Culinary fluid mechanics and other currents in food science

Arnold J. T. M. Mathijssen[*]

Department of Physics and Astronomy, University of Pennsylvania, 209 South 33rd Street, Philadelphia, Pennsylvania 19104, USA

Maciej Lisicki[†]

Institute of Theoretical Physics, Faculty of Physics, University of Warsaw, Pasteura 5, 02-093 Warsaw, Poland

Vivek N. Prakash[‡]

Departments of Physics, Biology, and Marine Biology and Ecology, University of Miami, 1320 Campo Sano Avenue, Coral Gables, Florida 33146, USA

Endre J. L. Mossige[§]

RITMO Centre for Interdisciplinary Studies in Rhythm, Time and Motion, University of Oslo (UiO), Forskningsveien 3A, 0373 Oslo, Norway

(published 15 June 2023)

Innovations in fluid mechanics have been leading to better food since ancient history, while creativity in cooking has inspired fundamental breakthroughs in science. This review addresses how recent advances in hydrodynamics are changing food science and the culinary arts and, reciprocally, how the surprising phenomena that arise in the kitchen are leading to new discoveries across the disciplines, including molecular gastronomy, rheology, soft matter, biophysics, medicine, and nanotechnology. This review is structured like a menu, where each course highlights different aspects of culinary fluid mechanics. Our main themes include multiphase flows, complex fluids, thermal convection, hydrodynamic instabilities, viscous flows, granular matter, porous media, percolation, chaotic advection, interfacial phenomena, and turbulence. For every topic, an introduction and its connections to food are provided, followed by a discussion of how science could be made more accessible and inclusive. The state-of-the-art knowledge is then assessed, the open problems, along with the likely directions for future research and indeed future dishes. New ideas in science and gastronomy are growing rapidly side by side.

DOI: 10.1103/RevModPhys.95.025004

CONTENTS

[*]amaths@upenn.edu
[†]mklis@fuw.edu.pl
[‡]vprakash@miami.edu
[§]endrejm@uio.no

I. INTRODUCTION

The origins of fluid mechanics trace back to ancient water technologies [Fig. 1(a)], which supplied our earliest civilizations with reliable food sources (Mays, 2010). Subsequently, as soon as the water flows, surprising phenomena emerge beyond number. Their abundance sparked the interest of the first inventors since the kitchen can serve as a laboratory (Kurti and This-Benckhard, 1994). As such, the scullery is a source of curiosity that has driven innovations throughout history (Drazin, 1987). The problems that emerge while cooking have led to creative solutions, which have improved food science. Moreover, as we explore in this review, these ideas have also led to breakthroughs in modern engineering, medicine, and the natural sciences. In turn, fundamental research has improved gastronomy, and thus the cycle continues. Hence, science and cooking are intrinsically connected across people and time.

Today numerous chefs have written extensive cookbooks from a scientific perspective. Well acclaimed is the work on molecular gastronomy by This (2006), which turned into a scientific discipline, as reviewed by Barham *et al.* (2010).

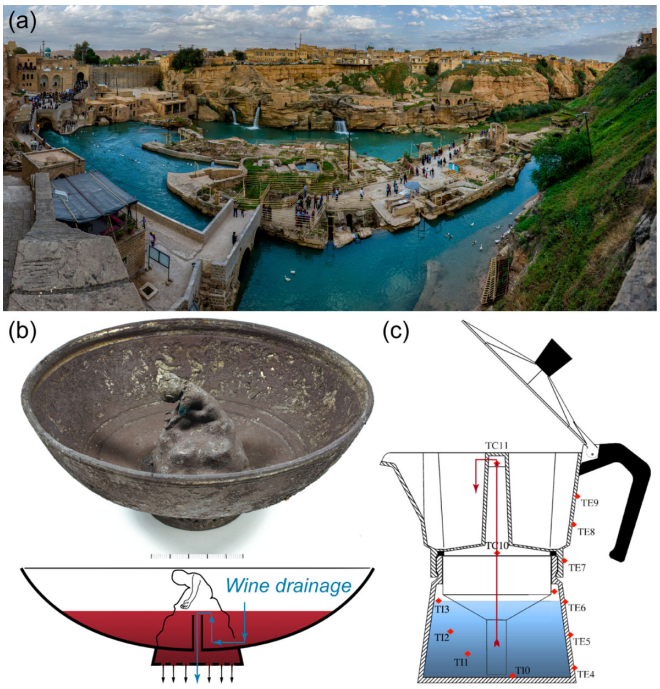

FIG. 1. Hidden channels. (a) Shushtar Historical Hydraulic System in Iran, described by UNESCO as a "masterpiece of creative genius." This irrigation system, dating back to the fifth century BCE, features canals, tunnels, dams, and water mills, which all work in unison. From Iman Yari. (b) First discovered specimen of a Tantalus bowl (Pythagorean cup) from the late Roman period, catalog no. 9 of the Vinkovci treasure. This silver-gilt bowl empties itself when filled above a critical level by a hidden siphon, soaking a greedy drinker in wine. Courtesy of Damir Doračić, Archaeological Museum in Zagreb, from Vulić *et al.*, 2017. (c) The moka pot, a traditional stove-top coffee maker, where the boiling water percolates through the coffee by following the arrows. From Navarini *et al.*, 2009.

Another recent movement, known for using advanced equipment including centrifuges and blow torches, is called modernist cuisine (Myhrvold, Young, and Bilet, 2021). With its striking photography, sometimes using optical illusions, it also connects science with art in the field of fine dining (Borkenhagen, 2017). The book by McGee (2007) is particularly influential too: Celebrity chef Heston Blumenthal called it "the book that has had the greatest single impact on my cooking" and then wrote eight books himself. Another noteworthy cookbook containing various experiments and scientific diagrams was written by López-Alt (2015). One of the first people to approach cooking systematically, a century earlier, was the "king of chefs and chef of kings" Escoffier (1903), whose 943-page culinary guide remains a gold standard in haute cuisine (Trubek, 2000).

In the scientific community, a wave of excitement hit when Kurti and Kurti (1988) solicited recipes or essays on cooking from the members of the Royal Society. Science can improve cooking, but they also showed that food can lead to better science, a notion that may not have been taken seriously at the time (Mermin, 1990). Later, in her essay "Food for thought," Dame Athene Donald FRS pleaded that the scientific challenges are as exciting in food as in any more conventional

area. They should not be overlooked or, worse, sneered at (Donald, 2004). Her early vision inspired scientists to regard food as an interdisciplinary research topic. Food science now spans many fields, including materials science (Mezzenga *et al.*, 2005), food chemistry and physical chemistry (Fennema, 2017), nutrition genetics (Capozzi and Bordoni, 2013), food engineering (Heldman, Lund, and Sabliov, 2018), food microbiology (Provost *et al.*, 2016; Doyle, Diez-Gonzalez, and Hill, 2019), food rheology (Ahmed, Ptaszek, and Basu, 2016), soft condensed matter (Vilgis, 2015; Assenza and Mezzenga, 2019; Pedersen and Vilgis, 2019), and biophysics (Foegeding, 2006; Nelson, 2020).

However, to our knowledge, and despite the overwhelming number of surprising hydrodynamic effects that emerge in the kitchen, there has been no comprehensive review of fluid mechanics in gastronomy and food science. Therefore, we address this topic here in a manner that first provides a broad overview and then highlights the frontier of modern research. As such, we aim to connect the following communities.

First, for chefs and gastronomy professionals fluid mechanics can make or break their culinary creations. Hydrodynamic instabilities can ruin a layered cocktail (Sec. III.A), while the Leidenfrost effect helps when searing a steak (Sec. V.B), and percolation methods help baristas to perfect their coffee (Sec. VII.D). We discuss these examples here, and quite a few more. Indeed, throughout this review we aim to connect the science with food applications. We also point out some common mistakes in cooking and think of new ideas for recipes.

Second, for food scientists it is important to unravel hydrodynamic effects in order to develop better food processing technologies (Knorr *et al.*, 2011). For example, microfluidic techniques are now extensively used for edible foam generation and emulsification (Skurtys and Aguilera, 2008; Gunes, 2018), but also for bioactive compound extraction and the design of novel food microstructures (He *et al.*, 2020). More generally fluid mechanics describes the transport of mass, momentum, and energy, which is to be optimized in food processing (Welti-Chanes and Velez-Ruiz, 2016) and food preservation (Gould, 2012; Amit *et al.*, 2017). We highlight a number of unexpected flow phenomena and their relation with food science technologies.

Third, from the perspective of medicine and nutrition professionals, flow physics has led to novel health care solutions and has provided insights on the physiology of digestion (Donald, 2017). For example, flow devices can detect foodborne pathogens or toxins (Kant *et al.*, 2018), which is essential for food safety (Bajpai *et al.*, 2018) and food quality control (Ozilgen, 2011). Similar technologies can equally be used for *in vitro* fertilization for agricultural animal breeding or other applications in animal health monitoring, vaccination, and therapeutics (Neethirajan *et al.*, 2011). Moreover, using next-generation DNA and protein sequencing with nanopore technology (Drndić, 2021), the field of foodomics could help to improve human nutrition (Capozzi and Bordoni, 2013). In this review we reflect on more of these food-related health innovations.

Fourth, for engineers and natural scientists kitchen flows have led to breakthrough discoveries, and continue to do so. To name a few here, Agnes Pockels established the modern discipline of surface science after her observations of soap film while washing dishes (Sec. IX.C), and Pyotr Kapitza discovered the roll-wave instability while under house arrest (Sec. IX.E). Most universities and labs were closed during the COVID-19 pandemic, which again led to an unsolicited wave of kitchen science (American Physical Society Press Office, 2020a). Moreover, culinary flows have given rise to engineering applications in completely different fields. The piston-and-cylinder steam engine was inspired by Papin's pressure cooker (Sec. II.A), and inkjet printers rely on capillary breakups observed in a sink (Sec. II.G). Indeed, because of the low activation barrier, the kitchen is a hot spot for curiosity-driven research where new ideas arise.

Fifth, for policy makers the evolution of food science often lies at the heart of historical developments (Toussaint-Samat, 2009; Mays, 2010), and it is key to the future of our planet (Foley *et al.*, 2011). Our soil resources are under stress worldwide (Amundson *et al.*, 2015), the use of land has global consequences (Foley *et al.*, 2005), and food from the sea is similarly limited (Costello *et al.*, 2020). Solutions may come from food technology innovations, global policy reforms, and science education improvements.

Finally, for science educators the kitchen can serve as an exceptional classroom (Benjamin, 1999; Rowat *et al.*, 2014; Vieyra, Vieyra, and Macchia, 2017) or indeed a lab (Kurti and This-Benckhard, 1994) that is accessible to people of different backgrounds, ages, and interests. As a natural gateway to learning about fluid mechanics, food science demonstrations equally connect to numerous other disciplines. Examples include teaching oceanography (Glessmer, 2020), chemistry education (Schmidt *et al.*, 2012; Piergiovanni and Goundie, 2019), geology (Giles, Jackson, and Stephen, 2020), soft matter physics (Ogborn, 2004), and the science of cooking for nonscientific individuals (Miles and Bachman, 2009). Recently, based on their successful edX (online) and Harvard University course, Brenner, Sörensen, and Weitz (2020) connected haute cuisine with soft matter science in a textbook. Indeed, a lot of science awaits to be discovered during our daily meals.

This review is structured like a menu, with each section corresponding to the course of a meal and subsections corresponding to different dishes. We begin by washing our hands in Sec. II, which is about kitchen sink fundamentals. There we provide an introduction to fluid mechanics in a manner that is accessible to scientists across the disciplines. We are then ready to pour ourselves a cocktail, which we discuss in Sec. III, which concerns multiphase flows. The first course might be a *consommé*, so in Sec. IV we focus on complex fluids and food rheology. The main course is often hot, so we review thermal effects in cooking in Sec. V. Tempted by dessert with honey and ice cream, we consider Stokesian flows in Sec. VI. We then brew a coffee after the lavish meal, the thought of which sparks interest in granular flows and porous media, as discussed in Sec. VII. Pouring another cup of tea, we discuss different aspects of nonlinear flow and turbulence in Sec. VIII. Once the meal comes to an end, it is time to wash the dishes, which turns our attention to interfacial flows in Sec. IX. We conclude the review with a discussion about making science more accessible and inclusive in Sec. X.

We do not recommend working one's way through this entire menu (review) in one sitting. Instead, to optimize

digestion of the material, it might be better to return a couple of times. For each visit, one could then compose a different meal (reading) with a few courses (sections) by selecting from the available dishes (subsections) *à la carte*.

II. KITCHEN SINK FUNDAMENTALS

We begin this review by introducing the basics of fluid mechanics in the context of food science. Starting with surprising aspects of hydrostatics, we quickly transition to topics such as the hydrodynamics of wine aeration, hydraulic jumps, and satellite dishes. Some of these concepts are not as simple as they may appear. In the words of Drazin (1987),

> "A child can ask in an hour more questions about fluid dynamics than a Nobel Prize winner can answer in a lifetime."

As things get more complicated in the later sections, we often refer back to these kitchen sink fundamentals.

A. Eureka: Surprising hydrostatics

In his work "On Floating Bodies," Archimedes of Syracuse (c. 287–c. 212 BCE) described the principles of hydrostatics. The buoyancy force on an immersed object equals the weight of the fluid that it displaces (Chalmers, 2017). To see this for a simple incompressible liquid, we note that the hydrostatic pressure increases with depth as a consequence of the incompressibility. Consider an immersed cube of volume $V = L^3$ that experiences a pressure difference of $\Delta p = \rho g L$ between its top and bottom surfaces, where ρ is the fluid density, ρ_0 is the object density, $\Delta\rho = \rho - \rho_0$ is the density contrast, and g is the gravitational acceleration. The buoyancy force is this pressure difference multiplied by the surface area (L^2), giving $F_b = \rho g V$, which indeed is the weight of the displaced fluid. The total force, including buoyancy and gravity on the object, is $F = \Delta\rho g V$, which vanishes for neutrally buoyant objects. Note that buoyancy applies not only to solid objects but also to fluids of different densities; see the discussion of layered cocktails of Sec. III.A.

As Greece is a seafaring nation, we note the importance of Archimedes's principle to describe the stability of ships: If the center of gravity is above the metacenter (which is related to the center of buoyancy), the boat will topple (Barrass and Derrett, 2011; Lautrup, 2011). We can test this by floating a cup upside down in the kitchen sink. Another classic experiment is throwing a stone out of a boat (or an upright floating cup). Does the water level rise? Furthermore, Archimedes's principle is often used in modern engineering. A notable example is the Falkirk Wheel in Scotland, one of the world's largest boat lifts, where it is ensured that the weights of the lift are always balanced (Kosowatz, 2011). As we see throughout this review, buoyancy is essential in many food science processes, including bubbly drinks (Sec. III.E), heat convection (Sec. V.C), and latte art (Sec. VII.D).

The concept of pressure became more established in the 17th century. Evangelista Torricelli (1608–1647) understood that "we live submerged at the bottom of an ocean of the element air, which by unquestioned experiments is known to have weight." Hence, he invented the barometer, by realizing that mercury in a top-sealed tube was supported by the pressure of the air (West, 2013). Torricelli also wrote that air pressure might decrease with altitude, a prediction later demonstrated by Blaise Pascal (1623–1662). Note that for compressible fluids the pressure does not necessarily decrease linearly with altitude, as was the case for the previously described simple incompressible liquid. Subsequently, these findings led to the discovery of Pascal's law, which states that a pressure change at any point in an enclosed fluid at rest is transmitted undiminished throughout the fluid (Batchelor, 2000). This law lies at the heart of many applications with "communicating vessels," including water towers, modern plumbing, water gauges, and barometers (Middleton, 1964).

While hydrostatics may seem elementary compared to hydrodynamics, it can still be counterintuitive. For example, gravity can be defied when a glass of water is turned upside down (Lindén, 2020). Another puzzling effect appears in siphons (Potter and Barnes, 1971). They are devices wherein fluids first flow upward, over a hill, and then downward without a pump. Siphons are used in many applications, including modern washing machines and anticolic baby bottles (Marshall *et al.*, 2021). While it is generally agreed upon that these flows are driven by gravity, it depends on the situation whether the fluid moves primarily because of pressure differences or intermolecular cohesion and capillary forces (Binder and Richert, 2011; Hughes, 2011; Richert and Binder, 2011; Jumper and Stanchev, 2014); see Sec. II.F. Hence, siphons remain an active topic of research (Boatwright, Hughes, and Barry, 2015; Wang *et al.*, 2022).

One of the oldest pranks in history that uses this siphon effect is the Tantalus bowl [Fig. 1b], also known as the Pythagoras cup. It is a drinking vessel that functions normally when filled moderately, but if the liquid level rises above a critical height, the siphon flow is initiated and the bowl will drain its entire contents. Therefore, the bowl concretizes a "Tantalean punishment," eliminating pleasure from those who get too greedy. While described in ancient literature, the earliest specimen of a Tantalus bowl was discovered only recently, in the Vinkovci treasure (Vulić *et al.*, 2017). Finally, in his treatise on pneumatics, Heron of Alexandria (c. 10–c. 70 CE) described 78 inventions based on nonintuitive hydrostatics (Woodcroft, 1851). Even today, modern chefs could use these nonintuitive discoveries to serve their dishes in a surprising fashion.

The use of pressure in the kitchen expanded upon the invention of the steam digester by Denis Papin (1647–1713). His improved designs included a stream-release valve to prevent the machine from exploding, an essential feature in all modern pressure cookers and in coffee makers like the moka pot; see Fig. 1(c) in Sec. VII.D. Besides kitchen appliances (Abu-Farah and Germann, 2022), the steam digester was the forerunner of the autoclave to disinfect medical instruments and the piston-and-cylinder steam engine (Ferguson, 1964). Pascal's principle also underpins the hydraulic press, a force amplifier capable of uprooting trees that was invented by Joseph Bramah (1748–1814). Bramah invented and improved many other culinary technologies during the industrial revolution, including high-pressure public water mains and the beer engine (Dickinson, 1941).

B. Navier-Stokes equations and the Reynolds number

Moving on from hydrostatics, we shift our attention to fluids in motion. These are described by the equations named after Claude-Louis Navier (1785–1836) and George Gabriel Stokes (1819–1903). When the velocity of the fluid is much smaller than the speed of sound, which is true for typical kitchen flows, the Navier-Stokes equations for a compressible Newtonian fluid (see Sec. IV.A) of constant dynamic viscosity μ, constant bulk viscosity ζ, and density ρ can be written as

$$\rho\frac{D\boldsymbol{u}}{Dt} = -\boldsymbol{\nabla}p + \mu\boldsymbol{\nabla}^2\boldsymbol{u} + \left(\zeta + \frac{\mu}{3}\right)\boldsymbol{\nabla}(\boldsymbol{\nabla}\cdot\boldsymbol{u}) + \boldsymbol{f}, \quad (1a)$$

$$\frac{D\rho}{Dt} = -\rho(\boldsymbol{\nabla}\cdot\boldsymbol{u}). \quad (1b)$$

In Eqs. (1a) and (1b) $\boldsymbol{u}(\boldsymbol{x},t)$ is the flow velocity at position $\boldsymbol{x}$ and time t, $p(\boldsymbol{x},t)$ is the pressure field, $\boldsymbol{f}$ is a body force (usually gravity) acting on the fluid, and the operator $D/Dt = \partial/\partial t + (\boldsymbol{u}\cdot\boldsymbol{\nabla})$ is the material derivative, which includes both temporal and spatial variations experienced by a fluid element. Physically, Eq. (1a) stems from the conservation of momentum, essentially Newton's second law applied to an infinitesimal fluid parcel. Equation (1b) is called the continuity equation, which describes the conservation of mass.

In typical kitchen flows, we often deal with incompressible fluids. In that case, the density of a moving fluid parcel remains constant, so its material derivative vanishes ($D\rho/Dt = 0$). Consequently, Eq. (2b) reduces to $\boldsymbol{\nabla}\cdot\boldsymbol{u} = 0$, and the term in Eq. (2a) concerning the bulk viscosity disappears. Hence, the Navier-Stokes equations for an incompressible fluid are written as

$$\rho\frac{D\boldsymbol{u}}{Dt} = -\boldsymbol{\nabla}p + \mu\boldsymbol{\nabla}^2\boldsymbol{u} + \boldsymbol{f}, \quad (2a)$$

$$0 = \boldsymbol{\nabla}\cdot\boldsymbol{u}. \quad (2b)$$

Note that Eqs. (2a) and (2b) are often appropriate for water but not for gases.

The Navier-Stokes equations give us insight into the character of flow. In his seminal work, Reynolds (1883) observed the shape of a streak of dye injected into a pipe flow. For low pumping speeds, the dye forms a straight line parallel to the streamlines [Fig. 2(a)(i)]. This flow is called laminar because the fluid parcels move in lamellae parallel to each other. With increasing pumping speed, we see a gradual distortion of this regular pattern and the flow transits to turbulence. Here the streak of dye is quickly smeared all over the flow domain [Fig. 2(a)(ii)] because of increased mixing and chaotic streamlines [Fig. 2(a)(iii)].

To characterize the transition from laminar (ordered) to turbulent (disordered) flow (Mullin, 2011), we may use the Navier-Stokes equations and examine the relative magnitude of the inertial to viscous forces that compete in shaping the flow. By considering a steady flow with a characteristic speed U_0 varying over a length scale L_0, we find that the relative magnitude of the convective term to the viscous term, called the Reynolds number, can be written as

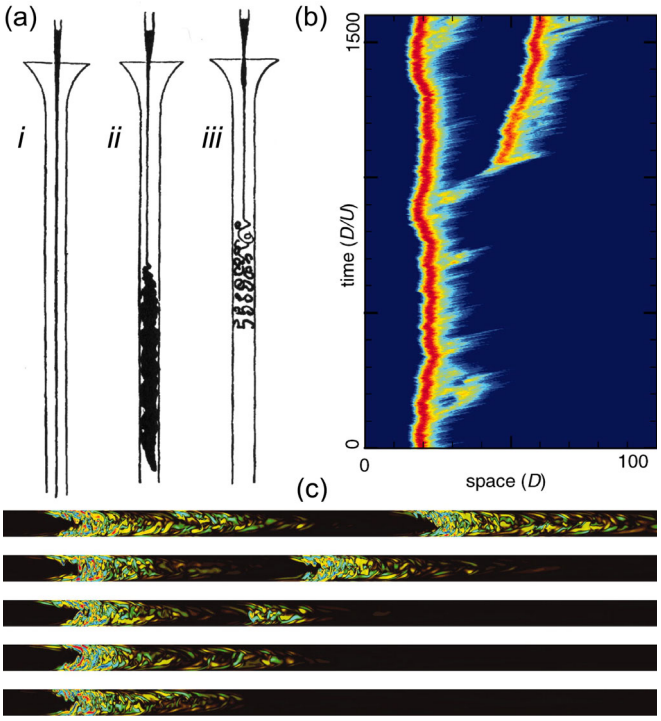

FIG. 2. Turbulent pipe flow. (a) Drawings showing (i) laminar pipe flow, (ii) turbulent flow, and (iii) turbulent flow observed under the stroboscopic illumination achieved with an electric spark, thereby revealing that the structure of the flow comprises eddies and vortices. From Reynolds, 1883. (b) Spacetime diagram from a numerical simulation at $\mathrm{Re} = 2300$ showing the process of turbulent puff splitting. (c) Visualization of puff splitting in a cross section of the pipe. Time increases in the snapshots from bottom to top. (b),(c) From Avila *et al.*, 2011.

$$\mathrm{Re} \equiv \frac{\text{inertial forces}}{\text{viscous forces}} = \frac{|\rho(\boldsymbol{u}\cdot\boldsymbol{\nabla})\boldsymbol{u}|}{|\mu\boldsymbol{\nabla}^2\boldsymbol{u}|} \sim \frac{\rho U_0 L_0}{\mu}. \quad (3)$$

The character of flow crucially depends on this quantity. The low Reynolds number regime ($\mathrm{Re} \ll 1$) is called Stokes flow (see Sec. VI.A), where viscosity dominates inertia, while the other limit $\mathrm{Re} \to \infty$ corresponds to inviscid flow (see Sec. VIII). The critical Reynolds number $\mathrm{Re}_c \approx 2300$ marks the value above which flow character turns from laminar to turbulent. In Sec. II.C, we examine this transition using the specific example of a pipe flow.

Today, more than 200 years after their formulation, much is still unknown about the Navier-Stokes equations. This is due mainly to the nonlinearity of the convective term $(\boldsymbol{u}\cdot\boldsymbol{\nabla})\boldsymbol{u}$ in the material derivative. One of the seven Millennium Prizes of $1 million can be earned for the "existence and smoothness problem" (Carlson, Jaffe, and Wiles, 2006). However, highly accurate approximative techniques for solving the Navier-Stokes equations have been developed and are used by physicists and engineers on a daily basis.

C. Drinking from a straw: Hagen-Poiseuille flow

Keeping in mind the mathematical difficulty of fluid mechanics, solutions to the Navier-Stokes equations can be found in specific cases. An important example is laminar pipe

flow, which occurs when we drink through a straw. This current is driven by a difference in pressure Δp, where we consider a cylindrical tube of radius R and length L with negligible gravity. The volumetric flow rate (the flux) going through the tube is described as follows using the Hagen-Poiseuille equation:

$$Q = \pi R^4 \Delta p / 8\mu L. \tag{4}$$

Equation (4) was first experimentally deduced independently by Gotthilf Hagen (1797–1884) and Jean Poiseuille (1797–1869). Soon thereafter, it was confirmed theoretically, as reviewed by Sutera and Skalak (1993). One of the most renowned theories was derived by Sir George Stokes (1819–1903) in 1845 (Stokes, 1880). However, he did not publish it until 1880, supposedly because he was not certain about the validity of the "no-slip" boundary condition of vanishing velocity at the walls (Sutera and Skalak, 1993). Stokes also derived the exact flow velocity $\boldsymbol{u}$ everywhere in the pipe. Starting with the Navier-Stokes equations (2) in cylindrical coordinates (ϱ, θ, z), assuming that the flow is steady, that it is axisymmetric, and that the radial and azimuthal components of the velocity are zero, one finds the parabolic flow profile,

$$u_z = -\Delta p (R^2 - \varrho^2)/4\mu L, \tag{5}$$

which as expected is strongest at the center line. The consequences of the Hagen-Poiseuille equation (4) can be substantial: It is 16 times more difficult to drink through a straw that is 2 times thinner to achieve the same flux. This fourth-power scaling is even more problematic for microscopic flow channels in the field of microfluidics; see Squires and Quake (2005), Tabeling (2005), Bruus (2008), Kirby (2010), and Sec. VI.F. However, wider pipes do not always make transport easier, because the hydraulic resistance (friction factor) increases when the flow becomes turbulent (Mullin, 2011; Cerbus *et al.*, 2018).

In the kitchen context, we can see this flow transition in a sink. When the tap is opened a little, the water column is clear and can be used as an optical lens. The Reynolds number is low and the flow is laminar. When the tap is opened further, the image begins to fluctuate. When the flow turns completely turbulent, the fluid layers no longer flow parallel to each other. This can cause the entrainment of air bubbles into the water stream, together with other instabilities. These bubbles can turn the water column opaque and white because of Mie scattering, which is roughly independent of the wavelength of light (van de Hulst, 1981), as opposed to the Rayleigh scattering that turns the sky blue, as explained independently by Smoluchowski (1908) and Einstein (1910).

The critical Reynolds number Re_c can be directly measured from this faucet experiment: The characteristic length scale L_0 is often chosen to be the diameter of the faucet nozzle ($d \sim 1$ cm), and the velocity scale U_0 can be easily determined by holding a cup under the faucet at the onset of turbulence (Thomsen, 1993). One should find a volumetric flow rate of $Q \sim 1.8\ \mathrm{cm}^3/\mathrm{s}$, which corresponds to $\mathrm{Re}_c \approx 2300$ in pipe flow (Heavers and Medeiros, 1990; Schlichting and Gersten, 2017). Near this critical value, one observes puff splitting events [Figs. 2(b) and 2(c)], showing that spatial proliferation of chaotic domains is critical to fluid turbulence (Avila *et al.*, 2011; Avila, Barkley, and Hof, 2022).

One can also determine the diameter of the valve inside the faucet. Without seeing it, the onset of turbulence can still be heard as a hissing sound. Using $\mathrm{Re} = 4Q/\nu\pi d$ with a known Re, we can find the critical Q at which the sound emerges and thus compute the valve diameter. Because the valve is usually smaller than the nozzle, this happens at a lower flow rate. In medicine, this listening technique, called auscultation (Chizner, 2008), can be used to detect a narrowing of blood vessels, sounds referred to as bruits or vascular murmurs (Stein and Sabbah, 1976; Marsden, 2014; Seo *et al.*, 2017), and, similarly, obstructions of the airways in respiratory conditions (Grotberg, 2001; Kleinstreuer and Zhang, 2010; Bohadana, Izbicki, and Kraman, 2014). In Sec. VIII.C we discuss more about hydrodynamic sound generation.

D. Wine aeration: The Bernoulli principle

In his book *Hydrodynamica*, Bernoulli (1700–1782) found that pressure decreases when the flow speed increases. More generally, Bernoulli's principle is a statement about the conservation of energy along a streamline. Swiss mathematician Leonhard Euler (1707–1783) used this principle to derive the modern form of the Bernoulli equation,

$$\tfrac{1}{2}u^2 + \Psi + w = \text{constant along a streamline}, \tag{6}$$

where it is assumed that the flow is steady and that friction due to viscosity is negligible, $\Psi = gz$ is the force potential due to gravity, and w is called the enthalpy of the fluid per unit mass. For an incompressible fluid, which is often an appropriate approximation for water, this enthalpy corresponds simply to the energy of the pressure field $w = p/\rho$. For a compressible fluid, the enthalpy also includes the internal energy of the fluid, such as the energy stored by the compression, which depends on the fluid's thermodynamic properties (Batchelor, 2000).

Despite its apparent simplicity, the Bernoulli principle is a powerful tool in many applications. On the one hand, it can be used to compute flow rates by measuring a pressure difference. A Pitot tube is a device that uses this idea, for example, to determine the speed of an aircraft (Anderson, 2017) or to measure airflow in food processing applications (Moyls, 1981). On the other hand, the Bernoulli principle can be used to compute pressure differences by measuring flow rates, for example, to determine the pressure distribution around a plane wing (airfoil) and thus the lift force (Anderson, 2017).

Together with the principle of mass conservation, the Bernoulli equation explains the Venturi effect: In a pipe constriction, the pressure decreases as the flow speed increases. In the kitchen, this Venturi effect is exploited in wine aerators [Fig. 3(a)]: The wine moves through a main tube with a constriction, where the lower pressure is used to draw in bubbles from a side tube. These air bubbles can improve wine flavor (Ribéreau-Gayon *et al.*, 2006; Balboa-Lagunero *et al.*, 2011). Indeed, this was already known to Louis Pasteur, who famously wrote, "*C'est l'oxygène qui fait le vin*," (Pasteur, 1873), or "It is the oxygen that makes the wine." Note that

FIG. 3. Wine aeration. (a) Oxygen injection using the Venturi effect. The wine moves down into a narrow funnel by gravity. In the funnel the liquid accelerates, which lowers the pressure relative to the surrounding atmosphere, as described by the Bernoulli principle [Eq. (6)]. Hence, air bubbles are drawn in, which aerates the wine. (b) Wine decanter. By pouring and swirling the liquid around, ripples form that mix oxygen in efficiently. Section IX.E addresses thin-film instability. (a),(b) Courtesy Vintorio Wine Accessories.

Fig. 3(b) shows aeration based on mixing with thin-film ripples, which we describe in Sec. IX.E. The Venturi effect is also used in gas stoves and grills, where inspirators mix air with flammable gas (instead of wine) to enhance combustion efficiency. The use of fire in the kitchen is further addressed in Sec. V.F. Finally, the Bernoulli principle can be used to regulate the pressure in hydraulic devices such as food grippers, which handle sliced fruits and vegetables (Davis, Gray, and Caldwell, 2008; Petterson *et al.*, 2010).

E. Pendant drops: Surface tension

The Bernoulli and Navier-Stokes equations describe the motion of fluids, but they do not say much about the phenomena that occur at interfaces: How can droplets hang upside down from a tap? Water molecules are attracted to each other by cohesion forces, particularly by hydrogen bonds (de Gennes *et al.*, 2004; Rowlinson and Widom, 2013). This cohesion leads to a surface tension γ, a force per unit length, which acts as if there were a taut elastic sheet covering the liquid interface (Marchand *et al.*, 2011). Indeed, surface tension acts to minimize the surface area, so free droplets tend to be spherical. This inward force is balanced by a higher pressure inside the droplet. The pressure difference across the water-air interface, called the Laplace pressure, is given by the Young-Laplace equation

$$\Delta p = -\gamma H, \tag{7}$$

where H is the mean curvature of the interface. For spherical droplets of radius R, we have $H = 2/R$. Equation (7) is named for Thomas Young (1773–1829) and Pierre-Simon Laplace (1749–1827).

In the kitchen, the surface tension of water-air interfaces can be measured with a dripping tap experiment. A drop of radius R hanging from a faucet balances the surface tension ($F_\gamma = 2\pi R\gamma$) with the force of gravity [$F_g = (4/3)\pi R^3 \Delta\rho g$]. Therefore, the pendant drop will fall if it grows larger than $R^* \sim \lambda_c$, with the capillary length

$$\lambda_c = \sqrt{\frac{\gamma}{\Delta\rho g}}. \tag{8}$$

By measuring this critical droplet radius, one can then estimate the surface tension using the known values for gravity g and the density difference $\Delta\rho$ between water and air. For a more accurate result, we should take the exact shape of the nozzle and the pendant drop into account (Berry *et al.*, 2015). To make this experiment accessible to students, they can be asked to use their smartphone cameras (Goy *et al.*, 2017). For water-air interfaces, one finds that the surface tension is $\gamma \approx 0.07$ N/m. This value (double O seven) might be easy to remember because the nondimensional parameter that characterizes the importance of gravity compared to surface tension is called the Bond number,

$$\mathrm{Bo} \equiv \frac{\text{gravitational forces}}{\text{capillary forces}} \sim \frac{2}{3}\frac{\Delta\rho g L_0^2}{\gamma} = \left(\frac{L_0}{\lambda_c}\right)^2, \tag{9}$$

which was named for the English physicist Wilfrid Noel Bond (1897–1937). In Eq. (9) L_0 is a characteristic length scale like the drop radius R. Note that the Bond number is also called the Eötvös number (Eo), which was named for the Hungarian physicist Loránd Eötvös (1848–1919).

Surface tension can lead to a vast number of counterintuitive phenomena, and new effects are still discovered every day. This is particularly important for nanotechnology and miniaturization in microfluidics because the characteristic length scale is much smaller than the capillary length. This leads to small Bond numbers [Eq. (9)], so surface tension dominates gravity and indeed most other bulk forces (Tabeling, 2005). In addition, in microgravity experiments the effects of surface tension are amplified (Kundan *et al.*, 2015). This is highlighted in a video where an astronaut tries to wring out a wet cloth in the International Space Station (Hadfield, 2013), but the water stays near the cloth because of surface tension. Back on Earth, when a pendant drop falls it makes a distinct "plinking" sound, which we explain in Sec. VIII.C. Not least, plinking droplets are a characteristic of drip coffee (discussed in Sec. VII.D).

F. Rising liquids: Wetting and capillary action

Besides cohesion forces that lead to surface tension, liquid molecules are also subject to adhesion forces, through which they are attracted to other molecules (Rowlinson and Widom, 2013). This can be observed directly when looking at a water droplet sitting on a kitchen benchtop (de Gennes *et al.*, 2004). The line where the liquid, gas, and solid meet is called the contact line, or the triple line. The contact angle θ_c is defined as the angle between the liquid-gas interface and the surface. If the benchtop is hydrophilic (it attracts water), the droplet spreads out and wets the surface (Bonn *et al.*, 2009), leading to a small contact angle of $0 \leq \theta_c < 90°$. But if the adhesion forces are weak, such as on waxed surfaces, the surface is

called hydrophobic (it fears water). The cohesion forces prevent spreading by pulling the drop together, leading to a large contact angle of $90° < \theta_c \leq 180°$. The equilibrium contact angle is found by minimizing the total free energy using the calculus of variations. This leads to the Young equation

$$\cos\theta_c = \frac{\gamma_{SG} - \gamma_{SL}}{\gamma_{LG}}, \tag{10}$$

where the interfacial energies γ_{ij} encode the relative strengths of the cohesion and adhesion forces between the three phases $i, j \in (\text{liquid}, \text{gas}, \text{solid})$. Note that without using a subscript we imply that $\gamma = \gamma_{LG}$, and the gas phase is sometimes also called the vapor phase. Indeed, instead of an energy balance, Eq. (10) can be interpreted as a force balance between the acting interfacial tensions. When these forces are no longer in equilibrium, the Young equation can be improved by accounting for advanced effects like contact line dynamics (Tadmor, 2004; Jasper and Anand, 2019).

The degree to which a drop will wet a substrate can be estimated with the spreading parameter (de Gennes *et al.*, 2004), which is given by

$$S = \gamma_{SG} - (\gamma_{LG} + \gamma_{SL}). \tag{11}$$

When $S > 0$, the drop spreads indefinitely toward a zero equilibrium contact angle, as is the case for silicone oil spreading on water. When $S < 0$, the drop instead forms a finite puddle, as when a drop of cooking oil is placed on a bath of water in a simple kitchen experiment. Owing to its weight, the drop deforms the water surface. The amount of distortion depends on the relative magnitude of buoyancy to surface tension forces, as characterized by the Bond number [Eq. (9)]. The spreading dynamics for partially wetting droplets was recently studied by Durian *et al.* (2022).

Leonardo da Vinci (1452–1519) first recorded that liquids tend to flow spontaneously into confined spaces, an effect now called capillary action or capillarity (de Gennes *et al.*, 2004). When dipping a narrow glass tube or a straw into water, the liquid will rise up until it reaches a constant height h. The narrower the capillary, the more the liquid ascends. It may take a longer time to reach the final height, though, because the hydraulic resistance increases significantly for smaller tube radii, as seen from the Hagen-Poiseuille equation (4).

This effect of capillarity is also explained by intermolecular adhesion and cohesion forces, as the liquid is pulled down by gravity but attracted up by the surfaces. Quantitatively, the height to which the water rises in a capillary can be calculated by balancing the hydrostatic pressure $\Delta p_g = \rho g h$, with the Laplace pressure as in Eq. (7). If the capillary is cylindrical with inner radius R_i and the meniscus has a spherical shape, its radius of curvature is $R = R_i/\cos\theta_c$ in terms of the contact angle. Combining these ingredients yields the Jurin's law (Jurin, 1718)

$$h = 2\gamma_{LG}\cos\theta_c/\rho g R_i. \tag{12}$$

For a typical glass microchannel of $R_i = 50$ μm, the water can rise up to ∼30 cm, and much higher for thinner tubes.

Hence, wetting and capillary action have many applications (de Gennes *et al.*, 2004). For example, you may like growing your own basil for cooking. Plants use capillarity for transporting water from the soil to their leaves, together with other mechanisms including osmosis and evaporation, which become more important for tall trees (Jensen *et al.*, 2016; Katifori, 2018). Conversely, if the contact angle $\theta_c > 90°$ for hydrophobic surfaces h turns negative in Jurin's law [Eq. (12)], liquid is expelled. One can then observe dewetting, the process of a liquid spontaneously retracting from a surface (Redon, Brochard-Wyart, and Rondelez, 1991; Reiter, 1992; Herminghaus *et al.*, 1998). Consequently, thin liquid films are metastable or unstable on these surfaces, as they break up into droplets. Therefore, dewetting is often not desirable in industrial applications, because it can peel off protective coatings or paint (Palacios *et al.*, 2019), and it can inhibit lubrication in machinery (Sec. VI.C). Dewetting also has important implications for human health. For example, dewetting of lung surfactant layers can inhibit breathing (Hermans *et al.*, 2015), and dewetting of the tear film caused by dry eye disease (Madl *et al.*, 2022) or by wearing contact lenses (Suja *et al.*, 2022) can cause ocular discomfort and vision loss. Dewetting is also important in solid-state physics because it can damage thin solid films. Sometimes this effect can be turned into an advantage for making photonic devices and for catalyzing the growth of nanotubes and nanowires (Thompson, 2012). An example of a fine-dining accessory exploiting the effects of surface tension is the "floral pipette" (Burton *et al.*, 2013), which presents a novel means of serving small volumes of fluid in an elegant fashion. Not least, wetting properties are crucial for making cooking equipment with nonstick coatings (Sec. V.H).

G. Breakup of jets: Plateau-Rayleigh instability

Dripping kitchen taps offer a direct example of an important hydrodynamic instability [Fig. 4(a)]: When a vertical stream of water leaves a worn tap, it narrows down, stretched by gravity. Once the liquid cylinder is sufficiently thin, we observe its breakdown into droplets before hitting the sink. Plateau (1873b) was the first to describe this instability systematically, which then enticed Rayleigh (1879) to provide a theoretical description and a stability analysis of an inviscid jet. He showed that a cylindrical fluid column is unstable to disturbances whose wavelengths λ exceed the circumference of the cylinder. The most unstable mode for a jet of radius R has the wave number $k = 2\pi/\lambda \approx 0.697/R$ and, from the growth rate of this mode, a characteristic jet breakup time can be estimated as $\tau_b \approx 3\sqrt{\rho R^3/\gamma}$, which in a kitchen sink is typically a fraction of a second. This estimate does not depend on the jet velocity, although that is no longer expected to be true when one would account for air drag. On a separate note, kitchen jets also exhibit cross-sectional shape oscillations attributed to capillary waves, which can easily be seen in homemade experiments (Wheeler, 2012). By measuring these variations of jet eccentricity, occurring at a frequency proportional to τ_b^{-1}, one can measure the surface tension following an experimental protocol designed by Bohr and Ramsay (1909).

The physics and stability of liquid jets are fundamentally important for a number of applications, as reviewed by Eggers

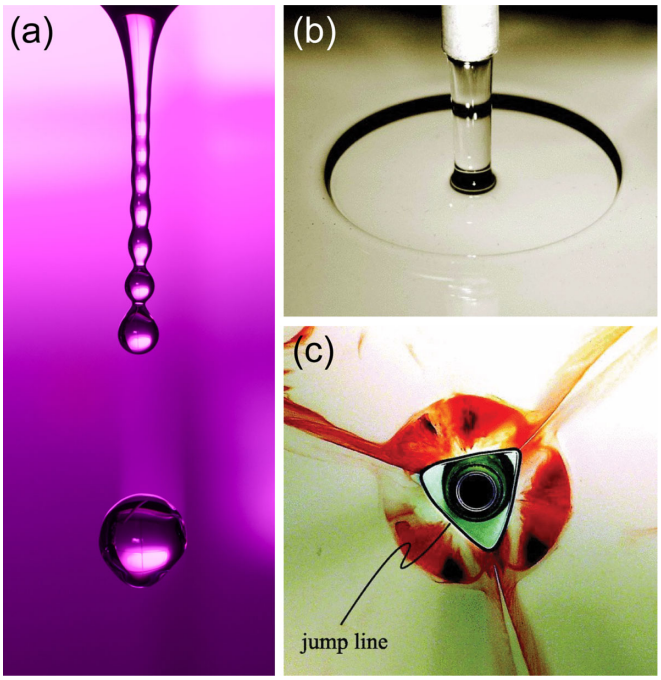

FIG. 4. Jets in the kitchen sink. (a) Example of the Rayleigh-Plateau instability, where a thin jet from a faucet breaks into droplets. From Niklas Morberg. (b) A circular hydraulic jump forms when a thicker liquid jet impinges on a planar surface. (c) A triangular hydraulic jump, seen from below through a glass plate. The impinging jet is the black center region, and the jump line is the triangular black line surrounding it. An additional roller structure, marked with a dye, extends from the jump line to the outer radius. In the corner region, the dyed fluid is expelled in radial jets. (b),(c) From Martens, Watanabe, and Bohr, 2012.

and Villermaux (2008). The breakup of jets has some universal features that result in a number of self-similar solutions. The scale invariance is manifested both in the conical shape of the tip of a French baguette [Fig. 4 in Eggers and Villermaux (2008)] and in a bimodal distribution of droplets produced, independently of the initial conditions, in the pinch-off process. The latter is an important technological problem in inkjet printing (Eggers, 1997; Martin, Hoath, and Hutchings, 2008). In microfluidic systems, the surface-tension-assisted breakup is also used to create monodisperse droplets (Anna, 2016), and drinking (lapping) mammals including cats and dogs may adjust their jaw-closing times to the pinch-off dynamics to maximize water intake (Jung, 2021). Citrus fruits can eject high-speed microjets from bursting oil gland reservoirs, up to 5000 g forces, which is comparable to the acceleration of a bullet leaving a rifle (Smith *et al.*, 2018). The breakup of these jets enables aerosolization, leading to a strong citrus scent.

H. Hydraulic jumps in the kitchen sink

When a thicker water jet (that does not break up) impinges on the kitchen sink, it will first spread out in a thin disk at high velocity. However, at some distance from its origin the thickness of the film suddenly increases; a hydraulic jump is formed [Fig. 4(b)]. Again, Leonardo da Vinci was first known to study hydraulic jumps (Hager, 2013), and Rayleigh (1914) first described it mathematically. He postulated that a balance between inertia and gravity forces lead to the jump. In other words, a jump is expected when the Froude number

$$\mathrm{Fr} \equiv \sqrt{\frac{\text{inertial forces}}{\text{gravitational forces}}} \sim \sqrt{\frac{\rho U_0^2/L_0}{\rho g}} \sim \frac{U_0}{\sqrt{gL_0}} \tag{13}$$

transitions through unity since the flow in the thin film continually loses momentum as is spreads out radially. In Eq. (13) U_0 is the velocity at the free surface of the film, g is gravity, and L_0 is the film thickness. Rayleigh did not include effects of surface tension (Sec. II.E) in his analysis. However, he wrote, "On the smallest scale surface-tension doubtless plays a considerable part, but this may be minimised by increasing the stream, and correspondingly the depth of the water over the plate, so far as may be convenient." Watson (1964) included effects of viscosity in his description of circular jumps, and two years later Olsson and Turkdogan (1966) performed complementary experiments to validate Watson's theory and hypothesized that surface tension contributed to the loss of kinetic energy at the jump. Bush and Aristoff (2003) expanded Watson's theory by exploring the role of surface tension on the formation of circular hydraulic jumps and Mathur *et al.* (2007) found that surface tension dominated over gravity for films on the micrometer scale. However, all of the aforementioned authors regarded capillary pressures [due to surface tension; see Eq. (7)] as being negligible compared to hydrostatic pressures (due to gravity) on the scale of kitchen sink hydraulic jumps. Bhagat *et al.* (2018) observed that when a strong jet impinges on a planar surface, the radius of the disk (the inner region before the jump) is independent of the orientation of the surface. They concluded that gravity does not cause the hydraulic jump when the film is sufficiently thin. Instead, a capillary pressure competes with the transport of momentum, and this balance is characterized by the Weber number

$$\mathrm{We} \equiv \frac{\text{inertial forces}}{\text{cohesion forces}} \sim \frac{\rho U_0^2 L_0}{\gamma}, \tag{14}$$

where γ denotes surface tension and ρ denotes the density of the impinging liquid. For weaker jets, however, gravity can no longer be neglected. By balancing the energy at the jump and adopting the approach of Watson (1964) by assuming a boundary layer flow inside the film, Bhagat *et al.* (2018) found the gradient of the radial velocity to be singular whenever

$$\mathrm{We}^{-1} + \mathrm{Fr}^{-2} = 1, \tag{15}$$

in which case a hydraulic jump can be expected. In Eq. (15) the first term is associated with capillary waves and the second is associated with gravity waves. The difference of the power of 2 comes out of the derivation because the Froude number [Eq. (13)] is historically defined as the square root of the force ratio.

As we have seen, the rich physics characterizing circular hydraulic jumps has attracted researchers for centuries, and the degree to which surface tension controls these jumps

remains an active research topic. Duchesne, Andersen, and Bohr (2019) and Bohr and Scheichl (2021) considered a static control volume and argued that surface tension has a negligible influence, as it is fully contained in the Laplace pressure, while Bhagat and Linden (2020, 2022) came to a different conclusion using an energy-based analysis. Another aspect of hydraulic jumps concerns the influence of different surface coatings on the jump radius and shape, and Walker *et al.* (2012) showed that when a water jet impinges on a shear-thinning liquid (see Sec. IV.A), the radius becomes time dependent. The same group later used viscoelastic liquids to enhance the degree of particle removal by inducing normal stresses (see Sec. IV.A) that "lift" the particles away from the substrate (Hsu *et al.*, 2014; Walker *et al.*, 2014). Abdelaziz and Khayat (2022) discussed noncircular jumps for inclined jets. Finally, it is also possible to create polygonal jumps, either by leveraging hydrodynamic instabilities in viscous liquids (Ellegaard *et al.*, 1998, 1999; Bush, Aristoff, and Hosoi, 2006; Martens, Watanabe, and Bohr, 2012; Nichols and Bostwick, 2020), as displayed in Fig. 4(c), or by utilizing micropatterned surfaces (Dressaire *et al.*, 2009).

I. How to cook a satellite dish

The importance of parabolas when focusing light rays has been known since classical antiquity: Diocles described it in his book *On Burning Mirrors*, and legend has it that Archimedes of Syracuse (c. 287–c. 212 BCE) used them to burn down the Roman fleet (Knorr, 1983). The latter is probably fictional, but Archimedes did write that the surface of a rotating liquid forms a paraboloid (Knorr, 1983). At hydrostatic equilibrium, the gravitational force on a fluid element is balanced by the centripetal force and buoyancy [Fig. 5(a)], such that the liquid height profile is given by

$$h(\rho) - h(0) = \omega^2\rho^2/2g, \tag{16}$$

where ρ is the radial distance from the rotation axis, ω is the angular velocity, and the corresponding focal distance is $f = g/2\omega^2$ [Fig. 5(a)]. Liquid-mirror telescopes use precisely this concept: the Large Zenith Telescope [Fig. 5(b)] was made of a 6 m pool of liquid mercury, which was rotated such that the camera sat at the focal point (Hickson *et al.*, 2007). Instead of a parabolic mirror, the earliest known functional reflecting telescope, which was made by Isaac Newton (1642–1727), used a spherical mirror because paraboloids are difficult to fabricate (Wilson, 2007). For modern large telescopes, the parabolic mirror is sometimes made by spinning molten glass in a rotating furnace. You can try to do this yourself in the kitchen by melting some wax (or gelatin) and letting it cool on a record turntable. Once it has solidified, you could even coat it with reflective paint. Parabolic reflectors are also widely used in solar cookers and large-scale solar engineering (Price *et al.*, 2002), opening up interesting avenues for future research in renewable energy technologies (Duffie, Beckman, and Blair, 2020).

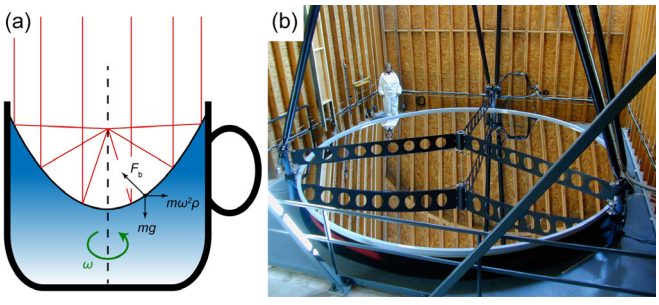

FIG. 5. Liquid mirrors. (a) Diagram of a rotating liquid that forms a parabolic reflector by the principle of hydrostatic equilibrium. The black arrows denote the force balance between gravity, rotation, and buoyancy. The red (vertical) lines represent light rays that come together at the focal point. (b) The Large Zenith Telescope used this principle. It was one of the largest optical telescopes in the world. Diameter, 6.0 m; rotation period, 8.5 s; mercury thickness, 1.2 mm; accessible area of sky, 64.2 deg^2. Person shown for scale. From Hickson *et al.*, 2007.

Equation (16) holds under the assumptions that the entire fluid rotates as a rigid body and that there is no local rotation of neighboring fluid elements. The flow is then called irrotational (Acheson, 1990). In closed containers, one must also account for surface tension and potential dewetting when the bottom becomes dry in the middle of the vessel (Lubarda, 2013). For higher rotation speeds, however, this static description is no longer valid as the flow becomes rotational. In fact, this transition is also highlighted by a symmetry breaking, leading to the formation of polygonal rotating structures (Jansson *et al.*, 2006; Bergmann *et al.*, 2011) before all symmetry is lost in turbulence at even higher rotation speeds.

This local rotation of fluid elements is quantified by the fluid vorticity (Acheson, 1990), which is defined as $\boldsymbol{\omega} = \boldsymbol{\nabla} \times \boldsymbol{u}$. The Navier-Stokes equation (2) for an incompressible fluid ($\boldsymbol{\nabla} \cdot \boldsymbol{u} = 0$) can be recast upon taking a curl of both sides, giving

$$\frac{D\boldsymbol{\omega}}{Dt} = (\boldsymbol{\omega} \cdot \boldsymbol{\nabla})\boldsymbol{u} + \nu\boldsymbol{\nabla}^2\boldsymbol{\omega}. \tag{17}$$

In Eq. (17) the first term on the right-hand side accounts for the stretching or tilting of vorticity due to the flow gradients, while the last term describes the diffusion of vorticity in the fluid. Vortices formed across all scales, from atmospheric to molecular processes, are described by their velocity or vorticity distribution. The simplest models assume an axisymmetric velocity field in which the fluid circles around the vortex axis. However, the flow field is more complex in most practical cases. For instance, secondary flows can arise due to this circling motion and friction with surfaces (Okulov *et al.*, 2022). These secondary flows give rise to the tea leaf effect; see Sec. VIII.A.

J. Washing and drying hands: Skin care

In Shakespeare's Scottish play, Lady Macbeth repeatedly washes her hands "for a quarter of an hour" to cleanse away her murderous guilty conscience. At the start of the COVID-19 pandemic, her troubled soliloquy was used to satirize World Health Organization posters that offer personal hygiene instructions in public restrooms (Smith, 2020). Humor aside,

washing hands with soap is "a modest measure with big effects" to combat pathogen dispersal (Handwashing Liaison Group, 1999), which is of particular importance to the food industry (Todd *et al.*, 2010). In addition, coronaviruses can be removed from the skin with soap or with hand sanitizers that contain sufficiently high concentrations of agents such as ethanol and isopropanol (Bar-On *et al.*, 2020; Chin *et al.*, 2020; Poon *et al.*, 2020). Dancer (2020) also reminded us that, besides our hands, we should not forget to clean the surfaces that we touch, following the legacy of Florence Nightingale (1820–1910), who is often called the founder of modern nursing. Despite the importance of proper sanitation, its hydrodynamics has not been well explored. Mittal, Ni, and Seo (2020) recently wrote, "Amazingly, despite the 170+ year history of hand washing in medical hygiene (Rotter, 1997), we were unable to find a single published research article on the flow physics of hand washing." There is a large body of literature about micelle formation and multiphase flows (Sec. III), foaming (Sec. III.F), and the physics of microorganisms (Sec. VI.E), but connecting this network of knowledge in the context of personal hygiene is only now starting.

Motivated by this gap in the literature and without access to a lab due to stay-at-home orders during the pandemic, Hammond (2021) conducted a theoretical assessment of handwashing. Using a lubrication approximation, he came a long way in describing how and when a virus particle is released from our hands when we rub them together. Hammond found that the rubbing speed needs to exceed a certain value set by the depth of the surface undulations of the skin, which in his model are represented by sinusoidal waves. Surprisingly, he found that multiple rubbing cycles are needed to remove a particle. More generally, the study of washing biological surfaces could widen our understanding of hydrodynamic interactions between particles, rough surfaces, and fluid flows, which is a largely unexplored research field with important implications in the food industry. A natural extension of this work is to include viscoelastic effects, which are likely to enhance the particle removal (Walker *et al.*, 2014) (see Sec. II.H) and which also might more realistically represent the material properties of the soap film. Moreover, Bar-On *et al.* (2020) and Poon *et al.* (2020) wrote recent reviews that discuss the biological physics and soft matter aspects of COVID-19.

After washing our hands, it is essential to dry them properly (Todd *et al.*, 2010; Gammon and Hunt, 2020). When we use a towel, the water gets pulled into the fabric by capillary action (see Sec. II.F). This works well only if the towel is more hydrophilic (water loving) than the surface of our hands. Paper and cotton cloth are especially hydrophilic, aided further by the large surface area of the fibers. Another method is to dry hands by evaporation. Whereas evaporation has been studied extensively on idealized surfaces (see Sec. VII.E), not much is known about wetting and evaporation on soft materials like the skin (Lopes and Bonaccurso, 2012; Gerber *et al.*, 2019). An ongoing debate is whether the dispersal of viruses and bacteria can be stopped more efficiently by warm air dryers or jet dryers, which, on the one hand, may let one avoid having to touch surfaces but, on the other hand, could cause pathogen aerosolization (Huang, Ma, and Stack, 2012; Best, Parnell, and Wilcox, 2014; Mittal, Ni, and Seo, 2020; Reynolds *et al.*, 2021), which is especially problematic in food processing plants (Kang and Frank, 1989).

A common medical condition that comes with washing and drying hands frequently is xeroderma, or dry skin (Walters *et al.*, 2012). This can lead to symptoms including itching, scaling, fissure, or wrinkling (Cerda and Mahadevan, 2003; Aharoni *et al.*, 2017). These problems can often be alleviated with moisturizers or emollients, but in more severe cases an effective treatment requires understanding the underlying biophysical mechanisms (Proksch *et al.*, 2020). Liquid transport has been studied in the networked microchannels of the skin surface (Dussaud, Adler, and Lips, 2003), as well as in the physics of stratum corneum lipid membranes (Das and Olmsted, 2016), and more generally in soft interfacial materials (Brooks *et al.*, 2016). Connecting the disciplines of physics and medicine will become increasingly important in future research.

III. DRINKS AND COCKTAILS: MULTIPHASE FLOWS

After washing our hands, it is time to start dinner with a beverage of choice. In this section we review a wealth of hydrodynamic phenomena that can emerge inside your drink. The Roman emperor Marcus Aurelius (121–180 CE) once said,

> "Look within. Within is the fountain of good, and it will ever bubble up, if thou wilt ever dig."

Examples of surprising effects happening inside beverages are shock waves in the tears of wine, effervescence in champagne, and "awakening the serpent" during whisky tasting. These multiphase flows (Brennen, 2005; Michaelides, Crowe, and Schwarzkopf, 2016) have seen rapid scientific advances recently, and they are applied extensively in industrial processes. Perfect to contemplate while waiting for the main course to arrive or to impress at a cocktail party. But, as the Dutch proverb says, "Do not look too deep into your glass."

A. Layered cocktails

A classic example of a culinary multiphase fluid is a layered cocktail [Fig. 6(a)]. For instance, an Irish flag cocktail is made by first pouring *crème de menthe*, then a layer of Irish cream, and finally some orange liqueur. This beverage is called stably stratified because each layer is less dense than the one beneath it, so buoyancy keeps the layers separate; see the discussion of Archimedes's principle in Sec. II.A. Note that densities of liquids can be measured with high accuracy using a hydrometer (Lorefice and Malengo, 2006), which can also be used in breweries to assess the strength of alcohol (alcoholometer) or in the dairy industry to measure the fat content of milk (lactometer). Multiple colored cocktail layers can be formed using a density chart also called a specific gravity chart for the different liquid ingredients (Ouimet, 2015). Stratification is essential for life on Earth, both in the atmosphere (Mahrt, 2014), where sharp cloud layers can be observed, and in the ocean (Li *et al.*, 2020), where water layers can be characterized by large gradients in density (pycnocline) and also by

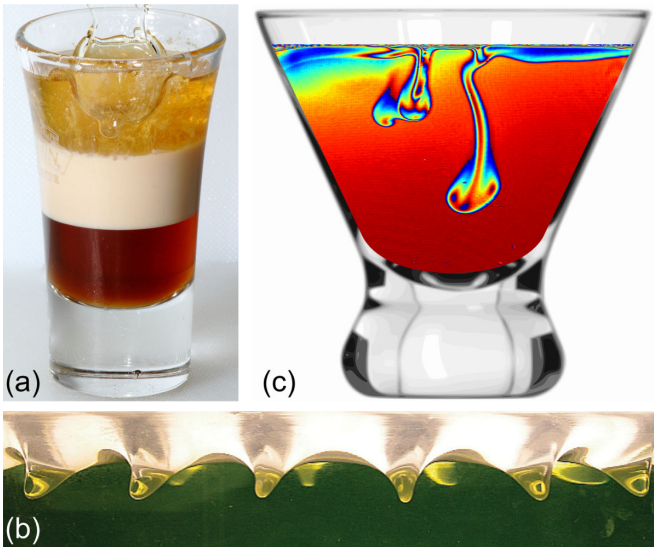

FIG. 6. Multiphase cocktails. (a) B-52 shot made by layering Kahlua, Bailey's Irish Cream, and Grand Marnier, with a splash on top. From J. D. Baskin on Flickr. (b) Kelvin-Helmholtz instability waves formed at an oscillated water-oil interface. From Yoshikawa and Wesfreid, 2011. (c) Evaporation-induced Rayleigh-Taylor instability. The ethanol concentration is measured using Mach-Zehnder interferometry, with plumes welling down from the top of the glass (low concentration) to the bottom (high concentration). Courtesy of Sam Dehaeck.

gradients in temperature (thermocline) or salinity (halocline), which can immediately impact environmental stratified flows (Grimshaw, 2002) or phytoplankton migration (Sengupta, Carrara, and Stocker, 2017), and more generally geophysical fluid mechanics (Pedlosky, 1987).

1. Inverted fountains

The cocktail layers will separate readily if the ingredients are immiscible, such as, say, lemon water and rose oil. However, if the liquids are miscible, it is recommended to pour the layers slowly (ideally along the side of the glass, with the help of a spoon) because otherwise the layers will mix. We can understand this turbulent and miscible mixing process as an "inverted fountain" (Turner, 1966; Hunt and Burridge, 2015), where the lighter fluid is forced down into the heavier fluid, opposed by buoyancy (Xue, Khodaparast, and Stone, 2019). The inverted height of the fountain z_f, and thus the mixing volume, depends strongly on the Reynolds number [Eq. (3)], where U_0 is the pouring velocity and L_0 is the radius of the injected jet, but also the densimetric Froude number, where g in Eq. (13) is replaced by $|g'|$, the reduced gravity due to buoyancy, which is given by

$$g' = g(\rho_i - \rho_a)/\rho_a \tag{18}$$

in terms of ρ_i and ρ_a, the densities of the injected and the ambient fluid. Conventionally, g' is negative for inverted fountains. For large Froude numbers, Turner (1966) showed that the fountain height is given by

$$z_f \approx 2.46 L_0 \mathrm{Fr}. \tag{19}$$

This classical result predicts a linear relation, which agrees well with modern experiments. Note that different scaling laws have been derived for weaker fountains with a smaller Froude number, as reviewed by Hunt and Burridge (2015).

2. Internal waves

Once the cocktail layers are established, more interesting flow phenomena can be observed. For example, when the glass is slightly disturbed, gravity waves (not to be confused with the gravitational waves in general relativity) can be seen, and these waves propagate inside the fluid instead of on its surface (Benjamin, 1967; Helfrich and Melville, 2006). Specifically, they are called interfacial (internal) waves when they propagate horizontally along an interface characterized by a density gradient $d\rho/dz < 0$. Consider a fluid parcel in a continuously stratified fluid, with a smooth density profile $\rho(z)$, that is in hydrostatic equilibrium at z_0. If the parcel of density $\rho_0 = \rho(z_0)$ is displaced a vertical distance $\Delta z = z - z_0$, where the surrounding fluid has a different density $\rho(z_0 + \Delta z)$, it will feel a gravitational restoring force (Sec. II.A). To first order, that leads to a simple harmonic motion (Vallis, 2017) with an oscillation frequency given by

$$f = \frac{1}{2\pi}\sqrt{-\frac{g}{\rho_0}\frac{d\rho}{dz}}. \tag{20}$$

Equation (20) was independently codiscovered by Väisälä (1925) and Brunt (1927), so it is called the Brunt-Väisälä frequency. These internal oscillations are typically slow compared to surface gravity waves at the liquid-air interface because the density gradient between the liquid layers is much smaller; see Sec. IX.D.

Internal waves are also common in oceanography (Garrett and Munk, 1979) and atmospheric science (Pedlosky, 1987), where they lead to beautiful patterns such as rippled clouds or lenticular clouds (Lamb and Verlinde, 2011). As such, internal waves appear in both compressible and incompressible media. Equation (20) is valid in the Boussinesq limit when the density differences are sufficiently small to be neglected, except where they appear in terms multiplied by g. This approximation is appropriate for weakly compressible fluids when the variations in density due to volume expansion are also small compared to buoyancy. Generalizations of the Brunt-Väisälä frequency can be derived outside the Boussinesq limit, which is important when the effects of compressibility become important, such as in stellar oscillations (Emanuel, 1994).

3. Kelvin-Helmholtz instability

Another spectacular atmospheric phenomenon is the formation of fluctus clouds, which look like breaking ocean waves in the sky. They are caused by the shear-induced Kelvin-Helmholtz (KH) instability (Kelvin, 1871; Drazin and Reid, 2010) when two fluid layers move alongside each other. Indeed, the same can be observed when a layered cocktail is sheared. By rotating the glass, a velocity gradient $\partial u/\partial z$ is created between the stratified layers. This shear is especially pronounced if the liquid spins up by friction with the bottom wall instead of the sidewalls; see Sec. VIII.A. The velocity

gradient drives the KH instability while it is opposed by buoyancy, quantified by the density gradient $\partial\rho/\partial z$. The ratio of these two forces is encoded by a dimensionless quantity named the densimetric Richardson number

$$\mathrm{Ri} \equiv \frac{\text{buoyancy forces}}{\text{shear forces}} \sim \frac{g}{\rho}\frac{\partial\rho/\partial z}{(\partial u/\partial z)^2}. \tag{21}$$

The fluid layers are unstable when the shear is large enough, when $\mathrm{Ri} \lesssim 1$, depending on the system configuration. In a setup resembling our cocktail, the instability was recently characterized in a spin-up rotating cylindrical vessel by Yan *et al.* (2017), and in an oscillatory cylindrical setup by Yoshikawa and Wesfreid (2011), as shown in Fig. 6(b). The KH instability will cause the stratified layers to mix with one another, as reviewed by Peltier and Caulfield (2003), or cause emulsion formation if the layers are immiscible (Sec. IV.D). In the latter case, surface tension stabilizes the short wavelength instability on top of buoyancy, which strongly affects emulsion formation (Thorpe, 1969; Drazin, 1970). Therefore, the KH instability is important for many processes in industry and food science. Think about making mayonnaise with a blender, for example. From a fundamental point of view, understanding these flows is intrinsically connected with the heart of theoretical physics: symmetries. Recently Qin *et al.* (2019) described how the KH instability results from parity-time symmetry breaking. Moreover, the Kelvin-Helmholtz instability also features in the magnetohydrodynamics of the Sun (Foullon *et al.*, 2011), ocean mixing (Pedlosky, 1987), relativistic fluids (Bodo, Mignone, and Rosner, 2004), and superfluids (Blaauwgeers *et al.*, 2002).

4. Rayleigh-Taylor instability

Until now we have discussed stably stratified cocktails. Yet, when a heavier fluid sits on top of a lighter fluid, the latter pushes into the former by gravity. Therefore, if there is no or little surface tension between the layers, the mechanical equilibrium is unstable. Any small perturbation then leads to a familiar pattern of fingerlike structures with a mushroom cap, as seen in Fig. 6(c). This phenomenon is explained by the Rayleigh-Taylor (RT) instability, which was discovered by Rayleigh (1882) and later mathematically described by Taylor (1950), together with systematic experiments by Lewis (1950). Many developments followed, and Chandrasekhar (1961) extended the theoretical description. Like the KH instability, the RT instability is relevant across the disciplines, from the astrophysics of supernovae (Kuranz *et al.*, 2018; Abarzhi *et al.*, 2019) to numerous technological applications (Drazin and Reid, 2010).

The RT instability arises because the system seeks to minimize its overall potential energy. Its onset is primarily governed by the Atwood number

$$\mathrm{At} = \frac{\rho_h - \rho_l}{\rho_h + \rho_l}, \tag{22}$$

the nondimensional difference between the densities of the heavier and the lighter fluid ρ_h and ρ_l. This number is most likely named after George Atwood (1745–1807), who also invented the Atwood machine, but we could not find the original source. To describe the RT instability more generally, one must account for the fluid viscosities and surface tension (Andrews and Dalziel, 2010), as well as potential effects due to fluid compressibility (Boffetta and Mazzino, 2017). Moreover, the dynamics depends strongly on the initial conditions: They begin with linear growth from perturbations, which transitions to a nonlinear growth phase involving characteristic structures of rising "plumes" and falling "spikes." Subsequently, these plumes and spikes interact with each other through merging and competition and roll up into vortices. The final stages are characterized by turbulent mixing; see Sec. VIII.

In the words of Benjamin (1999), the RT instability is a fascinating gateway to the study of fluid dynamics; see also Sec. X.B. It can readily be observed in kitchen experiments, but it also occurs spontaneously without us even noticing [Fig. 6(c)]: In a well-mixed (nonlayered) cocktail, the alcohol evaporates faster than water. Hence, at the air interface a water-rich layer develops that is denser than the bulk mixture, which gives rise to the RT instability (Dehaeck, Wylock, and Colinet, 2009). The plumes of such "evaporating cocktails" are observed using a Mach-Zehnder interferometer. By demodulating the fringe patterns using a Fourier transform method (Kreis, 1986), it is possible to compute the refractive index field, and hence the local ethanol concentration. Evaporation-induced Rayleigh-Taylor instabilities also occur in polymer solutions (Mossige *et al.*, 2020), so your cocktail need not necessarily be alcoholic.

The RT instability is often inseparable from the Kelvin-Helmholtz instability. RT flows create velocity gradients that trigger KH billows, while KH flows create density inversions that trigger RT fingers. Moreover, the RT instability is closely related to the Richtmyer-Meshkov instability, in which two fluids of different density are impulsively accelerated (Abarzhi *et al.*, 2019), and to the Rayleigh-Bénard convection, in which an instability occurs due to heating a single liquid from below or cooling it from above, which we describe in more detail in Sec. V.C.

B. Tears of wine

One of the most surprising phenomena in multiphase flows is the Marangoni effect, which is named for Carlo Marangoni (1825–1940) (Marangoni, 1871). You may have seen this effect already in the kitchen, when a droplet of dish soap falls into a bowl of water sprinkled with pepper: Within the blink of an eye, the pepper moves to the edges by an outward flow along the liquid-air interface. Another striking example is adding food coloring drops to a bowl of milk, where poking it with a soap-covered cotton bud generates beautiful flow patterns. These Marangoni flows arise because the surfactant molecules in the soap lower the surface tension (Levich and Krylov, 1969), leading to a difference in surface tension along the interface of $\Delta\gamma = f\gamma$, where the factor $f \sim 10^{-1}$ for most soaps. Consequently, the water without soap pulls more strongly on the water with soap, generating a current from regions of lower to higher surface tensions. For a difference in surface tension $\Delta\gamma$ over a characteristic length L_0 parallel to the interface, the Marangoni stress that drives the flow scales

as $\Delta\gamma/L_0$. The viscous stress that opposes this motion scales as $\mu u/L_0$. Hence, when these stresses balance each other, the flow strength can be roughly estimated as $u \approx \Delta\gamma/\mu = f\gamma/\mu$. Using $\gamma \sim 0.07$ N/m and viscosity $\mu \sim 0.9$ mPa s for water, we find that the flows are readily observable even for small fractions f. The ratio between advective and diffusive transport is then given by the Marangoni number

$$\mathrm{Ma} \equiv \frac{\text{advective transport rate}}{\text{diffusive transport rate}} \sim \frac{\Delta\gamma L_0}{\mu D}, \tag{23}$$

where D is the diffusivity of the surfactants or any additive that changes the surface tension. Note that the estimate $u \approx \Delta\gamma/\mu$ does not depend on L_0, which is only true if this is the only length scale in the problem. This assumption breaks down for shallow liquids. More detailed calculations must take these effects into account, including solubility, surface contamination, and system geometry (Levich and Krylov, 1969; Halpern and Grotberg, 1992; Lee and Starov, 2007; Roché *et al.*, 2014; Kim *et al.*, 2017).

The Marangoni effect occurs not only with soap but also with edible ingredients. In fact, the phenomenon was first identified by James Thomson (1822–1892) in the characteristic "tears" or "legs" of wine (Thomson, 1855), and indeed other alcoholic drinks including liquors and whisky; see Sec. III.C. These tears are formed because the alcohol is more volatile than water and it has a lower surface tension (Fournier and Cazabat, 1992). To see this, pour yourself a glass of wine; see Fig. 7(a). In the thin meniscus that the wine forms with the glass surface, the alcohol evaporates faster than the water, so the surface tension here is higher than in the bulk. The wine is then pulled up the meniscus, forming a thin film that starts climbing up along the side of the glass. After a few seconds, the film forms a ridge approximately 1 cm above the meniscus. This ridge becomes unstable under its own weight as more wine climbs up, so it collapses into tears that fall down toward the meniscus [Fig. 7(b)]. Large tears can fall back into the bulk, but small tears can be pulled up again by the continuously climbing film that replenishes the ridge. This can cause the tears to bounce up and down, especially at the meniscus. The effects are well imaged using the schlieren or shadow projection techniques (Settles, 2001).

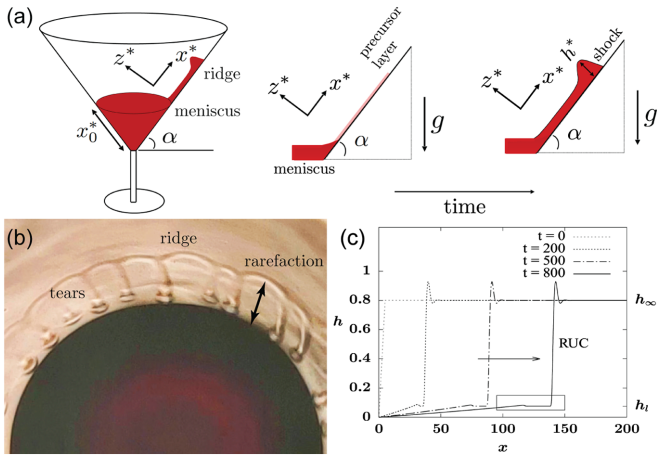

FIG. 7. Shock waves in tears of wine. (a) Schematic of a conical-shaped glass of inclination angle α, showing a one-dimensional thin wine film traveling up an inclined flat glass surface. The film height h^* is exaggerated for clarity. (b) Experiment using 18% ABV port wine and $\alpha = 65°$. Swirling the wine around the glass creates a front that forms out of the meniscus. The draining film advances up the glass and destabilizes into wine tears. (c) The formation of a reverse-undercompressive (RUC) shock. (a)–(c) From Dukler *et al.*, 2020.

In fact, the mechanism by which the droplets form and collapse is more complex. As the wine film climbs to its terminal height, when the Marangoni stresses are balanced by gravity, this transient stationary state is subject to various hydrodynamic instabilities (Vuilleumier *et al.*, 1995; Fanton and Cazabat, 1998; Hosoi and Bush, 2001). Besides alcohol concentration differences, the evaporation also induces temperature gradients that lead to additional Marangoni stresses (Venerus and Simavilla, 2015). The ridge instability that triggers the formation of wine tears was also studied and analyzed using Plateau-Rayleigh-Taylor theory (Nikolov, Wasan, and Lee, 2018). Yet, the dynamic formation of the ridge itself is still not well understood.

Until now we have discussed a wine film that spontaneously climbs up a dry wine glass, but it is common practice among connoisseurs to swirl the wine around. This often creates a wet coating film that is much higher than the terminal climbing height, which can give rise to vastly different behaviors. Dukler *et al.* (2020) showed that such swirled films can feature a "shock wave" that climbs out of the meniscus [Fig. 7(c)], again driven by Marangoni stresses due to evaporation. This wave can be observed as a ridge that propagates upward, where the wine film above the shock front is thicker than it is below the shock front. Specifically, the dynamics can be described as a reverse-undercompressive (RUC) shock. This type of shock wave is unstable: Small inhomogeneities in the wine film are amplified into thick drops, which then fall down as tears. As previously described for rising films driven by thermal gradients (Münch, 2003; Sur, Bertozzi, and Behringer, 2003), different shock morphologies can occur in other circumstances. This is of great scientific and technical interest, including dip-coating and painting applications. Moreover, it would be interesting if the dining experience could be improved by developing a new dish that uses the shock wave as a surprise effect.

C. Whisky tasting

We use all of our senses when we taste whisky, or whiskey (Velasco *et al.*, 2013). The spelling whiskey is common in Ireland and the United States, while the term whisky is common for products from the United Kingdom and most other countries. While complete volumes have been written about the art of whisky tasting [see MacLean (2020)], we instead highlight some of its hydrodynamic aspects, which are often clearly visible. That is, a good deal of information may be gained by assessing the appearance and dynamics of spirits (Russell, Bamforth, and Stewart, 2014; Miller, 2019). The following tests can give clues about the whisky quality and vintage before any smelling or tasting.

As a first examination, it is customary to inspect the tears that we described in Sec. III.B. This gives an indication of the

whisky's alcohol content, its viscosity, and its surface tension, which in turn depend on the exact chemical composition. When the tears run down slowly with thick legs, it indicates that it will give more mouthfeel (MacLean, 2010). Conversely, if the legs are thin and run quickly, the whisky is likely to be younger and of a lighter body. This is because the texture changes during the aging process, as viscous natural oils and other compounds are released from the wooden casks (Mosedale, 1995), which inevitably also influences the whisky color. The rheological and thermophysical properties are also affected by storage and temperature (Hlavác and Božiková, 2013). However, a whisky with more pronounced tears is not automatically sweeter or better in quality, since the tear formation is a purely physical phenomenon. Indeed, the tears vanish when the glass is covered since the evaporation-induced Marangoni stresses disappear.

A second experiment is the "beading" test (Davidson, 1981; MacLean, 2018; Miller, 2019). When a whisky bottle is shaken vigorously, a foam can appear on the liquid interface if the alcohol concentration is higher than approximately 50% alcohol by volume (ABV). The beading is not necessarily more pronounced at higher concentrations, but it is not observed below a certain percentage. Beading can also say something about the age of the whisky: The bubbles tend to last longer in older vintages because the compounds released from the wooden casks can stabilize the foam. Foam stability is further discussed in Sec. III.F.

A third inspection method is called whisky viscimetry (MacLean, 2010; Smith, 2011). When adding a little water to the whisky, small vortices called viscimetric whirls appear when the liquids of different viscosities mix with one another. Connoisseurs sometimes refer to this phenomenon as awakening the serpent (Smith, 2011). These vortices last for only a few seconds, but again they tell us something about the texture of the whisky. The more persistent the whirls, the thicker the mouthfeel and the higher the alcohol concentration. To our knowledge, this effect in whisky has not been quantified systematically in the scientific literature, but it is related to the miscible droplet dynamics discussed in Sec. IX.F.2.

Depending on the distillation method, spirits reach an initial strength of ∼70% ABV (pot still) or even higher (column still). Most whiskies are then diluted down to ∼60% ABV prior to storage in casks. After maturation, they are often mixed with more water to ∼40% ABV, the minimum in most countries. There are several reasons for this dilution: First, it can enhance the flavor because many of the taste-carrying molecules, such as guaiacol, are thermodynamically driven up to the liquid-air interface at low ethanol concentrations (Karlsson and Friedman, 2017). Second, the ethanol concentration influences the sensory perception (Velasco *et al.*, 2013; Harwood, Parker, and Drake, 2020), where lower strengths are more palatable for most consumers. Third, besides enhancing the flavor of spirits, dilution can lead to a better mouthfeel. At 20 °C, the viscosities of pure ethanol and water are $\mu_1 \approx 1.2$ mPa s and $\mu_2 \approx 1$ mPa s, respectively, but the viscosity of an ethanol-water mixture features a maximum of $\mu_{12} \approx 3$ mPa s at 40%–50% ABV (Dizechi and Marschall, 1982). This surprising nonlinear effect of binary mixture viscosities is described in more detail in Sec. IV.B.

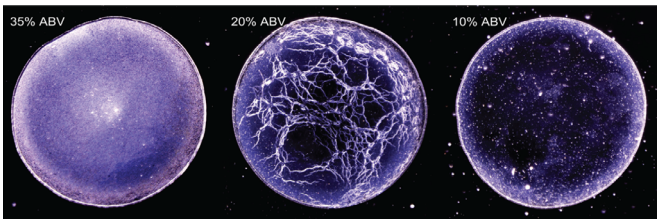

FIG. 8. Whiskey webs. Different patterns emerge after letting whiskey droplets of different alcohol percentages evaporate on a glass surface. At 35% ABV (left image), the deposits are evenly distributed, while at 10% ABV (right image), the deposits are distributed preferentially near the rim of the drop. At intermediate (20% ABV) concentration (middle image), the deposits form complex "whiskey web" patterns. From Williams, Brown, and Carrithers, 2019.

Diluting your drink can also help with distinguishing whether it is whisky or whiskey: An evaporating bourbon droplet of 40% ABV tends to leave a uniform surface deposition (Fig. 8), while a diluted droplet at 20% ABV leaves distinctive patterns called whiskey webs (Williams, Brown, and Carrithers, 2019; Carrithers *et al.*, 2020; Williams, 2021). Apparently, Scotch whisky and other distillates do not feature these web patterns and they are unique across different samples of American whiskey, so they could act like fingerprints. Indeed, the flavor profile results from the intricate chemical composition, which also affects the web patterns through the interplay of bulk chemistry with surfactants and polymers. Similarly, the webs do not form in droplets below 10% ABV, where instead the coffee-ring effect is observed; see Sec. VII.E. In general, this rich variety of surface depositions results from a combination of intrinsic (chemical composition) and extrinsic factors (temperature and humidity) that lead to an interplay of Marangoni flows and macromolecular surface adsorption. The nonuniform residues are often undesired in many industrial applications, including 3D printing, so whisky experiments could help us to understand and control uniform coatings (Kim *et al.*, 2016). Drying drop technologies may also be used for wine and hard alcohol quality control (Yakhno *et al.*, 2018).

D. Marangoni cocktails

Another well-known demonstration of the Marangoni effect is the "soap boat" (Keller, 1998; Wasin, 2017). These boats propel themselves in the kitchen sink by releasing surfactant molecules from the back: The surface tension of water is then higher at the front, so the boat is effectively pulled forward. The same effect is also used by water-walking insects as a quick escape mechanism (Bush and Hu, 2006). However, this propulsion is short-lived when soap is used as fuel in a closed geometry because the interface becomes saturated with surfactants. A prolonged motion can be achieved using other commonly available fuels (Renney, Brewer, and Mooibroek, 2013). Moreover, continuously moving boats can be made with camphor, a volatile surfactant that evaporates before the interface can saturate, allowing for persistent propulsion (Kohira *et al.*, 2001).

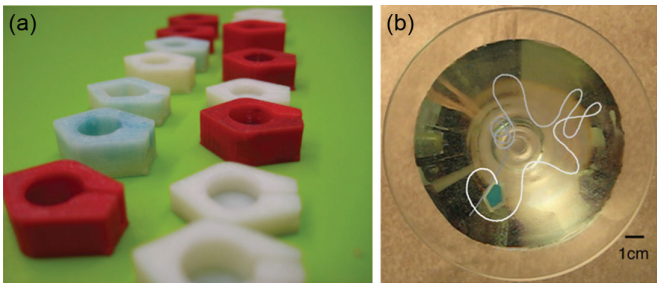

FIG. 9. Marangoni-stress powered cocktail boats. (a) Fleet of cocktail boats with different designs. The fuel (any liquor) is stored in the central cavity. The thin slit at the rear slowly releases the fuel into the glass, which establishes a surface tension gradient that drives the boat forward. (b) Trajectory in a cocktail glass. This boat is ∼1.5 cm long and fueled by Bacardi 151 (75% ABV). (a),(b) From Burton *et al.*, 2013.

This technology was extended to create alcohol-powered "cocktail boats" that move around in one's glass (Burton *et al.*, 2013; Burton, Cheng, and Bush, 2014). We depict them in Fig. 9. A typical commercial spirit can provide a surface tension difference up to $\Delta\gamma \sim 50$ mN/m compared to pure water, but sugar and other cocktail ingredients tend to somewhat reduce this value. By collaborating with chefs, various materials were tested to make the boats edible. Gelatin boats were found to be capable of sustained motion and suitable for a wide range of flavorings, but they are susceptible to dissolving and sticking to the glass walls. Wax boats performed the best, with speeds up to 11 cm/s and travel times up to 2 min, but they are not easily digestible (Schmidt-Nielsen and Randall, 1997). It would be interesting if future research could improve or discover new edible materials.

Marangoni propulsion lends itself not only to appetizing *divertissements*. The same mechanism can be used to create microscopic swimming droplets (Maass *et al.*, 2016), which can be used as cargo carriers that move deep inside complex flow networks (Jin *et al.*, 2021). Recently Dietrich *et al.* (2020) developed fast Marangoni surfers that can swim over 10 000 body lengths per second, and Timm *et al.* (2021) developed Marangoni surfers that can be remotely controlled. More generally, similar *phoretic* effects (Anderson, 1989), where interfacial flows are driven by gradients in concentration, electric fields, temperature, etc., can be exploited to make a broad range of self-propelled colloids that are of extraordinary interest to understand collective dynamics and emergent phenomena out of equilibrium (Howse *et al.*, 2007; Koch and Subramanian, 2011; Marchetti *et al.*, 2013; Cates and Tailleur, 2015; Elgeti, Winkler, and Gompper, 2015; Bechinger *et al.*, 2016; Zöttl and Stark, 2016). The same mechanisms are also at play in active emulsions (Weber *et al.*, 2019), the transport of molecules in biological systems (Anderson, 1986; Needleman and Dogic, 2017), and the fragmentation of binary mixtures into many small droplets, a process called Marangoni bursting (Keiser *et al.*, 2017).

E. Bubbly drinks

Go ahead and pour some nice sparkling wine into a glass, and observe the beautiful sight of rising bubbles and their effervescence [Fig. 10(a)]. Champagne and sparkling wines are supersaturated with dissolved CO_2 gas, which, along with ethanol, is a product of the wine fermentation process (Liger-Belair, Polidori, and Jeandet, 2008). When the bottle is uncorked, there is a continuous release of this dissolved CO_2 gas in the form of bubbles. Hence, this physicochemical system provides a great opportunity to study several fundamental fluid mechanics phenomena involving bubbles: their nucleation, rise, and bursting dynamics, which in turn affect the taste of carbonated drinks (Planinsic, 2004; Liger-Belair, Polidori, and Jeandet, 2008; Chandrashekar *et al.*, 2009; Polidori, Jeandet, and Liger-Belair, 2009; Zenit and Rodríguez-Rodríguez, 2018; Mathai, Lohse, and Sun, 2020; Rage *et al.*, 2020).

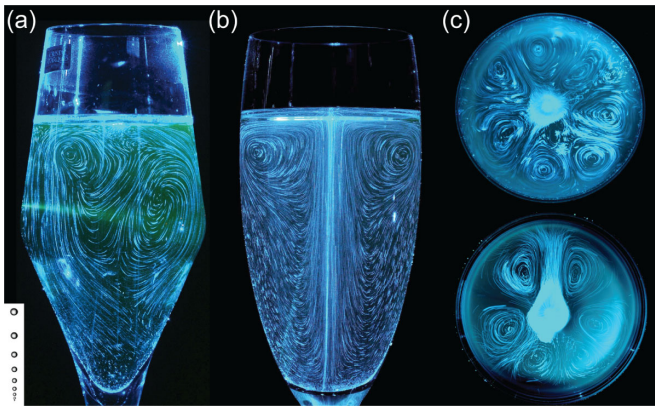

FIG. 10. Laser tomography of champagne glasses. (a) Natural, random effervescence in an untreated glass. Inset: growth of bubbles as they rise. (b) Stabilized eddies in a surface-treated glass. (a),(b) Courtesy of Gérard Liger-Belair. (c) Counterrotating convection cells self-organize at the air-champagne interface. From Beaumont, Liger-Belair, and Polidori, 2016.

Before savoring the wine or bubbles, you first need to open the bottle. We are all familiar with the curious "pop" sound, and the dangers of uncontrolled corks flying out. This uncorking process is also accompanied by the formation of a small fog cloud just above the bottle opening. It was recently shown that uncorking champagne creates supersonic CO_2 freezing jets (Liger-Belair, Cordier, and Georges, 2019). What is the underlying physical principle behind these interesting phenomena? It turns out that there is a sudden gas expansion when the bottle is uncorked (pressure drop from about 5 to 1 atm). This leads to a sudden drop in the temperature (about 90 °C), resulting in condensation of water vapor in the form of a fog cloud.

The uncorking also leads to a drop in the CO_2 partial pressure above the champagne surface. Hence, the dissolved CO_2 in the champagne is no longer in equilibrium with its partial pressure in the vapor phase. In fact, just after the uncorking it turns out that the champagne is supersaturated with CO_2. As Lubetkin and Blackwell (1988) described, this is quantified by the supersaturation ratio

$$S = (c_L/c_0) - 1, \tag{24}$$

where c_L is the CO_2 concentration in bulk liquid and c_0 is the equilibrium CO_2 concentration corresponding to a partial

pressure of CO_2 of 1 atm. Just after uncorking, $c_L/c_0 \approx 5$, so $S \approx 4$, and the champagne must degas in order to achieve stable thermodynamic equilibrium. The gas loss occurs through two mechanisms: by diffusion through the liquid surface (invisible to us) and by the vigorous bubbling (effervescence) that we can readily observe and also hear (Poujol *et al.*, 2021); see Sec. VIII.C.

How do these bubbles form in the first place? To answer this question, one should first look at the phase diagram of CO_2 and its solubility in water as a function of pressure and temperature (Bisweswar, Al-Hamairi, and Jin, 2020). Higher temperatures and lower pressures give a lower solubility, which encourages bubble formation. But these bubbles do not just pop out of nothing. The dissolved CO_2 molecules need to break free from the water molecules and cluster together. This bubble formation process is controlled by a nucleation energy barrier (Ford, 2004). As Jones, Evans, and Galvin (1999) described, the critical radius of curvature r^* that is necessary for gas pockets to overcome this barrier is

$$r^* \approx 2\gamma/p_{\mathrm{atm}}S, \tag{25}$$

where the surface tension of champagne is $\gamma \approx 50$ mN/m, the atmospheric pressure is $p_{\mathrm{atm}} \approx 10^5$ Pa, and $S \approx 4$ at the time of uncorking. Using these values, we find that this critical radius for bubble formation is $r^* \approx 0.25$ μm. Such large bubbles are not likely to form spontaneously. Indeed, instead of this homogeneous nucleation in the bulk of the liquid, bubble formation is more likely to occur at prenucleation sites on glass surfaces, typically at the bottom.

As such, the pleasing effervescence (bubbling) that we observe in champagne can arise from either natural or artificial sources (Liger-Belair, Polidori, and Jeandet, 2008; Polidori *et al.*, 2008), as shown in Figs. 10(a) and 10(b), respectively. On the one hand, natural effervescence refers to bubbling from a glass that has not received any specific surface treatment. The champagne contains hollow cylindrical cellulose fibers that naturally act as bubble nucleation sites. These fibers are approximately 100 μm long, and they contain trapped gas cavities (lumen) that are about 10 μm wide. Such hollow tubes are typically adsorbed on the walls of the champagne glass. Another source of natural effervescence are gas pockets trapped in tartrate crystals precipitated on the glass wall. Hence, natural effervescence can vary significantly depending on how the glasses are cleaned, dried, and stored. On the other hand, artificial effervescence refers to bubbling from a glass surface where precise imperfections have been engraved by the glass manufacturer. The typical imperfections introduced on the glass are microscale scratches to produce a specific pattern that give rise to bubbling phenomena that are markedly different from natural effervescence (Liger-Belair, Polidori, and Jeandet, 2008).

The bubble release mechanism from a fiber's lumen has been well studied (Liger-Belair, Polidori, and Jeandet, 2008). After a champagne bottle is uncorked, the supersaturation of carbon dioxide implies that such molecules will escape to the vapor phase using every available gas/liquid interface. The trapped small air pockets on fiber lumens offer gas/liquid interfaces to the dissolved carbon dioxide molecules, enabling them to cross the interface to gas pockets. The CO_2 gas pockets grow in size, and when a pocket reaches the fiber tip, it is ejected as a bubble. However, a portion of the gas pocket is left trapped behind in the lumen, and the bubble ejection cycle continues until the dissolved CO_2 supply is depleted. The detachment of bubbles from the nucleation site is analogous to a dripping faucet (Sec. II.E). The size of the bubble at the moment of detachment is approximately the radius of the mouth of the cellulose fiber ($R_0 \approx 10$ μm).

After the bubbles detach, they rise toward the liquid surface due to their buoyancy, and they also grow in size since they absorb more dissolved CO_2 molecules. The repetitive production of bubbles from the nucleation sites has been captured in a model by Liger-Belair *et al.* (2002), and it has been found that the bubble radius R increases linearly with time t as

$$R(t) = R_0 + kt, \tag{26}$$

where R_0 is the initial bubble radius and $k = dR/dt$ is the growth rate. Bubble rise experiments conducted with champagne and sparkling wines revealed k values around 400 μm/s and experiments in beer revealed growth rates of around 150 μm/s, indicating that the physicochemical properties of the liquids influenced the bubble growth rate (Liger-Belair *et al.*, 2002).

According to wine tasters, the smaller the better, which in this context means that small bubbles make a better wine. Hence, plenty of attention has been focused on modeling the average size of the rising bubbles [Fig. 10(a) inset], which is a result of their growth rate and velocity of ascent. As discussed in detail by Liger-Belair, Parmentier, and Jeandet (2006), the average bubble radius is

$$R \approx (2.7 \times 10^{-3})T^{5/9}\left(\frac{1}{\rho g}\right)^{2/9}\left(\frac{c_L - k_H p_{\mathrm{atm}}}{p_{\mathrm{atm}}}\right)^{1/3} h^{1/3}, \tag{27}$$

where T is the liquid temperature, ρ is the liquid density, g is gravity, Henry's law constant $k_H \approx 1.4$ kg/(m^{3}bar) for a typical champagne at room temperature, and h is the distance traveled by the bubble from the nucleation site. Note that so many factors can influence the average bubble size, which is typically in the submillimeter length scale in bubbly drinks. The bubble size in beer is significantly smaller than it is in champagne, and the reason for this is that the amount of dissolved CO_2 in champagne is about 2 times higher.

Bubble growth is beautifully visualized by the oscillating dynamics of a raisin in a glass of champagne, also known as the "fizz-ball" effect (Cordry, 1998; Moinester *et al.*, 2012). Initially the raisin sinks, but the textured surface of the raisin provides nucleation sites for bubbles to grow on the surface. As they grow larger, these attached bubbles pull up the raisin by buoyancy. However, when the raisin reaches the air interface, some of the bubbles pop, so the raisin sinks again. This cycle of rising and sinking continues for a long time, until the CO_2 is depleted. The fizz-ball effect can be observed in many carbonated drinks (beer, soda, etc.) and for many different objects (berries, seeds, chocolate chips, etc.).

In addition to the visual beauty and fascination, the bubbles actually play an important role in the drink: the bubbles have

been shown to generate large-scale time-varying convection currents and eddies inside the glass (Dijkstra, 1992; Liger-Belair, Polidori, and Jeandet, 2008; Beaumont, Liger-Belair, and Polidori, 2015, 2016, 2020), often with surprising self-organized flow patterns [Figs. 10(b) and 10(c)]. Since they cause a continuous mixing of the liquid, bubbles are thought to play a key role in the flavor and aromatic gas release from the wine-air interface. These release rates are dependent on the fluid velocity field close to the surface, which is in turn significantly influenced by the ascending bubbles. As the bubbles collapse at the air interface, they radiate a multitude of tiny droplets into aerosols (Liger-Belair *et al.*, 2009), which evaporate and release a distinct olfactory fingerprint (Ghabache *et al.*, 2016).

In the future, we can look forward to several innovations in bubbly drinks, where numerous factors must be taken into consideration: different types of glass shapes, natural versus artificial effervescence, engraving conditions, kinetics of flavor and CO_2 release under various conditions, and sensory analysis.

F. Foams

Bubbles (Sec. III.E) can burst when they reach the surface, but there is a finite lifetime associated with this process (Liger-Belair, Polidori, and Jeandet, 2008). Thus, when the bubble production rate is fast, greatly exceeding the surface bursting timescales, the bubbles start accumulating on the surface to create layers of bubbles called "foams" (Kraynik, 1988; Weaire and Hutzler, 2001; Weaire *et al.*, 2003; Cantat *et al.*, 2013). In many beers, these foams last for a long time since they tend to be stabilized by proteins. They add to the visual appeal and provide a creamy texture that enhances the mouthfeel (Fig. 11). However, in champagne the foam is more fragile and less stable due to the lack of proteins. Foams are formed in many other fizzy drinks and also in specially prepared coffees such as cappuccino, where the foam layer lasts for a long time since it is stabilized by milk proteins. These observations naturally bring up questions concerning the mechanisms behind the formation, stability, age and drainage of foams; we discuss these aspects in the review.

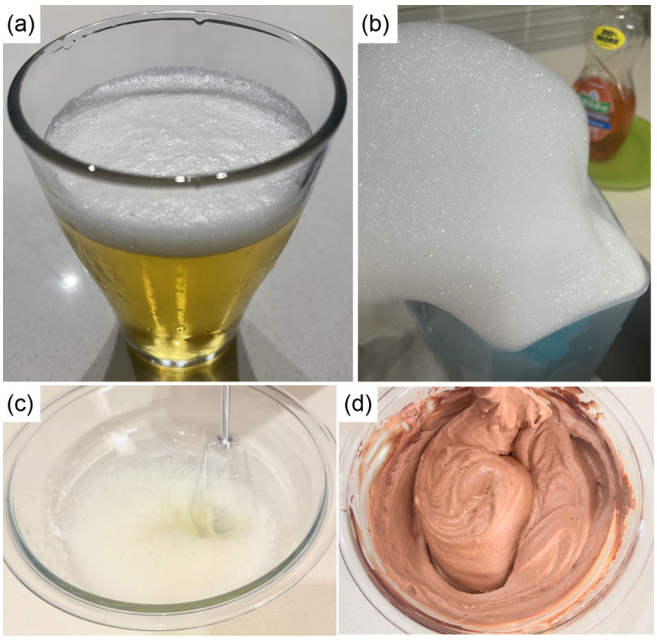

FIG. 11. Examples of foams in the kitchen. (a) Beer. (b) Dishwashing. (c) Egg beating. (d) Chocolate mousse.

A foam is essentially a dispersion of gas in liquid, and gas bubbles tightly occupy most of the volume. The liquid phase in the form of films and junctions is continuous, unlike the gas phase. Foams are also characterized by the presence of surface-active molecules called surfactants, which stabilize the bubbles at the interfaces of gas and liquid (Manikantan and Squires, 2020). The same type of molecule can also stabilize an oil/water interface in an emulsion (see Sec. IV.D) or on individual droplets (see Sec. IX.F). Foams consist of significant quantities of gas, hence being less dense than the liquid it contains, and this is why a foam floats on the surface of a liquid. Another interesting property of foam is the large surface area per unit volume, since the foam contains a large number of interfaces. Hence, foams enhance the possibilities for molecular transfer and find applications in foods for flavor enhancement (such as chocolate and spices) and also reduce the need for high sugar or salt content (Cantat *et al.*, 2013). Foams also have special mechanical properties: they exhibit both solidlike and liquidlike behavior (Janiaud and Graner, 2005). If the deformation is not too high, foams can show weak viscoelastic solid properties and can return to its original shape. However, if the foam is subjected to a high deformation, it can behave like a viscoplastic solid that can be sculpted. Foams can flow like liquids and seep through pores and cavities, so they can be poured into containers and tubes of various shapes. The foam's viscous resistance increases less quickly with flow rate compared to a normal fluid enabling it to reduce frictional losses. Moreover, most foams behave as "yield-stress fluids" (see Sec. IV.A) with intermittent flow via avalanchelike topological bubble rearrangements (Durian, 1995). Hence, given their unique properties, in addition to the food industry, foams find applications in many other areas of science and technology, including cosmetics (Durian, Weitz, and Pine, 1991), cleaning, reducing pollution, surface treatment, firefighting, and building materials (Cantat *et al.*, 2013). In food science, foams on beer, cream, and egg whites have been imaged and characterized using magnetic resonance imaging (MRI) to noninvasively estimate densities, drainage rates, and collapse throughout their structure (German and McCarthy, 1989).

We now examine the physical properties that allow a foam to exist in equilibrium. There are four relevant length scales to consider: (i) the meter scale, where the foam appears to be a soft and opaque solid, (ii) the millimeter scale, where individual bubbles can be distinguished in the foam, (iii) the micron scale, which reveals liquid distribution between bubbles, and (iv) the nanometer scale, where molecules (such as soap molecules) at the interfaces (including air/water interfaces) are relevant. The physics of foams is hence a broad subject covering so many length scales (Cantat *et al.*, 2013), and here we address only a few aspects.

At the scale of the gas/liquid interface, the surface tension (Sec. II.E) and the Young-Laplace law [Eq. (7)] determine the shape of the interface. An interface is flat if geometric constraints allow it, while the surface of an interface that is

completely surrounded by some fluid becomes spherical. The high pressure on the inside tries to curve the surface, while surface tension tries to flatten it.

Foams are prepared using additives that chemically consist of a polar head and a tail with a long carbon chain. The head is hydrophilic and the tail is hydrophobic; see Sec. II.F. The combination of these properties results in an amphiphilic molecule (both water loving and fat loving). Such a molecule, when dissolved in water, tends to adsorb at the air/water interface. This forms a monolayer, which greatly affects the interfacial surface tension properties. Hence, these molecules are called surface-active molecules or surfactants. In our everyday experience, there are several examples where we find many small bubbles that burst quickly (a few seconds), for instance, in sparkling wine or champagne. Here the small volume of gas in the bubble encloses a thin film that is unstable due to van der Waals forces, and hence breaks. However, the presence of surfactants such as soap molecules [Fig. 11(b)] carry a small charge, giving rise to an electrostatic repulsion, which cancels out the van der Waals forces and stabilizes the thin film, helping the foam last for a longer period.

A bubble is essentially a small volume of gas enclosed by a film of water. The bubble assumes the smallest possible surface area to contain the gas, which typically results in a spherical shape for an isolated bubble. The pressure inside most foam bubbles is only slightly greater than the atmospheric pressure and is not sufficient to compress the gas appreciably, so the volume of gas can be considered to be fixed. If the bubble has a large size, then the interface becomes deformed and is no longer spherical under external forces such as gravity (Prakash *et al.*, 2012). When two bubbles come into contact, they share an interface and hence change shape to reduce the total interfacial area and can no longer remain spherical.

Thus far we have mainly discussed foams in the context of air bubbles in liquid. However, edible foams (Briceño-Ahumada, Mikhailovskaya, and Staton, 2022) extend to soft solids or even hard solids, such as meringues, bread, and chocolate mousse [Figs. 11(c) and 11(d)]. They are a pleasure to eat because of their lightness and texture, which is determined by their complex mechanical properties (Kraynik *et al.*, 1999; Haedelt, Beckett, and Niranjan, 2007; Robin *et al.*, 2010; Cantat *et al.*, 2013; Janssen *et al.*, 2020). Edible foams are often prepared by solidification through refrigeration, cooking, or baking, such as bubbles in a pizza crust (Avallone *et al.*, 2022). Since these foams are solidified before their collapse, they often do not need a stabilizing agent. Another interesting point is that air is an important raw material in these edible foams: air contributes greatly to increasing the volume of the product, but it is practically free. On a final note, many other popular deserts are edible foams: these include favorites such as ice cream, marshmallows, many types of cakes, and baked Alaska.

We have mainly discussed foams that are stable for a finite duration of time. There are several interesting examples of dynamic and unstable foams; we show two popular examples in Fig. 12. We know in general that bubbles rise due to their buoyancy in a liquid, but in Guinness beer there is a collective downward movement of bubbles, creating a "cascade of bubble textures." It has been demonstrated that this bubble texture cascade motion [Fig. 12(a)] arises due to a roll-wave

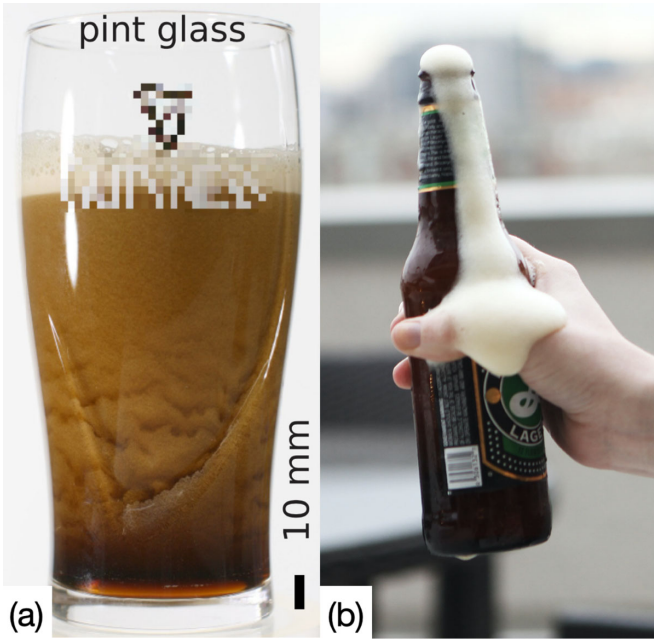

FIG. 12. Examples of dynamic and unstable foaming phenomena. (a) Unique foamy textures in stout with nitrogen bubbles. From Watamura *et al.*, 2021. (b) Foam overflow "volcano" due to tapping on a beer bottle. Public domain image.

instability of gravity currents (Watamura *et al.*, 2019), a phenomenon that is analogous to the roll-wave instability in liquid films that causes water films to slide downhill on rainy days (Sec. IX.E). Furthermore, it has been theoretically shown that these bubble cascades can occur in systems other than the Guinness beer (Watamura *et al.*, 2021).

Another interesting phenomenon is "beer tapping": a beer bottle foams up, resulting in an overflow when it is tapped from the top [Fig. 12(b)]. The fascinating fluid physics underlying this phenomenon was explained by Rodríguez-Rodríguez, Casado-Chacón, and Fuster (2014). It turns out that when the beer bottle is first hit at the top, a compression wave travels through the bottle. This wave gets rebounded through the liquid as an expansion wave. At the base of the bottle, the compression and expansion waves interact to cause "mother" bubbles to break up. This is a rapid cavitation process (see Sec. VIII.D) resulting in the formation of smaller "daughter" bubbles, which expand rapidly to create foam that starts to overflow (Rodríguez-Rodríguez, Casado-Chacón, and Fuster, 2014).

IV. SOUPS AND STARTERS: COMPLEX FLUIDS

Most foods are neither purely liquid nor purely solid, but rather something in between: they are called viscoelastic or complex materials. The fractalist Benoit Mandelbrot (1924–2010) once said,

> "A formula can be very simple, and create a universe of bottomless complexity."

Similarly, you can make excellent sauces following one simple recipe, where small variations in the ingredients can completely change the sauce flavor and consistency, because

changes in the molecular interactions lead to significantly different food properties. These complex properties strongly affect how we perceive taste since they are directly linked with mouthfeel, the oral processing and texture of foods (Sahin and Sumnu, 2006; Stokes, Boehm, and Baier, 2013). The rheology of complex fluids is also of extreme importance in the food industry because they affect transport phenomena, production processes, storage, and processing techniques that need to be adapted to the properties of materials at hand (Borwankar and Shoemaker, 1992; Brummer, 2006; Fischer and Windhab, 2011; Ahmed, Ptaszek, and Basu, 2016). Complex fluids are a rich and broad area, so we begin this section with an introduction to food rheology. We then get into the thick of it, reviewing the science of food suspensions, emulsions, and the mixing of sauces.

A. Food rheology

A large amount of syrup can be collected by pulling a knife vertically out of the jar. First, the syrup is lifted up by tangential forces, "dragging along" neighboring fluid layers. As the syrup slowly drips down, the stream is then stretched by tensile forces. Thus, a viscous fluid has two important properties: it resists both tangential and tensile stresses because of internal friction between the molecules. However, the same experiment done with oobleck (a solution of cornstarch in water) will show you an even richer phenomenology: Depending on the speed of lifting the knife, the solution flows easily, with difficulty, or even cracks like a solid. This is because the cornstarch solution has a complex internal microstructure that responds to external agitation with a certain delay. Viscosity alone is often not enough to determine the character of flow, but rather it is the interplay between the viscosity, elasticity, and inertia that gives rise to a wealth of different food properties.

To understand the rheology of the fluid is to know the stresses that arise in the effect of actuation, and vice versa. Consider a rheometer where a simple incompressible fluid is sheared between two parallel plates that translate in opposite directions. The fluid moves steadily along x, with a velocity $u_x(y)$ varying along y. The force (per unit area) required to shear the plates is then determined by the shear stress $\boldsymbol{\sigma}$. This tensor has only one component in our example (σ_{xy}), which is given by Newton's law of viscosity

$$\sigma_{xy} = \mu \frac{\partial u_x}{\partial y}, \tag{28}$$

where the constant of proportionality is the dynamic viscosity μ and the second term is called the shear rate $\dot{\gamma}$. Thus, a Newtonian fluid is defined by the linear relation between stress and shear rate. Most simple liquids are indeed Newtonian, including water, alcohol, and most thin oils. However, many kitchen fluids, such as milkshakes, emulsion dressings, and even chapati and bread dough, deviate from this linear relationship because of their complex internal structure. For example, Louhichi *et al.* (2022) studied dough by characterizing the linear and nonlinear viscoelastic properties of an aqueous gluten solutions. Such *non-Newtonian fluids* can feature many different types of behavior.

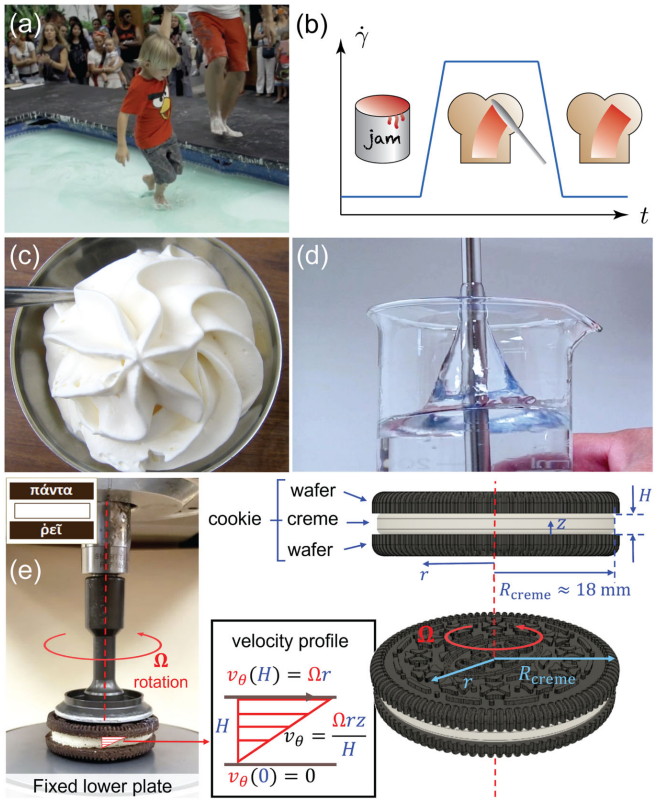

FIG. 13. Examples of complex rheological behavior of fluids. (a) People walking over a swimming pool full of oobleck, a mixture of cornstarch and water. From Ion Furjanic, We are KIX (2014). (b) Thixotropic fluids become thinner with time when they are sheared and solidify again at rest. Classic examples are paint and sandwich spread. (c) Whipped cream is an example of a Bingham plastic, which can be squeezed out like a fluid, but then turns solid in the absence of stresses. From Wikimedia Commons. (d) The Weissenberg rod climbing effect seen in a 2% solution of high molecular weight polyacrylamide. From Wikimedia Commons. (e) A sandwich cookie is mounted on a rheometer, where one wafer is rotated relative to the other. Hence, the properties of the creme between the wafers are measured. Courtesy of Crystal E. Owens.

In *shear-thickening* liquids, the viscosity increases with the shear rate. When agitated, they seem to harden and increase their resistance to motion. This is commonly seen in the previously mentioned oobleck and other starch solutions (Dintzis, 1996). In some cases, they can effectively behave as solids, as seen in the demonstrations of people walking on a swimming pool filled with an aqueous mixture of cornstarch [Fig. 13(a)]. However, if a person stops midway through the pool, they would start to sink, which demonstrates stress relaxation as the shear rate is reduced. But one needs to be careful because the material will solidify again when people try to resist the sinking. Fluids that gradually become more viscous with the duration of stress are called *rheopectic* fluids. A good example is the beating of egg whites, which slowly stiffen because the proteins unravel and form large networks. Rheopecty can also result from heat: think of pancake batter in a frying pan; see Sec. VI.D.

The contrary behavior is seen in shear-thinning fluids, whose viscosity decreases with increasing shear rate. Such

fluids appear less viscous when set in motion. Think of yogurt, mustard, clotted cream, or the well-known example of ketchup, reluctant to leave the bottle at first but spilling generously when shaken. Another example is paint, which should be easy to spread on a wall and stay there when the brush is removed. A particular subclass of shear-thinning substances is thixotropic fluids (Larson and Wei, 2019), which become less viscous over time when agitated, so their response is also time dependent. Thixotropy is often a consequence of their fibrous or polymeric internal composition. Ketchup and yogurt belong to this category, together with margarine and even honey at large strain (Munro, 1943). This quality is desirable in spreads and jams, which should be easy to spread on toast but stay solid once applied, as shown in Fig. 13(b). The shear rate is almost a step function in this case, and the viscosity of jam would show an inverted relationship, with decreased viscosity when it is spread at increased stress.

Some materials, called Bingham plastics or yield-stress materials, behave as solids at low stresses but start flowing above a critical stress. A prime example is our daily experience with toothpaste, which flows only when enough force is applied. Yield stress is also seen in numerous food products (Griebler and Rogers, 2022; Wilson and Strasser, 2022a, 2022b). Think about mayonnaise, where ridges and peaks on the surface show the existence of a critical stress above which it flows (Figoni and Shoemaker, 1983; Goshawk *et al.*, 1998; Balmforth, Frigaard, and Ovarlez, 2014). Similarly, Fig. 13(c) shows that cream, once whipped, can be squeezed out from a cone but will stay rigid on a piece of cake in the absence of forcing. Moreover, many emulsions (Sec. IV.D) and foams (Sec. III.F) behave as Bingham plastics because a certain minimal amount of force is required for the bubbles to rearrange within the material before it can flow.

In most non-Newtonian fluids subject to small or slowly varying deformations, it suffices to assume that stress and strain are linearly related, and a plethora of phenomenological models have been proposed to quantify this relationship. Many non-Newtonian fluids are called viscoelastic because they exhibit both viscous (creep) and elastic (relaxation) effects. In fact, they are something between fluids and elastic solids and can display either behavior, depending on the circumstances. To investigate them, two typical tests can be run (Borwankar and Shoemaker, 1992; Fischer and Windhab, 2011). The creep test consists of measuring a time-dependent strain upon the application of a steady stress. The material starts to flow with a certain delay, which is measured by this experiment. In the linear approximation, doubling the stress doubles the strain. This is widely observed in processed fruit tissues (Alzamora *et al.*, 2008) and in dynamic rheology measurements of honey (Yoo, 2004). A complementary experiment, the stress relaxation test, measures the time-dependent stress resulting from a steady strain. In the range of small deformations, many food products can be aptly described by linear models. Rheology measurements of frankfurters of various compositions show a good linear response for strains of up to about 3.8% (Skinner and Rao, 1986). Stress relaxation and creep recovery tests on oat grains also show linear behavior for a range of temperatures and moisture content (Zhao *et al.*, 2020). Linear models have been successfully used to describe stress relaxation behavior for a variety of semisolid food products, such as agar gel, meat, mozzarella cheese, ripened cheese, and white pan bread (Del Nobile *et al.*, 2007). Even systems with finer microstructure, such as protein-stabilized oil-in-water emulsions, can also exhibit linear viscoelastic behavior (Ruiz-Márquez *et al.*, 2013).

To assess whether the deformations are large or rapid enough for a fluid to exhibit linear response, we can compare the typical observation time (or the process under consideration) τ_0 to the typical stress relaxation time measured in the previously mentioned experiments to yield the dimensionless Deborah number

$$\mathrm{De} \equiv \frac{\text{timescale of relaxation}}{\text{timescale of process}} \sim \frac{\tau}{\tau_0}, \tag{29}$$

which indicates whether the material should behave like a fluid (at low De) or exhibit non-Newtonian properties, with an increasingly manifested elasticity at high De. For example, viscoelastic ice cream (Bolliger *et al.*, 2000) should preferably be consumed at high De for practical reasons; see Sec. VI.G.

However, some biological fluids are non-Newtonian at any De. Rheology measurements of yogurts show that overlapping polymer molecules cause viscoelastic behavior even at dilute concentrations, resulting in a sharp increase in viscosity with concentration (Benezech and Maingonnat, 1994). Yogurts are shear thinning in addition to being viscoelastic. Shear thinning or thickening cannot be explained using linear constitutive equations; thus, more complex models are needed to quantify their behavior. Non-Newtonian effects manifest themselves particularly in the material properties that become dynamic quantities and especially depend on the shear rate $\dot{\gamma}$.

The Weissenberg number is another dimensionless group that quantifies the ratio of elastic to viscous forces. For a fluid with a characteristic stress relaxation time λ under shear, we write this ratio as

$$\mathrm{Wi} \equiv \frac{\text{elastic forces}}{\text{viscous forces}} \sim \lambda\dot{\gamma}. \tag{30}$$

Although seemingly similar to De, the Weissenberg number has a different interpretation because it captures the degree of anisotropy introduced by the deformation, rather than the effect of time-dependent forcing (Poole, 2012). This is an intrinsic response of the fluid rather than the setup, whereas for the Deborah number the setup is more relevant. The two numbers span a phase space interpolating between purely viscous and purely elastic deformations, with linear (typically at moderate De and low Wi) and nonlinear viscoelasticity (at higher Wi) in between.

A first step into the nonlinear territory is the generalized Newtonian fluid model, in which the stress depends only on the instantaneous flow, but the viscosity in Eq. (28) is replaced by a shear-dependent function $\mu(\dot{\gamma})$. Its form is usually derived empirically from the available data. Some common approximations include a power-law fluid with $\mu(\dot{\gamma}) = k(\dot{\gamma})^{n-1}$, where k and n are the fitting parameters. If $n > 1$ the fluid is shear thickening (dilatant), and if $n < 1$ it is shear thinning. Most fruit and vegetable purees belong to the latter category and can be efficiently described by this model (Krokida,

Maroulis, and Saravacos, 2001). Another set of examples are Carreau-Yasuda-Cross models (Cross, 1965; Carreau, 1972; Yasuda, Armstrong, and Cohen, 1981), which interpolate between the different zero and infinite shear rate viscosities (μ_0 and μ_∞, respectively) by $\mu(\dot\gamma) = \mu_\infty + (\mu_0 - \mu_\infty) \times [1 + (\lambda\dot\gamma)^a]^{(n-1)/a}$, with additional fitting parameters λ, a, and n. Such models successfully describe the flow of skim milk concentrate (Karlsson *et al.*, 2005) and semisolid Spanish dairy desserts called natillas (Tárrega, Durán, and Costell, 2005). An important category is yield fluids, which flow only above some critical stress $\sigma > \sigma_c$. Within these, the Bingham models satisfy $\mu(\dot\gamma) = \mu_0 + \sigma_c/\dot\gamma$ (Bingham, 1922). This type of behavior is seen commonly in tahini, curry, and tomato pastes (Rao and Cooley, 1992). The Herschel-Bulkley models use $\mu(\dot\gamma) = k\dot\sigma^{n-1} + \sigma_c/\dot\gamma$ (Herschel and Bulkley, 1926) and have proven useful in aptly describing the rheology of stirred yogurts (Ramaswamy and Basak, 1991).

The truly nonlinear shear-dependent properties of kitchen matter can be seen in the context of mixing and whisking. The "Weissenberg effect" (Freeman and Weissenberg, 1948) is an illustrative proxy of viscoelasticity. As depicted in Fig. 13(d), it is seen when a spinning rod is inserted into an elastic fluid: Instead of the meniscus curving inward, the solution is attracted toward the rod and rises up its surface. This is due to normal stresses in the fluid acting as hoop stresses and pushing the fluid toward the rod (Muller, 1961). When egg whites are whisked with a mixer (Walker, 1978), we see the solution rise up close to the mixer shaft rather than move outward in a parabolic shape characteristic of Newtonian liquids, as described in Sec. II.I. Reiner, Scott Blair, and Hawley (1949) observed this effect in sweetened condensed milk after thickening, when it becomes a highly thixotropic gel; they linked it with the uncoiling of globular protein molecules during heat denaturation of the albumin-globulin fraction. Muller (1961) suggested that the extent to which cake batter exhibits the Weissenberg effect depends on its egg content and isolated the so-called thick white as the egg component that exhibits it most markedly. The rheology of the inside of an egg was also investigated by Bertho, Darbois Texier, and Pauchard (2022), who determined its shear-thinning properties and, motivated by the difficulty of distinguishing between raw and hard-boiled eggs, observed its residual rotation on a table to deduce its viscosity.

The viscosity may also change as a result of a change in the chemical composition under external stimuli, such as heat. This complex landscape is particularly important in the kitchen environment, where we often work with thickening agents such as roux or xanthan gum (also found in bubble gum), gently heat up egg yolks to make hollandaise sauce, or milk for the *béchamel*. For demonstration purposes in the home laboratory, Wiegand (1963) showed the transition from Newtonian to Weissenberg-like behavior of a gelatine solution when cooling down from 32 to 26 °C.

Composite food products typically respond in a non-Newtonian manner to deformation. Dynamic quantities that characterize the rheology of food products are of paramount importance in food processing, in which appropriate length and timescales should be chosen for the expected result. For example, pasta products such as curly spaghetti can be thought of as a hydrated gel (D'Angelo *et al.*, 2022). A chef can gauge pasta by its texture, but a rheological study of pasta cooking by Hwang *et al.* (2022) showed that an objective measure for spaghetti can be derived from its time-dependent length, and the measurement can be adjusted for other types of pasta. In a rheological study of lutefisk (Norwegian dry cod soaked in lye to rehydrate), Feneuil *et al.* (2022) measured the elastic modulus of the material to identify the key element of the preparation process that determines the mouthfeel. Working on plant-based meat surrogates, Ghebremedhin, Baechle, and Vilgis (2022) studied the structure and rheological properties of meat, vegetarian, and vegan sausages. Another subjective textural property of food products is spreadability, which can be effectively measured using the vane method (Daubert, Tkachuk, and Truong, 1998). In this method, a vane composed of four to eight blades is attached to the narrow shaft of a rheometer. This vane is then immersed and rotated through a sample, imitating a knife that spreads out a food product. Its spreadability is then related to the torque required for a given angular velocity.

Numerous articles have quantified the rheological response of food products: Nelson *et al.* (2018) measured the extensional yield stress of Nutella and showed that it can be modeled as a classical yield-stress fluid. However, other food products can have a more complex rheological signature: Martinetti *et al.* (2014) characterized a range of bubble and chewing gums under shear, finding that while in small-amplitude oscillatory shear and steady shear they behave like power-law critical gels in the linear regime, in start-up flows or large-amplitude oscillatory shear nonlinear viscoelastic effects were observed. They found, in particular, that extensional thickening, more pronounced in bubble gum than chewing gum, stabilizes film blowing, which is important for the ability to blow large bubbles, which are desired by consumers. Steady-shear measurements of the properties of various commercially available salad dressings by Elliott and Ganz (1977) showed that they can be described as modified Bingham bodies. On the other hand, the choice of a particular constitutive model depends on the physical situation: for example, the transient flow of mayonnaise in a coaxial viscometer is similar to that of polymer melts, and a similar mathematical description can be used (Campanella and Peleg, 1987). These are only a few examples of a wide current that aims to describe transient effects in the flow of food products (Kokini and Dickie, 1981).

Since the beginnings of rheologic characterization of materials, it has been tempting to answer the inverse question: Can we produce a material with the desired properties? Such questions have particular implications for cooking and food science. What properties do we need in terms of texture, ease of processing, and mouthfeel? What effect do we want the consumer to see or taste when they interact with it? And finally, once these qualities are identified, how can we get there from the basic microstructure or processing? The design of complex fluids has evolved into a prominent research field (Ewoldt and Saengow, 2022), with many open questions that can potentially be answered when physicists and cooks team up and interact.

We also note here that the kitchen might play an important educational role in the teaching of rheology. Hossain and Ewoldt (2022) recently proposed a do-it-yourself home

rheology course, where students were encouraged to select complex fluids and produce the desired flow types to infer their rheological properties, such as yield stress, extensional viscosity, and shear viscosity. Inspired by the similarity between a sandwich cookie, composed of two wafers separated by a cream filling, and a parallel plate rheometer, Owens *et al.* (2022) investigated "oreology" and the deformation of cream by torsional rotation and the subsequent separation of the cookie into two pieces, as shown in Fig. 13(e). They then presented a homemade rheometer (or "oreometer") that can be used for such measurements, thus providing a good example with an accessible home experiment.

Rheology is a vast field, discussed widely in classic textbooks, also in the context of the applicability and structure of different models (McCrum, Buckley, and Bucknall, 1988; Macosko, 1994). The rheological properties of food are also important for microbial motility in complex fluids (Spagnolie and Underhill, 2022) and for medical conditions including dysphagia (Nita *et al.*, 2013), where fluid dynamics can help predict the ease of swallowing (Marconati *et al.*, 2019). For a more detailed description of food rheology, see Bird, Armstrong, and Hassager (1987), Borwankar and Shoemaker (1992), Brummer (2006), Fischer and Windhab (2011), and Ahmed, Ptaszek, and Basu (2016), as well as the works on soft matter by Ubbink, Burbidge, and Mezzenga (2008), Piazza (2011), Vilgis (2015), Assenza and Mezzenga (2019), Pedersen and Vilgis (2019), and McLeish (2020), and references therein.

B. Mixing up a sauce

When we make a sauce rather counterintuitive effects can emerge: the combination of two thin liquids can suddenly lead to a thick mixture, or vice versa. Indeed, as discussed in Sec. III.C, an ethanol-water blend has a higher viscosity than both a pure liquid. In general, the viscosity μ_{12} of most binary mixtures is not a linear function of their relative composition (Bingham, 1914). Instead, a first approximation is given by the Arrhenius equation as

$$\ln \mu_{12} = x_1 \ln \mu_1 + x_2 \ln \mu_2, \tag{31}$$

where x_i and μ_i are the mole fraction and viscosity of the ith component, respectively. Equation (31) holds for an ideal binary mixture where the volume of the components is conserved, i.e., the excess volume of mixing is zero. Building on this work, a more accurate description was given by Grunberg and Nissan (1949) and Oswal and Desai (1998) and reads

$$\ln \mu_{12} = x_1 \ln \mu_1 + x_2 \ln \mu_2 + \epsilon x_1 x_2 + K_1 x_1 x_2 (x_1 - x_2) + K_2 x_1 x_2 (x_1 - x_2)^2, \tag{32}$$

where ϵ, K_1, and K_2 are empirical parameters that account for molecular interactions. While there is no universal theory that accurately predicts the viscosity of a liquid blend, more extended models have been derived that are important for many industrial applications, including food science (Zhmud, 2014; Schikarski, Peukert, and Avila, 2017).

In terms of mixing sauces, most ingredients have their own elastoviscoplastic properties. To describe the material properties of food mixtures, Nagasawa *et al.* (2019) considered a wide range of theoretical models and derived a viscosity blending model for shear-thinning fluids. Using rheometry experiments, they also tested these models with various sauces, including honey, mustard, mayonnaise, ketchup, hot chilli sauce, condensed milk, chocolate syrup, sweet bean sauce, oyster sauce, Japanese pork cutlet sauce, and barbecue sauce. When mixed together, unexpected behaviors can arise: The top row of Fig. 14 experimentally shows that pure honey flows down an inclined slope slowly because of its high viscosity (left image) and that pure mayonnaise remains stagnant because of its yield stress (right image) (Balmforth, Frigaard, and Ovarlez, 2014). However, a 50:50 mixture runs down the slope quickly, with a much lower viscosity μ_{12} than its constituents (middle image). In the bottom row, Balmforth, Frigaard, and Ovarlez (2014) accurately reproduced these surprising dynamics using numerical simulations combined with high-end computer-generated imagery (CGI) techniques.

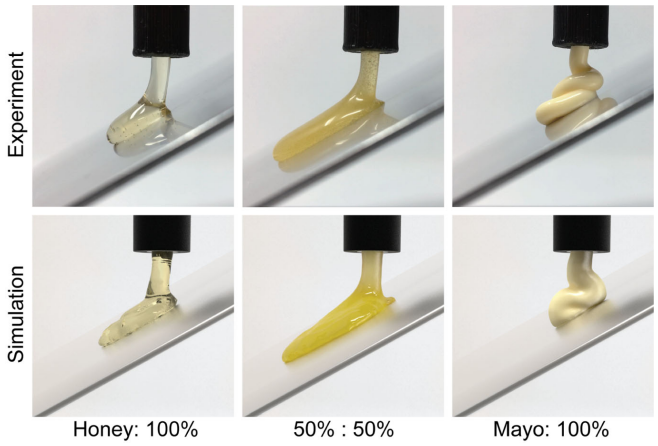

FIG. 14. Blending sauces. Left column: pure honey. Middle column: 50:50 mixture. Right column: pure mayonnaise. Top row: rheometry experiments of the sauces flowing down an inclined plane. While honey and mayo move slowly, the mixture runs down fast. Bottom row: the same dynamics simulated with a shear-thinning mixing model and displayed using CGI. Image courtesy of Yonghao Yue.

C. Suspensions

Drinks and foods often take the form of a particle suspension (Moelants *et al.*, 2014), with examples ranging from unfiltered coffee and wine to Turkish pepper paste and kimchi. The texture and mouthfeel of suspensions depend on their rheology (see Sec. IV.A), which is sensitive to the particle size, microstructure, and concentration. Dilute suspensions such as coffee and juices are typically Newtonian fluids, while concentrated suspensions such as pastes and purees typically display non-Newtonian behavior due to both long-ranged hydrodynamic interactions between the particles (see Sec. IV.A) and various short-ranged interactions including friction (Guazzelli and Morris, 2011; Zenit and Feng, 2018). Indeed, these rheological properties have been studied to optimize food paste 3D printing (Zhu *et al.*, 2019).

The influence of internal structure on macroscopic properties of suspensions has been actively investigated since the

birth of statistical physics. Einstein (1906) established that the viscosity of a dilute suspension increases by adding solute according to the Einstein viscosity

$$\mu = \mu_0(1 + \tfrac{5}{2}\phi), \tag{33}$$

where μ_0 is the dynamic viscosity of the solvent and ϕ is the volumetric concentration of particles. This relationship, which was later developed in the context of other transport coefficients, included the diffusion and sedimentation coefficients of suspended particles and accounted for higher volume fractions and different interactions between the particles (Guazzelli and Morris, 2011). This was reviewed in the context of food suspensions by Genovese, Lozano, and Rao (2007) and Moelants *et al.* (2014).

When we grind coffee beans or otherwise create a suspension, the particles are not all of the same size but instead follow a size distribution. The width of this size distribution is called the dispersity, and it can be tuned to control the rheology of a suspension. Notably the Farris effect (Farris, 1968) explains how the viscosity of a suspension decreases when the dispersity increases; that is, a broader distribution of particle sizes yields a lower viscosity than a narrow distribution of particle sizes. In food science, the Farris effect has been exploited to adjust the rheological properties of edible microgel suspensions such as cheese (Hahn *et al.*, 2015), and it has been used to minimize the apparent viscosity of cooked cassava pastes (Ojijo and Shimoni, 2008). Conversely, by narrowing the particle dispersity in coffee and unfiltered wine, it should be possible to enhance the mouthfeel by the opposite mechanism, but we are not aware of any reports on this topic. The Kaye effect is a phenomenon that occurs when a complex fluid is poured onto a flat surface, where a jet suddenly spouts upward (Kaye, 1963). Many non-Newtonian liquids including shampoo, feature this effect, and recent experiments have explained it using high-speed microscopy to show that the jet slips on a thin air layer (Versluis *et al.*, 2006; Lee *et al.*, 2013; King and Lind, 2019).

D. Emulsions

Food emulsions consist of oil drops dispersed in water (oil-in-water emulsion), or vice versa (water-in-oil emulsion), and are ubiquitous in gastronomy and food science (Dickinson, 2010; Berton-Carabin, Sagis, and Schroën, 2018) in everyday products such as cream, yogurt, mayonnaise, salad dressing, and sauces (McClements, 2015). Emulsions are easy to make, and even an amateur chef can make an emulsion in seconds by vividly shaking or stirring the oil and water phase, which efficiently breaks up the dispersed phase into droplets by a Rayleigh-Plateau instability; see Sec. II.G. But, as anyone who has tried to make a hollandaise sauce would painfully know, such colloidal systems are by design thermodynamically unstable and prone to phase separation, sometimes called a broken sauce.

In the food industry, phase separation is an even larger problem, as it can severely degrade the food product and shorten the shelf life, but fortunately stabilizers such as emulsifiers, texture modifiers, ripening inhibitors, and weighting agents can be added to keep the system in a metastable state (by creating a free energy barrier), efficiently extending the lifetime to hours, days, months, or even years (Friberg, Larsson, and Sjöblom, 2003). Protein molecules are particularly good stabilizers (Ferrari *et al.*, 2022). This is useful when making mayonnaise, where a full cup of oil is slowly added to an egg (or only the yolk) while stirring. The resulting emulsion is stabilized because the proteins reduce the interfacial tension, thereby reducing the capillary driving force for drop-drop coalescence, and by the formation of viscoelastic networks that act as physical barriers against coalescence (McClements, 2004; Tcholakova *et al.*, 2006). The stability of mayonnaise can be further increased by adding a teaspoon of mustard to the egg before adding the oil (Mayer and Krechetnikov, 2012). This is an example of a Pickering emulsion (Ramsden, 1904; Pickering, 1907), where nanoparticles coating the interface of the droplets prevent their coalescence. Pickering stabilization has promising applications in drug delivery and structured nanomaterials (Chevalier and Bolzinger, 2013; Zanini *et al.*, 2017), and also in food science. For example, Cuthill *et al.* (2021) used cocoa shells, which are a food grade industry coproduct, to produce colloidal lignin-rich extracts ready for use as Pickering-type stabilizers.

In addition to the stabilization, these surface proteins control the complex rheology of emulsions (Brummer, 2006), which is responsible for the appearance and our sensory perception of food products (Fischer and Windhab, 2011). Salad dressing is a widely studied kitchen emulsion that has been examined in the context of its complex rheological response (Barnes, 1994) and processing (Franco, Guerrero, and Gallegos, 1995), stability, and linear viscoelasticity (Franco, Berjano, and Gallegos, 1997). Owing to the large surface area of emulsion drops, the overall rheology and stability is controlled by interfacial properties and, in particular, by the surface coverage and structure of adsorbed protein layers (Fischer and Windhab, 2011). Animal proteins such as whey and casein readily form viscoelastic networks with high surface coverage, leading to emulsion stability, while plant-based proteins such as those from cereals and pulses are less efficient stabilizers, and this is due mainly to their poor solubility in the aqueous phase (Fischer, 2021). While heating can be used to increase the stabilizing abilities by denaturing the proteins (Amagliani and Schmitt, 2017), such treatment can degrade the taste as well as the texture and the nutritional value of plant-based foods. As such, the ability to control the interfacial properties of plant-based emulsions without denaturing the protein is an important goal, and an interesting new direction in food science for vegetarians and vegans (Liu *et al.*, 2021).

Emulsions are often used in food because of their creamy texture, where triborheology can be linked to mouthfeel (Mu *et al.*, 2022). As such, they even appear in forms that you may not expect. Espresso crema is an emulsion of coffee oil in water that floats on the coffee like a foam (Sec. VII.D), while *foie gras* and *pâté* are fatty liver-based emulsions (Via *et al.*, 2021). The process of converting separate fluids into an emulsion is called homogenization (Håkansson, 2019) and is industrially realized with high-energy mechanical methods, such as blenders and ultrasonics (Kentish *et al.*, 2008), where strong shear forces break the dispersed phase up into droplets. The degree of homogenization that translates to the distribution of sizes of constitutive droplets or suspended

particles affects the mouthfeel. For example, ice cream is a frozen emulsion made with water, milk fat, and air. Upon repeated heating and cooling when taking the box out from the refrigerator multiple times, the size of ice crystals within the mixture changes, giving a more gritty and crunchy texture while keeping the same chemical composition; see Sec. VI.G. Another example is rice flour batter, which was shown by Ichikawa *et al.* (2020) to change the bubble size distribution during whipping, with the potential aim of creating new textures for rice flour products. The manufacturing of an emulsion does not necessarily need mechanical processing. Another special type is spontaneous emulsification, as we discuss in Sec. IV.E.

E. Ouzo effect

Ouzo, raki, arak, pastis, and sambuca are popular aperitifs in Southern Europe. They are known for their anise aroma and the notable change in turbidity: Clear when pure, they turn milky white when clear water or ice is added, which has been called the ouzo effect (Vitale and Katz, 2003). The key to this puzzle lies in the chemical composition of the drink, a mixture mostly of water, alcohol, and essential oils, of which anethole is a prominent part. Anethole (also known as anise camphor) is highly soluble in ethanol but not in water (Ashurst, 2012), thus an undiluted spirit has a completely clear appearance. Upon the addition of small amounts of water, however, the oils start separating and create an emulsion of fine oil droplets that act as light scattering centers, resulting in the final cloudiness.

The ouzo effect, also called louching or the louche effect, can be regarded as spontaneous emulsification. Such emulsions are highly stable and require little mixing (Sitnikova *et al.*, 2005). In these multicomponent mixtures, the thermodynamic stability of the emulsion comes from the trapping between the binodal and spinodal curves in the phase diagram (Grillo, 2003; Ganachaud and Katz, 2005). The ouzo effect has been widely studied to elucidate its mechanisms (Vitale and Katz, 2003). However, the microscopic dynamics are still under active investigation. Small-angle neutron scattering studies in pastis (Grillo, 2003) and limoncello (Chiappisi and Grillo, 2018) measured the size of the demixing oil droplets to be on the order of a micron, a bit larger than the wavelength of visible light, giving rise to Mie scattering; see Sec. II.C. Sitnikova *et al.* (2005) established the mechanism for oil droplets growth to be Ostwald ripening without coalescence and observed the ripening rate to be lower at higher ethanol concentrations, with stable droplets reaching an average diameter of 3 μm. Lu *et al.* (2017) tried to disentangle the effects of concentration gradients from the extrinsic mixing dynamics by following the nanodroplet formation in a confined planar geometry and observed universal branch structures of the nucleating droplets under the external diffusive field, which is analogous to the ramification of stream networks on a large scale (Devauchelle *et al.*, 2012; Cohen *et al.*, 2015), and the enhanced local mobility of colloids driven by the emerging concentration gradient. The ouzo effect can be triggered not only by the addition of water but also by the evaporation of ethanol, as in sessile ouzo droplets (Tan *et al.*, 2016, 2017; Diddens *et al.*, 2017), leading to a rich drying dynamics involving multiple phase transitions.

The stability of the spontaneously formed emulsion gives hope for potential generation of surfactant-free microemulsions without the need to resort to mechanical stabilization, such as high-shear stabilization, which is often used in fat-filled milk formulations (O'Sullivan *et al.*, 2018). Thus, the ouzo effect has been used for the creation of a variety of pseudolatexes, silicone emulsions, and biodegradable polymeric capsules of nanometric size (Ganachaud and Katz, 2005). Nanoprecipitation can also be used for drug delivery and the design of nanocarriers (Lepeltier, Bourgaux, and Couvreur, 2014). Particles created using the ouzo effect are kinetically stabilized and provide an alternative to thermodynamically stabilized micelles formed when using surfactants (Almoustafa, Alshawsh, and Chik, 2017). Thus, this field offers many interesting directions of future research.

F. Cheerios effect

Thus far we have seen complex fluid effects in the bulk, but a similar complexity can arise at interfaces. Imagine sprinkling pepper on your soup. Small objects that are more dense than the fluid may still float at the air-fluid interface because of surface tension (Vella, 2015). Moreover, floating objects tend to aggregate at the surface, brought together by capillary forces induced by the presence of a curved meniscus around floating objects. Aptly named the Cheerios effect (Vella and Mahadevan, 2005), this is seen not only with cornflakes but also with bread crumbles (Singh and Joseph, 2005), foams, and generally objects that are large enough to create menisci of considerable size. The mechanism of lateral capillary interaction due to interfacial deformation admits a universal theoretical description for particle sizes ranging from nanometers to centimeters (Kralchevsky and Nagayama, 2000). Initially, the interaction of widely spaced particles may be regarded as a two-body problem (Paunov *et al.*, 1993), but multiparticle rafts are eventually formed (Lagarde, Josserand, and Protière, 2019). The dynamics of these aggregates are more complex since they may undergo internal redistribution and destabilization (Abkarian *et al.*, 2013). An interesting example is an active assembly of dozens of fire ants on a water surface (Mlot, Tovey, and Hu, 2011). The presence of surface tension allows one to sustain deformed surfaces that can support a load of an insect walking on water (Gao and Jiang, 2004; Bush and Hu, 2006; Childress, 2010) or a biomimetic water-walking device (Hu *et al.*, 2007). Similar behavior, called the inverted Cheerios effect, is seen when water droplets sit on a soft, deformable substrate, and the induced deformation drives their assembly (Karpitschka *et al.*, 2016; Pandey *et al.*, 2017).

By a combination of capillary forces and externally controlled fields, for instance, electromagnetic fields, both static and dynamic assemblies can be achieved in capillary disks (Wang *et al.*, 2017; Koens *et al.*, 2019). Capillary forces between spherical particles floating at a liquid-liquid interface have also been quantified to show a qualitatively similar behavior (Vassileva *et al.*, 2005). The same guiding principles are used at microscale for colloidal self-assembly, driven not by gravity but by an anisotropically curved interface (Ershov *et al.*, 2013). Finally, in active microrheology (MacKintosh and Schmidt, 1999; Mizuno *et al.*, 2008;

Squires and Mason, 2010; Furst and Squires, 2017; Zia, 2018), an external force field (usually magnetic or optical) is used to distort surface-active or bulk probes in order to extract viscoelastic responses of complex materials, with direct applications in food science (Yang *et al.*, 2017).

A separate class of interfacial interaction involves the dynamic problem of stone skipping, known in Britain as "ducks and drakes," where the interfacial properties determine the optimal angle of attack for the most successful rebound, and therefore maximal range (Clanet, Hersen, and Bocquet, 2004; Lorenz, 2006; Hewitt, Balmforth, and McElwaine, 2011). Moreover, elastic "stones" have been shown to demonstrate superior skipping ability by assuming hydrodynamically optimal shapes during the collision (Belden *et al.*, 2016). Although seemingly unrelated, the dynamics of interfacial deformation by contact with a boundary might be important in the development of ergonomic kitchen utensils such as spatulas and scrapers, optimal coatings for baking surfaces (Magens *et al.*, 2017), and dealing with food adhesion in industrial processing (Frabetti *et al.*, 2021), and may also inspire novel approaches to these procedures.

V. HOT MAIN COURSES: THERMAL EFFECTS

The word *cooking* refers to the preparation of food in general, but specifically to the operations involving temperature and heat such as boiling, frying, baking, and poaching, to transform food products into a final dish. Thus, many kitchen flows are subject to thermal effects that alter their taste, texture, and mouthfeel. Here we discuss such culinary processes involving heat transfer, the Leidenfrost effect, temperature-driven flows, the physics of seared steaks, and even hot vapors, smoke, and fire. Nothing beats a warm meal, but be careful not to get burned. In the words of William Shakespeare (c. 1564–1616),

> "Heat not a furnace for your foe so hot, that it do singe yourself."

A. Feel the heat: Energy transfer

Heat is transported in fluids in a manner similar to momentum (Sec. II.B). Fluid parcels are advected with the flow, and additionally exchange heat by conduction. Local variations in temperature can additionally induce density gradients, which can drive macroscale convective motion.

The relevant quantity characterizing the thermal properties of the fluid is the scalar temperature field $T(\boldsymbol{r}, t)$. The spread of temperature is described by the heat equation, which for a fluid of density ρ and heat capacity at constant pressure c_p can be written as

$$\rho c_p \frac{DT}{Dt} = k\boldsymbol{\nabla}^2 T + h + Q, \tag{34}$$

where k is the thermal conductivity, governing the diffusive spread of temperature by thermal conduction, h is a source term accounting for local heating (as by chemical or nuclear reactions), and Q is the viscous dissipation term, which can be neglected in most practical situations. In the absence of local heat sources, the heat equation simply becomes a Fourier diffusion equation with the thermal diffusivity $D_T = k/\rho c_p$. The dominant heat transport mechanism is determined by the thermal Péclet number

$$\mathrm{Pe}_{(T)} \equiv \frac{\text{diffusion time}}{\text{convection time}} \sim \frac{L_0 U_0}{D_{(T)}}, \tag{35}$$

which besides thermal diffusion can equally be used to characterize molecular diffusive transport.

The concept of heat diffusion suffices to explain several kitchen processes. Baking a cake requires the heat to reach the inner parts of the dough, but changing either the dimensions of the cake or the amount of batter used alters the baking time in a way that can indeed be predicted from the diffusion equation (Olszewski, 2006). Heat flow considerations can guide the development of an optimal flipping schedule when frying hamburgers (Thiffeault, 2022). And the problem of perfectly boiling an egg can also be quantified in terms of the energy equation (Roura, Fort, and Saurina, 2000) to aid many breakfast table discussions.

B. Levitating drops: The Leidenfrost effect

The Maillard reaction (Brenner, Sörensen, and Weitz, 2020) is what gives browned food its nutty, delicious flavor and is known for turning uncooked, raw meat into tender, tasty steaks or sausages (Ghebremedhin, Baechle, and Vilgis, 2022). When grilling steaks, a simple way to assess whether the frying pan is sufficiently hot is to sprinkle a handful of water droplets onto it. When the surface temperature slightly exceeds the water boiling point, the droplets start vigorously evaporating, producing a sizzling sound. However, if the pan is left on full heat for a while and becomes considerably hotter, small droplets change their behavior completely and start levitating above the hot surface without boiling [Figs. 15(a) and 15(b)]. This levitation can help prevent the meat from sticking (Herwig, 2018).

This phenomenon is known to have been observed by a Dutch scientist H. Boerhaave in 1732 and was later described in detail by German doctor Johan Gottlob Leidenfrost in 1756. He provided a record of water poured onto a heated spoon that "does not adhere to the spoon, as water is accustomed to do, when touching colder iron" (Leidenfrost, 1756). The Leidenfrost effect, as it was later called, has been studied extensively in the scientific context (Curzon, 1978; Thimbleby, 1989; Quéré, 2013), and even became a plot device in Jules Verne's novel Michel Strogoff in 1876.

The explanation of this effect boils down to the analysis of heat transfer rate between a hot plate and a droplet. For intermediate excess temperatures above the boiling temperature (between 1 and approximately 100 °C), the droplets undergo either nucleate boiling, with vapor bubbles forming inside, or transition boiling, when they sizzle explosively upon impact on the plate. However, above the Leidenfrost temperature, which for water on a metal plate is approximately 150–180 °C, the heat transfer dynamics change when a thin vapor layer is created between the droplet and the plate. This thin cushion both insulates the droplet and prevents it from touching the substrate, which would cause nucleate boiling

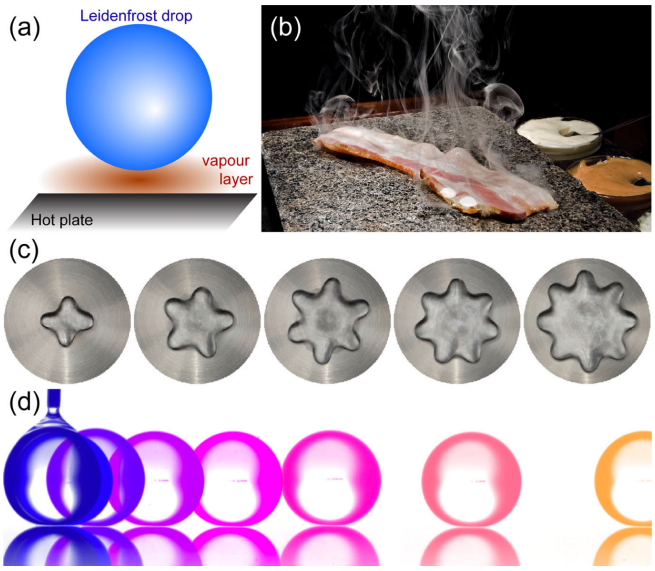

FIG. 15. Leidenfrost effect. (a) Diagram of a droplet levitating on a cushion of evaporated vapor above a heated surface. (b) The Leidenfrost effect prevents meat from sticking to a hot plate. Courtesy of Pedro Moura Pinheiro. (c) Star-shaped oscillations of Leidenfrost drops (Ma, Liétor-Santos, and Burton, 2017) that make characteristic sounds. Top view. From Singla and Rivera, 2020. (d) Time-lapse image of a self-propelled Leidenfrost drop on a reflective wafer heated at 300 °C. Side view. From Bouillant, Mouterde, Bourrianne, Clanet, and Quéré, 2018.

inside the droplet [Fig. 15(a)]. Owing to the competition between evaporation and film draining, the typical thickness of the insulating layer is about 100 μm. Because of this effect, the lifetime of droplets on a substrate can increase by an order of magnitude (Biance, Clanet, and Quéré, 2003). A further increase in the substrate temperature naturally decreases the lifetime, but the decrease is slow. The minimum temperature required for the Leidenfrost effect to occur on smooth surfaces was recently characterized by Harvey, Harper, and Burton (2021).

The presence of a thin lubricating vapor layer, which is characterized by a low Reynolds number (Sec. VI.A), prevents meat from sticking to a hot plate [Fig. 15(b)]. It makes water droplets highly mobile due to the diminished friction [Fig. 15(d)]. As soon as a spontaneous instability causes a slight difference in the thickness of the vapor layer, a flow emerges that triggers self-propulsion by rolling motion (Bouillant, Mouterde, Bourrianne, Lagarde *et al.*, 2018; Leon and Varanasi, 2021). The interaction with a structured substrate can also be used to induce directed motion, for example, across ratcheted grooves (Linke *et al.*, 2006; Würger, 2011; Jia, Chen, and Zhu, 2017), and the motion may be further controlled with thermal gradients (Sobac *et al.*, 2017). A video featured on BBC Earth shows how the Leidenfrost effect can be used to make water run uphill (BBC Earth Unplugged, 2013). Besides self-propulsion, the energy injected by droplet heating can cause droplet vibration with star-shaped droplet modes (Ma, Liétor-Santos, and Burton, 2017) that lead to distinct Leidenfrost sounds (Singla and Rivera, 2020) [Fig. 15(c)].

The Leidenfrost phenomenon is seen all across the temperature scale and is controlled mainly by the temperature difference between the substrate and the droplet and the surface roughness. The substrate need not be solid: a similar effect is observed with acetone droplets (nail polish remover) on a bath of hot water (Janssens, Koizumi, and Fried, 2017). More generally, the Leidenfrost state, in which an object hovers on a solid or on a liquid due to the presence of a vapor layer, can be seen in a variety of contexts. For example, it occurs when a block of sublimating solid carbon dioxide (dry ice) is placed on a plate at room temperature (Lagubeau *et al.*, 2011), which is also called the inverse Leidenfrost effect (Hall *et al.*, 1969), or when room temperature ethanol droplet falls on a bath of liquid nitrogen (Gauthier *et al.*, 2019) and starts moving. Furthermore, when two water droplets are placed on a hot plate, the vapor layer between them prevents their coalescence, which is called the triple Leidenfrost effect (Pacheco-Vázquez *et al.*, 2021). Frequently demonstrated in popular lectures and science fairs, the Leidenfrost effect allows a person to quickly dip a wet finger in molten lead or blow out a mouthful of liquid nitrogen without injury (Walker, 2010).

C. Heating and boiling: Rayleigh-Bénard convection

We now cook some pasta (Audoly and Neukirch, 2005; Heisser *et al.*, 2018; Tao *et al.*, 2021; Hwang *et al.*, 2022). We place a pot with water on the stove and start heating. Heat from the stove is transferred to the water, first through conduction and then through natural convection (Batchelor, 1954), which we see as characteristic structures called plumes near the bottom wall [Figs. 16(a) and 16(b)]. The fluid layer adjacent to the heated surface becomes unstable and starts to rise [Figs. 16(c) and 16(d)] since it is lighter than the bulk fluid; see also Sec. III.A. This fundamental process has been widely studied in many different configurations. One of the most well studied is the Rayleigh-Bénard convection (RBC) system, consisting of a fluid layer bound between two horizontal plates, heated from below and cooled from above, as reviewed by Kadanoff (2001), Ahlers, Grossmann, and Lohse (2009), and Lohse and Xia (2010). This occurs ubiquitously in natural contexts, including astrophysics (Moore and Weiss, 1973; Cattaneo, Emonet, and Weiss, 2003) and geophysics (Mckenzie, Roberts, and Weiss, 1974; Prakash, Sreenivas, and Arakeri, 2017), and in engineering applications such as metallurgy, chemical engineering, and nuclear engineering (Brent, Voller, and Reid, 1988; Zhong, Patterson, and Wettlaufer, 2010).

The key nondimensional parameters governing natural convection is the Rayleigh number

$$\mathrm{Ra} \equiv \frac{\text{heat diffusion time}}{\text{heat convection time}} \sim \frac{g\beta_T \Delta T H^3}{\nu D_T}, \tag{36}$$

and the Prandtl number

$$\mathrm{Pr} \equiv \frac{\text{momentum diffusivity}}{\text{thermal diffusivity}} \sim \frac{\nu}{D_T}, \tag{37}$$

where g is gravity, β_T is the coefficient of thermal expansion, ΔT is the temperature difference between the walls, H is the height of the fluid layer, ν is the kinematic viscosity of the

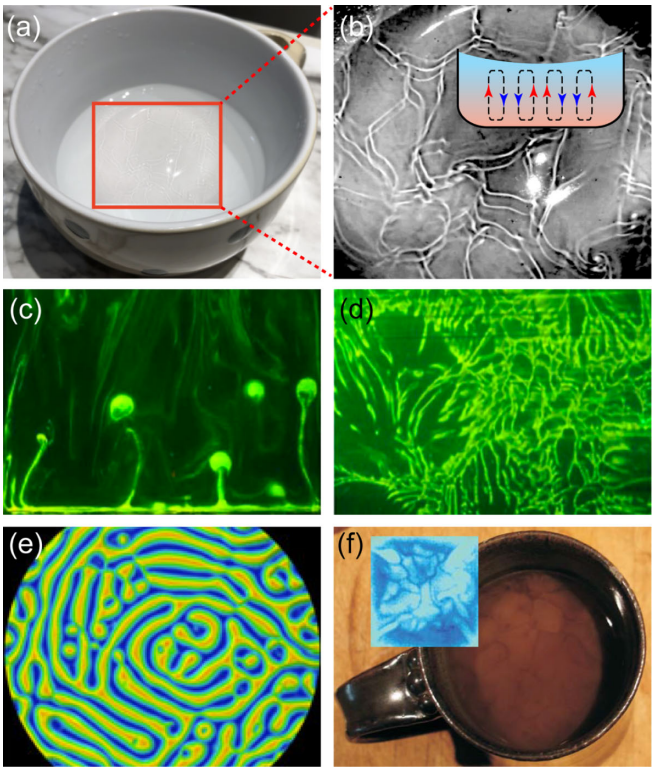

FIG. 16. Rayleigh-Bénard convection. (a) Rising plumes in a pot of water heated from below, visible because the refractive index changes with temperature differences. (b) Contrast-enhanced magnification. (c) Side view of mushroomlike plumes in a high-viscosity fluid. The green line at the bottom is the boundary layer. (d) Top view of dendritic line plumes. (c), (d) From Prakash, Sreenivas, and Arakeri, 2017. (e) Temperature field in a simulation of Rayleigh-Bénard convection at Ra = 5000 and Pr = 0.7. From Emran and Schumacher, 2015. (f) Vortex structures in a coffee cup with milk at the bottom, which gets displaced by cold plumes that sink down from the evaporating interface. Inset: IR thermograph showing convection cells of colder (downwelling) and warmer (upwelling) regions. From Wettlaufer, 2011.

fluid, and D_T is the thermal diffusivity of the fluid. Note that the Prandtl number depends only on the inherent properties of the liquid. Most oils have $\mathrm{Pr} \gg 1$, which means that heat diffuses slowly in oils. Depending on the magnitude of Ra, we can then identify different regimes of natural convection. The heat transfer through the fluid is solely through conduction until a critical $\mathrm{Ra}_{cr} \sim 1708$ (Krishnamurti, 1970a, 1970b), above which the convection consists of steady "laminar" rolls [Fig. 16(e)]. At $\mathrm{Ra} \sim 10^4$, these convection rolls become unsteady, and beyond $\mathrm{Ra} \sim 10^5$ the convection is characterized as turbulent natural convection. An example of this is seen when milk is poured into coffee [Fig. 16(f)]. Another important manifestation of thermally driven flows is found in deep-fat fryers, where plumes transport oxygen from the air interface into the hot oil, leading to reactive hydroperoxides and toxic compounds (Touffet *et al.*, 2021).

Now we come back to our water pot. As we continue to supply heat, the temperature will eventually reach the boiling point of water. At this point, the boiling process begins with vapor bubbles forming in a superheated layer adjacent to the heated surface (Dhir, 1998). In this two-phase system, the vapor bubbles enhance the convective heat transfer in the standard RBC system (Lakkaraju *et al.*, 2013). This boiling process is so complicated that we currently have only an empirical understanding of it (Dhir, 1998), and theoretical progress has been lacking. However, cutting-edge numerical simulations seem to be a promising direction to accurately model these processes (Dhir, 2006). We put the pasta into boiling water and allow it to cook for approximately 10 min [or until it extends to a desired length, as discussed by Hwang *et al.* (2022) and in Sec. IV.A]. Once the pasta is cooked, we drain the excess water and serve with a sauce; see Sec. IV.B.

D. Layered latte: Double-diffusive convection

In Sec. V.C we discussed Rayleigh-Bénard convection, which occurs because the fluid density depends on temperature. Often the density also depends on a second scalar like the salt or sugar concentration. Their molecular diffusivity D_S is smaller than the thermal diffusivity D_T, so heat is transported faster than mass. This explains why your tea cools down before the sugar diffuses up, but it can also lead to double-diffusive convection (DDC), which can cause a range of unexpected phenomena, as reviewed by Huppert and Turner (1981), and more recently by Radko (2013) and Garaud (2018). Besides the Rayleigh and Prandtl numbers [Eqs. (36) and (37)], DDC also depends on the Schmidt number, which is often used to characterize convective flows involving simultaneous momentum and mass diffusion processes,

$$\mathrm{Sc} \equiv \frac{\text{momentum diffusivity}}{\text{molecular diffusivity}} \sim \frac{\nu}{D_S}. \tag{38}$$

One surprising DDC phenomenon that is readily observed in the kitchen (Heavers and Colucci, 2009) is called salt fingering, which happens when warmer, saltier water rests on colder, fresher water of a higher density (Yang, Verzicco, and Lohse, 2016). Therefore, in the words of Stern (1960), "[the] 'gravitationally stable' stratification … is actually unstable." If a parcel of warm, salty water is perturbed to move down a bit, it loses its heat quicker than its salinity, so it will keep sinking further. Hence, salt fingers (vertical convection cells) spontaneously start growing downward, accelerated by thermal diffusion, which gives rise to strong mixing. Kerr (2002) joked that one might have a Martini cocktail "fingered, not stirred," which could in fact be quite a spectacle with colored layers [Fig. 17(a)]. This mixing effect is likely important for nutrient transport in the ocean and climate change (Johnson and Kearney, 2009; Fernández-Castro *et al.*, 2015). In astronomy, thermohaline mixing can occur in evolved low-mass stars (Cantiello and Langer, 2010). DDC can equally figure in porous media (Griffiths, 1981), which might be relevant for heat and mass transfer in porous materials under microwave heating (Dinčov, Parrott, and Pericleous, 2004).

Another striking example of DDC is the formation of distinct layers in a caffè latte (Xue *et al.*, 2017) [Fig. 17(b)]. To make one, warm a tall glass with 150 ml of milk up to 50 °C, and pour 30 ml of espresso at 50 °C into it. The milk is denser than espresso, so the dynamics will follow an inverted fountain effect (Sec. III.A), leading to stratification with a

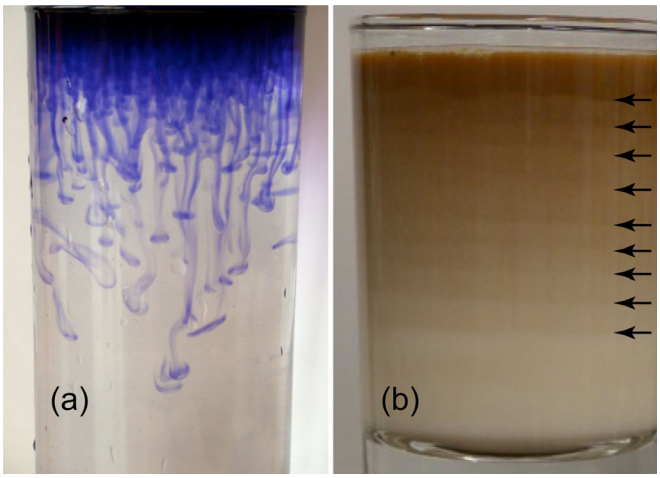

FIG. 17. Double-diffusive convection phenomena. (a) Cocktail with blue salt fingers, produced by warmer salty water resting on colder fresh water of a higher density. Courtesy of Matteo Cantiello (Flatiron Institute). (b) Layered caffè latte. Black arrows were added to highlight the layer boundaries. Adapted from Xue *et al.*, 2017.

vertical density gradient. Subsequently, a horizontal temperature gradient is established because the glass slowly cools down from the sides. This double gradient leads to stacked convection rolls separated by sharp interfaces, as seen in creaming emulsions (Mueth *et al.*, 1996). The coffee pouring (injection) velocity sets the initial density gradient, and thus the Rayleigh number, which much exceed a critical value for layers to form (Xue *et al.*, 2017). This was further investigated with direct numerical simulations by Chong *et al.* (2020), who also discussed the mechanism regulating how the layers merge over time: they found that as the circulation weakens, hot fluid accumulates by the hot sidewall, where buoyancy forces, larger for hotter fluid, eventually break the layer interface. The two layers merge, and a new circulation pattern is established within the thicker new layer. Besides *café au lait*, similar stacked layers are observed in the ocean, meters thick and kilometers wide, called thermohaline staircases (Tait and Howe, 1971; Yang, Chen *et al.*, 2020).

E. Tenderloin: Moisture migration

Thus far we have described various fluid mechanical phenomena related to drinks or liquids. When cooking solid foods, it is also important to understand moisture migration to achieve a tender result (Hwang *et al.*, 2022). We consider here the example of meat cooking (of tenderloin, for instance), where two important physical aspects include time-dependent protein denaturation and cooking loss (water loss). To reach the desired meat textures, the meat must be cooked at well-defined temperatures to ensure selective protein denaturation (Zielbauer *et al.*, 2016). Since our focus here is on fluid dynamics, we discuss water loss during the heat treatments, which also depends on the temperature (Zielbauer *et al.*, 2016). This cooking loss has been described using the Flory-Rehner theory of rubber elasticity (Vilgis, 1988; Van der Sman, 2007). This theory models the transport of liquid moisture due to denaturation and shrinkage when the protein is heated. The moisture transport is due to a shrinking protein matrix similar to a "self-squeezing sponge." It is assumed that the poroelastic theory applies here. Thus, this theory describes moisture transport by Darcy's law (see Sec. VII.D), where the fluid flow rate is linear with the pressure gradient. The pressure is due to the elasticity of the solid matrix of the porous material, and here it is referred to as the swelling pressure p_{swell}. According to Flory-Rehner theory, the swelling pressure can be decomposed into the following two components:

$$p_{\mathrm{swell}} = p_{\mathrm{mix}} + p_{\mathrm{el}}, \tag{39}$$

where p_{mix} is the mixing or osmotic pressure and p_{el} is the pressure due to elastic deformation of the cross-linked polymer gel (Vilgis, 2000). In equilibrium, the network pressure opposes the osmotic pressure and the swelling pressure is zero. The temperature rise during cooking causes an imbalance between the osmotic pressure and network pressure, leading to the expelling of excess fluid from the meat. Hence, the swelling pressure in meat is proportional to the difference between moisture content and water holding capacity. The gradient of this swelling pressure will drive the liquid moisture flow and is used in Darcy's law [Eq. (54)]. This model has been found to agree well with experimental data, proving that the Flory-Rehner theory provides a sound physical basis for the moisture migration in cooking meat (Van der Sman, 2007).

F. Flames, vapors, fire, and smoke

Next we consider the flows generated around the hot cookware, utensils, or hot beverages. There are various heat transfer processes in the kitchen that can give rise to vapors, fumes, fires, and smoke. We enjoy the aroma of a good dish that is cooking, and unexpected smoke is often an indicator that something is burning. Hence, in addition to increasing the overall room temperature, the vapors also play an important role in providing positive or negative feedback on how the cooking is going. Hot utensils transfer heat into the surrounding air setting up buoyancy-driven convection or natural convective flows around them. Figure 18 shows the flow of

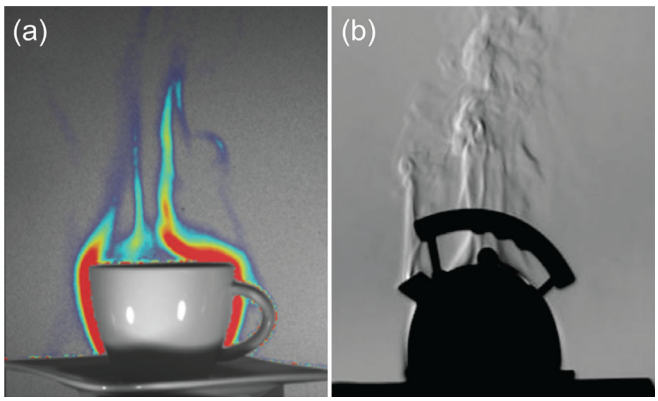

FIG. 18. Buoyancy-driven plumes. (a) Flows developing over an espresso cup visualized with schlieren imaging. The largest amount of fluid displacement is observed on the sides and above the cup. From Cai *et al.* (2021). (b) Plume around a hot teakettle captured with schlieren imaging. From Settles and Hargather, 2017.

vapors and convection around a hot espresso cup (Cai *et al.*, 2021) and around a hot teakettle, visualized with schlieren imaging, as reviewed by Settles (2001) and Settles and Hargather (2017). Such convective flows are present around all heated objects, and one can imagine how different geometries of vessels and cookware can give rise to complicated flows around them.

The kitchen is our safe place to prepare food, but we must remember that it is also a place where several safety hazards exist. At some point in our lives most of us have forgotten to turn off the kitchen stove and have suffered the consequences. When food is overheated, it starts to burn, and eventually the temperature gets so high that the carbon content gets converted to soot that give rise to smoke and fumes. Smoke decreases the overall air quality and inhaling it can adversely affect our health (Comstock *et al.*, 1981), especially if the burning becomes intense and the heating is continued. While the dispersion of smoke as a general pollutant in the atmosphere has been studied extensively, smoke in the kitchen has also been the subject of several studies (Comstock *et al.*, 1981; Rogge *et al.*, 1991). A critical issue related to this is ventilation, i.e., how well a kitchen is designed to get rid of harmful smoke and fumes. Most modern kitchens feature a ventilation or exhaust "hood" right above the stove. Both experimental fluid dynamics and computational fluid dynamics techniques such have been utilized to study the flow through kitchen hoods in order to maximize their performance (Chen *et al.*, 2018). Fires in the kitchen are the most dangerous safety hazard (Gao *et al.*, 2014) and can result in destruction of property and loss of life. Given the importance of minimizing safety hazards in the kitchen, fire engineers rely on fluid dynamics modeling to develop safe kitchen ventilation (Yeoh and Yuen, 2009; Norton, Tiwari, and Sun, 2013; Chen, Xin, and Liu, 2020).

G. Melting and freezing

We tend to naturally associate cooking with heat. Boiling, melting, freezing, solidifying, dissolving, and crystallizing food products need external heat stimulus to be transformed. Thermally driven reconfiguration can happen on a molecular level, but more often it is enough to consider phase transitions due to the heating or cooling of a substance.

Melting is another fundamental process of phase transition. From thawing to cooking, solid substances are transformed into soft matter or liquid products. The sole process of melting and flows induced therein are still of fundamental interest to physicists. The mechanism of heat transfer relies, in the simplest case described in Sec. V.A, on the Fourier law, where the heat flux q across a surface is locally proportional to the temperature gradient ∇T. The temperature field thus satisfies the advection-diffusion equation (34), which can then be solved numerically or analytically in specific geometric configurations. The geometry itself inspires questions on how the process of thawing can be exploited to create desired forms, i.e., those seen in constantly evolving ice sculptures or in ordinary ice cubes melting in a cocktail. Although the initial shapes of frozen structures may be arbitrary, macroscopic objects such as melting ice cubes and growing stalactites can approach nonintuitive geometric ideals. For the dissolution of noncrystalline objects, a paraboloidal shape was shown to be the geometric attractor (Nakouzi, Goldstein, and Steinbock, 2015). Even the simple melting of icicles is governed by a combination heat transfer from the air, the latent heat of condensation of water vapor, and the net radiative heat transfer from the environment to the ice (Neufeld, Goldstein, and Worster, 2010), which emphasizes the complexity of phase change processes.

In food products like chocolate, melting and freezing strongly affects the microstructure. Their flow properties are non-Newtonian, and their response to temperature variations is nonlinear for that reason. Even though the flow of molten chocolate in a fountain is aptly described by a power-law fluid (Townsend and Wilson, 2016), the process of melting involves different crystalline phases and is thus highly complex. Subsequent freezing typically leads to a change in structure and appearance, with different physical properties and even taste. The quality of chocolate products, in particular, their gloss, brittleness, texture, and melting behavior, depends primarily on two processing steps: the precrystallization of the chocolate mass and the eventual cooling process (Mehrle, 2007). These factors must be considered in confectionery manufacturing and, fundamentally, in the modeling of crystallization and melting kinetics of cocoa butter in chocolate (Le Révérend, Fryer, and Bakalis, 2009; Bhattacharyya and Joshi, 2022). For a good result, chocolate is often "tempered" by subsequently heating and cooling it in order to make the chocolate smoothly textured and glossy (Chevalley, 1975).

Butter (plant or animal based) itself, a vital product for cooking, responds strongly to external temperature, transiting from completely solid and brittle when taken out from the refrigerator, to spreadable at intermediate temperatures, to liquid. This empirical feeling can be related to its viscoelastic characteristics (Hayashi, 1994; Landfeld *et al.*, 2000), which additionally depend on the substance and the method of production (Shukla *et al.*, 1994). Rheology and texture (see Sec. IV.A) are often the basic characteristics when cheese is heated or baked (Lucey, Johnson, and Horne, 2003), as in the melting and browning of mozzarella in the oven (Rudan and Barbano, 1998). The temperature can be also coupled to the nonlinear viscoelastic properties, for instance, when one considers starch gelatinization while making gravies and thick sauces (Ratnayake and Jackson, 2008) or when one freezes and thaws a gelatin-filtered *consommé* (Lahne and Schmidt, 2010).

H. Nonstick coatings

Many nonstick pans or cookware are designed to be hydrophobic (water repellent) and oleophobic (oil repellent), which together are called amphiphobic (Williams, 2018; Tehrani-Bagha, 2019). Waterproof fabrics often use chemical coatings such as polyurethane, polyvinyl chloride (better known as PVC), or fluoropolymers. However, there are many concerns for these materials regarding toxicity and other environmentally damaging effects (Sajid and Ilyas, 2017), and to limit their destructive impact the European Union announced a ban on such chemicals by 2030 (European Commission, 2020b). As such, interest has risen for purely physical coatings that make use of the "lotus effect" (Marmur, 2004; Barthlott *et al.*, 2017). Like leaves of the lotus plant

(*Nelumbo* genus), micron-sized structures that give rise to superhydrophobicity can be designed (Feng *et al.*, 2002; Lafuma and Quéré, 2003; Dupuis and Yeomans, 2005). A droplet that impacts these surfaces can bounce off without wetting them (Richard, Clanet, and Quéré, 2002; Reyssat, Yeomans, and Quéré, 2008). Moreover, decorating submillimetric posts with nanotextures can lead to "pancake bouncing," where the contact time of droplets with the surface is significantly reduced (Liu *et al.*, 2014, 2015). This is important for anti-icing (Mishchenko *et al.*, 2010) and self-cleaning surfaces (Blossey, 2003), with possible applications for airplanes and cars. Superamphiphobic coatings can also be made with candle soot (Deng *et al.*, 2012).

VI. DESSERTS: VISCOUS FLOWS

Viscosity shapes our notion of thick substances such as coconut oil and honey (Wray and Cimpeanu, 2020). This notion is hard to grasp because, when a liquid is cooled by just a few degrees, its viscosity can increase by a factor of a million. Quoting the Nobel laureate Edward M. Purcell (Purcell, 1977),

> "The viscosity of a fluid is a very tough nut to crack."

Besides the nature of viscosity itself, the motion of thick liquids, often called creeping flow, can be equally puzzling. A notable example of this is G. I. Taylor's kinematic reversibility experiment, as depicted in Fig. 19(a): A mixing device with a cylindrical stirrer is filled with a viscous fluid containing dye streaks. When the stirrer is rotated in one direction, the dye streaks seem to mix with the fluid. However, the streaks are recovered when the stirrer is rotated back. This experiment, shown explicitly in a video by Taylor (1967), demonstrates that a time-reversible driving force will lead to time-reversible particle trajectories in Stokes flow. Another example is when honey or golden syrup is poured onto a pancake [Fig. 19(b)] and shows unexpected coiling dynamics because of the rich interplay among gravity, viscosity, and surface tension (Ribe, Habibi, and Bonn, 2006). Finally, as seen in Fig. 19(c), the complex shapes of sedimenting clouds of food coloring added to a cocktail can be aptly described using many-body hydrodynamic interactions between microparticles (Metzger, Nicolas, and Guazzelli, 2007; Zenit and Feng, 2018). Indeed, the theory of microhydrodynamics underlies the behavior of most composite food products, including emulsions, suspensions, and particle-laden fluid substances. Next we discuss how these viscous flows manifest themselves in a myriad of culinary aspects, and how they improve our understanding of science at a more fundamental level.

A. Honey: Flows at low Reynolds number

In thick fluids like honey, viscous forces tend to be much larger than inertial forces. As discussed in Sec. II.B, flows dominated by viscosity have a small Reynolds number ($\mathrm{Re} = \rho U_0 L_0/\mu \ll 1$). This condition is satisfied in highly viscous fluids, at low velocities, or at small length scales. For

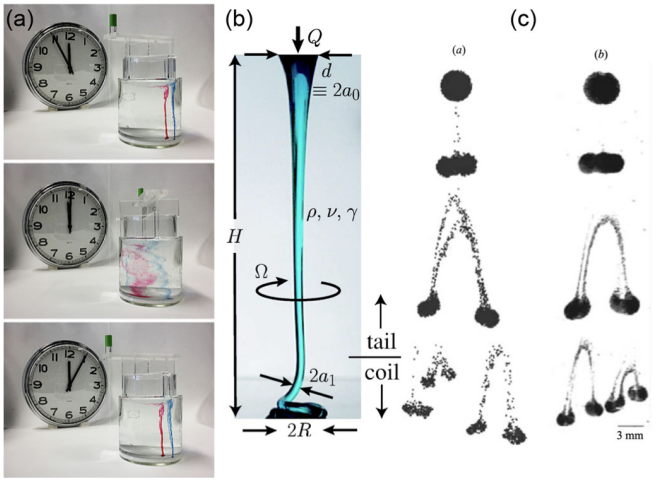

FIG. 19. Examples of Stokes flows relevant to kitchen setting. (a) Experimental demonstration of kinematic reversibility in an annular cylindrical space filled with silicone oil. Upon rotating the inner cylinder slowly a number of times and then reversing the forcing, the dyed fluid blobs remain unchanged, thus illustrating the difficulties in mixing viscous fluids. From Wikimedia Commons. (b) Coiling of a liquid rope made of a viscous fluid (corn syrup) demonstrates the complexities of free-surface gravity flows and also of pouring honey on pancakes. From Ribe, Habibi, and Bonn, 2006. (c) Snapshots of the falling cloud in (left images) point-particle Stokesian dynamics simulation with 3000 particles and (right images) sedimentation experiments using 70 μm glass beads in silicon oil. From Metzger, Nicolas, and Guazzelli, 2007.

example, when humans swim in water at a velocity of $U_0 \approx 1$ m/s with a dynamic viscosity $\mu \approx 0.9$ mPa s and density $\rho \approx 10^3$ kg/m^3, we find that $\mathrm{Re} \sim 10^6$. This means that the fluid inertia is much more important than viscosity and that the flow is likely turbulent. For microbes ($L_0 \approx 1$ μm) swimming in the same medium at, typically, $U_0 \approx 10$ μm/s, however, we have $\mathrm{Re} \sim 10^{-5}$, so the viscosity is overwhelmingly dominant (Purcell, 1977). For such creeping flows, the Navier-Stokes equations [Eqs. (2)] in the incompressible case reduce to the following Stokes equations:

$$0 = -\nabla p + \mu \nabla^2 \boldsymbol{u} + \boldsymbol{f}, \qquad \nabla \cdot \boldsymbol{u} = 0. \tag{40}$$

Equations (40) have several important properties. First, they are linear, which makes them much easier to solve than the Navier-Stokes equations. This also means that, for a given set of boundary conditions, there is only one unique solution (Kim and Karrila, 1991). Second, the Stokes equations do not depend explicitly on time. Viscosity-dominated flows will therefore respond effectively instantaneously to changes in the applied force, the applied pressure, or the boundary conditions. Third, Eqs. (40) are kinematically reversible; i.e., they are invariant under the simultaneous reversion of the direction of forces and the direction of time. This means that if the forces driving the flow are reversed, the fluid particles retrace their trajectories in time, as seen in Fig. 19(a), where a droplet of dye remains undeformed upon shearing it reversibly between two cylinders. As a consequence, it is difficult to

mix fluids at low Reynolds number; see Sec. VIII.E. Apart from demonstrations of mixing and demixing under reversed forcing in video experiments by Taylor (1967), this issue bears great significance for microfluidic flows where $L_0 \approx 1$ μm, which are becoming increasingly relevant for food science; see Secs. IV.D and VI.F].

The fundamental solution to the Stokes equations, the Green's function, is called the Stokeslet. It is the flow $\boldsymbol{u}_S(\boldsymbol{x},t)$ at position $\boldsymbol{x}$ and time t due to a point force, with the distribution $\boldsymbol{f}(\boldsymbol{x},\boldsymbol{y},t)=\delta(\boldsymbol{x}-\boldsymbol{y})\boldsymbol{F}(t)$. The force has a time-dependent strength $\boldsymbol{F}(t)$ exerted on the liquid and is located at position $\boldsymbol{y}(t)$, as expressed by the Dirac delta function. For an unbounded fluid, the boundary condition is $\boldsymbol{u}=0$ as $|\boldsymbol{x}|\to\infty$. Physically, one could think of this point force as a small particle being dragged through the liquid, such as a sedimenting coffee grain; see Sec. VI.B. The flow generated by this point force is given by

$$\boldsymbol{u}_S(\boldsymbol{x},t)=\mathcal{J}(\boldsymbol{x}-\boldsymbol{y}(t))\cdot\boldsymbol{F}(t), \tag{41}$$

where the Oseen tensor $\mathcal{J}_{ij}(\boldsymbol{r})$ has the Cartesian components

$$\mathcal{J}_{ij}(\boldsymbol{r})=\frac{1}{8\pi\mu}\left(\frac{\delta_{ij}}{r}+\frac{r_i r_j}{r^3}\right), \tag{42}$$

with indices $i,j\in\{1,2,3\}$, the relative distance is $\boldsymbol{r}=\boldsymbol{x}-\boldsymbol{y}$, and $r=|\mathbf{r}|$. There are different ways to derive this tensor, as summarized by Lisicki (2013).

This Stokeslet solution is powerful and analogous to Coulomb's law for electric point charges. Like the Stokes equations, it also reveals important properties of viscous flows. Equation (41) shows that the applied force is directly proportional to the flow velocity. As opposed to Newtonian mechanics, where the forces are proportional to acceleration, this reflects Aristotelian mechanics (Van Leeuwen, 2016), where there is no motion in the absence of forces. Inertia vanishes at low Reynolds number, that is, so the dynamics are overdamped. Second, hydrodynamic interactions are long ranged. The Stokeslet flow decays as $1/r$ with distance, as opposed to gravitation or electrostatics that both follow inverse-square laws. This has interesting consequences in the kitchen. For example, in a particle suspension such as sedimenting coffee grains, the motion of one grain will produce a flow that moves other grains, which in turn generate flows that affect the first grain again; see Sec. IV.C.

The fundamental solution can also be used to derive the Stokes law

$$\boldsymbol{F}=6\pi\mu a\boldsymbol{U}, \tag{43}$$

which describes the viscous drag force that a sphere of radius a moving with velocity $\boldsymbol{U}$ exerts on a viscous fluid (Stokes, 1851; Batchelor, 2000; Guazzelli and Morris, 2011; Yeomans, Pushkin, and Shum, 2014). The significance of Stokes's law cannot be overemphasized. Dusenbery (2009) writes that it is directly connected to at least three Nobel Prizes. Can you name them?

B. Coffee grounds in free fall: Sedimentation

In the words of Pendergrast (2010), "Possibly the cradle of mankind, the ancient land of Abyssinia, now called Ethiopia, is the birthplace of coffee." Thus, before discussing coffee brewing further in Sec. VII.D, we analyze here the oldest method of preparation: sedimentation of coffee grounds under gravity. To optimize our daily cup, we may want to assess the size distribution of the coffee particles after grinding. This can be achieved using the Stokes law, which was discussed in Sec. VI.A. The gravitational force $\boldsymbol{F}_g=m\boldsymbol{g}$ pulling on a sphere of radius a is proportional to the mass differential with the surrounding fluid $[m=(\rho_p-\rho)(4/3)\pi a^3]$. The same grain is slowed by a viscous drag force given by Eq. (43). When the drag force balances the gravitational force, the terminal velocity is

$$U_\infty=\frac{2}{9}\frac{a^2(\rho_p-\rho)g}{\mu}. \tag{44}$$

To measure U_∞ in the kitchen, we can use a mobile phone to videotape individual grains sedimenting. Equation (44) can be rearranged to solve for the particle size a. Conversely, it is possible to solve for μ if a is known, which is the principle of falling sphere viscometry (Sutterby, 1973). Millikan (1913) used a form of Eq. (44) to find the elementary electrical charge. Note that Eq. (44) was developed under several assumptions, and we now assess the validity of these.

The first assumption is that the grain sediments at a low Reynolds number (see Sec. II.B) given by $\mathrm{Re}=aU_\infty(\rho_p-\rho)/\mu$. Using Eq. (44), we find that a typical grain of radius $a=1$ mm sediments at 0.1 mm/s, yielding a Reynolds number just below the order of unity. We should therefore be cautious when using Stokes's law in this case (Arnold, 1911). To obtain the range of Reynolds numbers over which Eq. (44) gives a good approximation, one can turn to experiments. Numerous reports have been published on this topic (Rubey, 1933; Flemmer and Banks, 1986), and it is generally agreed that Eq. (44) gives good estimates up to $\mathrm{Re}\approx 1$ (Guyon *et al.*, 2001).

The second assumption is that the grain is spherical and smooth, as shape irregularities and surface heterogeneities increase the surface area. One might expect that this surface roughness increases the drag force and, since a coffee grain is neither smooth nor spherical, one might think that it falls slower than a sphere having the same density and volume. However, in the low Re limit, it turns out that the Stokes drag force is relatively insensitive to shape (Rubey, 1933), and Eq. (44) is thus likely to approximate U_∞ well even for irregular coffee grains. Moreover, at high Re surface roughness can even reduce drag, as seen with the dimples of a golf ball (Bearman and Harvey, 1976). If the particle is smooth because it is a liquid instead of a solid, then the boundary conditions will change, which typically reduces the drag force, as discussed in Sec. IX.F.

The sedimenting coffee grain generates a flow field that decays slowly with the distance from its center; see Sec. VI.A. Close to the particle viscous forces dominate, while in the far field the inertial terms dominate. It is the absence of walls that

facilitates this shift from viscous to inertial dominance, as walls provide friction to the flow. By accounting for inertial effects while considering an unbounded fluid, Oseen (1910) developed the following improved formula for the drag coefficient $C_D = F/p_{\mathrm{dyn}}A$:

$$C_D = \frac{24}{\mathrm{Re}}\left(1 + \frac{3}{16}\mathrm{Re}\right), \tag{45}$$

where $p_{\mathrm{dyn}} = \rho U_\infty^2/2$ is the dynamic pressure and A is the cross-sectional area of the sedimenting particle. The first term in Eq. (45) is the Stokes drag close to the particle, while the second term stems from inertial effects far from the particle. Oseen's formula agrees fairly well with experiments up to $\mathrm{Re} \approx 10$ (Dey, Zeeshan Ali, and Padhi, 2019).

Beyond the Oseen regime, inertial effects in the flow surrounding the particle can no longer be neglected. This causes the nearby fluid streamlines to divert from the particle, causing the flow to separate. The pressure drop across the particle is then reduced, which leads to a drag reduction. A simple experiment using coffee grains released in air (instead of water) can be performed to observe this behavior. By accounting for inertial effects around a sedimenting sphere, Stewartson (1956) found the drag coefficient to be approximately 1.06, which may be compared to the value of 7.2 using Eq. (45) for $\mathrm{Re} = 10$. For more details, see the review on Stokes's law and its legacy by Dey, Zeeshan Ali, and Padhi (2019).

Wall effects.—We now return to the assessment of the validity of Stokes's law for sedimenting coffee grains in bounded water. In developing Eq. (44), we assumed that the grain falls without influences of walls, and this is our third assumption. However, building on the pioneering works of Lorentz (1907) and Faxén (1923), O'Neill (1964) showed that hydrodynamic contributions due to walls can slow down a sedimenting grain (or a rising bubble) by as much as 5% when the distance to the walls is 10 times its size. The degree of retardation increases linearly as the grain gets closer to the vessel walls. Using matched asymptotic expansions, Goldman, Cox, and Brenner (1967) obtained the following solution for the drag force acting on a sedimenting sphere moving parallel to a wall:

$$\frac{F_{\parallel \mathrm{W}}}{F_S} = 1 - \frac{9}{16}\frac{a}{h} + \frac{1}{8}\left(\frac{a}{h}\right)^3 - \frac{45}{256}\left(\frac{a}{h}\right)^4 - \frac{1}{16}\left(\frac{a}{h}\right)^5, \tag{46}$$

which is normalized by the Stokes drag force [Eq. (43)]. Thorough experiments have been performed to validate Eq. (46) and have shown good agreement (Brown and Lawler, 2003).

For spheres close to a wall, lubrication effects become important (Sec. VI.C), yielding a logarithmic relationship between the force and the distance to the wall (Cichocki and Jones, 1998). This strong logarithmic dependence can be readily observed when making French press coffee: grains close to the vessel container sediment much slower than grains out in the bulk. Another important aspect of spheres moving parallel to the wall in a Newtonian fluid is that there is no lateral component (toward the wall) to the motion, the result of time-reversal symmetries (O'Neill and Stewartson, 1967). This intuition no longer holds for patterned surfaces (Chase, Kurzthaler, and Stone, 2022) and non-Newtonian fluids (Rad and Moradi, 2020), which has important biophysical implications for microbial biofilm formation; see Sec. VI.E.

Collective effects.—Our final assessment of Eq. (44) concerns the possible influence of multiple particles correlated by long-range hydrodynamic interactions (see Sec. VI.A) and, as Eq. (43) does not include such effects, our fourth and final assumption is that these can be neglected. However, when two spheres sediment side by side, they fall slower than in the absence of the other particle, while if they are separated by a vertical line going through their centers, the opposite is true (Guazzelli and Morris, 2011; Zenit and Feng, 2018). In a suspension containing several grains, the influence of other particles always leads to a decrease in sedimentation velocity. This observation is known as hindered settling (Richardson and Zaki, 1997) and is due mainly to an upward flow generated by each particle as it sediments. In a dilute suspension, the hindered settling velocity depends on the particle concentration as $U \approx U_\infty(1 - 6.55\phi)$, as shown by Batchelor (1972). Other effects such as Brownian motion (Lin *et al.*, 2019) and shape (Rubey, 1933) can also affect the sedimentation velocity and introduce memory effects (Szymczak and Cichocki, 2004). Finally, if particles sediment toward a surface covered with moving actuators, a self-cleaning effect can occur where hydrodynamic fluctuations repel the particles, leading to a non-Boltzmannian sedimentation profile (Guzmán-Lastra, Löwen, and Mathijssen, 2021). An important topic for future research is how such non-equilibrium distributions can evolve dynamically in active and living systems (Gompper *et al.*, 2020).

C. Pot stuck to stove top: Stefan adhesion and lubrication theory

If a pot of pasta overboils, a common subsequent problem is that the pan is "stuck" to the surface. This effect does not require any glue or the formation of molecular bonds. Instead, it stems from the viscous liquid film that is sandwiched between the objects, which requires a large force to be displaced. Josef (1874) first described this "apparent adhesion," and Reynolds (1886) later quantified it with a detailed treatise on lubrication theory.

It is important to notice a separation of length scales: The thickness h of the fluid layer is much smaller than the radius R of the pot. Thus, we can define a small parameter $\varepsilon = h/R \ll 1$. In a simplified 2D system, where the directions z and x are perpendicular and parallel to the substrate, respectively, we can expand the Stokes equations to leading order in this parameter as

$$\frac{\partial p}{\partial z} = 0, \qquad \frac{\partial p}{\partial x} = \mu\frac{\partial^2 u_x}{\partial z^2}. \tag{47}$$

The first expression in Eqs. (47) indicates that the pressure changes little with height in the thin gap above the substrate, and the second expression says that the pressure change along the substrate is related to the flow variation across the gap. The general three-dimensional case of Eqs. (47) are referred to as

the Reynolds equations, as reviewed by Oron, Davis, and Bankoff (1997), Batchelor (2000), and Szeri (2010). These equations may be solved analytically or numerically for a range of different applications.

For a cylindrical pot stuck to the surface, the Reynolds equations can be used to show that the force required to lift the pot, the Stefan adhesion force, is given by

$$F = \frac{3\pi\mu R^4}{2h^3}\frac{dh}{dt}. \tag{48}$$

Because it is hard to squeeze a viscous liquid through a narrow gap, this force can be large for thin films. For example, we estimate that for a pan of radius $R \sim 12$ cm, film thickness $h \sim 100$ μm, and separation speed $dh/dt = 100$ μm/s the force is $F \sim 10^2$ N, which can be larger than the weight of the pan filled with water. Conversely, it is difficult to bring two surfaces into close contact. However, in reality the force required is smaller than this estimate due to surface irregularities, dry spots in the film, and angling of the pot. Generalizations of these problems are described by squeeze flow theory, for example, for viscoelastic fluids (Engmann, Servais, and Burbidge, 2005).

Indeed, lubrication theory is used ubiquitously whenever one system dimension is significantly smaller than the others. In tribology, it is crucial for reducing wear and friction between bearings (Khonsari and Booser, 2017). In biology, tree frogs can climb vertical walls using liquid film flows, which has inspired new tire technology (Barnes, 1999), and biomimetic materials that adhere under wet conditions (Barnes, 2007; Meng *et al.*, 2019). Thin films significantly alter the motion of trapped microorganisms (Mathijssen, Doostmohammadi *et al.*, 2016), thereby governing their surface accumulation. Using ferrofluids, one can make adhesion switchable for use in smart adaptable materials (Wang *et al.*, 2018). Recent developments in nanoscale physics can improve lubricant design (Xu and Leng, 2018) and enhance painting and coating flows (Ruschak, 1985). Additionally, lubrication theory has been used to model air hockey (Weidman and Sprague, 2015) and, in the spirit of kitchen experiments, Reynolds (1886) used it to determine the viscosity of olive oil. Pan lubrication is also an important step in industrial baking (De La Cruz Garcia, Sánchez Moragas, and Nordqvist, 2014). Finally, the lubrication theory can also be used to model handwashing, as explained in Sec. II.J.

D. Making perfect crêpes: Viscous gravity currents

"Open the front door of a centrally-heated house and a gravity current of cold air immediately flows in." These opening words by Huppert (1982b) describe many processes in the kitchen: Opening the refrigerator or the oven door, and also the spreading of oil in a frying pan. To understand how long this spreading takes, we need to determine the evolution of the height profile $h(\boldsymbol{r}, t)$, which strongly depends on the dynamic viscosity and density of the oil μ and ρ, gravity g, and pouring rate Q.

The presence of inertia makes predictions of the radial spreading velocity difficult. If we instead pour the oil slowly, at low Reynolds number, assuming that both the oil layer thickness h and the "jet" radius R_j are small compared to the current R, we can use a lubrication approximation (see Sec. VI.C) to obtain the following simplified version of the radial force balance:

$$\frac{\partial h}{\partial t} - \frac{1}{3}\frac{\rho g}{\mu}\frac{1}{r}\frac{\partial}{\partial r}\left(rh^3\frac{\partial h}{\partial r}\right) = 0. \tag{49}$$

By adding a mass conservation equation to Eq. (49) and introducing a similarity variable, Huppert showed that the radial extent of the evolving puddle R is given exactly by

$$R = 0.715\left(\frac{\rho g Q^3}{3\mu}\right)^{1/8} t^{1/2}. \tag{50}$$

Note that Eq. (50) holds for the case of constant flow rather than constant volume.

The dominant balance of forces in Huppert's analysis is between the hydrostatic pressure head that drives the fluid and viscous stresses that slow the fluid down. Huppert discarded the effects of surface tension γ, and Eq. (50) requires the Bond number to be large: $\mathrm{Bo} = \rho R^2/\gamma \gg 1$; see Sec. II.E. Many geophysical flows are characterized by large Bond numbers, and the scalings by Huppert have seen widespread use for predicting spreading rates of saltwater currents into freshwater, lava flows, and many other geophysical gravity currents (Huppert, 2006; Craster and Matar, 2009; Meiburg and Kneller, 2010). The success of these scalings in miscible fluids might be surprising. However, geophysical flows are often characterized by high Péclet numbers [Eq. (35)], such that the transport of momentum outpaces the transport of mass; see Sec. V.A. On the fast timescale of the flow, diffusion does not have sufficient time to blur the interface separating miscible liquids, resulting in the liquids displaying immiscible behavior. Equation (50) was found to accurately describe the spreading rate of miscible sessile drops of corn syrup and glycerol in water (Walls, Meiburg, and Fuller, 2018). Other important contributions to the study of gravity currents include the spreading of French vinaigrette (Benabdelhalim and Brutin, 2022), the spreading of a saltwater current under a bath of freshwater (Didden and Maxworthy, 1982), spreading hot plumes in cold environments (Britter, 1979), and oil spreading on the sea (Hoult, 1972). These and other works were described in detail in a number of reviews (Simpson, 1982; Huppert, 2006) and in a book by Ungarish (2009).

Making the perfect crêpe.—When pouring pancake batter into a frying pan, it is tempting to speed up the spreading by holding the pan inclined. However, viscous currents down a slope can be unstable, as shown by Huppert (1982a). An initially uniform propagation front can break up into long fingers, leading to undesired stripes instead of a uniform *crêpe*. Another problem arises because the pan is heated, so the spreading problem becomes more complicated as the viscosity is a nonlinear function of time. Initially, a temperature rise is associated with a viscosity decrease, but later in the spreading process the batter starts to solidify, leading to a viscosity increase. Since the current continually loses momentum as it spreads, the solidification can arrest the flow long before it extends the entire pan. Motivated by the aim of making a perfectly flat and uniform *crêpe*, Boujo and Sellier

(2019) recently approached the spreading problem with both time-dependent viscosity and gravity. Armed with numerical tools, they identified different swirling modes and measured the resulting pancake shape. A swirling mode that is naturally adopted in pancake making (namely, draining all the batter in one place and then rotating the batter around the perimeter of the pan in one large swirling motion) appeared to optimize the pancake shape. To learn more about the rheology of pancake making and other cooking processes, see Sec. IV.A.

E. Microbial fluid mechanics

Microbes play an important role all across Eastern and Western cuisines (Tamang *et al.*, 2020). On the one hand, their presence can improve the texture and taste of foods such as sourdough bread (Arendt, Ryan, and Dal Bello, 2007), yogurt, and many fermented products (Şanlier, Gökcen, and Sezgin, 2019). On the other hand, their growth and development can cause illness (Chitlapilly Dass *et al.*, 2020). It is thus crucial to understand the mechanisms of their growth, interactions, and locomotion to control their influence on food products and the living systems they inhabit (Doyle, Diez-Gonzalez, and Hill, 2019).

Because of their size, the hydrodynamics of microorganisms is governed by the Stokes equations; see Sec. VI.A. As such, they experience the profound consequences of living at low Reynolds number (Purcell, 1977). Unlike us, cells cannot use inertia to coast forward after each swimming stroke; viscous dissipation slows them down almost instantly. Furthermore, microswimmers must obey the "scallop theorem," which states that a time-reversible swimming gait cannot lead to a net displacement (Elgeti, Winkler, and Gompper, 2015; Lauga, 2020). That is, a scallop would not be able to swim in viscous fluids: while closing and opening its shell, it would just move back and forth. Thus, microorganisms must employ more sophisticated mechanisms in order to propel themselves.

Most bacteria swim using helical flagella driven by a rotary motor, while eukaryotic swimmers often use whiplike beating organelles called cilia (Brennen and Winet, 1977; Lauga and Powers, 2009; Gilpin, Bull, and Prakash, 2020). These flagella and cilia can both be modeled as slender filaments that exert viscous drag forces on the liquid. To understand this better, we consider a generalization of the Stokes law [Eq. (43)] for a cylinder of length ℓ and radius a, with $\ell \gg a$. When it moves through the fluid sideways, perpendicular to its major axis, it will exert a viscous drag force

$$F_\perp \approx \frac{4\pi\mu\ell U}{\ln(\ell/a)}, \tag{51}$$

as predicted by slender-body theory (Gray and Hancock, 1955; Batchelor, 1970; Cox, 1970; Johnson, 1980). Note that Eq. (51) depends only weakly on the filament radius, which is on the order of $a \approx 10$ nm. Thus, a typical cilium of length $\ell \approx 10$ μm and velocity $U \approx 100$ μm/s can exert a force $F_\perp \approx 1$ pN. While this force is relatively large for a small cell, it is of little use if the same force is exerted forward and backward during periodic beating cycles. However, because of the structure of the Oseen tensor $\mathcal{J}_{ij}$ given by Eq. (42), the cylinder will exert a smaller drag force on the fluid when it moves parallel to its axis,

$$F_\parallel \approx F_\perp/2. \tag{52}$$

Both cilia and flagella rely on this fundamental principle. A cilium can exert more force on the liquid during its perpendicular "power stroke" and less force during its parallel "recovery stroke." Similarly, a bacterial flagellum can force liquid backward because each rotating helix element moves with velocity components parallel and perpendicular to the filament (Lauga, 2016). Equation (52) lies at the heart of many transport processes for viscous fluids. Indeed, numerous synthetic swimmers and microrobots are based on this hydrodynamic anisotropy (Bechinger *et al.*, 2016). Moreover, humans also use cilia to remove pathogens from our lungs (Sleigh, Blake, and Liron, 1988; Bruot and Cicuta, 2016; Ramirez-San Juan *et al.*, 2020) and to transport liquid in our brain ventricles (Faubel *et al.*, 2016).

Microbes cannot rely on external forces to swim: They are force free, such that their propulsion and drag forces balance. Therefore, instead of a Stokes monopole [Eq. (41)], the flows they generate are described by Stokes dipoles and higher multipoles (Mathijssen, Pushkin, and Yeomans, 2015). These flows can be used to model their long-range interactions with each other and with their environment (Wensink *et al.*, 2012; Elgeti and Gompper, 2013; Lauga, 2020). Cell motility takes on additional complexity because these flows often reside in viscoelastic fluids; see Sec. IV.A. This can change the swimming speed of the cells in a way that depends on the properties of the fluid and the nature of its complexity (Martinez *et al.*, 2014; Sznitman and Arratia, 2015; Spagnolie and Underhill, 2022). These non-Newtonian materials also break the time-reversal symmetry of Stokes flow, so Purcell's previously described scallop theorem no longer holds, allowing for different motility mechanisms (Lauga, 2009; Lauga, 2011; Qiu *et al.*, 2014).

Because the hydrodynamics of microorganisms has been studied so extensively recently, it is now possible to connect it with food science in terms of infectious disease transmission (Mittal, Ni, and Seo, 2020), bacterial contamination by upstream swimming (Mathijssen, Shendruk *et al.*, 2016), and the microbiology of bacterial coexistence (Gude *et al.*, 2020). Figure 20(a) shows how *E. coli* bacteria can reorient with respect to externally imposed rinsing flows, a phenomenon called rheotaxis (Mathijssen, Figueroa-Morales *et al.*, 2019). Moreover, recent engineering improvements have led to sensors capable of detecting harmful microbes. For example, a porous silk microneedle array can be used to sense the presence of *E. coli* in fish fillets (Kim *et al.*, 2021). In general, a wide spectrum of potential pathogens stimulates future research on food safety (Ali *et al.*, 2020), as we now discuss.

F. Microfluidics for improved food safety

Foodborne pathogens such as *E. coli* and *Salmonella* bacteria cause approximately 420 000 deaths and 600 million illnesses yearly (World Health Organization, 2015). Such pathogens often originate from bacterial biofilms in food processing plants (Mathijssen *et al.*, 2018; Vidakovic *et al.*, 2018)

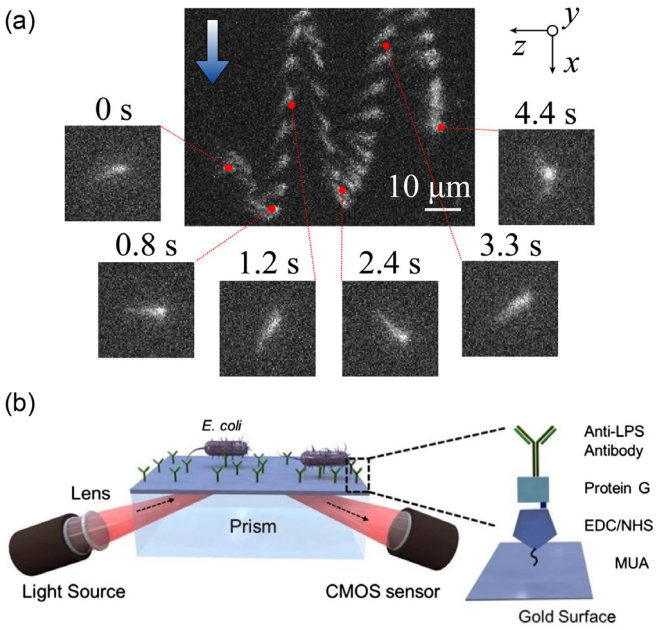

FIG. 20. Microbial dynamics and food safety. (a) Time lapse of an *E. coli* bacterium performing oscillatory rheotaxis, with fluorescently labeled flagella to reveal its reorientation with respect to the flow (large arrow, pointing down). From Mathijssen, Figueroa-Morales *et al.*, 2019. (b) Working principle of an optofluidic pathogen detector. When *E. coli* binds to Y-shaped monoclonal antibodies, it induces a shift in refractive index that can be detected with an optical sensor. From Tokel *et al.*, 2015.

and poor hygiene (Secs. II.J and IX.C). Therefore, on-site rapid detection is necessary to prevent these harmful bacteria from entering our grocery stores and ending up in food. The traditional way of detecting pathogens is by cultivating them in petri dishes, but slow bacterial growth limits the usefulness of such "babysitting" in food plants. This has led to alternatives such as nucleic-acid-based methods [including polymerase chain reactions (known as PCR) (Kant *et al.*, 2018), which is the primary method to test patients for COVID-19], but extensive training requirements, expensive equipment, and labor intensive steps prevent a robust and efficient implementation in food production facilities.

Microfluidic-based biosensors can detect or "sense" pathogens on much faster timescales thanks to small volumes and flow-mediated transport, with high-speed imaging enabling real-time monitoring (Skurtys and Aguilera, 2008; Mairhofer, Roppert, and Ertl, 2009; He *et al.*, 2020). Biosensors work by measuring an electrical or optical signal induced by a chemical reaction as a target molecule (pathogen) binds to a bioreceptor molecule (Van Dorst *et al.*, 2010; Karunakaran, Rajkumar, and Bhargava, 2015). The bioreceptors are designed to exactly match the surface elements of the pathogen (these elements are called antigens) in a lock and key fit. Owing to their excellent specificity, monoclonal antibodies (mAbs) are the most widely used bioreceptor molecules. Figure 20(b) shows the working principle a biosensor functionalized with Y-shaped mAb molecules for detecting *E. coli* (Tokel *et al.*, 2015).

The speed and accuracy of surface-based biosensors depend on a number of factors, with the most important being the pathogen concentration, the number of available binding sites on the sensor, the transport of pathogens from the bulk fluid to the sensor via flow and diffusion, and finally the kinetics of the binding reaction. Without flow, the sensing time is usually limited by the time it takes for a pathogen or a virus to diffuse to the sensor, which can be several hours in a microchannel due to the low diffusivity of such large particles. However, by leveraging microfluidic flow, solute transport can be sped up by several orders of magnitude, leading to reaction-limited kinetics. We recommend the pedagogical reviews on transport and reaction kinetics in surface-based biosensors by Gervais and Jensen (2006), Squires, Messinger, and Manalis (2008), and Sathish and Shen (2021).

G. Ice cream

Although first mentions of ice cream as "flavored snow or ice" date back to the Persian and Roman Empires, evidence suggests that dairy iced products originate from 12th century China (Marshall, Goff, and Hartel, 2003). From a chemical point of view, ice cream is an emulsion (see Sec. IV.D) made with water, ice, milk fat and protein, sugar, and air. The ingredients are mixed together and turned into foam upon the addition of air bubbles. The colloidal emulsion is then frozen to preserve the metastable mixture. The details of the process have been extensively studied within the food science community (Arbuckle, 2013; Goff and Hartel, 2013), and also from the physics and general science viewpoints (Clarke, 2003, 2015). Special attention has been paid to the colloidal character of the emulsion (Goff, 1997).

An appealing texture and rheology are crucial aspects of ice cream quality. Owing to its popularity, ice cream was apparently the first food product to have its extensional viscosity measured, as early as 1934 (Leighton, Leviton, and Williams, 1934). Since then, rheological properties of ice cream have been examined in detail, and various dynamical models have been proposed to account for their behavior (Martin *et al.*, 2008). The breadth of related topics even inspired an interdisciplinary undergraduate course taught within the physics program (Trout and Jacobsen, 2020).

The production of ice cream involves a flow undergoing a structural and phase transition through a combination of mechanical processing and freezing. The dynamics of ice crystallization therein are not fully understood. Because an ice cream mix is opaque, *in situ* crystallization has not been observed and its mechanism is a subject of debate (Cook and Hartel, 2010). In a typical ice cream freezer, ice is formed on externally cooled walls by surface nucleation and growth and is then scraped off to the bulk fluid, where secondary nucleation and ripening take place (Hartel, 1996). The number and size of ice crystals formed is heavily dependent on the mixture composition and also affects the melting rate and hardness of the final food product (Muse and Hartel, 2004). Studying the characteristics of ice cream production leads to the development of novel methods for rapid freezing and thawing of foods (Li and Sun, 2002). The structure of ice cream can be practically controlled in most common conditions. However, environments with large temperature fluctuations remain problematic, so developing a detailed description of the underlying processes remains an interesting pathway for future research.

In addition to frozen ice cream, one sometimes sees "hot ice cream" that seems to melt upon cooling. This effect can be achieved using methyl cellulose, a thickener that acts at high temperatures to produce a product with surprising, "opposite" melting properties (The Master Chef, 2021). Perhaps not the obvious choice on a hot summer day, but definitely worth a taste.

VII. COFFEE: GRANULAR MATTER AND POROUS MEDIA

The Hungarian probability theorist Alfréd Rényi (1921–1970) once said (Suzuki, 2002),

> "A mathematician is a device for turning coffee into theorems."

Coffee is arguably one of the most popular beverages worldwide, and many of us look forward to a cup several times a day. It is not surprising that we are fascinated with the fluid dynamics of coffee, which is the focus of this section. We start with the flow of coffee beans and other granular materials, including avalanches, hoppers, and the Brazil nut effect. We then consider brewing coffee using different methods in the context of porous media flows and percolation theory, and we finish with the coffee-ring effect. In the words of Wettlaufer (2011), there is a "universe in a cup of coffee."

A. Granular flows and avalanches

Granular materials (de Gennes, 1999) are found everywhere in the kitchen. Take flour, rice, nuts, coffee beans, sugar, or salt. Indeed, the food industry processes billions of kilograms of granular material every year (Gray, 2018). They are composed of discrete, solid particles (grains) over a wide range of sizes. Therefore, the grain diameter D is often denoted on the Krumbein φ scale $\varphi = -\log_2(D/D_0)$, with $D_0 = 1$ mm (Krumbein, 1934). For example, $\varphi = -6$ and 6 correspond to oranges and powdered sugar, respectively.

Granular matter can have many surprising properties (Herminghaus, 2005; Mehta, 2012). One such example is the Janssen effect: The hydrostatic pressure at the bottom of a cylindrical container does not grow linearly with the filling height of grains, unlike in a liquid (Sec. II.A). Instead, the pressure saturates exponentially to a value much less than the weight of the grains, because they are partially supported by the vertical silo walls due to friction forces (Aguirre *et al.*, 2010). Another example is that granular matter can behave like solids, liquids, or even gases, depending on the amount of kinetic energy per grain (Lun *et al.*, 1984; Jaeger, Nagel, and Behringer, 1996; Forterre and Pouliquen, 2008). For this reason, granular flows are challenging to analyze and predict.

A notorious example thereof is avalanche dynamics (Nagel, 1992; Frette *et al.*, 1996; Paczuski, Maslov, and Bak, 1996; Hunt and Vriend, 2010). A pile of grains [Fig. 21(a)] is held together by "chains" of frictional and compressive forces (Mueth, Jaeger, and Nagel, 1998), but the pile will suddenly collapse if the slope exceeds a maximum angle θ_m. This sliding will stop only after the slope has been reduced below the critical angle of repose θ_r of which typical values range from 45° for wheat flour to 25° for whole grains (Al-Hashemi and Al-Amoudi, 2018). The angle of repose is important across food industry, from silo roof design to conveyor belt transport (De-Song *et al.*, 2003) and the geology of hillslopes (Deshpande *et al.*, 2021), which limits farming. It also sets a fundamental rule for food plating, which in turn affects the perception of taste (Zellner *et al.*, 2011) and the design of food sculptures [Fig. 21(b)]. In this artwork the grains are sticky, but the weakest links are still susceptible to avalanche dynamics. From a fundamental point of view, avalanche dynamics exhibits self-organized critical behavior for rice grains with a large aspect ratio, as shown by Frette *et al.* (1996). Moreover, Einav and Guillard (2018) used a column of puffed rice to investigate the crumbling of a brittle porous medium by fluid flow. These "ricequake" experiments may give insight on how to prevent the collapse of rock-fill dams, sinkholes, and ice shelves. Avalanches can also be extremely dangerous in food science such as entrapment in grain storage facilities (Issa *et al.*, 2017), where a silo of grains can clog [Fig. 21(c)] because of force chains forming between grains that prevent them from relative motion [Fig. 21(d)]. However, a disruption of this delicate balance might lead to large-scale avalanche flows. There are helpful rescue strategies in the case of grain entrapment (Roberts *et al.*, 2011).

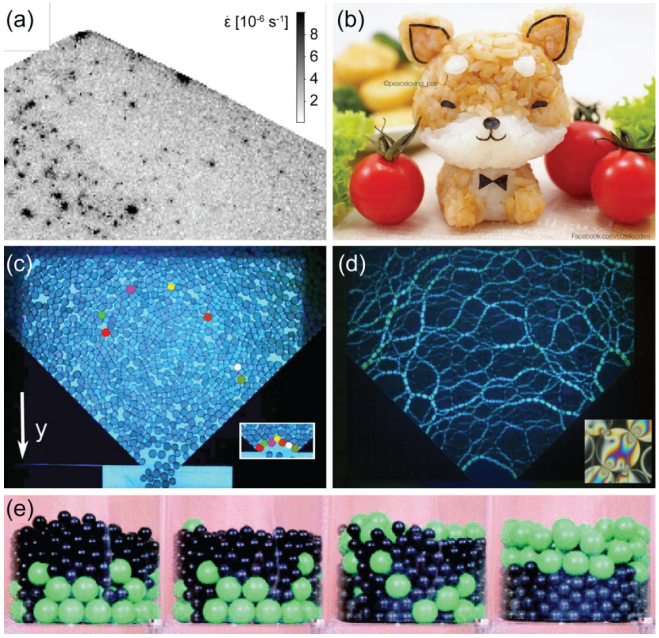

FIG. 21. Granular matter. (a) In a pile of grains, the motion is quantified by the rate of strain $\dot{\varepsilon}$ using spatially resolved diffusing wave spectroscopy. From Deshpande *et al.*, 2021. (b) Rice sculpture. From Piewpun, 2021. (c) The velocity field of grains flowing in a 2D hopper is measured by direct particle tracking. The seven particles that are marked form a jamming arch, shown in the inset. (d) Force chains in a jammed state, visualized using photoelastic particles that show intensity fringes under stress, highlighted in the inset. From Tang and Behringer, 2011. (e) The Brazil nut effect, with 8 mm black (small) glass beads and 15 mm green (gray, large) polypropylene beads. Evolution in time from left to right. From Breu *et al.*, 2003.

As opposed to avalanches, sometimes it is desirable to make granular matter flow faster. This can often be achieved with granulation (Cuq *et al.*, 2013), where a powder or small grains

are made to clump together. Perhaps counterintuitively, these aggregates can flow more easily. This has many important examples in the kitchen, including granulated sugar. Compared to powdered sugar, granulated sugar has a smaller angle of repose and considerably better flow characteristics (Teunou, Fitzpatrick, and Synnott, 1999) because the larger grains are less cohesive and more easily fluidized (Krantz, Zhang, and Zhu, 2009). Moreover, it is much easier to compactify granulated materials than powders, which is of vital importance for making tablets in the pharmaceutical and food industries (Kristensen and Schaefer, 1987). This is food for thought when you next sweeten your coffee.

B. Hoppers: Grains flowing through an orifice

An important quantity across food science is how quickly a granular material can pass through an orifice (Beverloo, Leniger, and Van de Velde, 1961). Chefs experience this daily when dispensing spices or grains from a hopper. The flow rate Q is given empirically by the Beverloo law

$$Q = C(\mu, \theta)\rho_b \sqrt{g}(D - kd)^{3/2}, \tag{53}$$

where C is a fitting parameter that depends on the friction coefficient μ and the hopper angle θ, ρ_b is the grain bulk density, D is the neck width, d is the grain diameter, and the parameter k is of order unity.

The Beverloo law can be partially explained using dimensional analysis, scaling arguments, and hourglass theory (Nedderman, 2005), but its foundations are still under active investigation, as recently discussed by Alonso-Marroquin and Mora (2021). This problem is difficult to solve because the grains behave like both a liquid and a solid near the opening (Zuriguel, 2014). This is the result of jamming (Liu and Nagel, 1998, 2010), where the effective viscosity increases dramatically above a critical particle density, so the flowing grains suddenly form a rigid arch or vault (Tang and Behringer, 2011), as shown in Figs. 21(c) and 21(d). This clogging becomes more unlikely as the opening size is increased, but all hoppers have a nonzero probability of clogging (Thomas and Durian, 2015). Clogging is particularly common in grain hoppers (To, Lai, and Pak, 2001) and microfluidic devices (Dressaire and Sauret, 2017), but also in sheep herds and pedestrian crowds moving through a bottleneck (Zuriguel *et al.*, 2014). Jamming is equally essential for food processing (Barker, 2013), biological tissue development (Lawson-Keister and Manning, 2021), and food structuring (Van der Sman, 2012).

The nonlinear nature of jamming can lead to surprising consequences. For example, the observed flow rate does not depend on the filling height of the hopper [Eq. (53)]. This was assumed to be due to the Janssen effect (Sec. VII.A), but Aguirre *et al.* (2010) showed that the grain flow rate remains constant even if the pressure at the orifice decreases during discharge, and that different flow rates can be achieved with the same pressure. More counterintuitively, inserting an obstacle just above the outlet of a silo can help with clogging reduction (Zuriguel *et al.*, 2011). In fact, it has been shown that "the sands of time run faster near the end," which is caused by a self-generated pumping of fluid through the packing (Koivisto and Durian, 2017); you may want to take this into account for your kitchen timer. By varying the softness of the grains, Tao, Wilson, and Weeks (2021) showed that clogging occurs more often for stiffer particles, and that clogging arches are larger for particles with larger frictional interactions. Hence, understanding jamming dynamics can help with the design of clog-free particle separation devices (Mossige, Jensen, and Mielnik, 2018).

C. Brazil nut effect

When you repeatedly shake a box of cereal, the larger (and heavier) grains often rise to the top [Fig. 21(e)]. This phenomenon was called the Brazil nut effect after the seminal work by Rosato *et al.* (1987) and is also known as granular segregation (Ottino and Khakhar, 2000; Kudrolli, 2004; Gray, 2018). One explanation is buoyancy, but the effect can happen even when the larger grains are denser than the smaller ones. A second contributing factor is called percolation (not to be confused with coffee brewing; Sec. VII.D). Here smaller grains fall into the gaps below the larger grains during shaking. However, a container shape can be designed in which the larger grains move downward (Knight, Jaeger, and Nagel, 1993). This was explained by a third effect called granular convection, where the shaking leads to a flow pattern of grains moving upward along the walls and downward in the middle of the container (Knight, Jaeger, and Nagel, 1993). Soon thereafter, granular convection was imaged directly using MRI (Ehrichs *et al.*, 1995; Knight *et al.*, 1996) and was studied using extensive computer simulations (Gallas *et al.*, 1996). However, the scientific trail was mixed up again by the discovery of the "reverse Brazil nut effect" by Shinbrot and Muzzio (1998), which was experimentally verified by Breu *et al.* (2003). Here larger but lighter particles can sink in a shaken bed of smaller grains that cannot be explained by granular convection alone, nor by percolation or buoyancy. Furthermore, Möbius *et al.* (2001) showed that particle segregation depends on the interstitial air between the grains and depends nonmonotonically on the density. Huerta and Ruiz-Suárez (2004) then found that there are two distinct regimes: At low vibration frequencies, inertia and convection drive segregation, whereas inertia (convection) dominates when the relative density is greater than (less than) 1. At high frequencies, segregation occurs due to buoyancy (or sinkage) because the granular bed is fluidized and convection is suppressed. Vibration-induced fluidization is used widely in the food industry to dry, cool, coat, or mix granular materials and powders (Turchiuli, 2013).

Granular convection can occur even in densely packed shaken containers, on the brink of jamming, where unexpected dynamic structures can arise under geometrical restrictions (Rietz and Stannarius, 2008). Murdoch *et al.* (2013) studied granular convection in microgravity during parabolic flights, revealing that gravity tunes the frictional particle-particle and particle-wall interactions, which have been proposed to drive secondary flow structures. Recently D'Ortona and Thomas (2020) discovered that a self-induced Rayleigh-Taylor instability (see Sec. III.A.4) can occur in segregating granular flows, where particles continuously mix and separate when they are flowing down an incline.

Granular separation is of vital importance in the food industry. It might be convenient if grains need to be sorted, but the effect is often undesirable when we require an even grain mixture. This is especially problematic when the product must be delivered within a narrow particle-sized distribution or with specific compositions of active ingredients (Gray, 2018). However, most food storage facilities (heaps and silos) and processing units (chutes and rotating tumblers) are prone to grain segregation (Baxter *et al.*, 1998). Researchers are learning how to prevent separation, but this is difficult because it strongly depends on details of the flow kinematics. One technique is to add small amounts of liquid to make the grains more cohesive (Li and McCarthy, 2003), but at the cost of reduced food longevity due to rot. Another strategy is to use modulation of the feeding flow rate onto heaps (Xiao *et al.*, 2017). The Brazil nut effect might also be suppressed using a system with cyclical shearing, where grains remain mixed or segregate slowly (Harrington, Weijs, and Losert, 2013). There are also new developments in machine vision systems for food grain quality evaluation (Vithu and Moses, 2016). Granular flows are often difficult to image with opaque particles, but powerful techniques to measure the 3D dynamics include MRI (Ehrichs *et al.*, 1995), positron emission particle tracking (Windows-Yule *et al.*, 2020) or x-ray computed tomography (referred to as CT) (Gajjar *et al.*, 2021).

Finally, returning to our kitchen, the Brazil nut effect may occur too when stir-frying. This is why chefs often toss the ingredients into the air repeatedly, fluidizing the grains to mix them evenly and to avoid burning them at high temperatures. Notably Ko and Hu (2020) recently described the physics of tossing fried rice. There is also an interesting connection between the Brazil nut effect and popcorn (Hoseney, Zeleznak, and Abdelrahman, 1983; Da Silva *et al.*, 1993; Virot and Ponomarenko, 2015), where the grains that have not popped sink to the bottom. Granular physics hence plays a key role in several culinary contexts, both in the food industry and in our kitchens.

D. Brewing coffee: Porous media flows

Henry Darcy (1803–1858) was a French hydrologist who studied the drinking water supply system of Dijon, France, a city also known for its mustard. In an appendix of his landmark publication (Darcy, 1856), he described experiments on water flowing through a bed of sand. From the results he obtained Darcy's law, an empirical expression for the average velocity $\boldsymbol{q}$ of the liquid moving through the bed. It was refined by Muskat (1938) and can be written as

$$\boldsymbol{q} = -\mathcal{K}(\boldsymbol{\nabla} p - \rho \boldsymbol{g})/\mu, \tag{54}$$

where $\mathcal{K}$ is a tensor that describes the permeability of the material in different directions, which sometimes is replaced by a constant k for isotropic materials. Note that the local velocity in the pores is $\boldsymbol{u} = \boldsymbol{q}/\phi$, where $\phi \in [0, 1]$ is called the porosity. Darcy's law can indeed be derived theoretically (Whitaker, 1986), and it is integral to many industrial processes in food science, such as sand filtration and antimicrobial water treatment (Hills *et al.*, 2001; Yang, Min *et al.*, 2020). Moreover, it can be applied to a much broader class of

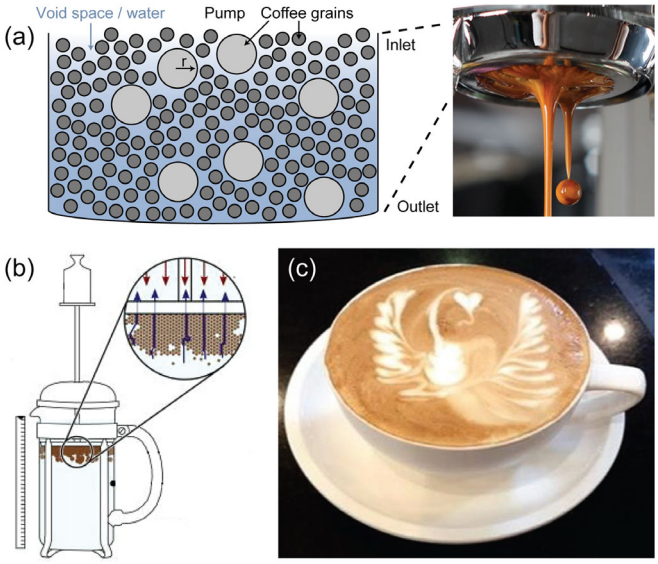

FIG. 22. Coffee brewing. (a) Schematic of percolation in an espresso machine basket. A pressure differential pushes water down through the pore spaces. Courtesy of Christopher H. Hendon. Inset: espresso drops by photographer theferdi. (b) Diagram of a French press. The water moves up around the coffee grounds (upward arrows) by applying a constant gravitational force on the plunger (downward arrows). From Wadsworth *et al.*, 2021. (c) Cappuccino with latte art in the shape of a phoenix. From Hsu and Chen, 2021.

porous media flows (Philip, 1970; Blunt, 2001; Bear, 2013), which are found everywhere in gastronomy. Examples include percolation in a salad spinner, drizzle cake, squeezing a sponge, and making coffee (Thurston, Morris, and Steiman, 2013; Egger and Orr, 2016).

For espresso brewing [see Giacomini *et al.* (2020)], one can use the first term in Darcy's law for pressure-driven flow [Fig. 22(a)], while drip coffee [see Angeloni *et al.* (2019)] can be described using the second term for gravity-driven flow in Eq. (54). In both cases, the permeability $\mathcal{K}$ can be changed by tamping the grounds or adjusting the grain size in order to tune the flow rate, and thus also the extraction time (Corrochano *et al.*, 2015). Another particularly well-studied method of making coffee is using the Italian "moka" pot; see Fig. 1(c). Its sophisticated design was patented by Alfonso Bialetti (1888–1970) (Binder and Scheidle, 2020). Gianino (2007) used a moka pot to measure the flow rate through a bed of grains and applied Darcy's law to measure its permeability. Later Navarini *et al.* (2009) improved this method by accounting for the decreasing permeability as aromatic substances dissolve in water. In a third study, King (2008) investigated the effect of packing and coffee grain temperature on the permeability. Percolation in a moka pot was well visualized by looking through the metal using neutron imaging (Kaestner, 2012).

Most studies on coffee extraction have showcased some direct applications of Darcy's law under idealized conditions, but they do not attempt a description beyond the Darcy regime (Fasano, Talamucci, and Petracco, 2000). For instance, they have ignored the initial stage of percolation, in which the water invades the initially dry coffee grain matrix. This process can be described using percolation theory

(Stauffer, 2018), where the pores between the coffee particles can be considered as a random network of microscopic flow channels (Blunt, 2001). If the coffee is coarsely ground or tamped lightly, the many open microchannels (bonds) allow the water to find a connecting path through the coffee. This process is first characterized by capillary wetting (Singh *et al.*, 2019) (see Sec. II.F) and considerable swelling of coffee grains (Mo *et al.*, 2022), after which Darcy's law becomes applicable. For intermediate tamping, as the permeability $\mathcal{K}$ decreases, we approach the percolation threshold. The extraction time will then significantly increase, which can result in overextraction (Severini *et al.*, 2017). Finally, if the coffee is tamped too strongly or too finely ground, the water cannot find a path between the grounds. Thus, either there is nothing to drink or the pressure builds up until we see hydraulic fracturing (Adler, Thovert, and Mourzenko, 2013). In that case, large flow channels suddenly crack open that bypass the microchannels (Berre, Doster, and Keilegavlen, 2019). Channelization might be induced by flow-mediated rearrangement of the porous coffee bed (Mahadevan *et al.*, 2012; Derr *et al.*, 2020). This "fracking" can give the coffee a bad taste because it leads to uneven extraction (Moroney *et al.*, 2019). Symptoms that your espresso is fractured are liquid spraying through the bottom of the basket, irregular flow, and a cracked coffee cake. Percolation theory has many other applications, including predictions for forest fires, disease spreading, and communication in biology (Sahimi, 2014; Mathijssen, Culver *et al.*, 2019). With these efforts to perfect the taste of the resulting beverage, there are still aspects of coffee brewing that are understood only qualitatively and described empirically. Microscopic details of swelling and extraction remain to be explored in order to fully understand the complex physics of reactive transport in espresso machine brewing.

Coffee can be made in many ways, each involving different fluid mechanics. Here we mention only a few preparation methods, with some recent results: To make an espresso, it is important to note that coffee beans are often prone to variations in quality. Even if the theory is perfect, the ingredients are not. To overcome this, Cameron *et al.* (2020) offered advice to systematically improve espresso brewing by proposing a set of guidelines for a uniform extraction yield. They also found that the smallest grains do not give the highest yield, as they tend to clump together and form aggregates; see the granulation discussion in Sec. VII.A. For drip brew coffee, it is common to use a precise temperature-controlled kettle, but Batali, Ristenpart, and Guinard (2020) surprisingly found that the brew temperature may not have as much of an impact on the sensory profile at fixed brew strength and extraction. Considering the French press, Wadsworth *et al.* (2021) recently determined the force required to operate the plunger [Fig. 22(b)]. They recommended using a maximum force of 32 N to complete the pressing action in 50 s, using 54 g of coffee grounds for 1 l of boiling water. Looking at cold brew coffee, Cordoba *et al.* (2019) evaluated the extraction time and flavor characteristics, Rao and Fuller (2018) investigated its acidity and antioxidant activity, and Ziefuß *et al.* (2022) showed that cold brewing can be achieved rapidly using picosecond-pulsed laser extraction. Finally, Greek and Turkish coffee rely on the sedimentation of fine particles, which we discuss in Sec. VI.B, and *café de olla* is a Mexican coffee drink that is made with aromatic spices and sugar.

After the perfect cup of coffee is made, it can be decorated with latte art [Fig. 22(c)]. Indeed, Hsu and Chen (2021) showed that coffee tastes sweeter with latte art, which they related to brain-wave activity using electroencephalography. The fluid mechanics of pouring steamed milk foam into the denser coffee can be described as an inverted fountain (see Sec. III.A), which depends on the jet diameter and the pouring height via the Froude number [Eq. (19)]. Large fountains lead to more mixing and brown foam, while gentle pouring gives white foam. After much practice, these colors can be combined in rapid succession to make intricate patterns, including a heart and the phoenix (Bez, 2021). Some people prefer their coffee without milk, but with a thin layer of espresso crema (Illy and Navarini, 2011). Undesirably this coffee foam can agglomerate along the perimeter. This effect can often be suppressed by heating the cup beforehand since it is caused by Bénard-Maragoni convection, which we discuss in Sec. VII.E.

E. Coffee-ring effect

When the last sip of coffee or wine is left overnight, it dries out, creating a stain with a brighter interior and much darker borders, where most residues are deposited (Fig. 23). The coffee-ring effect, as it has been called, can be observed in almost any kitchen mixture containing small particles. As explained by Deegan *et al.* (1997), the coffee-ring effect results from the drying dynamics of the droplet, combined with the pinning of its contact line with the substrate (Marín *et al.*, 2011; Mampallil and Eral, 2018). As the solvent evaporates, the outflow of matter decreases the thickness of the droplet at every point. If the contact line was not pinned, the droplet would shrink. This additional constraint, together with the surface tension requirement to keep the contact angle fixed (see Sec. II.F), induces an outward flow from the interior to replenish the evaporated liquid at the borders. This flow transports the sediment, which is then deposited at the outer ring, leaving the lower-concentration interior.

Instead of a solid particle suspension, the coffee-ring effect also emerges if the dissolved component is another liquid. In that case, the edge of the puddle remaining after a volatile solvent evaporates forms either "fingers" or spherical "pearls" or some combination of the two (Mouat *et al.*, 2020). Understanding the underpinning dynamics of coffee-ring formations remains an active research topic. An example of the many publications in recent years is the study by Moore, Vella, and Oliver (2021) on the effects of diffusion of solute from the pinned contact line to the bulk of the drop on the pattern formation.

By adding some alcohol to the drop to make it more volatile, the coffee-ring effect can be suppressed by consequential Marangoni flows from the contact line to the drop's interior (Hu and Larson, 2006). These flows are induced by a surface tension gradient along the surface of the drop (see Sec. III.B), which is in turn caused by nonuniform cooling as the droplet evaporates because the surface tension increases as the temperature decreases. This is referred to as Bénard-Marangoni convection; see also Sec. V.C.

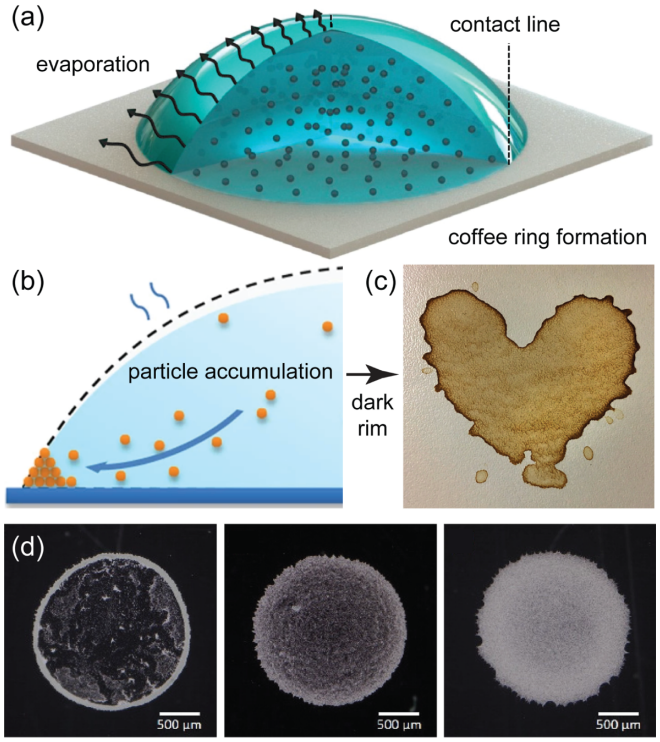

FIG. 23. Coffee-ring effect. (a) Schematic of an evaporating droplet containing a suspension of microparticles. Stronger evaporation near the contact line drives an internal flow to the outer edge. From Jafari Kang *et al.*, 2016. (b) A dark rim is formed by particles that accumulate at the pinned contact line. From Li *et al.*, 2016. (c) Example of a heart-shaped coffee ring. From Robert Couse-Baker. (d) Suppressing the coffee-ring effect by adding cellulose nanofibers (CNFs) to a drop of 0.1 wt% colloidal particles. From left to right: CNF concentration of 0, 0.01, 0.1 wt %. From Ooi *et al.*, 2017.

The deposition pattern then depends on the strength of the relative magnitude of thermocapillary stresses to viscous ones, as expressed by the dimensionless Marangoni number (Ma), as defined in Eq. (23) with $\Delta\gamma = (\partial\gamma/\partial T)\Delta T$. For large Ma the particles end up in the center, for intermediate Ma they are deposited evenly along the substrate, and for small Ma the coffee-ring effect is fully recovered. Therefore, by tuning Ma, for example, through tuning the alcohol percentage in the coffee, it is in principle possible to control the deposition pattern. Moreover, the coffee-ring effect can also be suppressed by shape-dependent capillary interactions (Yunker *et al.*, 2011, 2013) or the addition of cellulose nanofibers [Fig. 23(d)].

Applications of the coffee-ring effect and the drying of thin colloidal films in general go far beyond kitchen experiments (Routh, 2013; Mampallil and Eral, 2018). For example, it is the basis of controlled evaporative self-assembly, which is used to create functional surfaces with controllable features (Han and Lin, 2012). The coffee-ring effect can also be used for controlled inkjetting of a conductive pattern of silver nanoparticles (Zhang *et al.*, 2013), and particle deposition on surfaces could be further controlled using light-directed patterning by evaporative optical Marangoni assembly (Varanakkottu *et al.*, 2016). Moreover, the effect can be used for nanochromatography to separate particles such as proteins, microorganisms, and mammalian cells with a separation resolution on the order of 100 nm (Wong *et al.*, 2011). The growth dynamics of coffee rings are altered when active particles such as motile bacteria move around in the evaporating droplet (Nellimoottil *et al.*, 2007; Sempels *et al.*, 2013; Hennes *et al.*, 2017; Andac *et al.*, 2019), and bacterial suspensions can feature active depinning dynamics. Hence, in the spirit of frugal science it might be possible to exploit the coffee-ring effect to detect antimicrobial resistance (Kang *et al.*, 2020).

VIII. TEMPEST IN A TEACUP: NONLINEAR FLOWS, TURBULENCE, AND MIXING

What is turbulence? This intriguing question has fascinated fluid mechanicians throughout history. Leonardo da Vinci alluded to two important properties of turbulence (Marusic and Broomhall, 2021): the generation of motion at large scales and the destruction due to viscosity at the smallest scales. Arguably its main signature is the many scales of motion in turbulence ; for example, a volcanic plume spans over several kilometers, with eddies all the way down to the Kolmogorov microscales (Kolmogorov, 1941). As the turbulent structures break up, energy is transferred from large whirls to smaller ones. The poem by Richardson (2007) describes this energy cascade:

> Big whirls have little whirls
> That heed on their velocity,
> And little whirls have littler whirls
> And so on to viscosity.

The consequences of turbulence are numerous in our everyday lives. Turbulence gives us the characteristic sound of a kettle whistle, it helps with mixing milk into our tea or coffee, and it gives us some frictional losses when we bike home from the restaurant. In this section, we catch a whiff of turbulence in the kitchen.

A. Tea leaf paradox: Secondary flows

Before diving into chaotic realms, we consider the surprising effects that the nonlinearity of the Navier-Stokes equations [Eq. (2)] can bear in laminar flow. One such surprise is the "tea leaf paradox." Biological tissues tend to be denser than water (Aoyagi, Yokoi, and Tanaka, 1992); thus, soaked tea leaves will sink to the bottom of a cup. When the water is stirred around in circles, the leaves are expected to move toward the edge of the cup because of centrifugal action. The opposite happens, however: The leaves always migrate to the center of the cup, as seen in Fig. 24(a). Thomson (1892) first recognized that the solution of this paradox stems from "friction on the bottom." Later Einstein (1926) gave a detailed description of the tea leaf experiment itself in order to explain the erosion of a riverbank. A detailed theoretical treatment was later provided by Greenspan and Howard (1963).

The paradox is resolved with fluid mechanics as follows: As the liquid rotates in the cup, the first approximation of the fluid flow is just a solid-body rotation. Specifically, we have

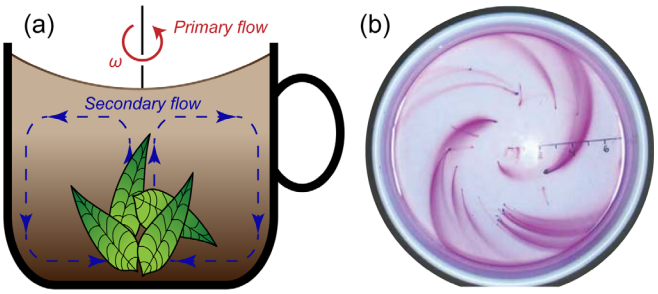

FIG. 24. Tea leaf effect due to secondary flows. (a) After stirring a cup of tea, rotating liquid (primary flow) slowly comes to a halt because of friction with the walls (spin down). This friction also induces toroidal recirculation (secondary flow) directed outward at the top and inward at the bottom, which causes the leaves to collect in the center. Adapted from Einstein, 1926. (b) Spiral dye streaks due to secondary flows in a cake pan. Instead of slowing down, the liquid is rotated increasingly fast (spin up), so the secondary flow is reversed such that the dye spirals outward at the bottom of the cake pan. From Heavers and Dapp, 2010.

$\boldsymbol{u} = \boldsymbol{\Omega} \times \boldsymbol{r}$ with a uniform angular velocity $\boldsymbol{\Omega}$. On the fluid acts a centrifugal force $\boldsymbol{F}_c \propto \boldsymbol{\Omega} \times (\boldsymbol{\Omega} \times \boldsymbol{r})$. If $\boldsymbol{\Omega}$ is constant in space, then this force does not modify the flow. However, frictional drag with the cup walls slows the fluid down in the boundary layer. In particular, near the bottom surface the angular velocity $\boldsymbol{\Omega}(\boldsymbol{r})$, and thus the centrifugal force, will be less than near the top water-air interface. Consequently, an in-up, out-down recirculation emerges [Fig. 24(a)] as the liquid slowly stops spinning. This recirculation can also be reversed [Fig. 24(b)] when the liquid is rotated increasingly faster (spin-up) from rest (Greenspan and Howard, 1963; Baker, 1968).

The tea leaf effect has many applications. In the kitchen, it can be applied conveniently when one poaches eggs (Moore, 1989; Heavers and Dapp, 2010). Before cracking the egg into the pot, the hot water can be gyred to keep the egg whites together at the center of the pot. But act quickly because the flow ceases after a time

$$\tau_E \sim \sqrt{\frac{H^2}{\nu\Omega}}, \tag{55}$$

called the Ekman time (Ekman, 1906; Greenspan and Howard, 1963), in terms of the kinematic viscosity ν and H is the height of the liquid layer, the depth. The same technique is also used to separate out trub during beer brewing (Bamforth, 2009) and to separate blood cells from plasma in microfluidics (Arifin, Yeo, and Friend, 2007). In geophysical flows, the same in-up, out-down circulation is seen in tornadoes (Rotunno, 2013). In modern additive manufacturing technologies, secondary flows can have a negative impact on the desired product, so the Ekman time sets a limit on how quickly objects can be 3D printed (Kelly *et al.*, 2019).

When discussing the tea leaf paradox, we saw that rotating a liquid in a cup gives rise to (1) a horizontal rigid body motion and (2) a vertical flow structure due to frictional drag with the surfaces [Fig. 24(a)]. Indeed, it is a powerful concept to understand such fluid flows in terms of a "primary flow," guessed from basic physical principles, and a "secondary flow," a correction due to high-order effects such as obstacles in the main flow.

Another classical example of secondary flows can be used when we inactivate microorganisms during the transport of fruit juices in pipes. This can be achieved by trapping the microbes in vortices and exposing them to UV-C light (Müller *et al.*, 2011). These so-called Dean vortices naturally emergence in a curved pipe (Dean, 1927). The primary structure can be taken as a straight Poiseuille flow (see Sec. II.C), and the secondary structure consists of vortices that can be explained using a perturbation method based on Poiseuille flow accounting for centrifugal forces (Germano, 1989; Boshier and Mestel, 2014). To tune the vertices, we must quantify the relative strength of the secondary flow compared to the primary. This is determined by the balance between inertial and centrifugal forces with respect to viscous forces, which is given by the Dean number

$$\mathrm{De} = \mathrm{Re}\sqrt{R_p/R_c}, \tag{56}$$

where Re is the Reynolds number [Eq. (3)], R_p is the radius of the pipe, and R_c is its radius of curvature. For small Dean numbers the current is unidirectional, mostly primary flow. Dean vortices emerge for intermediate values, and for large De the flow turns turbulent (Kalpakli, Örlü, and Alfredsson, 2012). This knowledge can also be used in applications to separate particles by size using inertia (Di Carlo, 2009). These vortices also emerge naturally in straight channels when two stratified fluid layers such as air and water flow through them (Vollestad, Angheluta, and Jensen, 2020), which is associated with large pressure losses in industrial (food) pipelines.

In the beer brewing industry, secondary flows are widely use in hot trub sediment removal (Jakubowski, 2015), where the suspension is injected tangentially to a cylindrical tank, called the whirlpool, where it gradually spins down, while the sediment migrates toward the center, following the so-called Ekman spirals, known from meteorological flow considerations (Bödewadt, 1940). A variant of this process involves a whirlpool kettle, in which a heating rod is placed at the axis, which distorts the flow and leads to the formation of a ring of deposit instead of the central cone (Jakubowski *et al.*, 2019).

Similar calculations can be performed to study secondary flows in many other applications, including kitchen sink vortices (Andersen *et al.*, 2003), turbomachinery compressors and turbines (Langston, 2001), and oceanic and atmospheric currents with Ekman layers (Ekman, 1906; Eliassen, 1982; Garratt, 1994). Ekman layers are associated with transport of biomaterials in the ocean through so-called Ekman transport processes. The secondary flow pattern of Ekman transport can lead to upwelling and downwelling of algae and nutrients that promote the growth of phytoplankton populations (Miller and Wheeler, 2012). A thorough understanding of the underpinning mechanisms is crucial to mitigate the devastating implications of harmful algal blooms that impact fish production and aquaculture. Secondary flows can also contribute to bridge scour (Wang, Yu, and Liang, 2017) by removing sediment such as sand and gravel from around bridge

abutments or piers, leading to one of the major causes of bridge failure around the world.

Thus, understanding secondary flows is useful in many scenarios (Bradshaw, 1987). However, not all currents can be decomposed in a simple primary and secondary flow structure. Care must be taken with such superpositions since the Navier-Stokes equations are nonlinear. However, secondary flows can give quick insights and more advanced perturbation methods can often be followed (Van Dyke, 1975).

B. Teakettles: Turbulent jets

When the water in the teakettle boils, a turbulent jet of steam emerges from the spout with a conical profile [Fig. 25(a)]. To describe the dynamics of a turbulent jet, it is useful to decompose the velocities into an average and a fluctuating component. This averaging procedure is named for its inventor Osborne Reynolds and is written as $u_i = \bar{u}_i + u_i'$, with $i = \{x, y\}$ for the velocity components in two dimensions (White and Corfield, 2006). By Reynolds averaging we arrive at the well-known equation for the conservation of momentum in turbulent flow,

$$\frac{\partial \bar{u}_i}{\partial t} + \bar{u}_j \frac{\partial \bar{u}_i}{\partial x_j} + \overline{u_j' \frac{\partial u_i'}{\partial x_j}} = -\frac{1}{\rho}\frac{\partial \bar{p}}{\partial x_i} + \nu \frac{\partial^2 \bar{u}_i}{\partial x_j^2}, \tag{57}$$

using Einstein notation. The third term is an apparent stress due to turbulent fluctuations, and the remaining ones are the

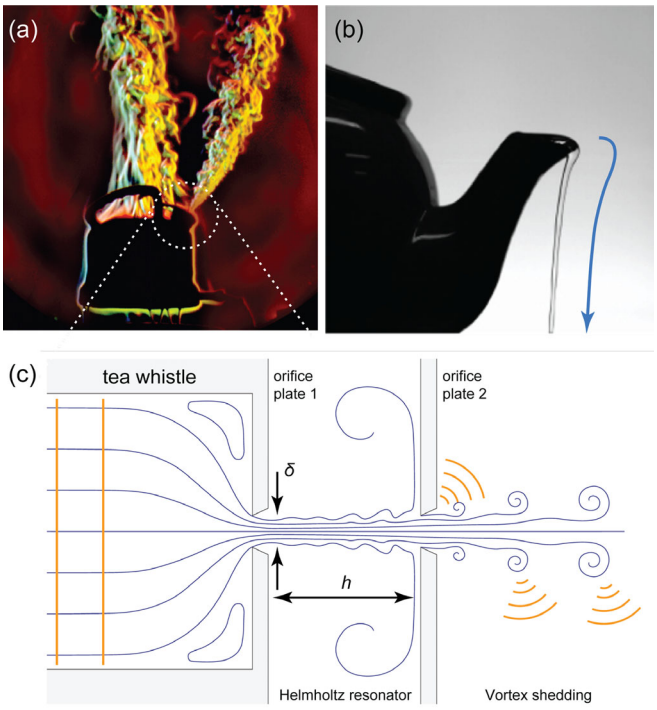

FIG. 25. Tea time. (a) A turbulent jet emanating from a teakettle. Courtesy of Gary S. Settles. (b) The teapot effect, showing a liquid stream following the curved surface of the spout (arrow). Pouring any slower will make the liquid stick to the pot entirely. From Scheichl, Bowles, and Pasias, 2021. (c) Diagram of a teakettle whistle. The steam passes from left to right through two orifice plates. From Henrywood and Agarwal, 2013.

averaged transport terms in the Navier-Stokes equation (see Sec. II.B), where the last (viscous stress) term can be neglected in inertia-dominated flows. The flux of momentum remains constant beyond a certain distance from the spout (Guyon *et al.*, 2001). To maintain its momentum, the jet must continually entrain ambient air. This is why blowing on a finger burnt by a hot kettle has a cooling effect.

Moreover, fluid jets tend to follow convex surfaces rather than being scattered off, which is called the Coanda effect (Barros *et al.*, 2016). This is sometimes demonstrated by extinguishing a candle by blowing around a tin can. Similarly, when a steam kettle jet curves around another pot, it can pose an unexpected safety hazard. An interesting application is robotic food processing using Coanda grippers (Lien and Davis, 2008). The Coanda effect should not be confused with the teapot effect (López-Arias *et al.*, 2009; Duez *et al.*, 2010; Scheichl, Bowles, and Pasias, 2021), in which a liquid follows a curved surface like a teapot spout [Fig. 25(b)], because this flow is dominated by surface tension and wetting (Sec. II.F). While the teapot effect can cause a mess when the liquid is poured too slowly, it can be advantageous for coating or making complex shapes (Jambon-Puillet *et al.*, 2019), perhaps in novel culinary decorations.

Other examples of turbulent jets include the contrails produced by aircrafts. According to one study (Burkhardt and Kärcher, 2011), this warms the planet even more than the carbon emitted by the jet engines, but it seems that these effects can be mitigated by avoiding certain altitudes (Teoh *et al.*, 2020). In any event, when flying it is best to steer clear of plumes, such as those emanating from smokestacks or volcanoes. As part of a safety assessment, we can use the predictions by Taylor (1946) for the shape and final height of such plumes. Taylor's theory is valid across many length scales: It could be used in the same way to estimate the shape of a plume rising from a cup of coffee (Fig. 18).

C. Sound generation by kitchen flows

The teakettle that we just discussed can make a pleasant whistle (Chanaud, 1970; Henrywood and Agarwal, 2013) that propagates by pressure waves at the speed on sound (Rayleigh, 1877a), approximately 343 m/s in air. Sir Isaac Newton (1642–1726) was the first known to measure the speed of sound, as reported in his book on classical mechanics *Principia* (Newton, 2020). Since then many creative attempts to measure this quantity have been reported, including the accurate experiments by the Reverend William Derham (1657–1735) involving a telescope and gunshots (Murdin, 2009). According to Rayleigh (1877b), the parameters determining the sound generation of a whistle are a characteristic length scale L_0, the frequency f_0, the fluid (steam) viscosity ν, and the steam jet velocity U_0. They form two dimensionless groups, namely, the Strouhal number

$$\mathrm{St} = \frac{\text{timescale of background flow}}{\text{timescale of oscillating flow}} = \frac{f_0 L_0}{U_0}, \tag{58}$$

and the Reynolds number [Eq. (3)]. Henrywood and Agarwal (2013) found that for a typical teakettle with two orifice plates [Fig. 25(c)], the frequency giving rise to the sound generation

is sensitive to the jet diameter δ and not the plate separation distance h in the diagram. Thus, L_0 is to be replaced with δ. Furthermore, Henrywood and Agarwal (2013) found that the whistle's behavior is divided into two regions: For $\mathrm{Re}_\delta \lesssim 2000$, the whistle operates like a Helmholtz resonator, with an approximately constant frequency (pitch). However, above a critical Reynolds number ($\mathrm{Re}_\delta \gtrsim 2000$) the whistle's tone is determined by vortex shedding (Bearman, 1984), with a frequency that increases with U_0 at an approximately constant $\mathrm{St}_\delta \approx 0.2$. This increases the whistle's pitch by the end and produces the characteristic shrieking sound.

Vortex shedding often occurs through the formation of von Kármán vortex streets, where counterrotating vortices detach from objects in an oscillatory fashion (von Kármán, 1954). These oscillations can drive the sound of our tea whistle, but also the "singing" of power cables in strong winds (Rienstra, 2005). Similarly, tall buildings or bridges can swing in a destructive manner if the aerodynamic driving frequency resonates with the structural eigenmodes (Irwin, 2010). To prevent damage from happening, newer buildings are designed to have several eigenfrequencies to effectively dissipate the energy, or to have roughness elements, as perfected by the glass sponge *Euplectella aspergillum* (Fernandes *et al.*, 2021). The sound of the teakettle whistle might inspire you to whistle for yourself while stirring your tea (Sec. VIII.A). The physiology of mouth whistling was discussed by Wilson *et al.* (1971), Shadle (1983), and Azola *et al.* (2018).

Plink. plink. plink.—Another kitchen sound is the maddening noise of a leaky tap (Schmidt and Marhl, 1997; Leighton, 2012a; Speirs *et al.*, 2018), which can be irregular because of its chaotic behavior (Schmidt and Marhl, 1997; D'Innocenzo, Paladini, and Renna, 2002). The paradox of why a single drop impacting on a liquid surface can be so loud compared to a more energetic continuous stream is still not fully understood. Franz (1959) discussed the fact that the droplet can entrain air bubbles, which oscillate to make a sound at a frequency $f = (1/2\pi a)\sqrt{3\gamma p_0/\rho}$ given by Minnaert (1933), where a is the bubble radius, γ is the ratio of specific heats of air, and p_0 is the pressure outside the bubble. However, not every drop makes a sound. Longuet-Higgins (1990) and Oguz and Prosperetti (1990) developed the first detailed analytical models to explain this in terms of the Froude number [Eq. (13)] and the Weber number [Eq. (14)] given the droplet radius and impact velocity. The sound volume is set by the wave amplitude, but how does sound generated underwater cross the water-air interface? Prosperetti and Oguz (1993) reviewed the underwater noise of rain, and Leighton (2012b) discussed whether goldfish can hear their owners talking. Looking at the dripping tap, Phillips, Agarwal, and Jordan (2018) tested previous theories by comparing sound recordings with direct high-speed camera imaging. They wrote that the airborne sound field is not simply the underwater field propagating through the water-air interface, but that the oscillating bubble induces oscillations of the water surface itself, which could explain the surprisingly strong airborne sound.

Glug. Glug. Glug.—Another classical kitchen sound is made when liquid is poured from a bottle (Whalley, 1987). Recently this was studied in more detail by Rohilla and Das (2020), who described how sounds are formed by the breaking and making of interacting interfaces.

Ting. Ting. Ting.—The "hot chocolate effect" (Crawford, 1982) occurs when a cup of cold milk is heated up in the microwave, cocoa powder is mixed in, and the bottom of the cup is tapped with a spoon. The sound pitch initially descends by nearly three octaves, comparable to the vocal range of an operatic soprano, after which the pitch gradually rises again. This happens because air is less soluble in hot liquids, so it becomes supersaturated with heating, and adding a fine powder provides nucleation sources for fine bubbles. Air is more compressible than water, which lowers the speed of sound, and thus the pitch. The same musical scales are heard when one opens a fresh beer (Crawford, 1990) that is supersaturated with CO_2 (Sec. III.E). The hot chocolate effect was visualized directly by Trávníček *et al.* (2012).

Pop. Pop. Pop.—It is impossible to cook without making noise, sometimes because of intense hydrodynamic phenomena. We already mentioned the supersonic pop made by cracking open a champagne bottle (Sec. III.E). Similarly, supersonic shock waves can be generated by snapping a tea towel (Bernstein, Hall, and Trent, 1958; Lee *et al.*, 1993). Dropping an object in a filled kitchen sink can also create a supersonic air jet (Gekle *et al.*, 2010). By investigating the popping sound of a bursting soap bubble, Bussonnière *et al.* (2020) found a way to acoustically measure the forces that drive fast capillary flows. Finally, Kiyama *et al.* (2022) investigated the morphology and sound generation of water droplets in heated oil baths such as deep-fat fryers.

D. Imploding bubbles: Cavitation

After having discussed flows that break the sound barrier in Sec. VIII.C, we now focus on another intense hydrodynamic phenomenon called cavitation (Plesset and Prosperetti, 1977). Here cavities (sometimes called bubbles or voids) are formed in the fluid under low pressure or rapid motion. These cavities can implode and lead to shock waves, often damaging nearby objects (Sreedhar, Albert, and Pandit, 2017). In nature, mantis shrimp use this effect to crush the shells of their prey (Patek, Korff, and Caldwell, 2004). Sometimes, cavitation causes ultrasonic fields that are so intense that they produce light flashes, a process called sonoluminescence (Jarman and Taylor, 1964; Patek, Korff, and Caldwell, 2004), with internal temperatures reaching thousands of kelvins (McNamara, Didenko, and Suslick, 1999).

Numerous situations in food science involve cavitation. In Sec. III.F and Fig. 12, we discussed how beer tapping leads to cavitation and bottles overflowing with foam (Rodríguez-Rodríguez, Casado-Chacón, and Fuster, 2014). Cavitation also occurs at the rotating tips of a smoothie blender, aiding the homogenization process (Gogate and Kabadi, 2009).

Indeed, the power of cavitation can be used in many positive ways. For example, beer brewing could benefit from cavitation by accelerating the production process and reducing gluten in beer (Albanese *et al.*, 2017a, 2017b). Cavitation may also be used as a nonthermal and energy-efficient tool to enhance emulsification, mixing, homogenization, pasteurization, and sterilization (Gogate, 2011a;

Asaithambi *et al.*, 2019), to process food and water (Gogate, 2011b), to improve the structure and functionality of proteins (Dash, Singh, and Singha, 2022), or to accelerate wine aging and coffee brewing, and more generally to increase flavor extraction (Gavahian *et al.*, 2022).

E. Making macarons: Chaotic advection

A droplet of milk with a typical diffusivity of $D \sim 10^9$ m^2/s takes a long time to mix in a cup of coffee in the absence of fluid motion, typically $\tau = L_0^2/D$, i.e., days, and much slower than the diffusion of heat (Sec. V.D). However, stirring reduces the mixing time dramatically, down to seconds, as turbulent eddies stretch the drop into thin filaments so diffusion can act efficiently (Dimotakis, 2005). Moreover, hydrodynamic instabilities (Sec. III.A) can lead to turbulence, which enhances the mixing rate by maximizing the exposed surface area and the concentration gradient between adjacent fluids (Chandrasekhar, 1961). However, turbulence does not occur in viscous fluids at low Reynolds numbers (Sec. II.B). Instead, mixing can be achieved by combining diffusion with chaotic advection (Aref, 1984). This is demonstrated by the baker's map (Fox, 1997). Imagine a piece of dough that is stretched out and folded on top of itself. Repeating these steps creates many exponentially thin layers, or laminae. A minimal amount of diffusion then mixes the layers together. This is called chaotic mixing (Ottino, 1989; Arnold and Khesin, 1998). Notably examples of Stokes flows in a bounded region exhibiting chaotic streamlines have also been found, inspired by "stretch-twist-fold" flows that arise naturally in dynamo theory (Bajer and Moffatt, 1990), but they seem to be impractical in the kitchen context.

A culinary example of chaotic advection is making macarons, where highly viscous batter must be mixed gently to maintain its foam structure (Özer and Ağan, 2021). The choice of stirring protocol has a dramatic impact on the mixing rate: If we move a spatula back and forth through a viscous Newtonian fluid, we see no mixing at all because of kinematic reversibility (see Fig. 19 in Sec. VI), as explained by the scallop theorem (Purcell, 1977). Thus, to mix fluids at low Re we must break time-reversal symmetry. This is already achieved naturally to some extent if the fluid is viscoelastic (Qiu *et al.*, 2014). To enhance this effect, we change our stirring protocol to moving the spatula in circular patterns instead of back and forth motion. Now the fluids do mix, but slowly, because they are stretched only linearly. Next we stir in figure-eight patterns (Thiffeault, Gouillart, and Dauchot, 2011) [see Fig. 26(a)], which speeds up the mixing rate dramatically as this strategy yields exponential stretching (Meunier and Villermaux, 2003). This can also be achieved by rotating two rods at the same speed but in opposite directions, as in commercial egg beaters (Franjione, Ottino, and Smith, 1992).

To come up with an optimal mixing protocol is a difficult, nonlinear task (Eggl and Schmid, 2020), but a number of good ideas have been proposed. A particularly efficient mixing protocol is the "blinking vortex" (Aref, 1984), where two rotors alternately spin in the same direction. For the first half period, the first rod rotates while the other one is stationary, then vice versa, a task that could perhaps be performed by a cooking robot (Bollini *et al.*, 2013). This

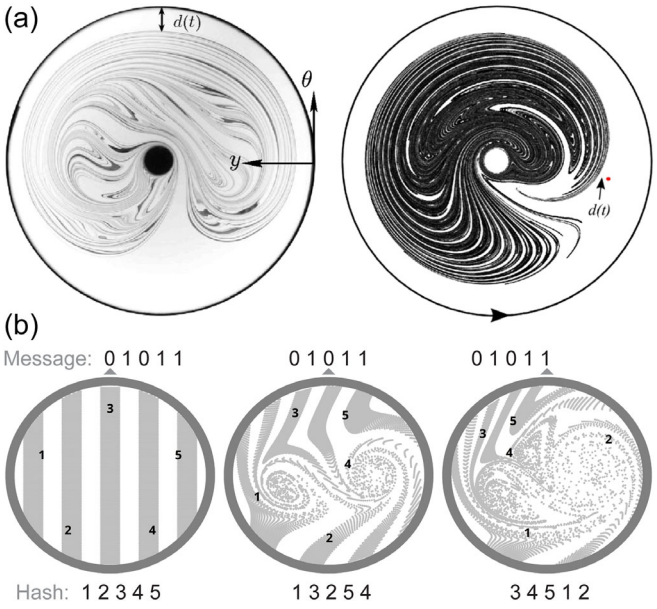

FIG. 26. Chaotic stirring protocols can be used for a broad range of applications, from making macarons to cryptography. (a) Experiment (left image) and simulation (right image) of the figure-eight stirring protocol used to mix a blob of dye into sugar syrup. From Thiffeault, Gouillart, and Dauchot, 2011. (b) Chaotic advection used to create a digital message hashing function. Courtesy of William Gilpin.

canonical and time-periodic blinking vortex is used ubiquitously in chaotic mixing theory to compare the effectiveness of different mixing protocols (Aref *et al.*, 2017). Similarly, Arnold-Beltrami-Childress flow is often considered the archetypal flow for many studies on chaotic advection in three dimensions (Arnold and Khesin, 1998). Besides expedient cooking, chaotic advection has numerous applications in other disciplines (Stroock *et al.*, 2002). For example, Gilpin (2018) used a blinking vortex model to create digital hash functions with potential applications in cryptography [Fig. 26(b)].

By adding another pair of counterrotating rods, for example, using two eggbeaters, one obtains the "four-roll mill." This concept was invented by Taylor (1934) to study the formation of emulsions (Sec. IV.D). Oil drops immersed in golden syrup (ideal for baking) were placed at the center of the mill in a stagnation-point flow, which elongates them. The drops split when the viscous stresses on their surface exceed the stabilizing surface tension, as described by the capillary number

$$\mathrm{Ca} \equiv \frac{\text{viscous stresses}}{\text{surface tension}} \sim \frac{\mu U_0}{\gamma}, \tag{59}$$

where the characteristic velocity $U_0 = \dot{\gamma} L_0$ can be written as the local shear rate times the droplet size. The four-roll mill laid the basis for studies of droplet breakup and stability, but fluctuating stagnation points made practical implementation difficult. To alleviate this issue, Bentley and Leal (1986a) implemented an image-based feedback loop that controlled the speed of each roller independently. Using their invention, Bentley and Leal (1986b) validated theoretical limits for drop

deformation (Barthes-Biesel and Acrivos, 1973; Hinch and Acrivos, 1979) and paired their experiments with theory for studying drop dynamics (Stone and Leal, 1989). Flow fields generated by the automated four-roll mill also pioneered polymer elongational rheometry (Fuller and Leal, 1980, 1981). More recently Hudson *et al.* (2004) introduced the microfluidic analog of the four-roll mill, which has been used extensively to characterize the material properties of biomaterials and single cells by extensional rheometry (Haward, 2016). And in applications of microfluidic stagnation-point flows, it has been extended to include substrate patterning (Juncker, Schmid, and Delamarche, 2005; Perrault, Qasaimeh, and Juncker, 2009; Safavieh *et al.*, 2015) and the trapping of cells by hydrodynamic confinements, allowing new developments in analytical chemistry and life sciences (Brimmo and Qasaimeh, 2017).

F. Sweetening tea with honey

Returning to the mixing of two liquids, we now make a cup of tea sweetened with a drop of honey. By pure dissolution, a viscous drop mixes slowly with the tea, but stirring can help us again. However, since the drop is viscous turbulent eddies cannot stretch the drop into thin filaments, as was the case with much less viscous milk drops; see Sec. VIII.E. Instead, the sharp flow velocity gradients around the drop increase the mass transfer by maintaining a correspondingly sharp concentration gradient (Leal, 2007). We seek an estimate of the mixing time. We consider a drop of honey of size $L_0 \sim 1$ mm and diffusivity $D \sim 10^{-10}$ m^2/s in water (Fan and Tseng, 1967). We also assume a viscous honey drop, so the mass transport is dominated by advection due to large Schmidt numbers [Eq. (38)]. Using a stirring speed of $U_0 \sim 1$ mm/s, the Péclet number [Eq. (35)] is large ($\mathrm{Pe} \sim 10^4$), but the flow close to the drop is still laminar at an intermediate Reynolds number ($\mathrm{Re} \lesssim 1$). As the drop dissolves, a diffusion layer develops between the pure phases. Acrivos and Goddard (1965) showed that, in the low Reynolds number and high Péclet number limit, this diffusion layer has a thickness

$$\delta \sim L_0 \mathrm{Pe}^{-1/3}. \tag{60}$$

In our case, at high Pe the boundary layer is rather thin ($L_0/\delta \sim 20$). By substituting δ for L_0 in the expression for the diffusion time $\tau_D \sim L_0^2/D$, following Mossige *et al.* (2021) we obtain a typical mixing time

$$\tau_{\mathrm{mix}} \sim (L_0^2/D)\mathrm{Pe}^{-2/3}. \tag{61}$$

By inspecting Eq. (61), we can immediately appreciate the dramatic effect of fluid flow: It can reduce the mixing time by a factor of 1000 or more. When the numbers are plugged in, it takes ∼22 s to stir the viscous honey droplets (or sugar grains) into our tea. This is surprisingly long compared to milk mixed by turbulence in a matter of seconds. This approximation can be improved by accounting for open streamlines and inertial effects (Krishnamurthy and Subramanian, 2018a, 2018b).

Instead of stirring, we can also let the honey drop sediment down. If it is sufficiently small, it will remain spherical and sediment at low Reynolds number (Sec. VI.B). When we substitute the terminal velocity U_∞ [Eq. (44)] for U_0 in Eq. (61), we obtain a characteristic timescale of mixing for the sinking drop,

$$\tau_{\mathrm{mix,sink}} \sim \left(\frac{\mu^2}{(\Delta\rho g)^2 D}\right)^{1/3}. \tag{62}$$

This timescale also applies to the inverted system of a water drop rising in another viscous, miscible liquid, such as corn syrup, as recently examined experimentally (Mossige *et al.*, 2021), theoretically (Nordbotten and Mossige, 2022), and numerically (Vorobev, Zagvozkin, and Lyubimova, 2020).

IX. WASHING THE DISHES: INTERFACIAL FLOWS

After our long meal, from cocktails to coffee and tea (Secs. III–VIII), it is now time to do the dishes. Food hygiene is paramount (see also Sec. II.J), and the cleaning will not be difficult if everyone helps out. As Johann Wolfgang von Goethe (1749–1832) wrote,

> "Let everyone sweep in front of his own door, and the whole world will be clean."

Moreover, doing the dishes is much alleviated by the mesmerizing colors of soap bubbles and the startling wave dynamics. Fun, you might think, but interfacial phenomena have led to exceptional scientific discoveries ranging from cell biology to nanotechnology; see Rosen and Kunjappu (2012) and Myers (2020). In this penultimate section, we will pop the bubble of some old misconceptions and catch the wave of the latest developments concerning interfacial flows.

A. Greasy galleys smooth the waves

Benjamin Franklin (1706–1790) noticed a noteworthy phenomenon during one of his journeys at sea, sailing in a fleet of 96 ships. "I observed the wakes of two of the ships to be remarkably smooth, while all the others were ruffled by the wind, which blew fresh" (Franklin and Brownrigg, 1774). Puzzled about the differing appearance, Franklin at last pointed it out to the captain and asked him the meaning of it. The captain's answer may come as a surprise: "The cooks, says he, have, I suppose, been just emptying their greasy water." The calming effect of oil on water was common knowledge to seamen at the time and had indeed been described since the ancient Greeks. However, legends circulated about a ship that miraculously survived a storm by taming it with olive oil [Fig. 27(a)], so Franklin decided to initiate a series of systematic experiments (Franklin and Brownrigg, 1774). The amusing details of these stories, and the scientific interest that have emerged since, were described by Tanford (2004) and Mertens (2006).

While the dampening of surface waves was known for millennia, its precise cause was a mystery until recently, as described by Henderson and Miles (1994), Nicolas and Vega (2000), Behroozi *et al.* (2007), and Kidambi (2011), and references therein. Franklin thought that the oil film stopped the wind from catching the water, but over a century passed before more progress was made. In her kitchen, Agnes

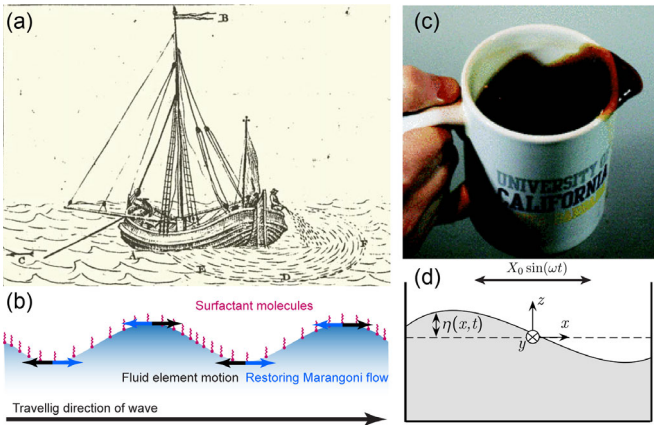

FIG. 27. Waves and splashes. (a) Protecting a ship by calming the waves with oil. The Dutch fisherman Isak Kalisvaar was reported to have conducted this experiment, in a letter to Frans van Lelyveld in 1776, after his ship got into a violent storm. From Mertens, 2006. (b) Diagram of capillary wave dampening by surfactants. (c) Representative image of coffee spilling. From Mayer and Krechetnikov, 2012. (d) Schematic of sloshing dynamics in an oscillated container. From Sauret *et al.*, 2015.

Pockels performed pioneering experiments on the surface tension of oil films; see Sec. IX.C. We now know that this surface tension increases when the oil film is stretched thin, as by the wind. Because of the Marangoni effect (see Sec. III.B), the resulting gradients in surface tension then induce flows that oppose the film deformation, thus dampening surface waves [Fig. 27(b)]. This interfacial restoring force is referred to as the Gibbs surface elasticity, or the Marangoni elasticity (Kim and Mandre, 2017), which is a multiphase flow effect that occurs in many other applications, as extensively reviewed by Brennen (2005).

B. Splashing and sloshing

No culinary achievement happens without a small mess left behind, be it an accidental spill or the usual drop of wine from the cook's glass on the kitchen table; see Sec. VII.E. Splashes and spills can be dangerous, though. Carmody *et al.* (2022) recently investigated the health concerns of washing raw chicken, where splashes can contaminate culinary surfaces. The question of sloshing, why liquids spill out of a container under acceleration, has previously received attention in the context of space vehicles and ballistics. Depending on the size of the container and the type of agitation, large-scale oscillations of the encased fluid can be enhanced to the point of spilling (Ibrahim, 2005; Herczyński and Weidman, 2012). In the academic context, sloshing is known to everyone trying to walk to a seminar with their coffee cup [Fig. 27(c)]. It turns out that spilling results from a combination of excess acceleration for a given coffee level when we start walking, and a complex enhancement of vibrations present in the range of common coffee cup sizes (Mayer and Krechetnikov, 2012). With some relief came the realization that beer does not slosh so easily, since the presence of even a few layers of foam bubbles on the free surface introduces strong damping of surface oscillations (Sauret *et al.*, 2015) [Fig. 27(d)].

We generally want to avoid or control splashing or spreading, especially when mixing and pouring liquids. The impact and breakdown of droplets on a solid or liquid surface is controlled mainly by the Reynolds number [Eq. (3)] and the Weber number [Eq. (14)]. Another important factor determining the splashing behavior is the type of substrate, which regulates the contact angle dynamics of impinging droplets (Quetzeri-Santiago *et al.*, 2019). The elasticity of the substrate also plays a role (Vella, 2019), because soft solids absorb kinetic energy from fluids in motion and noticeably reduce or even eliminate splashing. Estimates and experiments show that the droplet kinetic energy needed to splash on a soft substrate can be almost twice as large as in the rigid case (Howland *et al.*, 2016). Droplet spreading and recoil can result in a number of complex fluid dynamics phenomena when the elongating and stretching drops form jets and sheets that further destabilize into smaller droplets via the Rayleigh-Plateau instability (Sec. II.G). The possible outcomes of a collision of a droplet with a solid substrate involve deposition; a fervent splash; so-called corona splash, in which the liquid forms a circular layer that detaches from the wall; and retraction in which the droplet can destabilize and break up or rebound (partially or entirely) (Richard and Quéré, 2000; Richard, Clanet, and Quéré, 2002; Liu *et al.*, 2014). The process is controlled by the wettability of the surface, the parameters of the droplet, and its impact speed. At a larger scale, inverted bell structures are formed when a jet impacts a liquid container, as observed during the washing of vials (Mohd, Yadav, and Das, 2022).

Before a stream separates into impacting droplets, liquid jets are frequently seen and used in the kitchen (Eggers and Villermaux, 2008). When one plates a gourmet meal, the way sauces are spread on a plate is carefully engineered to achieve a variety of shapes and textures. The same questions appear when a cake is glazed, where various edible jets and streams are produced on surfaces in a manner that manages buckling instabilities. In artistic paining, the understanding of hydrodynamics was crucial to Jackson Pollock, who used a stick to drizzle paint on his canvas in a variety of ways (Palacios *et al.*, 2019). The complex fluid dynamics behind different painting effects was recently analyzed and reviewed by Herczyński, Chernuschi, and Mahadevan (2011) and Zenit (2019).

C. Dishwashing and soap film dynamics

The interference patterns on soap bubbles have fascinated physicists for centuries (Patsyk *et al.*, 2020), which has resulted in pioneering discoveries in optics, statistical mechanics, and fluid mechanics by Plateau (1873a), de Gennes *et al.* (2004), and Newton (2012). An even more noteworthy story is how the self-taught chemist Agnes Pockels (1862–1935) was inspired to study surface tension while doing the dishes. Women were not allowed to enter universities, so she did not have scientific training and could not publish her work in scientific journals (Byers and Williams, 2006). Ten years after her first experiments, she was encouraged to write a letter explaining her findings to Lord Rayleigh, who then forwarded it to the journal *Nature* (Rayleigh, 1891). Along with her

subsequent papers (Pockels, 1892, 1893, 1894, 1926), all of which appeared in top-level journals, she contributed to the establishment of the field of surface science. Without formal training and without access to a lab, Pockels also used simple kitchen tools to develop the precursor to the now widely celebrated Langmuir trough, which is now used to measure the surface pressure of soap molecules and other surfactants upon compression (Fuller and Vermant, 2012).

Soap bubbles comprise a thin aqueous film that is sandwiched between two surfactant layers, where each color corresponds to a different film thickness. The film starts to drain immediately due to gravity (Bhamla and Fuller, 2016). The drainage causes a small deficit in soap concentration at the bubble apex and the formation of a small dimple [Fig. 28(a), left panel]. This gradient in surfactant concentration sets up a Marangoni flow toward the apex. By replenishing interfacial material, these flows stabilize the bubble against rupture. However, such Marangoni flows are short-lived and are quickly destroyed by chaotic flows that destabilize the soap film [Fig. 28(a), right panel]. A simple trick can solve this issue. Bhamla *et al.* (2017) showed that by elevating the soap bubble in multiple small steps through a soap solution (instead of in one large step), it is possible to induce a cascade of Marangoni instabilities. Each Marangoni instability arrests the previous one, and this prevents chaotic flows from developing. This method, called "placing Marangoni instabilities under arrest," produces intricate flow patterns, as displayed in Fig. 28(b).

The rate of draining depends on the viscosity of the soap film. Adding glycerol, a natural ingredient in soap, effectively extends the life span of a bubble. Adding corn syrup or honey does the same job, but it might not help to clean your dishes.

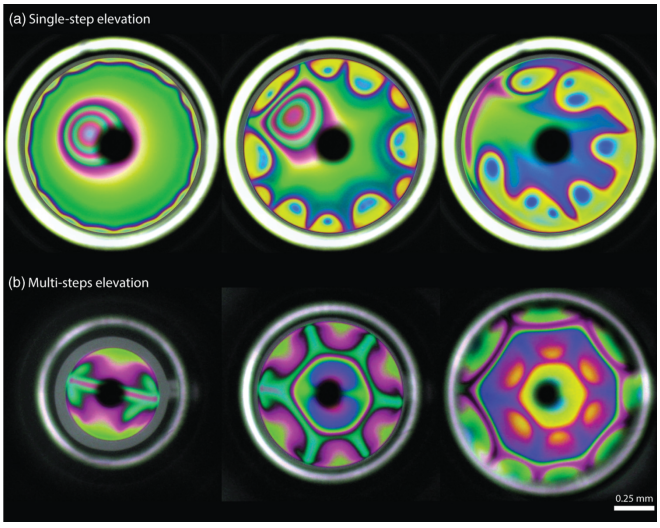

FIG. 28. Thin-film interferograms showing the evolution of surfactant-driven flows in soap bubbles. (a) When the soap bubble is brought through an air-liquid interface in a single step, an unstable dimple forms at the apex. The dimple is quickly washed away by surfactant plumes rising from the periphery. (b) When the bubble is instead elevated in multiple small steps, controllable Marangoni instabilities can be utilized to stabilize the bubble and to prolong its life span. From Bhamla and Fuller, 2016.

However, it will help to make large soap bubbles. By retarding film drainage and reducing the evaporation rate, a bubble stabilized by viscosity has sufficient time to grow before it eventually pops. Another approach was taken by Frazier, Jiang, and Burton (2020). They appreciated the central role of viscoelasticity in bubble stability, where a network of polymer chains holds the thin liquid film together. Using polyethylene glycol, a long-chain polymer commonly found in hand sanitizers, they created bubbles with surface areas of $\sim 100\ \mathrm{m}^2$, the area of a badminton field.

Interfacial fluid mechanics offers interesting avenues for future research. Recently, looking at the hardness of domestic tap water, Giacomin and Fischer (2021) used interfacial rheometry to study how this affects thin films floating on black tea, which crack like sea ice. These films are composed primarily of oxidized polyphenols, salts, and calcium carbonate, and they can be reduced by decreasing water hardness and pH, such as by adding a slice of lemon. Revisiting the work by Sir James Dewar after 100 years, Seimiya and Seimiya (2021) shed new light on the emergence of pearl string structures during bubble drainage. In modern video games, to render bubbles realistically CGI techniques are coupled with interfacial flow models that vary soap film thickness (Ishida *et al.*, 2020). Moreover, in biology the nature of the boundary between water and oil is crucial to many nanometer-scale assembly processes, including biological functions such as protein folding and liquid-liquid phase separation (Chandler, 2007; Hyman, Weber, and Jülicher, 2014).

Finally, when we have finished doing the dishes and we pull the plug from the kitchen sink so that the liquid drains, we observe a vortex (Andersen *et al.*, 2003). When the drain flux is small enough to avoid the formation of a central surface dip, this vortex can be approximated as a Rankine vortex (Tyvand, 2022). The hysteresis in two-liquid whirlpools was investigated by Naumov *et al.* (2022).

D. Ripples and waves

Whenever an interface between two fluids is disturbed, ripples and waves emerge and propagate along the surface; see also Sec. III.A. When a group of waves moves across a pond, we see waves of different wavelengths λ propagating at different speeds and groups of waves traveling at different speeds than the crests and troughs of individual sinusoidal perturbations. The reason for this is the dispersity of water waves. Dispersity refers to the dependence of the wave propagation speed on the wavelength, with longer waves generally traveling faster. For a wave of frequency ω, the relationship between the wave speed c and the wave number k is $c = \omega/k$, where the dependence of the frequency $\omega = \omega(k)$ on the wave number is called the dispersion relation. In a wave packet, where each crest travels at the speed c, the velocity of travel of the entire group is $c_g = d\omega/dk$ and is called the group velocity.

In deep water, where the dispersion relation reads $\omega^2 = gk$, the wave speed $c = \sqrt{g/k}$ is twice as large as the group propagation speed. This is why in a traveling wave packet individual crests will seem to continuously appear at the back of the packet, propagate through it toward the front, and

eventually vanish. Here deep water means that the depth of the layer is much larger than the wavelength ($\lambda = 2\pi/k$), in which case the previously mentioned dispersion relation is obtained from the assumption of a potential flow with a linearized boundary condition at the free surface, which is appropriate when the wave amplitude is smaller than the wavelength (Acheson, 1990). Such waves are referred to as gravity waves.

However, in many small-scale flows, the surface tension forces at the interface cannot be neglected. Accounting for them leads to a dispersion relation for *capillary-gravity waves* $\omega^2 = gk + \gamma k^3/\rho$, where the importance of the surface tension parameter is measured by the dimensionless number $S = \gamma k^2/\rho g$.

For short waves the capillary term dominates, so $S \ll 1$, and the dispersion relation simplifies to $\omega^2 = \gamma k^3/\rho$. Such waves are termed capillary waves, and for water the typical crossover wavelength when $S = 1$ is about 1.7 cm. Notably for capillary waves the group velocity exceeds the wave (or phase) velocity ($c_g = 3c/2$). Therefore, crests move backward in a propagating wave packet. In most small-scale kitchen flows, surface tension has a pronounced effect on the appearance and propagation of waves. A familiar example of this kitchen phenomenon is the waves created by a dripping faucet in a filled sink.

Moreover, in various food science circumstances, we might have to consider waves of wavelength comparable to the depth of the vessel in which they propagate. For such *shallow-water waves*, the propagation speed depends on the local depth, with larger speeds at deeper water. In particular, for gravity waves the dispersion relation becomes in this case $\omega^2 = gk\tanh(kh)$, with h the water depth. This again holds for wavelengths smaller than h. The general case is much more complex and nonlinear in nature, yet the linear wave theory is often enough to grasp the dominant behavior. We have considered here only free-surface flows, but the reasoning can easily be generalized to any fluid-fluid interface (Lamb, 1993).

E. Rinsing flows: Thin-film instabilities

Thin fluid films lead to noteworthy kitchen flows. For example, in a wine decanter thin-film instabilities give rise to ripples that enhance wine aeration [Fig. 3(b)], and similar ripples are seen when one rinses a plate or a chopping board. The stability of falling films was the subject of an investigation by a father-son team of the Kapitza family, led by the elder Nobel Prize winner Pyotr Leonidovich Kapitza, in the 1940s (Kapitza and Kapitza, 1948). After World War II, Kapitza was removed from all his positions, including the directorship of his own Institute for Physical Problems, for refusing to work on nuclear weapons. He was ordered to stay at his house and, deprived of advanced equipment, devised experiments to work on there, including a well-known set of experiments on falling films of liquid (Kalliadasis *et al.*, 2012). Kapitza and Kapitza (1965) were the first to experimentally investigate traveling waves on the free surface of a liquid film falling down a smooth plate. The emerging Kapitza instability takes the form of roll waves (Balmforth and Mandre, 2004) and evolves from a two-dimensional disturbance (i.e., invariant in the spanwise direction) into a fully developed three-dimensional flow (Liu, Schneider, and Gollub, 1995). Since the early works of Kapitza, the dynamics of waves in viscous films over the flat substrates have been extensively reviewed (Chang, 1994; Oron, Davis, and Bankoff, 1997; Craster and Matar, 2009). We often encounter such waves after a rainfall, on an inclined asphalt road, or even in flowing mud (Balmforth and Liu, 2004). Film and rivulet flows at solid surfaces are also important for gas exchange in industrial applications, including distillation columns (De Santos, Melli, and Scriven, 1991), and in coating processes they must be suppressed to obtain a smooth surface without ripples. In the kitchen context, they emerge predominantly in rinsing flows or spreading flows, where the thin-film dynamics may be governed by either capillarity or external driving, such as gravity or centrifugal forces (Walls *et al.*, 2019). We discussed the viscous spreading phenomenon in Sec. VI.D; thus, here we focus purely on the waving instability.

In the Kapitza instability, the formation of the roll waves is governed by two dimensionless parameters: the Reynolds number describing the flow character and the Kapitza number

$$\mathrm{Ka} \sim \frac{\gamma}{\rho g^{1/3}\nu^{1/4}}, \tag{63}$$

where g is the gravitational acceleration driving the flow. The Kapitza number is derived as the ratio of capillary to viscous damping forces $\mathrm{Ka} = (\lambda_c/\lambda_\nu)^2$, where $\lambda_c = (\gamma/\rho g)^{1/2}$ is the capillary length and $\lambda_\nu = (\nu^2/g)^{1/3}$ is the viscous gravity length scale (Kalliadasis *et al.*, 2012; Mendez, Scheid, and Buchlin, 2017). For a flow down a slope with an inclination angle β, the gravitational acceleration g is replaced by its streamwise component $g\sin\beta$. In the context of thin-film flows down an inclined slope, the formation of roll waves can also be discussed in terms of the Froude number (Fr), which is defined in Eq. (13) in Sec. II.H. For moderate Reynolds numbers, the value of $\mathrm{Fr} \approx 2$ marks the onset of instability in the thin-film flow equations (Barker *et al.*, 2017). However, Benjamin showed in his seminal paper (Benjamin, 1957) that such a flow is unstable for all values of Re. He also found that the rates of amplification of unstable waves become small when Re is made fairly small, while their wavelengths tend to increase greatly. He proposed a criterion that, for an observable instability of flow down a slope, the critical Reynolds number is $\mathrm{Re} = (5/6)\cot\beta$, as later corroborated by Yih (1963).

F. Dynamics of falling and rising drops

1. Immiscible drops

When a drop of water is released in cooking oil (or vice versa) it falls (or rises) due to gravity. During its journey, surface traction from the outer liquid mobilizes the fluid-fluid interface, and the degree of surface mobility is given by the viscosity ratio between the ambient and drop fluid $\hat{\mu}/\mu$. For viscous drops translating through low-viscosity liquids [such as a drop of oil rising through water ($\hat{\mu}/\mu \to 0$)], the small surface traction is insufficient to mobilize the interface: this results in the drop translating at the velocity of a rigid Stokes sphere of the same size and volume [see Eq. (43)], which we discussed in Sec. VI.B in regard to the sedimentation

dynamics of coffee grounds. The opposite mobility limit is reached when the viscosity ratio is reversed such that $\hat{\mu}/\mu \to \infty$: the interface is then expected to be completely mobile, which causes a vortex ring to develop within the drop. A completely mobile interface is not able to resist viscous stresses, which reduces the prefactor from 6π to 4π in the Stokes law [Eq. (43)]. This leads to the terminal drop velocity becoming 1.5 times as high as that of a Stokes sphere of the same size and density [Figs. 29(a) and 29(b)]. The solution to the flow field within a translating, rigid drop at low Reynolds number was worked out simultaneously and independently by the French mathematician Hadamard (1911) and the Polish physicist and mathematician Rybczynski (1911).

In reality, most small droplets rise or descend at velocities that lie between the theoretical prediction by Hadamard and Rybczyński and the Stokes prediction for rigid spheres (Manikantan and Squires, 2020), and this is true even in pure liquids with no surfactants added. The terminal velocity generally depends strongly on size, as reported by Bond (1927), who found that small water droplets descended through castor oil at only 1.16 times the Stokes velocity,

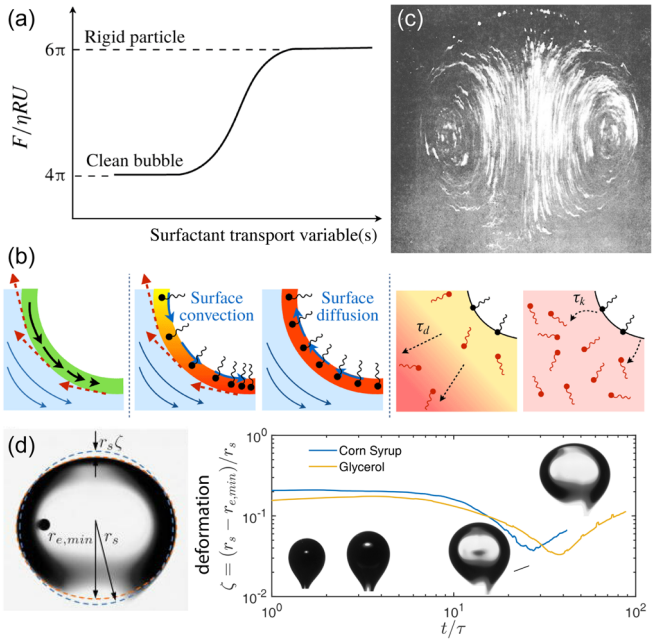

FIG. 29. Interfacial phenomena in bubbles and drops at low Reynolds number. (a) The drag force on a rigid particle is 1.5 times higher than the drag force on a clean bubble having the same size and density. (b) This drag force is affected by "hidden" surfactant transport variables including (i) interfacial viscosity, which can resist the surface flow, (ii) surfactant concentration gradients that generate Marangoni stresses, (iii) Marangoni forces weakened by surface diffusion against the gradient, (iv) diffusive transport of surfactants in the bulk, and (v) adsorption and desorption kinetics of soluble surfactants. (a),(b) From Manikantan and Squires, 2020. (c) Streakline visualization showing the flow field inside a water drop falling through castor oil. From Savic (1953). (d) Water drops ascending through corn syrup and glycerol undergo shape transformations from prolate to oblate spheroids. The travel time t is rescaled by the characteristic mixing time τ from Eq. (61). From Mossige *et al.*, 2021.

while drops exceeding a critical radius of about 0.6 cm descended at 1.4 times the Stokes velocity. To explain the sudden jump in velocity with drop size, Bond and Newton (1928) postulated that a ratio of buoyancy to surface tension determines the mobility of the interface. Boussinesq (1913) instead suggested that an increased viscosity at the drop's surface is responsible for slowing the drop. However, without experimental evidence of the flow field within the drop, it is impossible to judge the correctness of these models.

Aiming to obtain a better description, Savic (1953) published photographic evidence of the flow streamlines inside water droplets descending through castor oil [Fig. 29(c)]. His visualizations showed that the streamline patterns of drops exceeding 1 cm in radius are almost indistinguishable from the Hadamard-Rybczyński solution and that the terminal velocities for large drops are in good agreement with theory as well. However, for smaller drops the vortex rings are shifted forward, and this occurs as a stagnant cap emerges in the rear of the drop. As the drop size is further reduced, the stagnant region covers a larger and larger portion until it envelops the entire drop, with the result of the drop sedimenting as a Stokes sphere.

To explain his observations, Savic (1953) proposed that the interface is immobilized by *surface-active* molecules, which are in turn destabilized by viscous stresses from the outer fluid. For the smallest drops, the viscous stress is insufficient to distort the surface layer; this leads to a complete immobilization. However, as the drop size increases, the shear stress increases as well, and this leads to a gradual removal of the surface layer until the Hadamard-Rybczyński theory is fully recovered for the largest drops.

Savic (1953) developed a theory to calculate the drag of a drop from the degree of surface coverage, which he extracted from the flow visualizations. He also attempted to calculate the critical drop size of the transition between a mobile and an immobile no-slip boundary. However, the transition occurred at larger radii than predicted, and he suggested that this discrepancy was due to a finite solubility between water and castor oil not accounted for in the theoretical model. Later Davis and Acrivos (1966) improved Savic's analysis to obtain better agreement with experiments, and Sadhal and Johnson (1983) extended these results to obtain an exact solution of the drag force on the drop for a given surface coverage. For a droplet sedimenting at a given rate, Sadhal and Johnson (1983) also obtained an analytical expression for the total amount of surfactant adsorbed to the interface. However, the solution to the internal flow field and the corresponding sedimentation rate for a drop of a given size remains an open question.

The literature describing buoyant immiscible drops is vast. We refer the interested reader to the many reviews and books written on this topic; see Harper (1972) and Leal (2007).

2. Miscible drops

Compared to immiscible drops covered in Sec. IX.F.1, transport problems involving buoyant miscible drops have enjoyed far less attention, and as a result their dynamics is far from understood. Or, in the words of Joseph and Renardy, "A basic and basically unsolved problem of fluid dynamics is

to determine the evolution of rising bubbles and falling drops of one miscible liquid in another" (Joseph and Renardy, 2013). In Sec. VIII.F we looked at how fluid motion can accelerate the mixing rate between a viscous drop and its surroundings in the low Reynolds number case. In this section, we discuss how finite inertia may influence the shape of falling drops, and we also address the stabilizing effects of transient tensions between miscible liquids.

When a miscible drop descends into another liquid, it changes shape in response to the viscous drag acting on it, and when it reaches a critical velocity, inertial effects also start to play a role. A simple way to visualize the effect of inertia on the drop shape is to produce a drop of food dye in air and let it fall into a glass of water. Upon impact with the water surface, the central part of the drop gets accelerated upward in a Rayleigh-Taylor instability, and this causes the drop to evolve into an open torus. For drops made of honey or corn syrup, this shape transformation is delayed by the high viscosity, but on a long timescale even the most viscous drops deform into oblate spheroids or donuts.

Kojima, Hinch, and Acrivos (1984) developed a theory to explain the shape transitions of miscible drops and validated their theory against experiments with corn syrup drops falling through diluted corn syrup solutions. They showed that when the drop is created in air immediately above a water surface, the descending drop does not experience inertia in the early stages of its descent. In this case, it is deformed solely by viscous traction forces, causing the drop to develop into an oblate spheroid. However, later in the drop's descent, inertia does play a key role in its shape evolution, and this causes the drop to develop into an open torus. The fact that inertia is relevant at long timescales is intuitive; however, they also had to incorporate a small but finite tension across the miscible interface to fully explain the material deformation. Recently Mossige *et al.* (2021) examined the inverted system concerning water drops ascending through corn syrup [Fig. 29(d)].

The tension existing between miscible liquids is not a surface tension as defined in the classical sense between immiscible phases; see Sec. II.E. Instead, it is caused by sharp gradients in composition between the pure phases by giving rise to so-called Korteweg stresses (Joseph, Huang, and Hu, 1996) that mimic the effect of a surface tension. These tensions are typically at least 2 orders of magnitude smaller than the surface tension between immiscible fluids [for example, 0.43 mN/m between glycerol and water (Petitjeans and Maxworthy, 1996), as compared to 73 mN/m between water and air] and diminish in time as diffusion smears out the miscible interface. As a result, they are inherently difficult to measure and are usually neglected. However, in many situations, including miscible displacements in capillary tubes (Chen and Meiburg, 2002) and in Hele-Shaw geometries (Chen *et al.*, 2008), effective interfacial tensions must be accounted for to accurately describe a deforming, miscible interface; theoretical and experimental evidence for this was given by Davis (1988), Joseph (1990), Pojman *et al.* (2006), Zoltowski *et al.* (2007), Lacaze *et al.* (2010), and Joseph and Renardy (2013). Nonequilibrium stresses not only are of academic interest but also can be tuned to control the morphology of miscible interfaces in modern industrial processes. Notably Krishne Gowda *et al.* (2019) utilized transient tensions to align nanofibrils in microfluidic flow focusing geometries, with implications for the paper production industry and in the development of new, sustainable alternatives to plastics, and Wylock *et al.* (2014) explored its potential for controlling gravitational instabilities, with relevance to carbon sequestration plants.

X. DISCUSSION

In this review, we presented an overview of culinary fluid mechanics and other currents in food science. We discussed the notion that, starting in ancient times, the connection between cooking and fluid mechanics has led to innovations that benefit both. As Toussaint-Samat (2009) put it,

> "Eating, at first a purely visceral pleasure, became an intellectual process."

We explored throughout this review how the connection between science and food grows stronger every day, all the way to the frontier of modern research and gastronomy. Since kitchen science is so accessible, we can learn a great deal just by observing simple phenomena and seeing how they are connected. Therefore, innovations in fluid mechanics lead to better food, but creativity in cooking can also generate new knowledge in different areas. Indeed, culinary fluid mechanics brings together people from across society, from chefs to food scientists, physicists and chemical engineers, medical and nutrition specialists, and students across the disciplines.

A. Summary

To make this review accessible to a broad audience, we started our discussion with an overview of kitchen sink fundamentals (Sec. II), where we summarized the basics of fluid mechanics in the context of food science. Beginning the meal with drinks (Sec. III), we reviewed hydrodynamic instabilities in cocktails, Marangoni flows, bubble effervescence, and culinary foams. Getting into the thick of it with a soup for starter (Sec. IV), we discussed the rheological properties of viscoelastic food, nonlinear sauces, suspensions, and emulsions. Moving on to a hot main course (Sec. V), we analyzed the role of heat in cooking, including the Leidenfrost effect, Rayleigh-Bénard convection, double-diffusive convection, flames, and smoke. Going for a sticky desert (Sec. VI), we described flows at low Reynolds numbers, from Stokes's law to lubrication theory, viscous gravity currents, ice cream, and microbial fluid dynamics. Eager for a postprandial espresso (Sec. VII), we examined the physics of granular matter and porous media flows, different brewing methods, and the coffee-ring effect. Thirsty for another cup of tea (Sec. VIII), we delineated the tea leaf paradox and other nonlinear flows, succeeded by turbulence and chaos. Finally, when doing the dishes (Sec. IX), we explored interfacial phenomena including the Gibbs surface elasticity, soap film dynamics, waves and jets, miscible drops, and roll-wave instabilities. It was quite a bit to digest, but a place worth coming back to.

B. Learning from kitchen experiments

Humans are naturally curious. From infancy, we explore by actively interacting with our surroundings (Lindholm, 2018). Through touch, smell, and taste, we learn about the natural world. Becoming a scientist starts with questions like "what?," "why?," and "how?"

In physics education, we try to answer these questions by comparing observations to theoretical descriptions. Traditionally, this knowledge is transferred from teacher to students through in-class lecturing and instructor-made assignments (Cagiltay, Yildirim, and Aksu, 2006), but this linear learning protocol is not necessarily compatible with curiosity-driven exploration and observation (Kallick and Zmuda, 2017). As a result, the physics topics taught in class often feel alien to students (Rowat *et al.*, 2014), who subsequently lose the natural intuition and curiosity that is so important for learning (Jirout, Vitiello, and Zumbrunn, 2018; Gruber, Valji, and Ranganath, 2019). Inevitably physics has a reputation for being difficult and abstract, with little relevance to students' daily lives, and this disconnect is largely responsible for the relatively poor recruitment in science and education disciplines in higher education (Tobias and Birrer, 1999). To address this issue, it is vital to develop effective teaching strategies that foster intuition, engagement, and curiosity. This is best achieved through a hands-on active learning strategy (Deslauriers, Schelew, and Wieman, 2011; Freeman *et al.*, 2014), without creating the perception of learning by ineffective engagement (Deslauriers *et al.*, 2019), where experiments that relate to our daily lives play a prominent role.

The kitchen is an accessible learning environment where simple physics experiments can be performed at home with humble ingredients. Nelson (2022) recently described how rheology can be made more accessible using food materials, and Hossain and Ewoldt (2022) provided a detailed toolbox for do-it-yourself rheometry. Morover, Benjamin (1999) showed that students in elementary physics education can learn about surface tension, mixing, and gravity by studying Rayleigh-Taylor instabilities (see Sec. III.A) in their own kitchens. The simple experimental design allowed for a high degree of flexibility and was formulated in such a way that they could be performed either individually or in groups to foster collective accomplishment and collaborative learning. Compared to experiments conducted in school laboratories, kitchen experiments have a greater potential for engagement, as we encounter them every day. Moreover, since they require little equipment, they offer a low-cost "frugal science" alternative that is less susceptible to budget cuts, and more accessible to students from underrepresented socioeconomic backgrounds (Whitesides, 2011; Byagathvalli, Challita, and Bhamla, 2021).

Affordable and accessible kitchen experiments can also be utilized to develop intuition for advanced mathematical concepts. Notably a famous class at Harvard and the University of California, Los Angeles teaches general physics concepts such as heat transfer and phase transformations to nonscience majors through the lens of cooking [Figs. 30(a)–30(c)] (Rowat *et al.*, 2014). In this popular course, top chefs give weekly seminars for further engagement. Kitchen experiments can also be used to learn

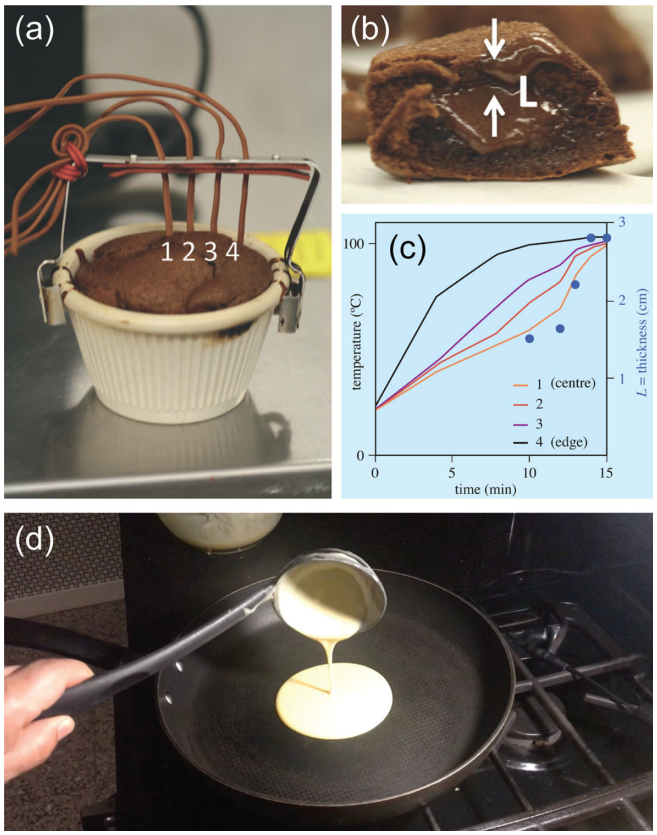

FIG. 30. Kitchen-based learning is an affordable and accessible strategy to foster curiosity and intuition for a wide range of physics topics and to engage people of different backgrounds, ages, and interests. In a science class for nonscience majors, cake making was used to demonstrate heat transfer and elasticity. (a) Thermocouples are used to measure the rise in temperature at different points inside a molten chocolate cake as it bakes in the oven. (b) The thickness of the solid crust of the cake L increases over time. (c) Results of experiments. (a)–(c) From Rowat *et al.*, 2014. (d) Students pour pancake batter to learn about viscous gravity currents. They used cell phones to video-record the spreading rate and fit their data into a theoretical model to back-calculate the viscosity. Courtesy of Roberto Zenit.

about more specialized topics in fluid mechanics. For example, take-home experiments such as measurement of the flow rate from a hose and estimation of the density and the viscosity of household fluids have been used to enhance learning in an introductory fluid mechanics class (Kaye, 2021). In addition, the kitchen can be a gateway to learning about the intrinsic fluid properties that govern these flows. Notably, in a special session on "Kitchen Flows" at the 73rd Annual Meeting of the APS Division of Fluid Dynamics, Zenit *et al.* (2020) demonstrated how pancake making can be used to teach students about fluid viscosity. Instead of extracting the viscosity from a classical sedimenting-sphere experiment (Sutterby, 1973), which is less common in our daily lives, the students were asked to pour pancake batter and other viscous fluids like honey and syrup into frying pans and then to measure the spreading rate [Fig. 30(d)]. By fitting their data to a theoretical prediction (Huppert, 1982b) that is described in Sec. VI.D, the students were able to back-calculate the viscosity. In the proposed course of

do-it-yourself rheometry, Hossain and Ewoldt (2022) outlined an efficient way to convey the key notions of rheology to students confined to their homes due to the pandemic. Even twisting an Oreo can be an inspiring physics experiment (Owens *et al.*, 2022). Such *in situ* kitchen measurements can be used for numerous other scientific concepts, as discussed throughout this review, thus creating direct links between physics and everyday experiences.

In addition, many canonical flows can be generated with simple kitchen tools, including circular hydraulic jumps (see Sec. II.H) and Poiseuille flows (Sec. II.C), which can be used to validate theoretical predictions taught in class as a means of developing intuition for advanced mathematical concepts. Moreover, Kaye and Ogle (2022) developed a pedagogical approach with hands-on activities to tackle common misconceptions in fluid mechanics education. Finally, to further accelerate the learning in fluid mechanics, e-learning tools can be implemented (Rahman, 2017), such as the extremely extensive Multimedia Fluid Mechanics Online (Homsy, 2019).

From these examples, it is evident that easy-to-perform kitchen experiments can be implemented for enhanced learning and engagement at all ages. They are highly scalable and can even be taught on an online platform to make learning available for large groups of students, including students who cannot afford enrollment in an educational program. Therefore, kitchen-based learning represents a viable strategy to increase the number of competent scientists and engineers in the world, which is necessary to address immediate threats to humankind and ensure a sustainable future (Sheppard *et al.*, 2008).

C. Curiosity-driven research

As well as being a vehicle for accessible and affordable science education, culinary fluid mechanics is a hot spot for curiosity-driven research (Agar, 2017; Fuller *et al.*, 2022). Indeed, Agnes Pockels found inspiration for her breakthrough discoveries in surface science and hydrodynamic instabilities from dishwashing (Sec. IX). Valuable data can be extracted relatively quickly from a kitchen-based laboratory, in the spirit of a "Friday afternoon experiment" (Smith, 2015). A minimum of investment in time, training, and equipment is needed, which makes this field approachable not only to experimentalists but also to theorists and researchers in other fields. Since many kitchen flows can be described by scaling theories and other analytical techniques, they can serve to validate theoretical models in fluid mechanics and materials science (Tao *et al.*, 2021). As such, kitchen experiments are attractive to theorists and, by lowering the activation barrier to start a new experiment, they can be combined with mathematical models to solve a large class of problems in science and engineering. Curiosity-driven learning is foundational to human cognition (Ten *et al.*, 2021), and sometimes the best discoveries are made in a few hours.

Perhaps the most influential fluid mechanician of all time Sir G. I. Taylor, was known for his special ability to make groundbreaking discoveries from humble ingredients and to design simple experiments that could be described theoretically (Batchelor, 1996). Instead of following the hype in science and "going with the flow," Taylor was driven merely by his own interest and curiosity, without consideration of specific applications. Outstanding contributions in fundamental science always find useful applications, which is immediately evident when we look at the great implications of Taylor's contributions to science and engineering. However, today's funding schemes often require research to preferentially address a particular problem and have immediate impact (Amon, 2015), which leaves little room for curiosity-driven research or scientific investigations for their own sake (Woxenius, 2015). But, since curiosity is a prerequisite for exploration and discovery, the scientific philosophy of Taylor and his predecessors could serve as inspiration for the modern physicist.

D. Conclusion

Culinary fluid mechanics is the study of everything that flows in the food supply chain, covering a wide range of surprising phenomena that can be harnessed for the benefit of gastronomy, for the benefit of food science, and for our planet as a whole. This field naturally connects practical technologies with basic research, which is just how fluid mechanics started. Culinary flows are accessible to experimentalists and theorists alike: Their intuitive geometry and well-defined conditions are suitable for mathematical modeling, while the relatively low equipment costs reduce the activation energy for pilot investigations, thus catalyzing curiosity-driven education (Sec. X.B) and research (Sec. X.C).

Where "kitchen science" papers may initially have been considered occasional or incidental, their breadth and depth now constitute a rapidly growing field. It is a field that this review can cover only partially because it is so interconnected. Yet, culinary fluid mechanics is unified by a number of well-defined research directions and goals: First, it aims to establish a sustainable and fair global food supply (Bloemhof and Soysal, 2017). Second, it has the potential to develop reliable food technologies with a strong fundamental backbone (Knorr *et al.*, 2011; López-Alt, 2015). Third, it can facilitate new discoveries far beyond gastronomy, particularly by making science and engineering more accessible (White and Frederiksen, 1998; Lee and Butler, 2003; Tuosto *et al.*, 2020; Nelson, 2022). Finally, it can advise policy makers on important decisions for our future generations, such as the announced European Union ban on PFAS nonstick coatings by 2030 (European Commission, 2020b), and help to reduce climate change (Dauxois *et al.*, 2021; Masson-Delmotte *et al.*, 2021). To achieve these goals, scientists from related fields must become even more interconnected.

Indeed, as discussed, culinary fluid mechanics directly links to other disciplines across the sciences, from molecular gastronomy to biological tissue mechanics and rheology. Furthermore, it has extensive engineering applications ranging from the steam engine to 3D printing and nanotechnology. Not least, there are immediate connections with food safety, microbiology, and medicine. However, unlike many fields in science, kitchen flows create a bond with people who do not have any scientific training: people who want to learn more and people who want to make contributions, like when Agnes Pockels wrote to Lord Rayleigh. So much talent is lost in this world full of inequality, and we have a responsibility to make

science more inclusive and accessible to people from underrepresented backgrounds through science communication, education, and research itself. We hope that more scientists will stand up to this challenge.

ACKNOWLEDGMENTS

We express our gratitude to many colleagues and friends, including but not limited to Anurag Agarwal, Paulo Arratia, Andrea Bertozzi, Michael Brenner, Rajesh Bhagat, Saad Bhamla, Tomas Bohr, Daniel Bonn, John Bush, Otger Campas, Matteo Cantiello, Sam Dehaeck, Damir Dorančić, Douglas Durian, Jan Engmann, Pere Castells Esqué, Peter Fischer, Jamie Foster, Gerald G. Fuller, Ion Furjanic, Yuqian Gan, Jeffrey Giacomin, William Gilpin, Nigel Goldenfeld, Elisabeth Guazzelli, Christopher Hendon, Andrzej Herczyński, Douglas Jerolmack, George Karniadakis, Kiran Kembhavimathada, Rouslan Krechetnikov, Gérard Liger-Belair, Harishankar Manikantan, Hassan Masoud, Philip Nelson, Enrico Nobile, Crystal Owens, Rosanna Pasquino, Pax Piewpun, David Quéré, Ingo Rehberg, Daniel Rosenberg, Amy Rowat, Alban Sauret, Bernhard Scheichl, Gary Settles, Tanu Singla, Pia Sorensen, Todd Squires, Howard Stone, Jean-Luc Thiffeault, Hugo Ulloa, Jan Vermant, Fabian Wadsworth, David Weitz, Tomoaki Watamura, John Wettlaufer, Stuart Williams, Nan Xue, Harunori Yoshikawa, Yonghao Yue, and Roberto Zenit for engaging in stimulating conversations, suggesting changes, providing figures, sharing their enthusiasm, and offering invaluable support. A. J. T. M. M. acknowledges funding from the U.S. Department of Agriculture (USDA-NIFA AFRI Grants No. 2020-67017-30776 and No. 2020-67015-32330) and the University of Pennsylvania (Klein Family Social Justice Grant).

REFERENCES

Abarzhi, S. I., A. K. Bhowmick, A. Naveh, A. Pandian, N. C. Swisher, R. F. Stellingwerf, and W. D. Arnett, 2019, "Supernova, nuclear synthesis, fluid instabilities, and interfacial mixing," Proc. Natl. Acad. Sci. U.S.A. **116**, 18184–18192.

Abdelaziz, A., and R. E. Khayat, 2022, "On the non-circular hydraulic jump for an impinging inclined jet," Phys. Fluids **34**, 023603.

Abkarian, M., S. Protière, J. M. Aristoff, and H. A. Stone, 2013, "Gravity-induced encapsulation of liquids by destabilization of granular rafts," Nat. Commun. **4**, 1895.

Abu-Farah, L., and N. Germann, 2022, "Simulations of thermal phase changes and bacterial inactivation in a superheated steam dishwasher," Phys. Fluids **34**, 085137.

Acheson, D. J., 1990, *Elementary Fluid Dynamics* (Clarendon Press, Oxford).

Acrivos, A., and J. D. Goddard, 1965, "Asymptotic expansions for laminar forced-convection heat and mass transfer," J. Fluid Mech. **23**, 273–291.

Adler, P. M., J.-F. Thovert, and V. V. Mourzenko, 2013, *Fractured Porous Media* (Oxford University Press, New York).

Agar, J., 2017, "2016 Wilkins-Bernal-Medawar lecture: The curious history of curiosity-driven research," Notes Rec. R. Soc. **71**, 409–429.

Aguirre, M. A., J. G. Grande, A. Calvo, L. A. Pugnaloni, and J.-C. Géminard, 2010, "Pressure Independence of Granular Flow through an Aperture," Phys. Rev. Lett. **104**, 238002.

Aharoni, H., D. V. Todorova, O. Albarrán, L. Goehring, R. D. Kamien, and E. Katifori, 2017, "The smectic order of wrinkles," Nat. Commun. **8**, 1–7.

Ahlers, G., S. Grossmann, and D. Lohse, 2009, "Heat transfer and large scale dynamics in turbulent Rayleigh-Bénard convection," Rev. Mod. Phys. **81**, 503–537.

Ahmed, J., P. Ptaszek, and S. Basu, 2016, *Advances in Food Rheology and Its Applications* (Woodhead Publishing, Sawston, England).

Albanese, L., R. Ciriminna, F. Meneguzzo, and M. Pagliaro, 2017a, "Beer-brewing powered by controlled hydrodynamic cavitation: Theory and real-scale experiments," J. Cleaner Prod. **142**, 1457–1470.

Albanese, L., R. Ciriminna, F. Meneguzzo, and M. Pagliaro, 2017b, "Gluten reduction in beer by hydrodynamic cavitation assisted brewing of barley malts," LWT Food Sci. Technol. **82**, 342–353.

Al-Hashemi, H. M. B., and O. S. B. Al-Amoudi, 2018, "A review on the angle of repose of granular materials," Powder Technol. **330**, 397–417.

Ali, A. A., A. B. Altemimi, N. Alhelfi, and S. A. Ibrahim, 2020, "Application of biosensors for detection of pathogenic food bacteria: A review," Biosensors **10**, 58.

Almoustafa, H. A., M. A. Alshawsh, and Z. Chik, 2017, "Technical aspects of preparing PEG-PLGA nanoparticles as carrier for chemotherapeutic agents by nanoprecipitation method," Int. J. Pharm. **533**, 275–284.

Alonso-Marroquin, F., and P. Mora, 2021, "Beverloo law for hopper flow derived from self-similar profiles," Granular Matter **23**, 1–8.

Alzamora, S. M., P. E. Viollaz, V. Y. Martínez, A. B. Nieto, and D. Salvatori, 2008, "Exploring the linear viscoelastic properties structure relationship in processed fruit tissues," in *Food Engineering: Integrated Approaches*, edited by G. F. Gutiérrez-López, G. V. Barbosa-Cánovas, J. Welti-Chanes, and E. Parada-Arias (Springer, New York), pp. 155–181.

Amagliani, L., and C. Schmitt, 2017, "Globular plant protein aggregates for stabilization of food foams and emulsions," Trends Food Sci. Technol. **67**, 248–259.

American Physical Society Press Office, 2020a, "Lab closed? Head to the kitchen," https://aps.org/newsroom/vpr/dfd/2020/11-22-2020-03.cfm.

Amit, S. K., M. M. Uddin, R. Rahman, S. R. Islam, and M. S. Khan, 2017, "A review on mechanisms and commercial aspects of food preservation and processing," Agric. Food Secur. **6**, 1–22.

Amon, A., 2015, "A case for more curiosity-driven basic research," Mol. Biol. Cell **26**, 3690–3691.

Amundson, R., A. A. Berhe, J. W. Hopmans, C. Olson, A. E. Sztein, and D. L. Sparks, 2015, "Soil and human security in the 21st century," Science **348**, 1261071.

Andac, T., P. Weigmann, S. K. Velu, E. Pinçe, G. Volpe, G. Volpe, and A. Callegari, 2019, "Active matter alters the growth dynamics of coffee rings," Soft Matter **15**, 1488–1496.

Andersen, A., T. Bohr, B. Stenum, J. J. Rasmussen, and B. Lautrup, 2003, "Anatomy of a Bathtub Vortex," Phys. Rev. Lett. **91**, 104502.

Anderson, J. L., 1986, "Transport mechanisms of biological colloids," Ann. N.Y. Acad. Sci. **469**, 166.

Anderson, J. L., 1989, "Colloid transport by interfacial forces," Annu. Rev. Fluid Mech. **21**, 61–99.

Anderson, Jr., J. D., 2017, *Fundamentals of Aerodynamics*, 6th ed. (McGraw-Hill, New York).

Andrews, M. J., and S. B. Dalziel, 2010, "Small Atwood number Rayleigh-Taylor experiments," Phil. Trans. R. Soc. A **368**, 1663–1679.

Angeloni, G., L. Guerrini, P. Masella, M. Innocenti, M. Bellumori, and A. Parenti, 2019, "Characterization and comparison of cold brew and cold drip coffee extraction methods," J. Sci. Food Agric. **99**, 391–399.

Anna, S. L., 2016, "Droplets and bubbles in microfluidic devices," Annu. Rev. Fluid Mech. **48**, 285–309.

Aoyagi, H., H. Yokoi, and H. Tanaka, 1992, "Measurement of fresh and dry densities of suspended plant cells and estimation of their water content," J. Ferment. Bioeng. **73**, 490–496.

Arbuckle, W. S., 2013, *Ice Cream* (Springer, Boston).

Aref, H., 1984, "Stirring by chaotic advection," J. Fluid Mech. **143**, 1–21.

Aref, H., *et al.*, 2017, "Frontiers of chaotic advection," Rev. Mod. Phys. **89**, 025007.

Arendt, E. K., L. A. Ryan, and F. Dal Bello, 2007, "Impact of sourdough on the texture of bread," Food Microbiol. **24**, 165–174.

Arifin, D. R., L. Y. Yeo, and J. R. Friend, 2007, "Microfluidic blood plasma separation via bulk electrohydrodynamic flows," Biomicrofluidics **1**, 014103.

Arnold, H. D., 1911, "Limitations imposed by slip and inertia terms upon Stokes's law for the motion of spheres through liquids," Phys. Rev. **32**, 233.

Arnold, V. I., and B. A. Khesin, 1998, *Topological Methods in Hydrodynamics*, Applied Mathematical Sciences Vol. 125 (Springer-Verlag, New York).

Asaithambi, N., P. Singha, M. Dwivedi, and S. K. Singh, 2019, "Hydrodynamic cavitation and its application in food and beverage industry: A review," J. Food Process Eng. **42**, e13144.

Ashurst, P. R., 2012, *Food Flavorings* (Springer, New York).

Assenza, S., and R. Mezzenga, 2019, "Soft condensed matter physics of foods and macronutrients," Nat. Rev. Phys. **1**, 551–566.

Audoly, B., and S. Neukirch, 2005, "Fragmentation of Rods by Cascading Cracks: Why Spaghetti Does Not Break in Half," Phys. Rev. Lett. **95**, 095505.

Avallone, P. R., P. Iaccarino, N. Grizzuti, R. Pasquino, and E. Di Maio, 2022, "Rheology-driven design of pizza gas foaming," Phys. Fluids **34**, 033109.

Avila, K., D. Moxey, A. De Lozar, M. Avila, D. Barkley, and B. Hof, 2011, "The onset of turbulence in pipe flow," Science **333**, 192–196.

Avila, M., D. Barkley, and B. Hof, 2022, "Transition to turbulence in pipe flow," Annu. Rev. Fluid Mech. **55**, 575–602.

Azola, A., J. Palmer, R. Mulheren, R. Hofer, F. Fischmeister, and W. T. Fitch, 2018, "The physiology of oral whistling: A combined radiographic and MRI analysis," J. Appl. Physiol. **124**, 34–39.

Bajer, K., and H. K. Moffatt, 1990, "On a class of steady confined Stokes flows with chaotic streamlines," J. Fluid Mech. **212**, 337–363.

Bajpai, V. K., M. Kamle, S. Shukla, D. K. Mahato, P. Chandra, S. K. Hwang, P. Kumar, Y. S. Huh, and Y.-K. Han, 2018, "Prospects of using nanotechnology for food preservation, safety, and security," J. Food Drug Anal. **26**, 1201–1214.

Baker, Jr., D. J., 1968, "Demonstrations of fluid flow in a rotating system II: The 'spin-up' problem," Am. J. Phys. **36**, 980–986.

Balboa-Lagunero, T., T. Arroyo, J. M. Cabellos, and M. Aznar, 2011, "Sensory and olfactometric profiles of red wines after natural and forced oxidation processes," Am. J. Enol. Vitic. **62**, 527–535.

Balmforth, N. J., I. A. Frigaard, and G. Ovarlez, 2014, "Yielding to stress: Recent developments in viscoplastic fluid mechanics," Annu. Rev. Fluid Mech. **46**, 121–146.

Balmforth, N. J., and J. J. Liu, 2004, "Roll waves in mud," J. Fluid Mech. **519**, 33–54.

Balmforth, N. J., and S. Mandre, 2004, "Dynamics of roll waves," J. Fluid Mech. **514**, 1–33.

Bamforth, C., 2009, *Beer: Tap into the Art and Science of Brewing* (Oxford University Press, New York).

Barham, P., L. H. Skibsted, W. L. P. Bredie, M. Bom Frøst, P. Møller, J. Risbo, P. Snitkjær, and L. M. Mortensen, 2010, "Molecular gastronomy: A new emerging scientific discipline," Chem. Rev. **110**, 2313–2365.

Barker, B., M. A. Johnson, P. Noble, L. M. Rodrigues, and K. Zumbrun, 2017, "Note on the stability of viscous roll waves," C.R. Mec. **345**, 125–129.

Barker, G. C., 2013, "Granular and jammed food materials," in *Food Microstructures: Microscopy, Measurement and Modelling*, edited by V. J. Morris and K. Groves (Elsevier, New York), pp. 325–335.

Barnes, H. A., 1994, "Rheology of emulsions—A review," Colloids Surf. A **91**, 89–95.

Barnes, W. J. P., 1999, "Tree frogs and tire technology," Tire Technol. Int. **99**, 42–47, https://www.researchgate.net/publication/313714428_Tree_frogs_and_tire_technology.

Barnes, W. J. P., 2007, "Biomimetic solutions to sticky problems," Science **318**, 203–204.

Bar-On, Y. M., A. Flamholz, R. Phillips, and R. Milo, 2020, "Science forum: SARS-CoV-2 (COVID-19) by the numbers," eLife **9**, e57309.

Barrass, B., and D. R. Derrett, 2011, *Ship Stability for Masters and Mates* (Elsevier, New York).

Barros, D., Borée, J., B. R. Noack, A. Spohn, and T. Ruiz, 2016, "Bluff body drag manipulation using pulsed jets and Coanda effect," J. Fluid Mech. **805**, 422–459.

Barthes-Biesel, D., and A. Acrivos, 1973, "Deformation and burst of a liquid droplet freely suspended in a linear shear field," J. Fluid Mech. **61**, 1–22.

Barthlott, W., M. Mail, B. Bhushan, and K. Koch, 2017, "Plant surfaces: Structures and functions for biomimetic innovations," Nano-Micro Lett. **9**, 23.

Batali, M. E., W. D. Ristenpart, and J.-X. Guinard, 2020, "Brew temperature, at fixed brew strength and extraction, has little impact on the sensory profile of drip brew coffee," Sci. Rep. **10**, 1–14.

Batchelor, G. K., 1954, "Heat convection and buoyancy effects in fluids," Q. J. R. Meteorol. Soc. **80**, 339–358.

Batchelor, G. K., 1970, "Slender-body theory for particles of arbitrary cross-section in Stokes flow," J. Fluid Mech. **44**, 419–440.

Batchelor, G. K., 1972, "Sedimentation in a dilute dispersion of spheres," J. Fluid Mech. **52**, 245–268.

Batchelor, G. K., 1996, *The Life and Legacy of G. I. Taylor* (Cambridge University Press, Cambridge, England).

Batchelor, G. K., 2000, *An Introduction to Fluid Dynamics* (Cambridge University Press, Cambridge, England).

Baxter, J., U. Tüzün, D. Heyes, I. Hayati, and P. Fredlund, 1998, "Stratification in poured granular heaps," Nature (London) **391**, 136–136.

BBC Earth Unplugged, 2013, "Water flows uphill! Leidenfrost effect," https://www.youtube.com/watch?v=hIXFxP_6m7I (accessed May 25, 2020).

Bear, J., 2013, *Dynamics of Fluids in Porous Media* (Dover Publications, New York).

Bearman, P. W., 1984, "Vortex shedding from oscillating bluff bodies," Annu. Rev. Fluid Mech. **16**, 195–222.

Bearman, P. W., and J. K. Harvey, 1976, "Golf ball aerodynamics," Aeronaut. Q. **27**, 112–122.

Beaumont, F., G. Liger-Belair, and G. Polidori, 2015, "Flow analysis from PIV in engraved champagne tasting glasses: Flute versus coupe," Exp. Fluids **56**, 1–6.

Beaumont, F., G. Liger-Belair, and G. Polidori, 2016, "Unveiling self-organized two-dimensional (2D) convective cells in champagne glasses," J. Food Eng. **188**, 58–65.

Beaumont, F., G. Liger-Belair, and G. Polidori, 2020, "Computational fluid dynamics (CFD) as a tool for investigating self-organized ascending bubble-driven flow patterns in champagne glasses," Foods **9**, 972.

Bechinger, C., R. Di Leonardo, H. Löwen, C. Reichhardt, G. Volpe, and G. Volpe, 2016, "Active particles in complex and crowded environments," Rev. Mod. Phys. **88**, 045006.

Behroozi, P., K. Cordray, W. Griffin, and F. Behroozi, 2007, "The calming effect of oil on water," Am. J. Phys. **75**, 407–414.

Belden, J., R. C. Hurd, M. A. Jandron, A. F. Bower, and T. T. Truscott, 2016, "Elastic spheres can walk on water," Nat. Commun. **7**, 10551.

Benabdelhalim, H., and D. Brutin, 2022, "Phase separation and spreading dynamics of French vinaigrette," Phys. Fluids **34**, 012120.

Benezech, T., and J. Maingonnat, 1994, "Characterization of the rheological properties of yoghurt—A review," J. Food Eng. **21**, 447–472.

Benjamin, R. F., 1999, "Rayleigh-Taylor instability—Fascinating gateway to the study of fluid dynamics," Phys. Teach. **37**, 332–336.

Benjamin, T. B., 1957, "Wave formation in laminar flow down an inclined plane," J. Fluid Mech. **2**, 554–573.

Benjamin, T. B., 1967, "Internal waves of permanent form in fluids of great depth," J. Fluid Mech. **29**, 559–592.

Bentley, B. J., and L. G. Leal, 1986a, "A computer-controlled four-roll mill for investigations of particle and drop dynamics in two-dimensional linear shear flows," J. Fluid Mech. **167**, 219–240.

Bentley, B. J., and L. G. Leal, 1986b, "An experimental investigation of drop deformation and breakup in steady, two-dimensional linear flows," J. Fluid Mech. **167**, 241–283.

Bergmann, R., L. Tophøj, T. A. M. Homan, P. Hersen, A. Andersen, and T. Bohr, 2011, "Polygon formation and surface flow on a rotating fluid surface," J. Fluid Mech. **679**, 415.

Bernstein, B., D. A. Hall, and H. M. Trent, 1958, "On the dynamics of a bull whip," J. Acoust. Soc. Am. **30**, 1112–1115.

Berre, I., F. Doster, and E. Keilegavlen, 2019, "Flow in fractured porous media: A review of conceptual models and discretization approaches," Transp. Porous Media **130**, 215–236.

Berry, J. D., M. J. Neeson, R. R. Dagastine, D. Y. C. Chan, and R. F. Tabor, 2015, "Measurement of surface and interfacial tension using pendant drop tensiometry," J. Colloid Interface Sci. **454**, 226–237.

Bertho, Y., B. Darbois Texier, and L. Pauchard, 2022, "Egg-speriments: Stretch, crack, and spin," Phys. Fluids **34**, 033101.

Berton-Carabin, C. C., L. Sagis, and K. Schroën, 2018, "Formation, structure, and functionality of interfacial layers in food emulsions," Annu. Rev. Food Sci. Technol. **9**, 551–587.

Best, E. L., P. Parnell, and M. H. Wilcox, 2014, "Microbiological comparison of hand-drying methods: The potential for contamination of the environment, user, and bystander," J. Hosp. Infect. **88**, 199–206.

Beverloo, W. A., H. A. Leniger, and J. Van de Velde, 1961, "The flow of granular solids through orifices," Chem. Eng. Sci. **15**, 260–269.

Bez, I., 2021, "Latte art guide," https://www.latteartguide.com/ (accessed October 27, 2021).

Bhagat, R. K., N. Jha, P. Linden, and D. I. Wilson, 2018, "On the origin of the circular hydraulic jump in a thin liquid film," J. Fluid Mech. **851**, R5.

Bhagat, R. K., and P. F. Linden, 2020, "The circular capillary jump," J. Fluid Mech. **896**, A25.

Bhagat, R. K., and P. F. Linden, 2022, "The circular hydraulic jump; the influence of downstream flow on the jump radius," Phys. Fluids **34**, 072111.

Bhamla, M. S., C. Chai, M. A. Alvarez-Valenzuela, J. Tajuelo, and G. G. Fuller, 2017, "Interfacial mechanisms for stability of surfactant-laden films," PLoS One **12**, e0175753.

Bhamla, M. S., and G. G. Fuller, 2016, "Placing Marangoni instabilities under arrest," Phys. Rev. Fluids **1**, 050506.

Bhattacharyya, T., and Y. M. Joshi, 2022, "Effect of thermal and mechanical rejuvenation on the rheological behavior of chocolate," Phys. Fluids **34**, 037111.

Biance, A.-L., C. Clanet, and D. Quéré, 2003, "Leidenfrost drops," Phys. Fluids **15**, 1632–1637.

Binder, P., and C. B. Scheidle, 2020, "The moka pot: Thoughts and experiments," Phys. Educ. **55**, 065024.

Binder, P. M., and A. Richert, 2011, "The explicit siphon," Phys. Educ. **46**, 710.

Bingham, E. C., 1914, "The viscosity of binary mixtures," J. Phys. Chem. **18**, 157–165.

Bingham, E. C., 1922, *Fluidity and Plasticity* (McGraw-Hill, New York).

Bird, R. B., R. C. Armstrong, and O. Hassager, 1987, *Dynamics of Polymeric Liquids, Vol. 1: Fluid Mechanics*, (Wiley, New York).

Bisweswar, G., A. Al-Hamairi, and S. Jin, 2020, "Carbonated water injection: An efficient EOR approach. A review of fundamentals and prospects," J. Pet. Explor. Prod. Technol. **10**, 673–685.

Blaauwgeers, R., V. B. Eltsov, G. Eska, A. P. Finne, R. P. Haley, M. Krusius, J. J. Ruohio, L. Skrbek, and G. E. Volovik, 2002, "Shear Flow and Kelvin-Helmholtz Instability in Superfluids," Phys. Rev. Lett. **89**, 155301.

Bloemhof, J. M., and M. Soysal, 2017, "Sustainable food supply chain design," in *Sustainable Supply Chains: A Research-Based Textbook on Operations and Strategy*, edited by Y. Bouchery, C. J. Corbett, J. C. Fransoo, and T. Tan (Springer, New York), pp. 395–412.

Blossey, R., 2003, "Self-cleaning surfaces—Virtual realities," Nat. Mater. **2**, 301–306.

Blunt, M. J., 2001, "Flow in porous media—Pore-network models and multiphase flow," Curr. Opin. Colloid Interface Sci. **6**, 197–207.

Boatwright, A., S. Hughes, and J. Barry, 2015, "The height limit of a siphon," Sci. Rep. **5**, 16790.

Bödewadt, V. U., 1940, "Die Drehströmung über festem Grunde [On rotary flows over solid surfaces]," Z. Angew. Math. Mech. **20**, 241–253.

Bodo, G., A. Mignone, and R. Rosner, 2004, "Kelvin-Helmholtz instability for relativistic fluids," Phys. Rev. E **70**, 036304.

Boffetta, G., and A. Mazzino, 2017, "Incompressible Rayleigh-Taylor turbulence," Annu. Rev. Fluid Mech. **49**, 119–143.

Bohadana, A., G. Izbicki, and S. S. Kraman, 2014, "Fundamentals of lung auscultation," N. Engl. J. Med. **370**, 744–751.

Bohr, N., and W. Ramsay, 1909, "Determination of the surface-tension of water by the method of jet vibration," Phil. Trans. R. Soc. A **209**, 281–317.

Bohr, T., and B. Scheichl, 2021, "Surface tension and energy conservation in a moving fluid," Phys. Rev. Fluids **6**, L052001.

Bolliger, S., H. Wildmoser, H. D. Goff, and B. W. Tharp, 2000, "Relationships between ice cream mix viscoelasticity and ice crystal growth in ice cream," Int. Dairy J. **10**, 791–797.

Bollini, M., S. Tellex, T. Thompson, N. Roy, and D. Rus, 2013, "Interpreting and executing recipes with a cooking robot," in

Experimental Robotics Springer Tracts in Advanced Robotics Vol. 88, edited by J. P. Desai, G. Dudek, O. Khatib, and V. Kumar (Springer, New York), pp. 481–495, 10.1007/978-3-319-00065-7_33.

Bond, W. N., 1927, "Bubbles and drops and Stokes' law," Philos. Mag. **4**, 889–898.

Bond, W. N., and D. A. Newton, 1928, "Bubbles, drops, and Stokes' law II," Philos. Mag. **5**, 794–800.

Bonn, D., J. Eggers, J. Indekeu, J. Meunier, and E. Rolley, 2009, "Wetting and spreading," Rev. Mod. Phys. **81**, 739–805.

Borkenhagen, C., 2017, "Evidence-based creativity: Working between art and science in the field of fine dining," Soc. Stud. Sci. **47**, 630–654.

Borwankar, R. P., and C. F. Shoemaker, 1992, Eds., *Rheology of Foods* (Elsevier, New York).

Boshier, F. A. T., and A. J. Mestel, 2014, "Extended series solutions and bifurcations of the Dean equations," J. Fluid Mech. **739**, 179–195.

Bouillant, A., T. Mouterde, P. Bourrianne, C. Clanet, and D. Quéré, 2018, "Symmetry breaking in Leidenfrost flows," Phys. Rev. Fluids **3**, 100502.

Bouillant, A., T. Mouterde, P. Bourrianne, A. Lagarde, C. Clanet, and D. Quéré, 2018, "Leidenfrost wheels," Nat. Phys. **14**, 1188–1192.

Boujo, E., and M. Sellier, 2019, "Pancake making and surface coating: Optimal control of a gravity-driven liquid film," Phys. Rev. Fluids **4**, 064802.

Boussinesq, M. J., 1913, "Sur l'existence d'une viscosité superficielle, dans la mince couche de transition séparant un liquide d'un autre fluide contigu [On the existence of a surface viscosity, in the thin transition layer separating a liquid from another contiguous fluid]," C.R. Hebd. Seances Acad. Sci. **156**, 983.

Bradshaw, P., 1987, "Turbulent secondary flows," Annu. Rev. Fluid Mech. **19**, 53–74.

Brennen, C., and H. Winet, 1977, "Fluid mechanics of propulsion by cilia and flagella," Annu. Rev. Fluid Mech. **9**, 339–398.

Brennen, C. E., 2005, *Fundamentals of Multiphase Flow* (Cambridge University Press, Cambridge, England).

Brenner, M., P. Sörensen, and D. A. Weitz, 2020, *Science and Cooking: Physics Meets Food, From Homemade to Haute Cuisine* (W. W. Norton, New York).

Brent, A. D., V. R. Voller, and K. J. Reid, 1988, "Enthalpy-porosity technique for modeling convection-diffusion phase change: Application to the melting of a pure metal," Numer. Heat Transfer **13**, 297–318.

Breu, A. P. J., H. M. Ensner, C. A. Kruelle, and I. Rehberg, 2003, "Reversing the Brazil-Nut Effect: Competition between Percolation and Condensation," Phys. Rev. Lett. **90**, 014302.

Briceño-Ahumada, Z., A. Mikhailovskaya, and J. A. Staton, 2022, "The role of continuous phase rheology on the stabilization of edible foams: A review," Phys. Fluids **34**, 031302.

Brimmo, A. T., and M. A. Qasaimeh, 2017, "Stagnation point flows in analytical chemistry and life sciences," RSC Adv. **7**, 51206–51232.

Britter, R. E., 1979, "The spread of a negatively buoyant plume in a calm environment," Atmos. Environ. (1967–1989) **13**, 1241–1247.

Brooks, N., M. Cates, P. Clegg, A. Lips, W. Poon, and J. Seddon, 2016, "Soft interfacial materials: From fundamentals to formulation," Phil. Trans. R. Soc. A **374**, 20150135.

Brown, P. P., and D. F. Lawler, 2003, "Sphere drag and settling velocity revisited," J. Environ. Eng. **129**, 222–231.

Brummer, R., 2006, *Rheology Essentials of Cosmetic and Food Emulsions* (Springer, New York).

Brunt, D., 1927, "The period of simple vertical oscillations in the atmosphere," Q. J. R. Meteorol. Soc. **53**, 30–32.

Bruot, N., and P. Cicuta, 2016, "Realizing the physics of motile cilia synchronization with driven colloids," Annu. Rev. Condens. Matter Phys. **7**, 323–348.

Bruus, H., 2008, *Theoretical Microfluidics*, Vol. 18 (Oxford University Press, Oxford).

Burkhardt, U., and B. Kärcher, 2011, "Global radiative forcing from contrail cirrus," Nat. Clim. Change **1**, 54–58.

Burton, L. J., N. Cheng, and J. W. M. Bush, 2014, "The cocktail boat," Integr. Comp. Biol. **54**, 969–973.

Burton, L. J., N. Cheng, C. Vega, J. Andrés, and J. W. M. Bush, 2013, "Biomimicry and the culinary arts," Bioinspiration Biomimetics **8**, 044003.

Bush, J. W. M., and J. M. Aristoff, 2003, "The influence of surface tension on the circular hydraulic jump," J. Fluid Mech. **489**, 229–238.

Bush, J. W. M., J. M. Aristoff, and A. E. Hosoi, 2006, "An experimental investigation of the stability of the circular hydraulic jump," J. Fluid Mech. **558**, 33–52.

Bush, J. W. M., and D. L. Hu, 2006, "Walking on water: Biolocomotion at the interface," Annu. Rev. Fluid Mech. **38**, 339–369.

Bussonnière, A., A. Antkowiak, F. Ollivier, M. Baudoin, and R. Wunenburger, 2020, "Acoustic Sensing of Forces Driving Fast Capillary Flows," Phys. Rev. Lett. **124**, 084502.

Byagathvalli, G., E. J. Challita, and M. S. Bhamla, 2021, "Frugal science powered by curiosity," Ind. Eng. Chem. Res. **60**, 15874–15884.

Byers, N., and G. Williams, 2006, *Out of the Shadows: Contributions of Twentieth-Century Women to Physics* (Cambridge University Press, Cambridge, England).

Cagiltay, N. E., S. Yildirim, and M. Aksu, 2006, "Students' preferences on Web-based instruction: Linear or non-linear," Educ. Technol. Soc. **9**, 122–136, https://www.jstor.org/stable/jeductechsoci.9.3.122.

Cai, S., Z. Wang, F. Fuest, Y. J. Jeon, C. Gray, and G. E. Karniadakis, 2021, "Flow over an espresso cup: Inferring 3-D velocity and pressure fields from tomographic background oriented schlieren via physics-informed neural networks," J. Fluid Mech. **915**, A102.

Cameron, M. I., D. Morisco, D. Hofstetter, E. Uman, J. Wilkinson, Z. C. Kennedy, S. A. Fontenot, W. T. Lee, C. H. Hendon, and J. M. Foster, 2020, "Systematically improving espresso: Insights from mathematical modeling and experiment," Matter **2**, 631–648.

Campanella, O. H., and M. Peleg, 1987, "Analysis of the transient flow of mayonnaise in a coaxial viscometer," J. Rheol. **31**, 439–452.

Cantat, I., S. Cohen-Addad, F. Elias, F. Graner, R. Höhler, O. Pitois, F. Rouyer, and A. Saint-Jalmes, 2013, *Foams: Structure and Dynamics* (Oxford University Press, New York).

Cantiello, M., and N. Langer, 2010, "Thermohaline mixing in evolved low-mass stars," Astron. Astrophys. **521**, A9.

Capozzi, F., and A. Bordoni, 2013, "Foodomics: A new comprehensive approach to food and nutrition," Genes Nutr. **8**, 1–4.

Carlson, J. A., A. Jaffe, and A. Wiles, 2006, Eds., *The Millennium Prize Problems* (American Mathematical Society, Providence).

Carmody, C. D., R. C. Mueller, B. M. Grodner, O. Chlumsky, J. N. Wilking, and S. G. McCalla, 2022, "Chickensplash! Exploring the health concerns of washing raw chicken," Phys. Fluids **34**, 031910.

Carreau, P. J., 1972, "Rheological equations from molecular network theories," Trans. Soc. Rheol. **16**, 99–127.

Carrithers, A. D., M. J. Brown, M. Z. Rashed, S. Islam, O. D. Velev, and S. J. Williams, 2020, "Multiscale self-assembly of distinctive weblike structures from evaporated drops of dilute American whiskeys," ACS Nano **14**, 5417–5425.

Cates, M. E., and J. Tailleur, 2015, "Motility-induced phase separation," Annu. Rev. Condens. Matter Phys. **6**, 219.
Cattaneo, F., T. Emonet, and N. Weiss, 2003, "On the interaction between convection and magnetic fields," Astrophys. J. **588**, 1183–1198.
Cerbus, R. T., C.-c. Liu, G. Gioia, and P. Chakraborty, 2018, "Laws of Resistance in Transitional Pipe Flows," Phys. Rev. Lett. **120**, 054502.
Cerda, E., and L. Mahadevan, 2003, "Geometry and Physics of Wrinkling," Phys. Rev. Lett. **90**, 074302.
Chalmers, A. F., 2017, *One Hundred Years of Pressure: Hydrostatics from Stevin to Newton* (Springer, New York).
Chanaud, R. C., 1970, "Aerodynamic whistles," Sci. Am. **222**, No. 1, 40–47.
Chandler, D., 2007, "Oil on troubled waters," Nature (London) **445**, 831–832.
Chandrasekhar, S., 1961, *Hydrodynamic and Hydromagnetic Stability* (Dover Publications, New York).
Chandrashekar, J., D. Yarmolinsky, L. von Buchholtz, Y. Oka, W. Sly, N. J. Ryba, and C. S. Zuker, 2009, "The taste of carbonation," Science **326**, 443–445.
Chang, H., 1994, "Wave evolution on a falling film," Annu. Rev. Fluid Mech. **26**, 103–136.
Chase, D. L., C. Kurzthaler, and H. A. Stone, 2022, "Hydrodynamically induced helical particle drift due to patterned surfaces," Proc. Natl. Acad. Sci. U.S.A. **119**, e2202082119.
Chen, C., and E. Meiburg, 2002, "Miscible displacements in capillary tubes: Influence of Korteweg stresses and divergence effects," Phys. Fluids **14**, 2052–2058.
Chen, C.-Y., C.-W. Huang, H. Gadêlha, and J. A. Miranda, 2008, "Radial viscous fingering in miscible Hele-Shaw flows: A numerical study," Phys. Rev. E **78**, 016306.
Chen, W., J. Li, C. Wang, X. Dai, and J. Liu, 2018, "2D-PIV measurement of range hood-driven flow in a domestic kitchen," Energy Build. **177**, 64–76.
Chen, Z., J. Xin, and P. Liu, 2020, "Air quality and thermal comfort analysis of kitchen environment with CFD simulation and experimental calibration," Build. Environ. **172**, 106691.
Chevalier, Y., and M.-A. Bolzinger, 2013, "Emulsions stabilized with solid nanoparticles: Pickering emulsions," Colloids Surf. A **439**, 23–34.
Chevalley, J., 1975, "Rheology of chocolate," J. Texture Stud. **6**, 177–196.
Chiappisi, L., and I. Grillo, 2018, "Looking into limoncello: The structure of the Italian liquor revealed by small-angle neutron scattering," ACS Omega **3**, 15407–15415.
Childress, S., 2010, "Walking on water," J. Fluid Mech. **644**, 1–4.
Chin, A., J. Chu, M. Perera, K. Hui, H.-L. Yen, M. Chan, M. Peiris, and L. Poon, 2020, "Stability of SARS-CoV-2 in different environmental conditions," Lancet Microbe **1**, E10.
Chitlapilly Dass, S., J. M. Bosilevac, M. Weinroth, C. G. Elowsky, Y. Zhou, A. Anandappa, and R. Wang, 2020, "Impact of mixed biofilm formation with environmental microorganisms on *E. coli* O157: H7 survival against sanitization," npj Sci. Food **4**, 1–9.
Chizner, M. A., 2008, "Cardiac auscultation: Rediscovering the lost art," Curr. Probl. Cardiol. **33**, 326–408.
Chong, K. L., R. Yang, Q. Wang, R. Verzicco, and D. Lohse, 2020, "Café latte: Spontaneous layer formation in laterally cooled double diffusive convection," J. Fluid Mech. **900**, R6.
Cichocki, B., and R. B. Jones, 1998, "Image representation of a spherical particle near a hard wall," Physica (Amsterdam) **258A**, 273–302.
Clanet, C., F. Hersen, and L. Bocquet, 2004, "Secrets of successful stone-skipping," Nature (London) **427**, 29–29.
Clarke, C., 2003, "The physics of ice cream," Phys. Educ. **38**, 248–253.
Clarke, C., 2015, *The Science of Ice Cream* (Royal Society of Chemistry, Cambridge, England).
Cohen, Y., O. Devauchelle, H. F. Seybold, R. S. Yi, P. Szymczak, and D. H. Rothman, 2015, "Path selection in the growth of rivers," Proc. Natl. Acad. Sci. U.S.A. **112**, 14132–14137.
Comstock, G. W., M. B. Meyer, K. J. Helsing, and M. S. Tockman, 1981, "Respiratory effects of household exposures to tobacco smoke and gas cooking," Am. Rev. Respir. Dis. **124**, 143–148, https://www.atsjournals.org/doi/abs/10.1164/arrd.1981.124.2.143.
Cook, K. L. K., and R. W. Hartel, 2010, "Mechanisms of ice crystallization in ice cream production," Compr. Rev. Food Sci. Food Saf. **9**, 213–222.
Cordoba, N., L. Pataquiva, C. Osorio, F. L. M. Moreno, and R. Y. Ruiz, 2019, "Effect of grinding, extraction time and type of coffee on the physicochemical and flavour characteristics of cold brew coffee," Sci. Rep. **9**, 1–12.
Cordry, S. M., 1998, "Finicky clay divers," Phys. Teach. **36**, 82–83.
Corrochano, B. R., J. R. Melrose, A. C. Bentley, P. J. Fryer, and S. Bakalis, 2015, "A new methodology to estimate the steady-state permeability of roast and ground coffee in packed beds," J. Food Eng. **150**, 106–116.
Costello, C., *et al.*, 2020, "The future of food from the sea," Nature (London) **588**, 95–100.
Cox, R. G., 1970, "The motion of long slender bodies in a viscous fluid. Part 1. General theory," J. Fluid Mech. **44**, 791–810.
Craster, R. V., and O. K. Matar, 2009, "Dynamics and stability of thin liquid films," Rev. Mod. Phys. **81**, 1131.
Crawford, F. S., 1982, "The hot chocolate effect," Am. J. Phys. **50**, 398–404.
Crawford, F. S., 1990, "Hot water, fresh beer, and salt," Am. J. Phys. **58**, 1033–1036.
Cross, M. M., 1965, "Rheology of non-Newtonian fluids: A new flow equation for pseudoplastic systems," J. Colloid Sci. **20**, 417–437.
Cuq, B., S. Mandato, R. Jeantet, K. Saleh, and T. Ruiz, 2013, "Agglomeration/granulation in food powder production," in *Handbook of Food Powders*, Woodhead Publishing Series in Food Science, Technology and Nutrition Vol. 255, edited by B. Bhandari, N. Bansal, M. Zhang, and P. Schuck (Elsevier, New York), pp. 150–177.
Curzon, F. L., 1978, "The Leidenfrost phenomenon," Am. J. Phys. **46**, 825–828.
Cuthill, H., C. Elleman, T. Curwen, and B. Wolf, 2021, "Colloidal particles for Pickering emulsion stabilization prepared via antisolvent precipitation of lignin-rich cocoa shell extract," Foods **10**, 371.
Dancer, S. J., 2020, "Revising Nightingale's legacy," J. Hosp. Infect. **105**, 344–345.
D'Angelo, M. V., L. Pauchard, H. Auradou, and B. D. Texier, 2022, "Shaping gels and gels mixture to create helices," Phys. Fluids **34**, 077116.
Darcy, H., 1856, *Les Fontaines Publiques de la Ville de Dijon: Exposition et Application …* (Victor Dalmont, Paris).
Das, C., and P. D. Olmsted, 2016, "The physics of stratum corneum lipid membranes," Phil. Trans. R. Soc. A **374**, 20150126.
Dash, D. R., S. K. Singh, and P. Singha, 2022, "Recent advances on the impact of novel non-thermal technologies on structure and functionality of plant proteins: A comprehensive review," Crit. Rev. Food Sci. Nutrit. 1–16.
Da Silva, W. J., B. C. Vidal, M. E. Q. Martins, H. Vargas, C. Pereira, M. Zerbetto, and L. C. M. Miranda, 1993, "What makes popcorn pop," Nature (London) **362**, 417.

Daubert, C. R., J. A. Tkachuk, and V. D. Truong, 1998, "Quantitative measurement of food spreadability using the vane method," J. Texture Stud. **29**, 427–435.
Dauxois, T., *et al.*, 2021, "Confronting grand challenges in environmental fluid mechanics," Phys. Rev. Fluids **6**, 020501.
Davidson, J. A., 1981, "Foam stability as an historic measure of the alcohol concentration in distilled alcoholic beverages," J. Colloid Interface Sci. **81**, 540–542.
Davis, H. T., 1988, "A theory of tension at a miscible displacement front," in *Numerical Simulation in Oil Recovery*, edited by M. Wheeler (Springer, New York).
Davis, R. E., and A. Acrivos, 1966, "The influence of surfactants on the creeping motion of bubbles," Chem. Eng. Sci. **21**, 681–685.
Davis, S., J. O. Gray, and D. G. Caldwell, 2008, "An end effector based on the Bernoulli principle for handling sliced fruit and vegetables," Robot. Comput. Integr. Manuf. **24**, 249–257.
Dean, W. R., 1927, "Note on the motion of fluid in a curved pipe," Philos. Mag. **4**, 208–223.
Deegan, R. D., O. Bakajin, T. F. Dupont, G. Huber, S. R. Nagel, and T. A. Witten, 1997, "Capillary flow as the cause of ring stains from dried liquid drops," Nature (London) **389**, 827–829.
de Gennes, P. G., 1999, "Granular matter: A tentative view," Rev. Mod. Phys. **71**, S374–S382.
de Gennes, P.-G., *et al.*, 2004, *Capillarity and Wetting Phenomena: Drops, Bubbles, Pearls, Waves* (Springer, New York).
Dehaeck, S., C. Wylock, and P. Colinet, 2009, "Evaporating cocktails," Phys. Fluids **21**, 091108.
De La Cruz Garcia, C., G. Sánchez Moragas, and D. Nordqvist, 2014, "Food contact materials," in *Food Safety Management. A Practical Guide for the Food Industry*, edited by Y. Motarjemi and H. Lelievelt (Academic Press, New York).
Del Nobile, M., S. Chillo, A. Mentana, and A. Baiano, 2007, "Use of the generalized Maxwell model for describing the stress relaxation behavior of solid-like foods," J. Food Eng. **78**, 978–983.
Deng, X., L. Mammen, H.-J. Butt, and D. Vollmer, 2012, "Candle soot as a template for a transparent robust superamphiphobic coating," Science **335**, 67–70.
Derr, N. J., D. C. Fronk, C. A. Weber, A. Mahadevan, C. H. Rycroft, and L. Mahadevan, 2020, "Flow-Driven Branching in a Frangible Porous Medium," Phys. Rev. Lett. **125**, 158002.
De Santos, J. M., T. R. Melli, and L. E. Scriven, 1991, "Mechanics of gas-liquid flow in packed-bed contactors," Annu. Rev. Fluid Mech. **23**, 233–260.
Deshpande, N., D. Furbish, P. Arratia, and D. Jerolmack, 2021, "The perpetual fragility of creeping hillslopes," Nat. Commun. **12**, 3909.
Deslauriers, L., L. S. McCarty, K. Miller, K. Callaghan, and G. Kestin, 2019, "Measuring actual learning versus feeling of learning in response to being actively engaged in the classroom," Proc. Natl. Acad. Sci. U.S.A. **116**, 19251–19257.
Deslauriers, L., E. Schelew, and C. Wieman, 2011, "Improved learning in a large-enrollment physics class," Science **332**, 862–864.
De-Song, B., Z. Xun-Sheng, X. Guang-Lei, P. Zheng-Quan, T. Xiao-Wei, and L. Kun-Quan, 2003, "Critical phenomenon of granular flow on a conveyor belt," Phys. Rev. E **67**, 062301.
Devauchelle, O., A. P. Petroff, H. F. Seybold, and D. H. Rothman, 2012, "Ramification of stream networks," Proc. Natl. Acad. Sci. U.S.A. **109**, 20832–20836.
Dey, S., S. Zeeshan Ali, and E. Padhi, 2019, "Terminal fall velocity: The legacy of Stokes from the perspective of fluvial hydraulics," Proc. R. Soc. A **475**, 20190277.
Dhir, V. K., 1998, "Boiling heat transfer," Annu. Rev. Fluid Mech. **30**, 365–401.
Dhir, V. K., 2006, "Mechanistic prediction of nucleate boiling heat transfer—Achievable or a hopeless task?," J. Heat Transfer **128**, 1–12.
Di Carlo, D., 2009, "Inertial microfluidics," Lab Chip **9**, 3038–3046.
Dickinson, E., 2010, "Food emulsions and foams: Stabilization by particles," Curr. Opin. Colloid Interface Sci. **15**, 40–49.
Dickinson, H. W., 1941, "Joseph Bramah and his inventions," Trans. Newcomen Soc. **22**, 169–186.
Didden, N., and T. Maxworthy, 1982, "The viscous spreading of plane and axisymmetric gravity currents," J. Fluid Mech. **121**, 27–42.
Diddens, C., H. Tan, P. Lv, M. Versluis, Kuerten, J. G. M., X. Zhang, and D. Lohse, 2017, "Evaporating pure, binary and ternary droplets: Thermal effects and axial symmetry breaking," J. Fluid Mech. **823**, 470–497.
Dietrich, K., N. Jaensson, I. Buttinoni, G. Volpe, and L. Isa, 2020, "Microscale Marangoni Surfers," Phys. Rev. Lett. **125**, 098001.
Dijkstra, H. A., 1992, "On the structure of cellular solutions in Rayleigh-Bénard-Marangoni flows in small-aspect-ratio containers," J. Fluid Mech. **243**, 73–102.
Dimotakis, P. E., 2005, "Turbulent mixing," Annu. Rev. Fluid Mech. **37**, 329–356.
Dinčov, D., K. A. Parrott, and K. Pericleous, 2004, "Heat and mass transfer in two-phase porous materials under intensive microwave heating," J. Food Eng. **65**, 403–412.
D'Innocenzo, A., F. Paladini, and L. Renna, 2002, "Experimental study of dripping dynamics," Phys. Rev. E **65**, 056208.
Dintzis, F. R., 1996, "Shear-thickening behavior and shear-induced structure in gently solubilized starches," Cereal Chem. **73**, 638–643, https://pubag.nal.usda.gov/download/25172/pdf.
Dizechi, M., and E. Marschall, 1982, "Viscosity of some binary and ternary liquid mixtures," J. Chem. Eng. Data **27**, 358–363.
Donald, A. M., 2004, "Food for thought," Nat. Mater. **3**, 579–581.
Donald, A. M., 2017, "Understanding starch structure and functionality," in *Starch in Food: Structure, Function and Applications*, 2nd ed., edited by A.-C. Eliasson, M. Sjöö, and L. Nilsson (Woodhead Publishing, Sawston, England), pp. 156–184.
D'Ortona, U., and N. Thomas, 2020, "Self-Induced Rayleigh-Taylor Instability in Segregating Dry Granular Flows," Phys. Rev. Lett. **124**, 178001.
Doyle, M. P., F. Diez-Gonzalez, and C. Hill, 2019, *Food Microbiology: Fundamentals and Frontiers* (John Wiley & Sons, New York).
Drazin, P., 1987, "Fluid mechanics," Phys. Educ. **22**, 350.
Drazin, P. G., 1970, "Kelvin-Helmholtz instability of finite amplitude," J. Fluid Mech. **42**, 321–335.
Drazin, P. G., and Reid, 2010, *Hydrodynamic Stability* (Cambridge University Press, Cambridge, England).
Dressaire, E., L. Courbin, J. Crest, and H. A. Stone, 2009, "Thin-Film Fluid Flows over Microdecorated Surfaces: Observation of Polygonal Hydraulic Jumps," Phys. Rev. Lett. **102**, 194503.
Dressaire, E., and A. Sauret, 2017, "Clogging of microfluidic systems," Soft Matter **13**, 37–48.
Drndić, M., 2021, "20 years of solid-state nanopores," Nat. Rev. Phys. **3**, 606.
Duchesne, A., A. Andersen, and T. Bohr, 2019, "Surface tension and the origin of the circular hydraulic jump in a thin liquid film," Phys. Rev. Fluids **4**, 084001.
Duez, C., C. Ybert, C. Clanet, and L. Bocquet, 2010, "Wetting Controls Separation of Inertial Flows from Solid Surfaces," Phys. Rev. Lett. **104**, 084503.
Duffie, J. A., W. A. Beckman, and N. Blair, 2020, *Solar Engineering of Thermal Processes, Photovoltaics and Wind* (Wiley, New York).

Dukler, Y., H. Ji, C. Falcon, and A. L. Bertozzi, 2020, "Theory for undercompressive shocks in tears of wine," Phys. Rev. Fluids **5**, 034002.

Dupuis, A., and J. M. Yeomans, 2005, "Modeling droplets on superhydrophobic surfaces: Equilibrium states and transitions," Langmuir **21**, 2624–2629.

Durian, D. J., 1995, "Foam Mechanics at the Bubble Scale," Phys. Rev. Lett. **75**, 4780–4783.

Durian, D. J., D. A. Weitz, and D. J. Pine, 1991, "Scaling behavior in shaving cream," Phys. Rev. A **44**, R7902–R7905.

Durian, S. C., S. Dillavou, K. Markin, A. Portales, B. O. T. Maldonado, W. T. Irvine, P. E. Arratia, and D. J. Durian, 2022, "Spatters and spills: Spreading dynamics for partially wetting droplets," Phys. Fluids **34**, 012112.

Dusenbery, D. B., 2009, *Living at Micro Scale: The Unexpected Physics of Being Small* (Harvard University Press, Cambridge, MA).

Dussaud, A. D., P. M. Adler, and A. Lips, 2003, "Liquid transport in the networked microchannels of the skin surface," Langmuir **19**, 7341–7345.

Egger, S., and R. A. Orr, 2016, *The Home Barista: How to Bring Out the Best in Every Coffee Bean* (The Experiment, New York).

Eggers, J., 1997, "Nonlinear dynamics and breakup of free-surface flows," Rev. Mod. Phys. **69**, 865–930.

Eggers, J., and E. Villermaux, 2008, "Physics of liquid jets," Rep. Prog. Phys. **71**, 036601.

Eggl, M. F., and P. J. Schmid, 2020, "Mixing enhancement in binary fluids using optimised stirring strategies," J. Fluid Mech. **899**, A24.

Ehrichs, E. E., H. M. Jaeger, G. S. Karczmar, J. B. Knight, V. Y. Kuperman, and S. R. Nagel, 1995, "Granular convection observed by magnetic resonance imaging," Science **267**, 1632–1634.

Einav, I., and F. Guillard, 2018, "Tracking time with ricequakes in partially soaked brittle porous media," Sci. Adv. **4**, eaat6961.

Einstein, A., 1906, "Eine neue Bestimmung der Moleküldimensionen [A new determination of the size of molecules]," Ann. Phys. (Berlin) **324**, 289–306.

Einstein, A., 1910, "Theorie der Opaleszenz von homogenen Flüssigkeiten und Flüssigkeitsgemischen in der Nähe des kritischen Zustandes [A theory for opalescence of homogeneous fluids and fluid mixtures close to the critical state]," Ann. Phys. (Berlin) **338**, 1275–1298.

Einstein, A., 1926, "Die Ursache der Mäanderbildung der Flußläufe und des sogenannten Baerschen Gesetzes [The cause of the formation of meanders in the courses of rivers and of the so-called Baer's law]," Naturwissenschaften **14**, 223–224.

Ekman, V. W., 1906, "Beiträge zur Theorie der Meeresströmungen [Contributions to the theory of ocean currents]," Ann. Hydrogr. Mar. Meteorol. **34**, 527–540.

Elgeti, J., and G. Gompper, 2013, "Emergence of metachronal waves in cilia arrays," Proc. Natl. Acad. Sci. U.S.A. **110**, 4470–4475.

Elgeti, J., R. G. Winkler, and G. Gompper, 2015, "Physics of microswimmers—Single particle motion and collective behavior: A review," Rep. Prog. Phys. **78**, 056601.

Eliassen, A., 1982, "Vilhelm Bjerknes and his students," Annu. Rev. Fluid Mech. **14**, 1–12.

Ellegaard, C., A. E. Hansen, A. Haaning, K. Hansen, A. Marcussen, T. Bohr, J. L. Hansen, and S. Watanabe, 1998, "Creating corners in kitchen sinks," Nature (London) **392**, 767–768.

Ellegaard, C., A. E. Hansen, A. Haaning, K. Hansen, A. Marcussen, T. Bohr, J. L. Hansen, and S. Watanabe, 1999, "Cover illustration: Polygonal hydraulic jumps," Nonlinearity **12**, 1–7.

Elliott, J. H., and A. J. Ganz, 1977, "Salad dressings—Preliminary rheological characterization," J. Texture Stud. **8**, 359–371.

Emanuel, K. A., 1994, *Atmospheric Convection* (Oxford University Press, New York).

Emran, M. S., and J. Schumacher, 2015, "Large-scale mean patterns in turbulent convection," J. Fluid Mech. **776**, 96–108.

Engmann, J., C. Servais, and A. S. Burbidge, 2005, "Squeeze flow theory and applications to rheometry: A review," J. Non-Newtonian Fluid Mech. **132**, 1–27.

Ershov, D., J. Sprakel, J. Appel, M. A. C. Stuart, and J. van der Gucht, 2013, "Capillarity-induced ordering of spherical colloids on an interface with anisotropic curvature," Proc. Natl. Acad. Sci. U.S.A. **110**, 9220–9224.

Escoffier, G. A., 1903, *Le Guide Culinaire: Aide-Mémoire de Cuisine Pratique* (Editions Flammarion, Paris) [*The Complete Guide to the Art of Modern Cookery*, translated by (Mayflower Publishing, London, 1979)].

European Commission, 2020b, "Poly- and perfluoroalkyl substances (PFAS)," Report No. SWD(2020) 249, https://ec.europa.eu/environment/pdf/chemicals/2020/10/SWD_PFAS.pdf.

Eweldt, R. H., and C. Saengow, 2022, "Designing complex fluids," Annu. Rev. Fluid Mech. **54**, 413–441.

Fan, L. T., and J. T. Tseng, 1967, "Apparent diffusivity in honey-water system," J. Food Sci. **32**, 633–636.

Fanton, X., and A. M. Cazabat, 1998, "Spreading and instabilities induced by a solutal Marangoni effect," Langmuir **14**, 2554–2561.

Farris, R. J., 1968, "Prediction of the viscosity of multimodal suspensions from unimodal viscosity data," Trans. Soc. Rheol. **12**, 281–301.

Fasano, A., F. Talamucci, and M. Petracco, 2000, "The espresso coffee problem," in *Complex Flows in Industrial Processes*, edited by A. Fasano (Birkhäuser, Boston), pp. 241–280.

Faubel, R., C. Westendorf, E. Bodenschatz, and G. Eichele, 2016, "Cilia-based flow network in the brain ventricles," Science **353**, 176–178.

Faxén, H., 1923, Ark. Mat. Astron. Fys. **17**, 1.

Feneuil, B., E. Strøm Lillebø, C. L. Honstad, A. Jensen, and A. Carlson, 2022, "Elastic modulus measurements of cooked lutefisk," Phys. Fluids **34**, 047122.

Feng, L., S. Li, Y. Li, H. Li, L. Zhang, J. Zhai, Y. Song, B. Liu, L. Jiang, and D. Zhu, 2002, "Super-hydrophobic surfaces: From natural to artificial," Adv. Mater. **14**, 1857–1860.

Fennema, O. R., 2017, *Fennema's Food Chemistry*, 5th ed., edited by S. Damodaran and K. L. Parkin (CRC Press, Boca Raton).

Ferguson, E. S., 1964, "The origins of the steam engine," Sci. Am. **210**, No. 1, 98–107.

Fernandes, M. C., M. Saadat, P. Cauchy-Dubois, C. Inamura, T. Sirota, G. Milliron, H. Haj-Hariri, K. Bertoldi, and J. C. Weaver, 2021, "Mechanical and hydrodynamic analyses of helical strake-like ridges in a glass sponge," J. R. Soc. Interface **18**, 20210559.

Fernández-Castro, B., *et al.*, 2015, "Importance of salt fingering for new nitrogen supply in the oligotrophic ocean," Nat. Commun. **6**, 8002.

Ferrari, M., Handgraaf, J.-W., G. Boccardo, A. Buffo, M. Vanni, and D. L. Marchisio, 2022, "Molecular modeling of the interface of an egg yolk protein-based emulsion," Phys. Fluids **34**, 021903.

Figoni, P. I., and C. F. Shoemaker, 1983, "Characterization of time dependent flow properties of mayonnaise under steady shear," J. Texture Stud. **14**, 431–442.

Fischer, P., 2021 (private communication).

Fischer, P., and E. J. Windhab, 2011, "Rheology of food materials," Curr. Opin. Colloid Interface Sci. **16**, 36–40.

Flemmer, R. L. C., and C. L. Banks, 1986, "On the drag coefficient of a sphere," Powder Technol. **48**, 217–221.

Foegeding, E. A., 2006, "Food biophysics of protein gels: A challenge of nano and macroscopic proportions," Food Biophys. **1**, 41–50.
Foley, J. A., *et al.*, 2005, "Global consequences of land use," Science **309**, 570–574.
Foley, J. A., *et al.*, 2011, "Solutions for a cultivated planet," Nature (London) **478**, 337–342.
Ford, I. J., 2004, "Statistical mechanics of nucleation: A review," Proc. Inst. Mech. Eng., Part C **218**, 883–899.
Forterre, Y., and O. Pouliquen, 2008, "Flows of dense granular media," Annu. Rev. Fluid Mech. **40**, 1–24.
Foullon, C., E. Verwichte, V. M. Nakariakov, K. Nykyri, and C. J. Farrugia, 2011, "Magnetic Kelvin-Helmholtz instability at the Sun," Astrophys. J. Lett. **729**, L8.
Fournier, J. B., and A. M. Cazabat, 1992, "Tears of wine," Europhys. Lett. **20**, 517.
Fox, R. F., 1997, "Construction of the Jordan basis for the Baker map," Chaos **7**, 254–269.
Frabetti, A. C. C., J. O. de Moraes, V. Jury, L. Boillereaux, and J. B. Laurindo, 2021, "Adhesion of food on surfaces: Theory, measurements, and main trends to reduce it prior to industrial drying," Food Eng. Rev. **13**, 884–901.
Franco, J. M., M. Berjano, and C. Gallegos, 1997, "Linear viscoelasticity of salad dressing emulsions," J. Agric. Food Chem., **45**, 713–719.
Franco, J. M., A. Guerrero, and C. Gallegos, 1995, "Rheology and processing of salad dressing emulsions," Rheol. Acta **34**, 513–524.
Franjione, J. G., J. M. Ottino, and F. T. Smith, 1992, "Symmetry concepts for the geometric analysis of mixing flows," Phil. Trans. R. Soc. A **338**, 301–323.
Franklin, B., and W. Brownrigg, 1774, "Of the stilling of waves by means of oil," Phil. Trans. R. Soc. London **64**, 445–460.
Franz, G. J., 1959, "Splashes as sources of sound in liquids," J. Acoust. Soc. Am. **31**, 1080–1096.
Frazier, S., X. Jiang, and J. C. Burton, 2020, "How to make a giant bubble," Phys. Rev. Fluids **5**, 013304.
Freeman, S., S. L. Eddy, M. McDonough, M. K. Smith, N. Okoroafor, H. Jordt, and M. P. Wenderoth, 2014, "Active learning increases student performance in science, engineering, and mathematics," Proc. Natl. Acad. Sci. U.S.A. **111**, 8410–8415.
Freeman, S. M., and K. Weissenberg, 1948, "Some new rheological phenomena and their significance for the constitution of materials," Nature (London) **162**, 320–323.
Frette, V., K. Christensen, A. Malthe-Sørenssen, J. Feder, T. Jøssang, and P. Meakin, 1996, "Avalanche dynamics in a pile of rice," Nature (London) **379**, 49–52.
Friberg, S., K. Larsson, and J. Sjöblom, 2003, *Food Emulsions*, 4th ed. (CRC Press, Boca Raton).
Fuller, G. G., and L. G. Leal, 1980, "Flow birefringence of dilute polymer solutions in two-dimensional flows," Rheol. Acta **19**, 580–600.
Fuller, G. G., and L. G. Leal, 1981, "Flow birefringence of concentrated polymer solutions in two-dimensional flows," J. Polym. Sci. **19**, 557–587.
Fuller, G. G., M. Lisicki, A. J. T. M. Mathijssen, E. J. L. Mossige, R. Pasquino, V. N. Prakash, and L. Ramos, 2022, "Kitchen flows: Making science more accessible, affordable, and curiosity driven," Phys. Fluids **34**, 110401.
Fuller, G. G., and J. Vermant, 2012, "Complex fluid-fluid interfaces: Rheology and structure," Annu. Rev. Chem. Biomol. Eng. **3**, 519–543.
Furst, E. M., and T. M. Squires, 2017, *Microrheology* (Oxford University Press, New York).
Gajjar, P., C. G. Johnson, J. Carr, K. Chrispeels, J. M. N. T. Gray, and P. J. Withers, 2021, "Size segregation of irregular granular materials captured by time-resolved 3D imaging," Sci. Rep. **11**, 1–6.
Gallas, J. A., H. J. Herrmann, T. Pöschel, and S. Sokołowski, 1996, "Molecular dynamics simulation of size segregation in three dimensions," J. Stat. Phys. **82**, 443–450.
Gammon, J., and J. Hunt, 2020, "COVID-19 and hand hygiene: The vital importance of hand drying," Br. J. Nurs. **29**, 1003–1006.
Ganachaud, F., and J. L. Katz, 2005, "Nanoparticles and nanocapsules created using the ouzo effect: Spontaneous emulsification as an alternative to ultrasonic and high-shear devices," ChemPhysChem **6**, 209–216.
Gao, X., and L. Jiang, 2004, "Water-repellent legs of water striders," Nature (London) **432**, 36.
Gao, Y., Q. K. Liu, W. K. Chow, and M. Wu, 2014, "Analytical and experimental study on multiple fire sources in a kitchen," Fire Saf. J. **63**, 101–112.
Garaud, P., 2018, "Double-diffusive convection at low Prandtl number," Annu. Rev. Fluid Mech. **50**, 275–298.
Garratt, J. R., 1994, "The atmospheric boundary layer," Earth-Sci. Rev. **37**, 89–134.
Garrett, C., and W. Munk, 1979, "Internal waves in the ocean," Annu. Rev. Fluid Mech. **11**, 339–369.
Gauthier, A., C. Diddens, R. Proville, D. Lohse, and D. van der Meer, 2019, "Self-propulsion of inverse Leidenfrost drops on a cryogenic bath," Proc. Natl. Acad. Sci. U.S.A. **116**, 1174–1179.
Gavahian, M., T. S. Manyatsi, A. Morata, and B. K. Tiwari, 2022, "Ultrasound-assisted production of alcoholic beverages: From fermentation and sterilization to extraction and aging," Compr. Rev. Food Sci. Food Saf. **21**, 5243–5271.
Gekle, S., I. R. Peters, J. M. Gordillo, D. van der Meer, and D. Lohse, 2010, "Supersonic Air Flow due to Solid-Liquid Impact," Phys. Rev. Lett. **104**, 024501.
Genovese, D. B., J. E. Lozano, and M. A. Rao, 2007, "The rheology of colloidal and noncolloidal food dispersions," J. Food Sci. **72**, R11–R20.
Gerber, J., T. Lendenmann, H. Eghlidi, T. M. Schutzius, and D. Poulikakos, 2019, "Wetting transitions in droplet drying on soft materials," Nat. Commun. **10**, 1–10.
German, J. B., and M. J. McCarthy, 1989, "Stability of aqueous foams: Analysis using magnetic resonance imaging," J. Agric. Food Chem. **37**, 1321–1324.
Germano, M., 1989, "The Dean equations extended to a helical pipe flow," J. Fluid Mech. **203**, 289–305.
Gervais, T., and K. F. Jensen, 2006, "Mass transport and surface reactions in microfluidic systems," Chem. Eng. Sci. **61**, 1102–1121.
Ghabache, E., G. Liger-Belair, A. Antkowiak, and T. Séon, 2016, "Evaporation of droplets in a champagne wine aerosol," Sci. Rep. **6**, 1–10.
Ghebremedhin, M., M. Baechle, and T. A. Vilgis, 2022, "Meat-, vegetarian-, and vegan sausages: Comparison of mechanics, friction, and structure," Phys. Fluids **34**, 047112.
Giacomin, C. E., and P. Fischer, 2021, "Black tea interfacial rheology and calcium carbonate," Phys. Fluids **33**, 092105.
Giacomini, J., G. Khamitova, P. Maponi, S. Vittori, and L. Fioretti, 2020, "Water flow and transport in porous media for *in-silico* espresso coffee," Int. J. Multiphase Flow **126**, 103252.
Gianino, C., 2007, "Experimental analysis of the Italian coffee pot 'moka,' " Am. J. Phys. **75**, 43–47.
Giles, S., C. Jackson, and N. Stephen, 2020, "Barriers to fieldwork in undergraduate geoscience degrees," Nat. Rev. Earth Environ. **1**, 77–78.

Gilpin, W., 2018, "Cryptographic hashing using chaotic hydrodynamics," Proc. Natl. Acad. Sci. U.S.A. **115**, 4869–4874.
Gilpin, W., M. S. Bull, and M. Prakash, 2020, "The multiscale physics of cilia and flagella," Nat. Rev. Phys. **2**, 74–88.
Glessmer, M. S., 2020, "How to teach motivating and hands-on laboratory and field courses in a virtual setting," Oceanography **33**, 130–132.
Goff, H., 1997, "Colloidal aspects of ice cream—A review," Int. Dairy J. **7**, 363–373.
Goff, H. D., and R. W. Hartel, 2013, *Ice Cream* (Springer, New York).
Gogate, P. R., 2011a, "Application of hydrodynamic cavitation for food and bioprocessing," in *Ultrasound Technologies for Food and Bioprocessing*, Food Engineering Series, edited by H. Feng, G. Barbosa-Canovas, and J. Weiss (Springer, New York), pp. 141–173.
Gogate, P. R., 2011b, "Hydrodynamic cavitation for food and water processing," Food Bioprocess Technol. **4**, 996–1011.
Gogate, P. R., and A. M. Kabadi, 2009, "A review of applications of cavitation in biochemical engineering/biotechnology," Biochem. Eng. J. **44**, 60–72.
Goldman, A. J., R. G. Cox, and H. Brenner, 1967, "Slow viscous motion of a sphere parallel to a plane wall—I. Motion through a quiescent fluid," Chem. Eng. Sci. **22**, 637–651.
Gompper, G., *et al.*, 2020, "The 2020 motile active matter roadmap," J. Phys. Condens. Matter **32**, 193001.
Goshawk, J., D. Binding, D. Kell, and R. Goodacre, 1998, "Rheological phenomena occurring during the shearing flow of mayonnaise," J. Rheol. **42**, 1537–1553.
Gould, G. W., 2012, Ed., *New Methods of Food Preservation* (Springer, Boston).
Goy, N.-A., Z. Denis, M. Lavaud, A. Grolleau, N. Dufour, A. Deblais, and U. Delabre, 2017, "Surface tension measurements with a smartphone," Phys. Teach. **55**, 498–499.
Gray, J., and G. J. Hancock, 1955, "The propulsion of sea-urchin spermatozoa," J. Exp. Biol. **32**, 802–814.
Gray, J. M. N. T., 2018, "Particle segregation in dense granular flows," Annu. Rev. Fluid Mech. **50**, 407–433.
Greenspan, H. P., and L. N. Howard, 1963, "On a time-dependent motion of a rotating fluid," J. Fluid Mech. **17**, 385–404.
Griebler, J. J., and S. A. Rogers, 2022, "The nonlinear rheology of complex yield stress foods," Phys. Fluids **34**, 023107.
Griffiths, R. W., 1981, "Layered double-diffusive convection in porous media," J. Fluid Mech. **102**, 221–248.
Grillo, I., 2003, "Small-angle neutron scattering study of a world-wide known emulsion: *Le Pastis*," Colloids Surf. A **225**, 153–160.
Grimshaw, R., 2002, Ed., *Environmental Stratified Flows* (Springer, New York).
Grotberg, J. B., 2001, "Respiratory fluid mechanics and transport processes," Annu. Rev. Biomed. Eng. **3**, 421–457.
Gruber, M. J., A. Valji, and C. Ranganath, 2019, "Curiosity and learning: A neuroscientific perspective," in *The Cambridge Handbook of Motivation and Learning* (Cambridge University Press, Cambridge, England), pp. 397–417.
Grunberg, L., and A. H. Nissan, 1949, "Mixture law for viscosity," Nature (London) **164**, 799–800.
Guazzelli, E., and J. F. Morris, 2011, *A Physical Introduction to Suspension Dynamics* (Cambridge University Press, Cambridge, England).
Gude, S., E. Pinçe, K. M. Taute, A.-B. Seinen, T. S. Shimizu, and S. J. Tans, 2020, "Bacterial coexistence driven by motility and spatial competition," Nature (London) **578**, 588–592.
Gunes, D. Z., 2018, "Microfluidics for food science and engineering," Curr. Opin. Food Sci. **21**, 57–65.
Guyon, E., J.-P. Hulin, L. Petit, and C. D. Mitescu, 2001, *Physical Hydrodynamics* (Oxford University Press, New York).
Guzmán-Lastra, F., H. Löwen, and A. J. T. M. Mathijssen, 2021, "Active carpets drive non-equilibrium diffusion and enhanced molecular fluxes," Nat. Commun. **12**, 1–15.
Hadamard, J. S., 1911, "Mouvement permanent lent d'une sphère liquid et visqueuse dans un liquide visqueux [Slow, steady motion of a liquid viscous sphere through a viscous fluid]," C.R. Hebd. Seances Acad. Sci. **152**, 1735–1738, https://cir.nii.ac.jp/crid/1571417125808224640?lang=en.
Hadfield, C., 2013, "Wringing out a water soaked washcloth in space—Canadian Space Agency science HD video," https://www.youtube.com/watch?v=KFPvdNbftOY (accessed May 8, 2020).
Haedelt, J., S. Beckett, and K. Niranjan, 2007, "Bubble-included chocolate: Relating structure with sensory response," J. Food Sci. **72**, E138–E142.
Hager, W. H., 2013, *Energy Dissipators and Hydraulic Jump*, Vol. 8 (Springer, New York).
Hahn, C., S. Nöbel, R. Maisch, W. Rösingh, J. Weiss, and J. Hinrichs, 2015, "Adjusting rheological properties of concentrated microgel suspensions by particle size distribution," Food Hydrocolloids **49**, 183–191.
Håkansson, A., 2019, "Emulsion formation by homogenization: Current understanding and future perspectives," Annu. Rev. Food Sci. Technol. **10**, 239–258.
Hall, R. S., S. J. Board, A. J. Clare, R. B. Duffey, T. S. Playle, and D. H. Poole, 1969, "Inverse Leidenfrost phenomenon," Nature (London) **224**, 266–267.
Halpern, D., and J. B. Grotberg, 1992, "Dynamics and transport of a localized soluble surfactant on a thin film," J. Fluid Mech. **237**, 1–11.
Hammond, P. S., 2021, "Will we ever wash our hands of lubrication theory?," Phys. Fluids **33**, 081908.
Handwashing Liaison Group, 1999, "Hand washing: A modest measure—With big effects," Br. Med. J. **318**, 686.
Han, W., and Z. Lin, 2012, "Learning from 'coffee rings': Ordered structures enabled by controlled evaporative self-assembly," Angew. Chem., Int. Ed. Engl. **51**, 1534–1546.
Harper, J. F., 1972, "The motion of bubbles and drops through liquids," in *Advances in Applied Mechanics*, Vol. 12, edited by C.-S. Yih (Elsevier, New York), pp. 59–129.
Harrington, M., J. H. Weijs, and W. Losert, 2013, "Suppression and Emergence of Granular Segregation under Cyclic Shear," Phys. Rev. Lett. **111**, 078001.
Hartel, R. W., 1996, "Ice crystallization during the manufacture of ice cream," Trends Food Sci. Technol. **7**, 315–321.
Harvey, D., J. M. Harper, and J. C. Burton, 2021, "Minimum Leidenfrost Temperature on Smooth Surfaces," Phys. Rev. Lett. **127**, 104501.
Harwood, W. S., M. N. Parker, and M. Drake, 2020, "Influence of ethanol concentration on sensory perception of rums using temporal check-all-that-apply," J. Sens. Stud. **35**, e12546.
Haward, S. J., 2016, "Microfluidic extensional rheometry using stagnation point flow," Biomicrofluidics **10**, 043401.
Hayashi, H., 1994, "Viscoelasticity of butter," in *Developments in Food Engineering: Proceedings of the 6th International Congress on Engineering and Food*, edited by T. Yano, R. Matsuno, and K. Nakamura (Springer, Boston), pp. 75–77.
He, S., N. Joseph, S. Feng, M. Jellicoe, and C. L. Raston, 2020, "Application of microfluidic technology in food processing," Food Funct. **11**, 5726–5737.
Heavers, R. M., and L. A. Colucci, 2009, "Sugar fingers and double-diffusive convection," J. Chem. Educ. **86**, 1326.

Heavers, R. M., and R. M. Dapp, 2010, "The Ekman layer and why tea leaves go to the center of the cup," Phys. Teach. **48**, 96–100.
Heavers, R. M., and M. G. Medeiros, 1990, "Laminar and turbulent flow in a glass tube," Phys. Teach. **28**, 297–299.
Heisser, R. H., V. P. Patil, N. Stoop, E. Villermaux, and J. Dunkel, 2018, "Controlling fracture cascades through twisting and quenching," Proc. Natl. Acad. Sci. U.S.A. **115**, 8665–8670.
Heldman, D. R., D. B. Lund, and C. Sabliov, 2018, *Handbook of Food Engineering* (CRC Press, Boca Raton).
Helfrich, K. R., and W. K. Melville, 2006, "Long nonlinear internal waves," Annu. Rev. Fluid Mech. **38**, 395–425.
Henderson, D. M., and J. W. Miles, 1994, "Surface-wave damping in a circular cylinder with a fixed contact line," J. Fluid Mech. **275**, 285–299.
Hennes, M., J. Tailleur, G. Charron, and A. Daerr, 2017, "Active depinning of bacterial droplets: The collective surfing of *Bacillus subtilis*," Proc. Natl. Acad. Sci. U.S.A. **114**, 5958–5963.
Henrywood, R. H., and A. Agarwal, 2013, "The aeroacoustics of a steam kettle," Phys. Fluids **25**, 107101.
Herczyński, A., C. Chernuschi, and L. Mahadevan, 2011, "Painting with drops, jets, and sheets," Phys. Today **64**, No. 6, 31.
Herczyński, A., and P. D. Weidman, 2012, "Experiments on the periodic oscillation of free containers driven by liquid sloshing," J. Fluid Mech. **693**, 216–242.
Hermans, E., M. S. Bhamla, P. Kao, G. G. Fuller, and J. Vermant, 2015, "Lung surfactants and different contributions to thin film stability," Soft Matter **11**, 8048–8057.
Herminghaus, S., 2005, "Dynamics of wet granular matter," Adv. Phys. **54**, 221–261.
Herminghaus, S., K. Jacobs, K. Mecke, J. Bischof, A. Fery, M. Ibn-Elhaj, and S. Schlagowski, 1998, "Spinodal dewetting in liquid crystal and liquid metal films," Science **282**, 916–919.
Herschel, W. H., and R. Bulkley, 1926, "Konsistenzmessungen von Gummi-Benzollösungen [Material property measurements of rubber-petrol solutions]," Kolloid Z. **39**, 291–300.
Herwig, H., 2018, *Ach, So Ist Das!* (Springer, Wiesbaden).
Hewitt, I. J., N. J. Balmforth, and J. N. McElwaine, 2011, "Continual skipping on water," J. Fluid Mech. **669**, 328–353.
Hickson, P., *et al.*, 2007, "The Large Zenith Telescope: A 6 m liquid-mirror telescope," Publ. Astron. Soc. Pac. **119**, 444.
Hills, B. P., L. Arnould, C. Bossu, and Y. P. Ridge, 2001, "Microstructural factors controlling the survival of food-borne pathogens in porous media," Int. J. Food Microbiol. **66**, 163–173.
Hinch, E. J., and A. Acrivos, 1979, "Steady long slender droplets in two-dimensional straining motion," J. Fluid Mech. **91**, 401.
Hlavác, P., and M. Božiková, 2013, "Influence of storing and temperature on rheologic and thermophysical properties of whisky samples," J. Cent. Eur. Agric. **14**, 291–304.
Homsy, G. M., 2019, *Multimedia Fluid Mechanics Online* (Cambridge University Press, Cambridge, England).
Hoseney, R. C., K. Zeleznak, and A. Abdelrahman, 1983, "Mechanism of popcorn popping," J. Cereal Sci. **1**, 43–52.
Hosoi, A. E., and J. W. M. Bush, 2001, "Evaporative instabilities in climbing films," J. Fluid Mech. **442**, 217.
Hossain, M., and R. H. Ewoldt, 2022, "Do-it-yourself rheometry," Phys. Fluids **34**, 053105.
Hoult, D. P., 1972, "Oil spreading on the sea," Annu. Rev. Fluid Mech. **4**, 341–368.
Howland, C. J., A. Antkowiak, J. R. Castrejón-Pita, S. D. Howison, J. M. Oliver, R. W. Style, and A. A. Castrejón-Pita, 2016, "It's Harder to Splash on Soft Solids," Phys. Rev. Lett. **117**, 184502.
Howse, J. R., R. A. L. Jones, A. J. Ryan, T. Gough, R. Vafabakhsh, and R. Golestanian, 2007, "Self-Motile Colloidal Particles: From Directed Propulsion to Random Walk," Phys. Rev. Lett. **99**, 048102.
Hsu, L., and Y.-J. Chen, 2021, "Does coffee taste better with latte art? A neuroscientific perspective," Br. Food J. **123**, 1931–1946.
Hsu, T. T., T. W. Walker, C. W. Frank, and G. G. Fuller, 2014, "Instabilities and elastic recoil of the two-fluid circular hydraulic jump," Exp. Fluids **55**, 1645.
Hu, D. L., M. Prakash, B. Chan, and J. W. M. Bush, 2007, "Water-walking devices," Exp. Fluids, **43**769–778.
Hu, H., and R. G. Larson, 2006, "Marangoni effect reverses coffee-ring depositions," J. Phys. Chem. B **110**, 7090–7094.
Huang, C., W. Ma, and S. Stack, 2012, "The hygienic efficacy of different hand-drying methods: A review of the evidence," Mayo Clinic Proc. **87**, 791–798.
Hudson, S. D., F. R. Phelan, Jr., M. D. Handler, J. T. Cabral, K. B. Migler, and E. J. Amis, 2004, "Microfluidic analog of the four-roll mill," Appl. Phys. Lett. **85**, 335–337.
Huerta, D. A., and J. C. Ruiz-Suárez, 2004, "Vibration-Induced Granular Segregation: A Phenomenon Driven by Three Mechanisms," Phys. Rev. Lett. **92**, 114301.
Hughes, S. W., 2011, "The secret siphon," Phys. Educ. **46**, 298.
Hunt, G. R., and H. C. Burridge, 2015, "Fountains in industry and nature," Annu. Rev. Fluid Mech. **47**, 195–220.
Hunt, M. L., and N. M. Vriend, 2010, "Booming sand dunes," Annu. Rev. Earth Planet Sci. **38**, 281–301.
Huppert, H. E., 1982a, "Flow and instability of a viscous current down a slope," Nature (London) **300**, 427–429.
Huppert, H. E., 1982b, "The propagation of two-dimensional and axisymmetric viscous gravity currents over a rigid horizontal surface," J. Fluid Mech. **121**, 43–58.
Huppert, H. E., 2006, "Gravity currents: A personal perspective," J. Fluid Mech. **554**, 299–322.
Huppert, H. E., and J. S. Turner, 1981, "Double-diffusive convection," J. Fluid Mech. **106**, 299–329.
Hwang, J., J. Ha, R. Siu, Y. S. Kim, and S. Tawfick, 2022, "Swelling, softening, and elastocapillary adhesion of cooked pasta," Phys. Fluids **34**, 042105.
Hyman, A. A., C. A. Weber, and F. Jülicher, 2014, "Liquid-liquid phase separation in biology," Annu. Rev. Cell Dev. Biol. **30**, 39–58.
Ibrahim, R. A., 2005, *Liquid Sloshing Dynamics: Theory and Applications* (Cambridge University Press, Cambridge, England).
Ichikawa, C., D. Ishikawa, J. M. Yang, and T. Fujii, 2020, "Phenomenological analysis on whipping behavior of rice flour batter," J. Food Sci. **85**, 4327–4334.
Illy, E., and L. Navarini, 2011, "Neglected food bubbles: The espresso coffee foam," Food Biophys. **6**, 335–348.
Irwin, P. A., 2010, "Vortices and tall buildings: A recipe for resonance," Phys. Today **63**, No. 9, 68–69.
Ishida, S., P. Synak, F. Narita, T. Hachisuka, and C. Wojtan, 2020, "A model for soap film dynamics with evolving thickness," ACM Trans. Graph. **39**, 31:1–31:11.
Issa, S. F., W. E. Field, C. V. Schwab, F. S. Issa, and E. A. Nauman, 2017, "Contributing causes of injury or death in grain entrapment, engulfment, and extrication," J. Agromed. **22**, 159–169.
Jaeger, H. M., S. R. Nagel, and R. P. Behringer, 1996, "Granular solids, liquids, and gases," Rev. Mod. Phys. **68**, 1259–1273.
Jafari Kang, S., V. Vandadi, J. D. Felske, and H. Masoud, 2016, "Alternative mechanism for coffee-ring deposition based on active role of free surface," Phys. Rev. E **94**, 063104.

Jakubowski, M., 2015, "Secondary flows occurring in a whirlpool separator—A study of phenomena—observation, simulation and measurements," Chem. Proc. Eng. **36**, 277–289.

Jakubowski, M., M. Stachnik, M. Sterczyńska, R. Matysko, J. Piepiórka-Stepuk, A. Dowgiałło, O. V. Ageev, and R. Knitter, 2019, "CFD analysis of primary and secondary flows and PIV measurements in whirlpool and whirlpool kettle with pulsatile filling: Analysis of the flow in a swirl separator," J. Food Eng. **258**, 27–33.

Jambon-Puillet, E., W. Bouwhuis, J. H. Snoeijer, and D. Bonn, 2019, "Liquid Helix: How Capillary Jets Adhere to Vertical Cylinders," Phys. Rev. Lett. **122**, 184501.

Janiaud, E., and F. Graner, 2005, "Foam in a two-dimensional Couette shear: A local measurement of bubble deformation," J. Fluid Mech. **532**, 243–267.

Janssen, F., A. G. Wouters, Y. Meeus, P. Moldenaers, J. Vermant, and J. A. Delcour, 2020, "The role of non-starch polysaccharides in determining the air-water interfacial properties of wheat, rye, and oat dough liquor constituents," Food Hydrocolloids **105**, 105771.

Janssens, S. D., S. Koizumi, and E. Fried, 2017, "Behavior of self-propelled acetone droplets in a Leidenfrost state on liquid substrates," Phys. Fluids **29**, 032103.

Jansson, T. R. N., M. P. Haspang, K. H. Jensen, P. Hersen, and T. Bohr, 2006, "Polygons on a Rotating Fluid Surface," Phys. Rev. Lett. **96**, 174502.

Jarman, P. D., and K. J. Taylor, 1964, "Light emission from cavitating water," Br. J. Appl. Phys. **15**, 321.

Jasper, W. J., and N. Anand, 2019, "A generalized variational approach for predicting contact angles of sessile nano-droplets on both flat and curved surfaces," J. Mol. Liq. **281**, 196–203.

Jensen, K. H., K. Berg-Sørensen, H. Bruus, N. M. Holbrook, J. Liesche, A. Schulz, M. A. Zwieniecki, and T. Bohr, 2016, "Sap flow and sugar transport in plants," Rev. Mod. Phys. **88**, 035007.

Jia, Z.-h., M.-y. Chen, and H.-t. Zhu, 2017, "Reversible self-propelled Leidenfrost droplets on ratchet surfaces," Appl. Phys. Lett. **110**, 091603.

Jin, C., Y. Chen, C. C. Maass, and A. J. T. M. Mathijssen, 2021, "Collective Entrainment and Confinement Amplify Transport by Schooling Microswimmers," Phys. Rev. Lett. **127**, 088006.

Jirout, J. J., V. E. Vitiello, and S. K. Zumbrunn, 2018, "Curiosity in schools," in *The New Science of Curiosity*, edited by G. Gordon (Nova Science, Hauppauge, NY), pp. 243–266.

Johnson, G. C., and K. A. Kearney, 2009, "Ocean climate change fingerprints attenuated by salt fingering?," Geophys. Res. Lett. **36**, L21603.

Johnson, R. E., 1980, "An improved slender-body theory for Stokes flow," J. Fluid Mech. **99**, 411–431.

Jones, S. F., G. M. Evans, and K. P. Galvin, 1999, "The cycle of bubble production from a gas cavity in a supersaturated solution," Adv. Colloid Interface Sci. **80**, 51–84.

Josef, Stefan, 1874, "Versuche über die scheinbare Adhäsion [Experiments on apparent adhesion]," Sitz. Kaiserl. Akad. Wiss. Math.-Naturwiss. Wien **69**, 713–735.

Joseph, D. D., 1990, "Fluid dynamics of two miscible liquids with diffusion and gradient stresses," Eur. J. Mech. B **9**, 565–596, 10.1007/978-1-4615-7061-5_6.

Joseph, D. D., A. Huang, and H. H. Hu, 1996, "Non-solenoidal velocity effects and Korteweg stresses in simple mixtures of incompressible liquids," Physica (Amsterdam) **97D**, 104–125.

Joseph, D. D., and Y. Y. Renardy, 2013, *Fundamentals of Two-Fluid Dynamics*, Interdisciplinary Applied Mathematics Vol. 4 (Springer, New York).

Jumper, W. D., and B. Stanchev, 2014, "Towards explaining the water siphon," Phys. Teach. **52**, 474–478.

Juncker, D., H. Schmid, and E. Delamarche, 2005, "Multipurpose microfluidic probe," Nat. Mater. **4**, 622–628.

Jung, S., 2021, "Pinch-off dynamics to elucidate animal lapping," Phys. Rev. Fluids **6**, 073102.

Jurin, J., 1718, "An account of some experiments shown before the Royal Society; with an enquiry into the cause of the ascent and suspension of water in capillary tubes," Phil. Trans. R. Soc. London **30**, 739–747.

Kadanoff, L. P., 2001, "Turbulent heat flow: Structures and scaling," Phys. Today **54**, No. 8, 34–39.

Kaestner, A., 2012, "Neutron movie of coffee making," https://www.youtube.com/watch?v=VESMU7JfVHU (accessed April 16, 2020).

Kalliadasis, S., C. Ruyer-Quil, B. Scheid, and M. G. Velarde, 2012, *Falling Liquid Films* (Springer, New York).

Kallick, B., and A. Zmuda, 2017, *Students at the Center: Personalized Learning with Habits of Mind* (ASCD, Alexandria, VA).

Kalpakli, A., R. Örlü, and P. H. Alfredsson, 2012, "Dean vortices in turbulent flows: Rocking or rolling?," J. Visualization **15**, 37–38.

Kang, Y. K., S. H. Im, J. S. Ryu, J. Lee, and H. J. Chung, 2020, "Simple visualized readout of suppressed coffee ring patterns for rapid and isothermal genetic testing of antibacterial resistance," Biosens. Bioelectron. **168**, 112566.

Kang, Y.-j., and J. F. Frank, 1989, "Biological aerosols: A review of airborne contamination and its measurement in dairy processing plants," J. Food Prot. **52**, 512–524.

Kant, K., M.-A. Shahbazi, V. P. Dave, T. A. Ngo, V. A. Chidambara, L. Q. Than, D. D. Bang, and A. Wolff, 2018, "Microfluidic devices for sample preparation and rapid detection of foodborne pathogens," Biotechnol. Adv. **36**, 1003–1024.

Kapitza, P. L., and S. P. Kapitza, 1948, "Wave flow of thin layers of a viscous fluid. I–III," Zh. Eksp. Teor. Fiz. **18**, 3–18, https://ui.adsabs.harvard.edu/abs/1948ZhETF..18....3K/abstract.

Kapitza, P. L., and S. P. Kapitza, 1965, "Wave flow of thin layers of a viscous fluid," in *Collected Papers of P. L. Kapitza*, edited by D. Ter Haar (Pergamon, New York), pp. 662–709.

Karlsson, A., R. Ipsen, K. Schrader, and Y. Ardö, 2005, "Relationship between physical properties of casein micelles and rheology of skim milk concentrate," J. Dairy Sci. **88**, 3784–3797.

Karlsson, B. C., and R. Friedman, 2017, "Dilution of whisky—The molecular perspective," Sci. Rep. **7**, 1–9.

Karpitschka, S., A. Pandey, L. A. Lubbers, J. H. Weijs, L. Botto, S. Das, B. Andreotti, and J. H. Snoeijer, 2016, "Liquid drops attract or repel by the inverted Cheerios effect," Proc. Natl. Acad. Sci. U.S.A. **113**, 7403–7407.

Karunakaran, C., R. Rajkumar, and K. Bhargava, 2015, "Introduction to biosensors," *Biosensors and Bioelectronics*, edited by C. Karunakaran, K. Bhargava, and R. Benjamin (Elsevier, New York), pp. 1–68.

Katifori, E., 2018, "The transport network of a leaf," C.R. Phys. **19**, 244–252.

Kaye, A., 1963, "A bouncing liquid stream," Nature (London) **197**, 1001–1002.

Kaye, N. B., 2021, "Teaching fluid mechanics: In-class activities to enhance student understanding," https://teachingfluids.wordpress.com/category/take-home-lab-experiments/ (accessed November 4, 2021).

Kaye, N. B., and J. Ogle, 2022, "Overcoming misconceptions and enhancing student's physical understanding of civil and environmental engineering fluid mechanics," Phys. Fluids **34**, 041801.

Keiser, L., H. Bense, P. Colinet, J. Bico, and E. Reyssat, 2017, "Marangoni Bursting: Evaporation-Induced Emulsification of Binary Mixtures on a Liquid Layer," Phys. Rev. Lett. **118**, 074504.

Keller, J. B., 1998, "Surface tension force on a partly submerged body," Phys. Fluids **10**, 3009–3010.
Kelly, B. E., I. Bhattacharya, H. Heidari, M. Shusteff, C. M. Spadaccini, and H. K. Taylor, 2019, "Volumetric additive manufacturing via tomographic reconstruction," Science **363**, 1075–1079.
Kelvin, Lord, 1871, "Hydrokinetic solutions and observations," Philos. Mag. **42**, 362–377.
Kentish, S., T. J. Wooster, M. Ashokkumar, S. Balachandran, R. Mawson, and L. Simons, 2008, "The use of ultrasonics for nanoemulsion preparation," Innovative Food Sci. Emerging Technol. **9**, 170–175.
Kerr, R. A., 2002, "Salt fingers mix the sea," Science **295**, 1821.
Khonsari, M. M., and E. R. Booser, 2017, *Applied Tribology: Bearing Design and Lubrication* (John Wiley & Sons, New York).
Kidambi, R., 2011, "Damping of surface waves in a brimful circular cylinder with a contaminated free surface," Fluid Dyn. Res. **43**, 035504.
Kim, D., Y. Cao, D. Mariappan, M. S. Bono Jr., A. J. Hart, and B. Marelli, 2021, "A microneedle technology for sampling and sensing bacteria in the food supply chain," Adv. Funct. Mater. **31**, 2005370.
Kim, H., F. Boulogne, E. Um, I. Jacobi, E. Button, and H. A. Stone, 2016, "Controlled Uniform Coating from the Interplay of Marangoni Flows and Surface-Adsorbed Macromolecules," Phys. Rev. Lett. **116**, 124501.
Kim, H., K. Muller, O. Shardt, S. Afkhami, and H. A. Stone, 2017, "Solutal Marangoni flows of miscible liquids drive transport without surface contamination," Nat. Phys. **13**, 1105–1110.
Kim, I., and S. Mandre, 2017, "Marangoni elasticity of flowing soap films," Phys. Rev. Fluids **2**, 082001(R).
Kim, S., and S. J. Karrila, 1991, *Microhydrodynamics: Principles and Selected Applications* (Butterworth-Heinemann, Oxford).
King, J. R. C., and S. J. Lind, 2019, "The Kaye effect: New experiments and a mechanistic explanation," J. Non-Newtonian Fluid Mech. **273**, 104165.
King, W. D., 2008, "The physics of a stove-top espresso machine," Am. J. Phys. **76**, 558–565.
Kirby, B. J., 2010, *Micro- and Nanoscale Fluid Mechanics: Transport in Microfluidic Devices* (Cambridge University Press, Cambridge, England).
Kiyama, A., R. Rabbi, Z. Pan, S. Dutta, J. S. Allen, and T. T. Truscott, 2022, "Morphology of bubble dynamics and sound in heated oil," Phys. Fluids **34**, 062107.
Kleinstreuer, C., and Z. Zhang, 2010, "Airflow and particle transport in the human respiratory system," Annu. Rev. Fluid Mech. **42**, 301–334.
Knight, J. B., E. E. Ehrichs, V. Y. Kuperman, J. K. Flint, H. M. Jaeger, and S. R. Nagel, 1996, "Experimental study of granular convection," Phys. Rev. E **54**, 5726–5738.
Knight, J. B., H. M. Jaeger, and S. R. Nagel, 1993, "Vibration-Induced Size Separation in Granular Media: The Convection Connection," Phys. Rev. Lett. **70**, 3728–3731.
Knorr, D., A. Froehling, H. Jaeger, K. Reineke, O. Schlueter, and K. Schoessler, 2011, "Emerging technologies in food processing," Annu. Rev. Food Sci. Technol. **2**, 203–235.
Knorr, W., 1983, "The geometry of burning-mirrors in antiquity," Isis **74**, 53–73.
Ko, H., and D. L. Hu, 2020, "The physics of tossing fried rice," J. R. Soc. Interface **17**, 20190622.
Koch, D. L., and G. Subramanian, 2011, "Collective hydrodynamics of swimming microorganisms: Living fluids," Annu. Rev. Fluid Mech. **43**, 637–659.
Koens, L., W. Wang, M. Sitti, and E. Lauga, 2019, "The near and far of a pair of magnetic capillary disks," Soft Matter **15**, 1497–1507.
Kohira, M. I., Y. Hayashima, M. Nagayama, and S. Nakata, 2001, "Synchronized self-motion of two camphor boats," Langmuir **17**, 7124–7129.
Koivisto, J., and D. J. Durian, 2017, "The sands of time run faster near the end," Nat. Commun. **8**, 1–6.
Kojima, M., E. J. Hinch, and A. Acrivos, 1984, "The formation and expansion of a toroidal drop moving in a viscous fluid," Phys. Fluids **27**, 19–32.
Kokini, J. L., and A. Dickie, 1981, "An attempt to identify and model transient viscoelastic flow in foods," J. Texture Stud. **12**, 539–557.
Kolmogorov, A. N., 1941, "The local structure of turbulence in incompressible viscous fluid for very large Reynolds numbers," C.R. Acad. Sci. URSS **30**, 301–305, https://cir.nii.ac.jp/crid/1573950401146140416?lang=en.
Kosowatz, J. (American Society of Mechanical Engineers), 2011, "Symbol of the millennium: The Falkirk Wheel," https://www.asme.org/topics-resources/content/symbol-of-the-millennium-the-falkirk-wheel (accessed December 7, 2022).
Kralchevsky, P. A., and K. Nagayama, 2000, "Capillary interactions between particles bound to interfaces, liquid films and biomembranes," Adv. Colloid Interface Sci. **85**, 145–192.
Krantz, M., H. Zhang, and J. Zhu, 2009, "Characterization of powder flow: Static and dynamic testing," Powder Technol. **194**, 239–245.
Kraynik, A. M., 1988, "Foam flows," Annu. Rev. Fluid Mech. **20**, 325–357.
Kraynik, A. M., M. K. Neilsen, D. A. Reinelt, and W. E. Warren, 1999, "Foam micromechanics," in *Foams and emulsions*, NATO ASI Ser., Vol. 354, edited by J. F. Sadoc and N. Rivier (Springer, New York), pp. 259–286, 10.1007/978-94-015-9157-7_15.
Kreis, T., 1986, "Digital holographic interference-phase measurement using the Fourier-transform method," J. Opt. Soc. Am. A **3**, 847–855.
Krishnamurthy, D., and G. Subramanian, 2018a, "Heat or mass transport from drops in shearing flows. Part 1. The open-streamline regime," J. Fluid Mech. **850**, 439–483.
Krishnamurthy, D., and G. Subramanian, 2018b, "Heat or mass transport from drops in shearing flows. Part 2. Inertial effects on transport," J. Fluid Mech. **850**, 484–524.
Krishnamurti, R., 1970a, "On the transition to turbulent convection. Part 1. The transition from two- to three-dimensional flow," J. Fluid Mech. **42**, 295–307.
Krishnamurti, R., 1970b, "On the transition to turbulent convection. Part 2. The transition to time-dependent flow," J. Fluid Mech. **42**, 309–320.
Krishne Gowda, V., C. Brouzet, T. Lefranc, L. D. Söderberg, and F. Lundell, 2019, "Effective interfacial tension in flow-focusing of colloidal dispersions: 3-D numerical simulations and experiments," J. Fluid Mech. **876**, 1052–1076.
Kristensen, H. G., and T. Schaefer, 1987, "Granulation: A review on pharmaceutical wet-granulation," Drug Dev. Ind. Pharm. **13**, 803–872.
Krokida, M. K., Z. B. Maroulis, and G. D. Saravacos, 2001, "Rheological properties of fluid fruit and vegetable puree products: Compilation of literature data," Int. J. Food Prop. **4**, 179–200.
Krumbein, W. C., 1934, "Size frequency distributions of sediments," J. Sediment. Res. **4**, 65–77.
Kudrolli, A., 2004, "Size separation in vibrated granular matter," Rep. Prog. Phys. **67**, 209.
Kundan, A., J. L. Plawsky, P. C. Wayner, D. F. Chao, R. J. Sicker, B. J. Motil, T. Lorik, L. Chestney, J. Eustace, and J. Zoldak, 2015,

"Thermocapillary Phenomena and Performance Limitations of a Wickless Heat Pipe in Microgravity," Phys. Rev. Lett. **114**, 146105.

Kuranz, C. C., *et al.*, 2018, "How high energy fluxes may affect Rayleigh-Taylor instability growth in young supernova remnants," Nat. Commun. **9**, 1564.

Kurti, N., and G. Kurti, 1988, *But the Crackling is Superb: An Anthology on Food and Drink by Fellows and Foreign Members of the Royal Society* (Adam Hilger Publishers, Philadelphia).

Kurti, N., and H. This-Benckhard, 1994, "The kitchen as a lab," Sci. Am. **270**, No. 4, 120–123.

Lacaze, L., P. Guenoun, D. Beysens, M. Delsanti, P. Petitjeans, and P. Kurowski, 2010, "Transient surface tension in miscible liquids," Phys. Rev. E **82**, 041606.

Lafuma, A., and D. Quéré, 2003, "Superhydrophobic states," Nat. Mater. **2**, 457–460.

Lagarde, A., C. Josserand, and S. Protière, 2019, "The capillary interaction between pairs of granular rafts," Soft Matter **15**, 5695–5702.

Lagubeau, G., M. Le Merrer, C. Clanet, and D. Quéré, 2011, "Leidenfrost on a ratchet," Nat. Phys. **7**, 395–398.

Lahne, J. B., and S. J. Schmidt, 2010, "Gelatin-filtered consommé: A practical demonstration of the freezing and thawing processes," J. Food Sci. Educ. **9**, 53–58.

Lakkaraju, R., R. J. A. M. Stevens, P. Oresta, R. Verzicco, D. Lohse, and A. Prosperetti, 2013, "Heat transport in bubbling turbulent convection," Proc. Natl. Acad. Sci. U.S.A. **110**, 9237–9242.

Lamb, D., and J. Verlinde, 2011, *Physics and Chemistry of Clouds* (Cambridge University Press, Cambridge, England).

Lamb, H., 1993, *Hydrodynamics*, 6th ed. (Cambridge University Press, Cambridge, England) .

Landfeld, A., P. Novotna, J. Strohalm, M. Houska, and K. Kyhos, 2000, "Viscosity of cocoa butter," Int. J. Food Prop. **3**, 165–169.

Langston, L. S., 2001, "Secondary flows in axial turbines—A review," Ann. N.Y. Acad. Sci. **934**, 11–26.

Larson, R. G., and Y. Wei, 2019, "A review of thixotropy and its rheological modeling," J. Rheol. **63**, 477–501.

Lauga, E., 2009, "Life at high Deborah number," Europhys. Lett. **86**, 64001.

Lauga, E., 2011, "Life around the scallop theorem," Soft Matter **7**, 3060–3065.

Lauga, E., 2016, "Bacterial hydrodynamics," Annu. Rev. Fluid Mech. **48**, 105–130.

Lauga, E., 2020, *The Fluid Dynamics of Cell Motility*, Cambridge Texts in Applied Mathematics Vol. 62 (Cambridge University Press, Cambridge, England).

Lauga, E., and T. R. Powers, 2009, "The hydrodynamics of swimming microorganisms," Rep. Prog. Phys. **72**, 096601.

Lautrup, B., 2011, *Physics of Continuous Matter: Exotic and Everyday Phenomena in the Macroscopic World* (CRC Press, Boca Raton).

Lawson-Keister, E., and M. L. Manning, 2021, "Jamming and arrest of cell motion in biological tissues," Curr. Opin. Cell Biol. **72**, 146–155.

Leal, L. G., 2007, *Advanced Transport Phenomena: Fluid Mechanics and Convective Transport Processes* (Cambridge University Press, Cambridge, England).

Lee, H.-S., and N. Butler, 2003, "Making authentic science accessible to students," Int. J. Sci. Educ. **25**, 923–948.

Lee, K. S., and V. M. Starov, 2007, "Spreading of surfactant solutions over thin aqueous layers: Influence of solubility and micelles disintegration," J. Colloid Interface Sci. **314**, 631–642.

Lee, N., S. Allen, E. Smith, and L. M. Winters, 1993, "Does the tip of a snapped towel travel faster than sound?," Phys. Teach. **31**, 376–77.

Lee, S., E. Q. Li, J. O. Marston, A. Bonito, and S. T. Thoroddsen, 2013, "Leaping shampoo glides on a lubricating air layer," Phys. Rev. E **87**, 061001.

Leidenfrost, J. G., 1756, *De Aquae Communis Nonnullis Qualitatibus Tractatus* (Ovenius, Frankfurt).

Leighton, A., A. Leviton, and O. E. Williams, 1934, "The apparent viscosity of ice cream: I. The sagging beam method of measurement. II. Factors to be controlled. III. The effects of milkfat, gelatin and homogenization temperature," J. Dairy Sci. **17**, 639–650.

Leighton, T. G., 2012a, *The Acoustic Bubble* (Academic Press, New York).

Leighton, T. G., 2012b, "How can humans, in air, hear sound generated underwater (and can goldfish hear their owners talking)?," J. Acoust. Soc. Am. **131**, 2539–2542.

Leon, V. J., and K. K. Varanasi, 2021, "Self-Propulsion of Boiling Droplets on Thin Heated Oil Films," Phys. Rev. Lett. **127**, 074502.

Lepeltier, E., C. Bourgaux, and P. Couvreur, 2014, "Nanoprecipitation and the 'ouzo effect': Application to drug delivery devices," Adv. Drug Delivery Rev. **71**, 86–97.

Le Révérend, B. J. D., P. J. Fryer, and S. Bakalis, 2009, "Modelling crystallization and melting kinetics of cocoa butter in chocolate and application to confectionery manufacturing," Soft Matter **5**, 891–902.

Levich, V. G., and V. S. Krylov, 1969, "Surface-tension-driven phenomena," Annu. Rev. Fluid Mech. **1**, 293–316.

Lewis, D. J., 1950, "The instability of liquid surfaces when accelerated in a direction perpendicular to their planes. II," Proc. R. Soc. A **202**, 81–96.

Li, B., and D.-W. Sun, 2002, "Novel methods for rapid freezing and thawing of foods—A review," J. Food Eng. **54**, 175–182.

Li, G., L. Cheng, J. Zhu, K. E. Trenberth, M. E. Mann, and J. P. Abraham, 2020, "Increasing ocean stratification over the past half-century," Nat. Clim. Change **10**, 1116–1123.

Li, H., and J. J. McCarthy, 2003, "Controlling Cohesive Particle Mixing and Segregation," Phys. Rev. Lett. **90**, 184301.

Li, Y., Q. Yang, M. Li, and Y. Song, 2016, "Rate-dependent interface capture beyond the coffee-ring effect," Sci. Rep. **6**, 1–8.

Lien, T., and P. Davis, 2008, "A novel gripper for limp materials based on lateral Coanda ejectors," CIRP Ann. **57**, 33–36.

Liger-Belair, G., C. Cilindre, R. D. Gougeon, M. Lucio, I. Gebefügi, P. Jeandet, and P. Schmitt-Kopplin, 2009, "Unraveling different chemical fingerprints between a champagne wine and its aerosols," Proc. Natl. Acad. Sci. U.S.A. **106**, 16545–16549.

Liger-Belair, G., D. Cordier, and R. Georges, 2019, "Under-expanded supersonic CO_2 freezing jets during champagne cork popping," Sci. Adv. **5**, eaav5528.

Liger-Belair, G., M. Parmentier, and P. Jeandet, 2006, "Modeling the kinetics of bubble nucleation in champagne and carbonated beverages," J. Phys. Chem. B **110**, 21145–21151.

Liger-Belair, G., G. Polidori, and P. Jeandet, 2008, "Recent advances in the science of champagne bubbles," Chem. Soc. Rev. **37**, 2490–2511.

Liger-Belair, G., M. Vignes-Adler, C. Voisin, B. Robillard, and P. Jeandet, 2002, "Kinetics of gas discharging in a glass of champagne: The role of nucleation sites," Langmuir **18**, 1294–1301.

Lin, C.-Y., W. Zhou, C.-T. Hu, F. Yang, and S. Lee, 2019, "Brownian motion and Einstein relation for migration of coffee particles in coffee suspensions," J. Sci. Food Agric. **99**, 3950–3956.

Lindén, J., 2020, "Upside down glass of water experiment revisited," Phys. Educ. **55**, 055023.

Lindholm, M., 2018, "Promoting curiosity?," Sci. Educ. **27**, 987–1002.
Linke, H., B. J. Alemán, L. D. Melling, M. J. Taormina, M. J. Francis, C. C. Dow-Hygelund, V. Narayanan, R. P. Taylor, and A. Stout, 2006, "Self-Propelled Leidenfrost Droplets," Phys. Rev. Lett. **96**, 154502.
Lisicki, M., 2013, "Four approaches to hydrodynamic Green's functions—The Oseen tensors," arXiv:1312.6231.
Liu, A. J., and S. R. Nagel, 1998, "Jamming is not just cool any more," Nature (London) **396**, 21–22.
Liu, A. J., and S. R. Nagel, 2010, "The jamming transition and the marginally jammed solid," Annu. Rev. Condens. Matter Phys. **1**, 347–369.
Liu, J., J. B. Schneider, and J. P. Gollub, 1995, "Three-dimensional instabilities of film flows," Phys. Fluids **7**, 55–67.
Liu, J., H. Zhou, Y. Tan, J. L. M. Mundo, and D. J. McClements, 2021, "Comparison of plant-based emulsifier performance in water-in-oil-in-water emulsions: Soy protein isolate, pectin and gum arabic," J. Food Eng. **307**, 110625.
Liu, Y., M. Andrew, J. Li, J. M. Yeomans, and Z. Wang, 2015, "Symmetry breaking in drop bouncing on curved surfaces," Nat. Commun. **6**, 10034.
Liu, Y., L. Moevius, X. Xu, T. Qian, J. M. Yeomans, and Z. Wang, 2014, "Pancake bouncing on superhydrophobic surfaces," Nat. Phys. **10**, 515–519.
Lohse, D., and K.-Q. Xia, 2010, "Small-scale properties of turbulent Rayleigh-Bénard convection," Annu. Rev. Fluid Mech. **42**, 335–364.
Longuet-Higgins, M. S., 1990, "An analytic model of sound production by raindrops," J. Fluid Mech. **214**, 395–410.
Lopes, M. C., and E. Bonaccurso, 2012, "Evaporation control of sessile water drops by soft viscoelastic surfaces," Soft Matter **8**, 7875–7881.
López-Alt, J. K., 2015, *The Food Lab: Better Home Cooking through Science* (W. W. Norton, New York).
López-Arias, T., L. M. Gratton, S. Bon, and S. Oss, 2009, "Back of the spoon: Outlook of Coanda effect," Phys. Teach. **47**, 508–512.
Lorefice, S., and A. Malengo, 2006, "Calibration of hydrometers," Meas. Sci. Technol. **17**, 2560.
Lorentz, H. A., 1907, *Abhandlung über Theoretische Physik* (B. G. Teubner, Leipzig).
Lorenz, R. D., 2006, *Spinning flight: Dynamics of frisbees, boomerangs, samaras, and skipping stones* (Springer-Verlag, New York).
Louhichi, A., M.-H. Morel, L. Ramos, and A. Banc, 2022, "Flow of gluten with tunable protein composition: From stress undershoot to stress overshoot and strain hardening," Phys. Fluids **34**, 051906.
Lu, Z., M. H. K. Schaarsberg, X. Zhu, L. Y. Yeo, D. Lohse, and X. Zhang, 2017, "Universal nanodroplet branches from confining the ouzo effect," Proc. Natl. Acad. Sci. U.S.A. **114**, 10332–10337.
Lubarda, V. A., 2013, "The shape of a liquid surface in a uniformly rotating cylinder in the presence of surface tension," Acta Mech. **224**, 1365–1382.
Lubetkin, S., and M. Blackwell, 1988, "The nucleation of bubbles in supersaturated solutions," J. Colloid Interface Sci. **126**, 610–615.
Lucey, J., M. Johnson, and D. Horne, 2003, "Invited review: Perspectives on the basis of the rheology and texture properties of cheese," J. Dairy Sci. **86**, 2725–2743.
Lun, C. K. K., S. B. Savage, D. J. Jeffrey, and N. Chepurniy, 1984, "Kinetic theories for granular flow: Inelastic particles in Couette flow and slightly inelastic particles in a general flowfield," J. Fluid Mech. **140**, 223–256.
Ma, X., J.-J. Liétor-Santos, and J. C. Burton, 2017, "Star-shaped oscillations of Leidenfrost drops," Phys. Rev. Fluids **2**, 031602.
Maass, C. C., C. Krüger, S. Herminghaus, and C. Bahr, 2016, "Swimming droplets," Annu. Rev. Condens. Matter Phys. **7**, 171–193.
MacKintosh, F. C., and C. F. Schmidt, 1999, "Microrheology," Curr. Opin. Colloid Interface Sci. **4**, 300–307.
MacLean, C., 2010, "Whisky university—what about the legs—viscimetry?," https://www.youtube.com/watch?v=_OwVN6mGHhA (accessed October 8, 2020).
MacLean, C., 2018, "The Scotch Malt Whisky Society (SMWS) masterclass: What beading can tell us," https://www.youtube.com/watch?v=x_WDNHyfsOQ (accessed October 8, 2020).
MacLean, C., 2020, *Malt Whisky* (Octopus, London).
Macosko, C. W., 1994, *Rheology: Principles, Measurements, and Applications* (Wiley-VCH, Weinheim).
Madl, A. C., C. Liu, D. Cirera-Salinas, G. G. Fuller, and D. Myung, 2022, "A mucin-deficient ocular surface mimetic platform for interrogating drug effects on biolubrication, antiadhesion properties, and barrier functionality," ACS Appl. Mater. Interfaces **14**, 18016–18030.
Magens, O. M., Y. Liu, J. F. Hofmans, J. A. Nelissen, and D. Ian Wilson, 2017, "Adhesion and cleaning of foods with complex structure: Effect of oil content and fluoropolymer coating characteristics on the detachment of cake from baking surfaces," J. Food Eng. **197**, 48–59.
Mahadevan, A., A. V. Orpe, A. Kudrolli, and L. Mahadevan, 2012, "Flow-induced channelization in a porous medium," Europhys. Lett. **98**, 58003.
Mahrt, L., 2014, "Stably stratified atmospheric boundary layers," Annu. Rev. Fluid Mech. **46**, 23–45.
Mairhofer, J., K. Roppert, and P. Ertl, 2009, "Microfluidic systems for pathogen sensing: A review," Sensors **9**, 4804–4823.
Mampallil, D., and H. B. Eral, 2018, "A review on suppression and utilization of the coffee-ring effect," Adv. Colloid Interface Sci. **252**, 38–54.
Manikantan, H., and T. M. Squires, 2020, "Surfactant dynamics: Hidden variables controlling fluid flows," J. Fluid Mech. **892**, P1.
Marangoni, C., 1871, "Ueber die Ausbreitung der Tropfen einer Flüssigkeit auf der Oberfläche einer anderen [On the spreading of drops of one liquid on the surface of another fluid]," Ann. Phys. (Berlin) **219**, 337–354.
Marchand, A., J. H. Weijs, J. H. Snoeijer, and B. Andreotti, 2011, "Why is surface tension a force parallel to the interface?," Am. J. Phys. **79**, 999–1008.
Marchetti, M. C., J. F. Joanny, S. Ramaswamy, T. B. Liverpool, J. Prost, M. Rao, and R. A. Simha, 2013, "Hydrodynamics of soft active matter," Rev. Mod. Phys. **85**, 1143–1189.
Marconati, M., J. Engmann, A. Burbidge, V. Mathieu, I. Souchon, and M. Ramaioli, 2019, "A review of the approaches to predict the ease of swallowing and post-swallow residues," Trends Food Sci. Technol. **86**, 281–297.
Marín, A. G., H. Gelderblom, D. Lohse, and J. H. Snoeijer, 2011, "Order-to-Disorder Transition in Ring-Shaped Colloidal Stains," Phys. Rev. Lett. **107**, 085502.
Marmur, A., 2004, "The lotus effect: Superhydrophobicity and metastability," Langmuir **20**, 3517–3519.
Marsden, A. L., 2014, "Optimization in cardiovascular modeling," Annu. Rev. Fluid Mech. **46**, 519–546.
Marshall, J., S. Clarke, C. Escott, and B. F. Pados, 2021, "Assessing the flow rate of different bottles and teats for neonates with feeding difficulties: An Australian context," J. Neonat. Nurs **27**, 285–290.
Marshall, R., H. Goff, and R. Hartel, 2003, *Ice Cream* (Kluwer Academic, Amsterdam).

Martens, E. A., S. Watanabe, and T. Bohr, 2012, "Model for polygonal hydraulic jumps," Phys. Rev. E **85**, 036316.
Martin, G. D., S. D. Hoath, and I. M. Hutchings, 2008, "Inkjet printing—The physics of manipulating liquid jets and drops," J. Phys. Conf. Ser. **105**, 012001.
Martin, P. J., K. N. Odic, A. B. Russell, I. W. Burns, and D. I. Wilson, 2008, "Rheology of commercial and model ice creams," Appl. Rheol. **18**, 12913-1–12913-11.
Martinetti, L., A. M. Mannion, W. E. Voje, R. Xie, R. H. Ewoldt, L. D. Morgret, F. S. Bates, and C. W. Macosko, 2014, "A critical gel fluid with high extensibility: The rheology of chewing gum," J. Rheol. **58**, 821–838.
Martinez, V. A., J. Schwarz-Linek, M. Reufer, L. G. Wilson, A. N. Morozov, and W. C. K. Poon, 2014, "Flagellated bacterial motility in polymer solutions," Proc. Natl. Acad. Sci. U.S.A. **111**, 17771–17776.
Marusic, I., and S. Broomhall, 2021, "Leonardo da Vinci and fluid mechanics," Annu. Rev. Fluid Mech. **53**, 1–25.
Masson-Delmotte, V., *et al.* (IPCC), 2021, "Climate Change 2021: The Physical Science Basis. Contribution of Working Group I to the Sixth Assessment Report of the Intergovernmental Panel on Climate Change," 10.1017/9781009157896.
The Master Chef, 2021, "Hot ice cream!," https://www.instructables.com/Hot-Ice-Cream/ (accessed June 23, 2021).
Mathai, V., D. Lohse, and C. Sun, 2020, "Bubbly and buoyant particle-laden turbulent flows," Annu. Rev. Condens. Matter Phys. **11**, 529–559.
Mathijssen, A. J. T. M., J. Culver, M. S. Bhamla, and M. Prakash, 2019, "Collective intercellular communication through ultra-fast hydrodynamic trigger waves," Nature (London) **571**, 560–565.
Mathijssen, A. J. T. M., A. Doostmohammadi, J. M. Yeomans, and T. N. Shendruk, 2016, "Hydrodynamics of micro-swimmers in films," J. Fluid Mech. **806**, 35–70.
Mathijssen, A. J. T. M., N. Figueroa-Morales, G. Junot, E. Clément, A. Lindner, and A. Zöttl, 2019, "Oscillatory surface rheotaxis of swimming *E. coli* bacteria," Nat. Commun. **10**, 1–12.
Mathijssen, A. J. T. M., F. Guzmán-Lastra, A. Kaiser, and H. Löwen, 2018, "Nutrient Transport Driven by Microbial Active Carpets," Phys. Rev. Lett. **121**, 248101.
Mathijssen, A. J. T. M., D. O. Pushkin, and J. M. Yeomans, 2015, "Tracer trajectories and displacement due to a micro-swimmer near a surface," J. Fluid Mech. **773**, 498–519.
Mathijssen, A. J. T. M., T. N. Shendruk, J. M. Yeomans, and A. Doostmohammadi, 2016, "Upstream Swimming in Microbiological Flows," Phys. Rev. Lett. **116**, 028104.
Mathur, M., R. DasGupta, N. R. Selvi, N. S. John, G. U. Kulkarni, and R. Govindarajan, 2007, "Gravity-Free Hydraulic Jumps and Metal Femtoliter Cups," Phys. Rev. Lett. **98**, 164502.
Mayer, H. C., and R. Krechetnikov, 2012, "Walking with coffee: Why does it spill?," Phys. Rev. E **85**, 046117.
Mays, L., 2010, Ed., *Ancient Water Technologies* (Springer, New York).
McClements, D. J., 2004, "Protein-stabilized emulsions," Curr. Opin. Colloid Interface Sci. **9**, 305–313.
McClements, D. J., 2015, *Food Emulsions: Principles, Practices, and Techniques*, 3rd ed. (CRC Press, Boca Raton).
McCrum, N. G., C. P. Buckley, and C. B. Bucknall, 1988, *Principles of Polymer Engineering* (Oxford University Press, New York).
McGee, H., 2007, *On Food and Cooking: The Science and Lore of the Kitchen* (Scribner, New York).
Mckenzie, D. P., J. M. Roberts, and N. O. Weiss, 1974, "Convection in the Earth's mantle: Towards a numerical simulation," J. Fluid Mech. **62**, 465–538.
McLeish, T., 2020, *Soft Matter: A Very Short Introduction* (Oxford University Press, New York).
McNamara, W. B., Y. T. Didenko, and K. S. Suslick, 1999, "Sonoluminescence temperatures during multi-bubble cavitation," Nature (London) **401**, 772–775.
Mehrle, Y. E., 2007, *Solidification and Contraction of Confectionery Systems in Rapid Cooling Processing* (ETH Zürich, Zurich).
Mehta, A., 2012, *Granular Matter: An Interdisciplinary Approach* (Springer-Verlag, Berlin).
Meiburg, E., and B. Kneller, 2010, "Turbidity currents and their deposits," Annu. Rev. Fluid Mech. **42**, 135–156.
Mendez, M., B. Scheid, and J.-M. Buchlin, 2017, "Low Kapitza falling liquid films," Chem. Eng. Sci. **170**, 122–138.
Meng, F., Q. Liu, X. Wang, D. Tan, L. Xue, and W. J. P. Barnes, 2019, "Tree frog adhesion biomimetics: Opportunities for the development of new, smart adhesives that adhere under wet conditions," Phil. Trans. R. Soc. A **377**, 20190131.
Mermin, N. D., 1990, "Book review of 'But the crackling is superb,' " Phys. Today **43**, No. 6, 78.
Mertens, J., 2006, "Oil on troubled waters: Benjamin Franklin and the honor of Dutch seamen," Phys. Today **59**, No. 1, 36.
Metzger, B., M. Nicolas, and E. Guazzelli, 2007, "Falling clouds of particles in viscous fluids," J. Fluid Mech. **580**, 283–301.
Meunier, P., and E. Villermaux, 2003, "How vortices mix," J. Fluid Mech. **476**, 213–222.
Mezzenga, R., P. Schurtenberger, A. Burbidge, and M. Michel, 2005, "Understanding foods as soft materials," Nat. Mater. **4**, 729–740.
Michaelides, E., C. T. Crowe, and J. D. Schwarzkopf, 2016, *Multiphase Flow Handbook*, 2nd ed. (CRC Press, Boca Raton).
Middleton, W. E. K., 1964, *The History of the Barometer* (Johns Hopkins University Press, Baltimore).
Miles, D. T., and J. K. Bachman, 2009, "Science of food and cooking: A non-science majors course," J. Chem. Educ. **86**, 311.
Miller, C. B., and P. A. Wheeler, 2012, *Biological Oceanography* (John Wiley & Sons, New York).
Miller, G. H., 2019, *Whisky Science: A Condensed Distillation*, 1st ed. (Springer International, New York).
Millikan, R. A., 1913, "On the elementary electrical charge and the Avogadro constant," Phys. Rev. **2**, 109.
Minnaert, M., 1933, "On musical air-bubbles and the sounds of running water," Philos. Mag. **16**, 235–248.
Mishchenko, L., B. Hatton, V. Bahadur, J. A. Taylor, T. Krupenkin, and J. Aizenberg, 2010, "Design of ice-free nanostructured surfaces based on repulsion of impacting water droplets," ACS Nano **4**, 7699–7707.
Mittal, R., R. Ni, and J.-H. Seo, 2020, "The flow physics of COVID-19," J. Fluid Mech. **894**, F2.
Mizuno, D., D. A. Head, F. C. MacKintosh, and C. F. Schmidt, 2008, "Active and passive microrheology in equilibrium and nonequilibrium systems," Macromolecules **41**, 7194–7202.
Mlot, N. J., C. A. Tovey, and D. L. Hu, 2011, "Fire ants self-assemble into waterproof rafts to survive floods," Proc. Natl. Acad. Sci. U.S.A. **108**, 7669–7673.
Mo, C., L. Navarini, F. S. Liverani, and M. Ellero, 2022, "Modeling swelling effects during coffee extraction with smoothed particle hydrodynamics," Phys. Fluids **34**, 043104.
Möbius, M. E., B. E. Lauderdale, S. R. Nagel, and H. M. Jaeger, 2001, "Size separation of granular particles," Nature (London) **414**, 270–270.
Moelants, K. R. N., R. Cardinaels, S. Van Buggenhout, A. M. Van Loey, P. Moldenaers, and M. E. Hendrickx, 2014, "A review on the relationships between processing, food structure, and rheological

properties of plant-tissue-based food suspensions," Compr. Rev. Food Sci. Food Saf. **13**, 241–260.
Mohd, J., A. Yadav, and D. Das, 2022, "Open inverted bell and bell formation during the washing of vials," Phys. Fluids **34**, 042126.
Moinester, M., L. Gerland, G. Liger-Belair, and A. Ocherashvili, 2012, "Fizz-ball fizzics," Phys. Teach. **50**, 284–287.
Moore, D. R., and N. O. Weiss, 1973, "Two-dimensional Rayleigh-Bénard convection," J. Fluid Mech. **58**, 289–312.
Moore, G. S. M., 1989, "Swirling tea leaves: Problem and solution," Phys. Educ. **24**, 358.
Moore, M. R., D. Vella, and J. M. Oliver, 2021, "The nascent coffee ring: How solute diffusion counters advection," J. Fluid Mech. **920**, A54.
Moroney, K. M., K. O'Connell, P. Meikle-Janney, S. B. G. O'Brien, G. M. Walker, and W. T. Lee, 2019, "Analysing extraction uniformity from porous coffee beds using mathematical modelling and computational fluid dynamics approaches," PLoS One **14**, e0219906.
Mosedale, J. R., 1995, "Effects of oak wood on the maturation of alcoholic beverages with particular reference to whisky," Forestry **68**, 203–230.
Mossige, E. J., V. Chandran Suja, M. Islamov, S. Wheeler, and G. G. Fuller, 2020, "Evaporation-induced Rayleigh-Taylor instabilities in polymer solutions," Phil. Trans. R. Soc. A **378**, 20190533.
Mossige, E. J., V. Chandran Suja, D. J. Walls, and G. G. Fuller, 2021, "Dynamics of freely suspended drops translating through miscible environments," Phys. Fluids **33**, 033106.
Mossige, E. J., A. Jensen, and M. M. Mielnik, 2018, "Separation and Concentration without Clogging Using a High-Throughput Tunable Filter," Phys. Rev. Appl. **9**, 054007.
Mouat, A. P., C. E. Wood, J. E. Pye, and J. C. Burton, 2020, "Tuning Contact Line Dynamics and Deposition Patterns in Volatile Liquid Mixtures," Phys. Rev. Lett. **124**, 064502.
Moyls, A. L., 1981, "Drying of apple purees," J. Food Sci. **46**, 939–942.
Mu, S., F. Ren, Q. Shen, H. Zhou, and J. Luo, 2022, "Creamy mouthfeel of emulsion-filled gels with different fat contents: Correlating tribo-rheology with sensory measurements," Food Hydrocolloids **131**, 107754.
Mueth, D. M., J. C. Crocker, S. E. Esipov, and D. G. Grier, 1996, "Origin of Stratification in Creaming Emulsions," Phys. Rev. Lett. **77**, 578.
Mueth, D. M., H. M. Jaeger, and S. R. Nagel, 1998, "Force distribution in a granular medium," Phys. Rev. E **57**, 3164–3169.
Muller, H. G., 1961, "Weissenberg effect in the thick white of the hen's egg," Nature (London) **189**, 213–214.
Müller, A., M. R. Stahl, V. Graef, C. M. Franz, and M. Huch, 2011, "UV-C treatment of juices to inactivate microorganisms using Dean vortex technology," J. Food Eng. **107**, 268–275.
Mullin, T., 2011, "Experimental studies of transition to turbulence in a pipe," Annu. Rev. Fluid Mech. **43**, 1–24.
Münch, A., 2003, "Pinch-Off Transition in Marangoni-Driven Thin Films," Phys. Rev. Lett. **91**, 016105.
Munro, J. A., 1943, "The viscosity and thixotropy of honey," J. Econ. Entomol. **36**, 769–777.
Murdin, P., 2009, *Full Meridian of Glory: Perilous Adventures in the Competition to Measure the Earth* (Springer, New York).
Murdoch, N., B. Rozitis, K. Nordstrom, S. F. Green, P. Michel, T.-L. de Lophem, and W. Losert, 2013, "Granular Convection in Microgravity," Phys. Rev. Lett. **110**, 018307.
Muse, M., and R. Hartel, 2004, "Ice cream structural elements that affect melting rate and hardness," J. Dairy Sci. **87**, 1–10.
Muskat, M., 1938, *The Flow of Homogeneous Fluids through Porous Media* (McGraw-Hill, New York).
Myers, D., 2020, *Surfactant Science and Technology*, 4th ed. (John Wiley & Sons, New York).
Myhrvold, N., C. Young, and M. Bilet, 2021, *Modernist Cuisine*, 7th ed. (The Cooking Lab, Port Washington, NY).
Nagasawa, K., T. Suzuki, R. Seto, M. Okada, and Y. Yue, 2019, "Mixing sauces: A viscosity blending model for shear thinning fluids," ACM Trans. Graphics **38**, 95.
Nagel, S. R., 1992, "Instabilities in a sandpile," Rev. Mod. Phys. **64**, 321–325.
Nakouzi, E., R. E. Goldstein, and O. Steinbock, 2015, "Do dissolving objects converge to a universal shape?," Langmuir **31**, 4145–4150.
Naumov, I. V., S. G. Skripkin, G. E. Gusev, and V. N. Shtern, 2022, "Hysteresis in a two-liquid whirlpool," Phys. Fluids **34**, 032108.
Navarini, L., E. Nobile, F. Pinto, A. Scheri, and F. Suggi-Liverani, 2009, "Experimental investigation of steam pressure coffee extraction in a stove-top coffee maker," Appl. Therm. Eng. **29**, 998–1004.
Nedderman, R. M., 2005, *Statics and Kinematics of Granular Materials* (Cambridge University Press, Cambridge, England).
Needleman, D., and Z. Dogic, 2017, "Active matter at the interface between materials science and cell biology," Nat. Rev. Mater. **2**, 17048.
Neethirajan, S., I. Kobayashi, M. Nakajima, D. Wu, S. Nandagopal, and F. Lin, 2011, "Microfluidics for food, agriculture and biosystems industries," Lab Chip **11**, 1574–1586.
Nellimoottil, T. T., P. N. Rao, S. S. Ghosh, and A. Chattopadhyay, 2007, "Evaporation-induced patterns from droplets containing motile and nonmotile bacteria," Langmuir **23**, 8655–8658.
Nelson, A. Z., 2022, "The soft matter kitchen: Improving the accessibility of rheology education and outreach through food materials," Phys. Fluids **34**, 031801.
Nelson, A. Z., R. E. Bras, J. Liu, and R. H. Ewoldt, 2018, "Extending yield-stress fluid paradigms," J. Rheol. **62**, 357–369.
Nelson, P. C., 2020, *Biological Physics: Energy, Information, Life*, 2nd ed. (Chiliagon Science, Napa, CA).
Neufeld, J. A., R. E. Goldstein, and M. G. Worster, 2010, "On the mechanisms of icicle evolution," J. Fluid Mech. **647**, 287–308.
Newton, I., 2012, *Opticks, or, a Treatise of the Reflections, Refractions, Inflections & Colours of Light* (Dover, New York).
Newton, I., 2020, *Mathematical Principles of Natural Philosophy* (Flame Tree Collections, London).
Nichols, T. E., and J. B. Bostwick, 2020, "Geometry of polygonal hydraulic jumps and the role of hysteresis," Phys. Rev. Fluids **5**, 044005.
Nicolas, J. A., and J. M. Vega, 2000, "A note on the effect of surface contamination in water wave damping," J. Fluid Mech. **410**, 367–373.
Nikolov, A., D. Wasan, and J. Lee, 2018, "Tears of wine: The dance of the droplets," Adv. Colloid Interface Sci. **256**, 94–100.
Nita, S. P., M. Murith, H. Chisholm, and J. Engmann, 2013, "Matching the rheological properties of videofluoroscopic contrast agents and thickened liquid prescriptions," Dysphagia **28**, 245–252.
Nordbotten, J. M., and E. J. L. Mossige, 2022, "The dissolution of a miscible drop rising or falling in another liquid at low Reynolds number," arXiv:2211.01242.
Norton, T., B. Tiwari, and D.-W. Sun, 2013, "Computational fluid dynamics in the design and analysis of thermal processes: A review of recent advances," Crit. Rev. Food Sci. Nutr. **53**, 251–275.
Ogborn, J., 2004, "Soft matter: Food for thought," Phys. Educ. **39**, 45.
Oguz, H. N., and A. Prosperetti, 1990, "Bubble entrainment by the impact of drops on liquid surfaces," J. Fluid Mech. **219**, 143–179.

Ojijo, N. K. O., and E. Shimoni, 2008, "Minimization of cassava paste flow properties using the 'Farris effect,' " LWT Food Sci. Technol. **41**, 51–57.
Okulov, V. L., B. R. Sharifullin, N. Okulova, J. Kafka, R. Taboryski, J. N. Sørensen, and I. V. Naumov, 2022, "Influence of nano- and micro-roughness on vortex generations of mixing flows in a cavity," Phys. Fluids **34**, 032005.
Olsson, R. G., and E. T. Turkdogan, 1966, "Radial spread of a liquid stream on a horizontal plate," Nature (London) **211**, 813–816.
Olszewski, E. A., 2006, "From baking a cake to solving the diffusion equation," Am. J. Phys. **74**, 502–509.
O'Neill, M. E., 1964, "A slow motion of viscous liquid caused by a slowly moving solid sphere," Mathematika **11**, 67–74.
O'Neill, M. E., and K. Stewartson, 1967, "On the slow motion of a sphere parallel to a nearby plane wall," J. Fluid Mech. **27**, 705–724.
Ooi, Y., I. Hanasaki, D. Mizumura, and Y. Matsuda, 2017, "Suppressing the coffee-ring effect of colloidal droplets by dispersed cellulose nanofibers," Sci. Technol. Adv. Mater. **18**, 316–324.
Oron, A., S. H. Davis, and S. G. Bankoff, 1997, "Long-scale evolution of thin liquid films," Rev. Mod. Phys. **69**, 931–980.
Oseen, C. W., 1910, "Über die Stokes'sche Formel und über eine verwandte Aufgabe in der Hydrodynamik [On Stokes's formula and a related problem in hydrodynamics]," Ark. Mat. Astron. Fys. **6**, 1–20.
O'Sullivan, J. J., K. P. Drapala, A. L. Kelly, and J. A. O'Mahony, 2018, "The use of inline high-shear rotor-stator mixing for preparation of high-solids milk protein-stabilised oil-in-water emulsions with different protein: Fat ratios," J. Food Eng. **222**, 218–225.
Oswal, S. L., and H. S. Desai, 1998, "Studies of viscosity and excess molar volume of binary mixtures," Fluid Phase Equilib. **149**, 359–376.
Ottino, J. M., 1989, *The Kinematics of Mixing: Stretching, Chaos, and Transport* (Cambridge University Press, Cambridge, England).
Ottino, J. M., and D. V. Khakhar, 2000, "Mixing and segregation of granular materials," Annu. Rev. Fluid Mech. **32**, 55–91.
Ouimet, M., 2015, "Bartending guide: Specific gravity chart," http://www.cocktailhunter.com/bartender-guide/specific-gravity-chart/ (accessed July 15, 2021).
Owens, C. E., M. R. Fan, A. J. Hart, and G. H. McKinley, 2022, "On Oreology, the fracture and flow of 'milk's favorite cookie,' " Phys. Fluids **34**, 043107.
Özer, Ç., and C. Ağan, 2021, "The influence of aging egg on foaming properties of different meringue types," J. Culin. Sci. Technol. **19**, 475–484.
Ozilgen, M., 2011, *Handbook of Food Process Modeling and Statistical Quality Control* (CRC Press, Boca Raton).
Pacheco-Vázquez, F., R. Ledesma-Alonso, J. L. Palacio-Rangel, and F. Moreau, 2021, "Triple Leidenfrost Effect: Preventing Coalescence of Drops on a Hot Plate," Phys. Rev. Lett. **127**, 204501.
Paczuski, M., S. Maslov, and P. Bak, 1996, "Avalanche dynamics in evolution, growth, and depinning models," Phys. Rev. E **53**, 414–443.
Palacios, B., A. Rosario, M. M. Wilhelmus, S. Zetina, and R. Zenit, 2019, "Pollock avoided hydrodynamic instabilities to paint with his dripping technique," PLoS One **14**, e0223706.
Pandey, A., S. Karpitschka, L. A. Lubbers, J. H. Weijs, L. Botto, S. Das, B. Andreotti, and J. H. Snoeijer, 2017, "Dynamical theory of the inverted Cheerios effect," Soft Matter **13**, 6000–6010.
Pasteur, L., 1873, *Études sur le Vin: Ses Maladies, Causes Qui les Provoquent, Procédés Nouveaux pour le Conserver et pour le Vieillir* (Simon Raçou et Comp., Paris).
Patek, S. N., W. Korff, and R. L. Caldwell, 2004, "Deadly strike mechanism of a mantis shrimp," Nature (London) **428**, 819–820.
Patsyk, A., U. Sivan, M. Segev, and M. A. Bandres, 2020, "Observation of branched flow of light," Nature (London) **583**, 60–65.
Paunov, V., P. Kralchevsky, N. Denkov, and K. Nagayama, 1993, "Lateral capillary forces between floating submillimeter particles," J. Colloid Interface Sci. **157**, 100–112.
Pedersen, M. T., and T. A. Vilgis, 2019, "Soft matter physics meets the culinary arts: From polymers to jellyfish," Int. J. Gastron. Food Sci. **16**, 100135.
Pedlosky, J., 1987, *Geophysical Fluid Dynamics* (Springer-Verlag, Berlin).
Peltier, W. R., and C. P. Caulfield, 2003, "Mixing efficiency in stratified shear flows," Annu. Rev. Fluid Mech. **35**, 135–167.
Pendergrast, M., 2010, *Uncommon Grounds: The History of Coffee and How It Transformed Our World* (Basic Books, New York).
Perrault, C. M., M. A. Qasaimeh, and D. Juncker, 2009, "The microfluidic probe: Operation and use for localized surface processing," J. Visualized Exp. **28**, 1418.
Petitjeans, P., and T. Maxworthy, 1996, "Miscible displacements in capillary tubes. Part 1. Experiments," J. Fluid Mech. **326**, 37–56.
Petterson, A., T. Ohlsson, D. G. Caldwell, S. Davis, J. O. Gray, and T. J. Dodd, 2010, "A Bernoulli principle gripper for handling of planar and 3D (food) products," Ind. Robot **37**, 518–526.
Philip, J. R., 1970, "Flow in porous media," Annu. Rev. Fluid Mech. **2**, 177–204.
Phillips, S., A. Agarwal, and P. Jordan, 2018, "The sound produced by a dripping tap is driven by resonant oscillations of an entrapped air bubble," Sci. Rep. **8**, 9515.
Piazza, R., 2011, *Soft Matter: The Stuff That Dreams Are Made of* (Springer, New York).
Pickering, S. U., 1907, "Emulsions," J. Chem. Soc. Trans. **91**, 2001–2021.
Piergiovanni, P., and D. Goundie, 2019, "Modernist cuisine as an introduction to chemical engineering," Chem. Eng. Educ. **53**, 80.
Nawaporn Pax Piewpun, 2021, "Personal blog of food artist Nawaporn Pax Piewpun, a.k.a. Peaceloving Pax," https://www.facebook.com/cutefoodies (accessed October 3, 2021).
Planinsic, G., 2004, "Fizziology," Phys. Educ. **39**, 65.
Plateau, J., 1873a, *Experimental and Theoretical Statics of Liquids Subject to Molecular Forces Only* (Gauthier-Villars, Paris).
Plateau, J. A. F., 1873b, *Statique Expérimentale et Théorique des Liquides Soumis aux Seules Forces Moléculaires* (Gauthier-Villars, Paris).
Plesset, M. S., and A. Prosperetti, 1977, "Bubble dynamics and cavitation," Annu. Rev. Fluid Mech. **9**, 145–185.
Pockels, A., 1892, "On the relative contamination of the water-surface by equal quantities of different substances," Nature (London) **46**, 418–419.
Pockels, A., 1893, "Relations between the surface-tension and relative contamination of water surfaces," Nature (London) **48**, 152–154.
Pockels, A., 1894, "On the spreading of oil upon water," Nature (London) **50**, 223–224.
Pockels, A., 1926, "The measurement of surface tension with the balance," Science **64**, 304–304.
Pojman, J. A., C. Whitmore, M. L. T. Liveri, R. Lombardo, J. Marszalek, R. Parker, and B. Zoltowski, 2006, "Evidence for the existence of an effective interfacial tension between miscible fluids: Isobutyric acid/water and 1-butanol/water in a spinning-drop tensiometer," Langmuir **22**, 2569–2577.
Polidori, G., F. Beaumont, P. Jeandet, and G. Liger-Belair, 2008, "Artificial bubble nucleation in engraved champagne glasses," J. Visualization **11**, 279.

Polidori, G., P. Jeandet, and G. Liger-Belair, 2009, "Bubbles and flow patterns in champagne: Is the fizz just for show, or does it add to the taste of sparkling wines?," Am. Sci. **97**, 294–301.

Poole, R. J., 2012, "The Deborah and Weissenberg numbers," Rheol. Bull. **53**, 32–39, https://pcwww.liv.ac.uk/~robpoole/PAPERS/POOLE_45.pdf.

Poon, W. C. K., *et al.*, 2020, "Soft matter science and the COVID-19 pandemic," Soft Matter **16**, 8310–8324.

Potter, A., and F. Barnes, 1971, "The siphon," Phys. Educ. **6**, 362.

Poujol, M., R. Wunenburger, F. Ollivier, A. Antkowiak, and J. Pierre, 2021, "Sound of effervescence," Phys. Rev. Fluids **6**, 013604.

Prakash, V. N., K. Sreenivas, and J. H. Arakeri, 2017, "The role of viscosity contrast on plume structure in laboratory modeling of mantle convection," Chem. Eng. Sci. **158**, 245–256.

Prakash, V. N., Y. Tagawa, E. Calzavarini, J. M. Mercado, F. Toschi, D. Lohse, and C. Sun, 2012, "How gravity and size affect the acceleration statistics of bubbles in turbulence," New J. Phys. **14**, 105017.

Price, H., E. Lüpfert, D. Kearney, E. Zarza, G. Cohen, R. Gee, and R. Mahoney, 2002, "Advances in parabolic trough solar power technology," J. Sol. Energy Eng. **124**, 109–125.

Proksch, E., E. Berardesca, L. Misery, J. Engblom, and J. Bouwstra, 2020, "Dry skin management: Practical approach in light of latest research on skin structure and function," J. Dermatol. Treat. **31**, 716–722.

Prosperetti, A., and H. N. Oguz, 1993, "The impact of drops on liquid surfaces and the underwater noise of rain," Annu. Rev. Fluid Mech. **25**, 577–602.

Provost, J. J., K. L. Colabroy, B. S. Kelly, and Wallert, M. A., 2016, *The Science of Cooking: Understanding the Biology and Chemistry behind Food and Cooking* (Wiley, New York).

Purcell, E. M., 1977, "Life at low Reynolds number," Am. J. Phys. **45**, 3–11.

Qin, H., R. Zhang, A. S. Glasser, and J. Xiao, 2019, "Kelvin-Helmholtz instability is the result of parity-time symmetry breaking," Phys. Plasmas **26**, 032102.

Qiu, T., T.-C. Lee, A. G. Mark, K. I. Morozov, R. Münster, O. Mierka, S. Turek, A. M. Leshansky, and P. Fischer, 2014, "Swimming by reciprocal motion at low Reynolds number," Nat. Commun. **5**, 5119.

Quéré, D., 2013, "Leidenfrost dynamics," Annu. Rev. Fluid Mech. **45**, 197–215.

Quetzeri-Santiago, M. A., K. Yokoi, A. A. Castrejón-Pita, and J. R. Castrejón-Pita, 2019, "Role of the Dynamic Contact Angle on Splashing," Phys. Rev. Lett. **122**, 228001.

Rad, V. F., and A.-R. Moradi, 2020, "Flat wall proximity effect on micro-particle sedimentation in non-Newtonian fluids," Sci. Rep. **10**, 1–9.

Radko, T., 2013, *Double-Diffusive Convection* (Cambridge University Press, Cambridge, England).

Rage, G., O. Atasi, M. M. Wilhelmus, J. F. Hernández-Sánchez, B. Haut, B. Scheid, D. Legendre, and R. Zenit, 2020, "Bubbles determine the amount of alcohol in mezcal," Sci. Rep. **10**, 1–16.

Rahman, A., 2017, "A blended learning approach to teach fluid mechanics in engineering," Eur. J. Eng. Educ. **42**, 252–259.

Ramaswamy, H. S., and S. Basak, 1991, "Rheology of stirred yogurts," J. Texture Stud. **22**, 231–241.

Ramirez-San Juan, G. R., A. J. T. M. Mathijssen, M. He, L. Jan, W. Marshall, and M. Prakash, 2020, "Multi-scale spatial heterogeneity enhances particle clearance in airway ciliary arrays," Nat. Phys. **16**, 958–964.

Ramsden, W., 1904, "Separation of solids in the surface-layers of solutions and 'suspensions' (observations on surface-membranes, bubbles, emulsions, and mechanical coagulation)—Preliminary account," Proc. R. Soc. London **72**, 156–164.

Rao, M. A., and H. J. Cooley, 1992, "Rheological behavior of tomato pastes in steady and dynamic shear," J. Texture Stud. **23**, 415–425.

Rao, N. Z., and M. Fuller, 2018, "Acidity and antioxidant activity of cold brew coffee," Sci. Rep. **8**, 16030.

Ratnayake, W. S., and D. S. Jackson, 2008, "Starch gelatinization," in *Advances in Food and Nutrition Research*, Vol. 55 (Academic Press, New York), pp. 221–268, 10.1016/S1043-4526(08)00405-1.

Rayleigh, Lord,, 1877a, *The Theory of Sound*, Vol. 1 (Cambridge University Press, Cambridge, England).

Rayleigh, Lord,, 1877b, *The Theory of Sound*, Vol. 2 (Cambridge University Press, Cambridge, England).

Rayleigh, Lord, 1879, "On the capillary phenomena of jets," Proc. R. Soc. London **29**, 71–97.

Rayleigh, Lord, 1882, "Investigation of the character of the equilibrium of an incompressible heavy fluid of variable density," Proc. London Math. Soc. **s1–14**, 170–177.

Rayleigh, Lord, 1891, "Surface tension," Nature (London) **43**, 437–439.

Rayleigh, Lord, 1914, "On the theory of long waves and bores," Proc. R. Soc. A **90**, 324–328, https://www.jstor.org/stable/93519.

Redon, C., F. Brochard-Wyart, and F. Rondelez, 1991, "Dynamics of Dewetting," Phys. Rev. Lett. **66**, 715–718.

Reiner, M., G. W. Scott Blair, and H. B. Hawley, 1949, "The Weissenberg effect in sweetened condensed milk," J. Soc. Chem. Ind. **68**, 327–328.

Reiter, G., 1992, "Dewetting of Thin Polymer Films," Phys. Rev. Lett. **68**, 75–78.

Renney, C., A. Brewer, and T. J. Mooibroek, 2013, "Easy demonstration of the Marangoni effect by prolonged and directional motion:'Soap Boat 2.0,' " J. Chem. Educ. **90**, 1353–1357.

Reynolds, K. A., J. D. Sexton, A. Norman, and D. J. McClelland, 2021, "Comparison of electric hand dryers and paper towels for hand hygiene: A critical review of the literature," J. Appl. Microbiol. **130**, 25–39.

Reynolds, O., 1883, "An experimental investigation of the circumstances which determine whether the motion of water shall be direct or sinuous, and of the law of resistance in parallel channels," Phil. Trans. R. Soc. London **35**, 84–99.

Reynolds, O., 1886, "On the theory of lubrication and its application to Mr. Beauchamp tower's experiments, including an experimental determination of the viscosity of olive oil," Phil. Trans. R. Soc. London **177**, 157–234.

Reyssat, M., J. M. Yeomans, and D. Quéré, 2008, "Impalement of fakir drops," Europhys. Lett. **81**, 26006.

Ribe, N. M., M. Habibi, and D. Bonn, 2006, "Stability of liquid rope coiling," Phys. Fluids **18**, 084102.

Ribéreau-Gayon, P., Y. Glories, A. Maujean, and D. Dubourdieu, 2006, *Handbook of Enology, Vol. 2: The Chemistry of Wine-Stabilization and Treatments* (John Wiley & Sons, New York).

Richard, D., C. Clanet, and D. Quéré, 2002, "Contact time of a bouncing drop," Nature (London) **417**, 811.

Richard, D., and D. Quéré, 2000, "Bouncing water drops," Europhys. Lett. **50**, 769–775.

Richardson, J. F., and W. N. Zaki, 1997, "Sedimentation and fluidisation: Part I," Chem. Eng. Res. Des. **75**, S82–S100.

Richardson, L. F., 2007, *Weather Prediction by Numerical Process* (Cambridge University Press, Cambridge, England).

Richert, A., and P.-M. Binder, 2011, "Siphons, revisited," Phys. Teach. **49**, 78–80.

Rienstra, S. W., 2005, "Nonlinear free vibrations of coupled spans of overhead transmission lines," J. Eng. Math. **53**, 337–348.

Rietz, F., and R. Stannarius, 2008, "On the Brink of Jamming: Granular Convection in Densely Filled Containers," Phys. Rev. Lett. **100**, 078002.

Roberts, M. J., G. R. Deboy, W. Field, and D. E. Maier, 2011, "Summary of prior grain entrapment rescue strategies," J. Agric. Saf. Health **17**, 303–325.

Robin, F., J. Engmann, N. Pineau, H. Chanvrier, N. Bovet, and G. Della Valle, 2010, "Extrusion, structure and mechanical properties of complex starchy foams," J. Food Eng. **98**, 19–27.

Roché, M., Z. Li, I. M. Griffiths, S. Le Roux, I. Cantat, A. Saint-Jalmes, and H. A. Stone, 2014, "Marangoni Flow of Soluble Amphiphiles," Phys. Rev. Lett. **112**, 208302.

Rodríguez-Rodríguez, J., A. Casado-Chacón, and D. Fuster, 2014, "Physics of Beer Tapping," Phys. Rev. Lett. **113**, 214501.

Rogge, W. F., L. M. Hildemann, M. A. Mazurek, G. R. Cass, and B. R. T. Simoneit, 1991, "Sources of fine organic aerosol. 1. Charbroilers and meat cooking operations," Environ. Sci. Technol. **25**, 1112–1125.

Rohilla, L., and A. K. Das, 2020, "Fluidics in an emptying bottle during breaking and making of interacting interfaces," Phys. Fluids **32**, 042102.

Rosato, A., K. J. Strandburg, F. Prinz, and R. H. Swendsen, 1987, "Why the Brazil Nuts Are on Top: Size Segregation of Particulate Matter by Shaking," Phys. Rev. Lett. **58**, 1038–1040.

Rosen, M. J., and J. T. Kunjappu, 2012, *Surfactants and Interfacial Phenomena* (John Wiley & Sons, New York).

Rotter, M. L., 1997, "150 years of hand disinfection—Semmelweis' heritage," Hyg. Med. **22**, 332–339.

Rotunno, R., 2013, "The fluid dynamics of tornadoes," Annu. Rev. Fluid Mech. **45**, 59–84.

Roura, P., J. Fort, and J. Saurina, 2000, "How long does it take to boil an egg? A simple approach to the energy transfer equation," Eur. J. Phys. **21**, 95.

Routh, A. F., 2013, "Drying of thin colloidal films," Rep. Prog. Phys. **76**, 046603.

Rowat, A. C., N. N. Sinha, P. M. Sörensen, O. Campàs, P. Castells, D. Rosenberg, M. P. Brenner, and D. A. Weitz, 2014, "The kitchen as a physics classroom," Phys. Educ. **49**, 512.

Rowlinson, J. S., and B. Widom, 2013, *Molecular Theory of Capillarity*, Dover Books on Chemistry (Dover, New York).

Rubey, W. W., 1933, "Settling velocity of gravel, sand, and silt particles," Am. J. Sci. **s5–25**, 325–338.

Rudan, M. A., and D. M. Barbano, 1998, "A model of mozzarella cheese melting and browning during pizza baking," J. Dairy Sci. **81**, 2312–2319.

Ruiz-Márquez, D., P. Partal, J. M. Franco, and C. Gallegos, 2013, "Linear viscoelastic behaviour of oil-in-water food emulsions stabilised by tuna-protein isolates," Food Sci. Technol. Int. **19**, 3–10.

Ruschak, K. J., 1985, "Coating flows," Annu. Rev. Fluid Mech. **17**, 65–89.

Russell, I., C. Bamforth, and G. Stewart, 2014, *Whisky: Technology, Production and Marketing* (Elsevier, New York).

Rybczynski, W., 1911, "O ruchu postępowym kuli ciekłej w ośrodku lepkim—Über die fortschreitende Bewegung einer flussigen Kugel in einem zähen Medium [On the progressive motion of a fluid sphere in a viscous medium]," Bull. Acad. Sci. Cracov. A **1**, 40–46, https://www.pdf-archive.com/2020/02/23/untitled-pdf-document/?.

Sadhal, S. S., and R. E. Johnson, 1983, "Stokes flow past bubbles and drops partially coated with thin films. Part 1. Stagnant cap of surfactant film—Exact solution," J. Fluid Mech. **126**, 237–250.

Safavieh, M., M. A. Qasaimeh, A. Vakil, D. Juncker, and T. Gervais, 2015, "Two-aperture microfluidic probes as flow dipoles: Theory and applications," Sci. Rep. **5**, 11943.

Sahimi, M., 2014, *Applications of Percolation Theory* (Taylor & Francis, London).

Sahin, S., and S. G. Sumnu, 2006, *Physical Properties of Foods*, Food Science Text Series (Springer, New York).

Sajid, M., and M. Ilyas, 2017, "PTFE-coated non-stick cookware and toxicity concerns: A perspective," Environ. Sci. Pollut. Res. **24**, 23436–23440.

Şanlier, N., B. B. Gökcen, and A. C. Sezgin, 2019, "Health benefits of fermented foods," Crit. Rev. Food Sci. Nutr. **59**, 506–527.

Sathish, S., and A. Q. Shen, 2021, "Toward the development of rapid, specific, and sensitive microfluidic sensors: A comprehensive device blueprint," JACS Au **1**, 1815–1833.

Sauret, A., F. Boulogne, J. Cappello, E. Dressaire, and H. A. Stone, 2015, "Damping of liquid sloshing by foams," Phys. Fluids **27**, 022103.

Savic, P., 1953, "Circulation and distortion of liquid drops falling through a viscous medium," National Research Council of Canada Technical Report No. MT-22, https://archive.org/details/mt-22.

Scheichl, B., R. Bowles, and G. Pasias, 2021, "Developed liquid film passing a smoothed and wedge-shaped trailing edge: Small-scale analysis and the 'teapot effect' at large Reynolds numbers," J. Fluid Mech. **926**, A25.

Schikarski, T., W. Peukert, and M. Avila, 2017, "Direct numerical simulation of water—Ethanol flows in a T-mixer," Chem. Eng. J. **324**, 168–181.

Schlichting, H., and K. Gersten, 2017, *Boundary-Layer Theory* (Springer-Verlag, Berlin).

Schmidt, S. J., D. M. Bohn, A. J. Rasmussen, and E. A. Sutherland, 2012, "Using food science demonstrations to engage students of all ages in science, technology, engineering, and mathematics (STEM)," J. Food Sci. Educ. **11**, 16–22.

Schmidt, T., and M. Marhl, 1997, "A simple mathematical model of a dripping tap," Eur. J. Phys. **18**, 377.

Schmidt-Nielsen, K., and D. J. Randall, 1997, *Animal Physiology: Adaptation and Environment* (Cambridge University Press, Cambridge, England).

Seimiya, T., and T. Seimiya, 2021, "Revisiting the 'pearl string' in draining soap bubble film first witnessed by Sir James Dewar some 100 years ago: A note of analyses for the phenomena with related findings," Phys. Fluids **33**, 104102.

Sempels, W., R. De Dier, H. Mizuno, J. Hofkens, and J. Vermant, 2013, "Auto-production of biosurfactants reverses the coffee ring effect in a bacterial system," Nat. Commun. **4**, 1757.

Sengupta, A., F. Carrara, and R. Stocker, 2017, "Phytoplankton can actively diversify their migration strategy in response to turbulent cues," Nature (London) **543**, 555–558.

Seo, J. H., H. Bakhshaee, G. Garreau, C. Zhu, A. Andreou, W. R. Thompson, and R. Mittal, 2017, "A method for the computational modeling of the physics of heart murmurs," J. Comput. Phys. **336**, 546–568.

Settles, G. S., 2001, *Schlieren and shadowgraph techniques: Visualizing phenomena in transparent media* (Springer, New York).

Settles, G. S., and M. J. Hargather, 2017, "A review of recent developments in schlieren and shadowgraph techniques," Meas. Sci. Technol. **28**, 042001.

Severini, C., A. Derossi, I. Ricci, A. G. Fiore, and R. Caporizzi, 2017, "How much caffeine in coffee cup? Effects of processing operations, extraction methods and variables," in *The Question of Caffeine*, edited by J. N. Latosińska and M. Latosińska (IntechOpen, London), pp. 45–85.

Shadle, C. H., 1983, "Experiments on the acoustics of whistling," Phys. Teach. **21**, 148–154.

Sheppard, S. D., K. Macatangay, A. Colby, and W. M. Sullivan, 2008, *Educating Engineers: Designing for the Future of the Field* (Jossey-Bass, San Francisco).

Shinbrot, T., and F. J. Muzzio, 1998, "Reverse Buoyancy in Shaken Granular Beds," Phys. Rev. Lett. **81**, 4365–4368.

Shukla, A., A. R. Bhaskar, S. S. H. Rizvi, and S. J. Mulvaney, 1994, "Physicochemical and rheological properties of butter made from supercritically fractionated milk fat," J. Dairy Sci. **77**, 45–54.

Simpson, J. E., 1982, "Gravity currents in the laboratory, atmosphere, and ocean," Annu. Rev. Fluid Mech. **14**, 213–234.

Singh, K., M. Jung, M. Brinkmann, and R. Seemann, 2019, "Capillary-dominated fluid displacement in porous media," Annu. Rev. Fluid Mech. **51**, 429–449.

Singh, P., and D. D. Joseph, 2005, "Fluid dynamics of floating particles," J. Fluid Mech. **530**, 31–80.

Singla, T., and M. Rivera, 2020, "Sounds of Leidenfrost drops," Phys. Rev. Fluids **5**, 113604.

Sitnikova, N. L., R. Sprik, G. Wegdam, and E. Eiser, 2005, "Spontaneously formed trans-anethol/water/alcohol emulsions: Mechanism of formation and stability," Langmuir **21**, 7083–7089.

Skinner, G. E., and V. N. M. Rao, 1986, "Linear viscoelastic behavior of frankfurters," J. Texture Stud. **17**, 421–432.

Skurtys, O., and J. M. Aguilera, 2008, "Applications of microfluidic devices in food engineering," Food Biophys. **3**, 1–15.

Sleigh, M. A., J. R. Blake, and N. Liron, 1988, "The propulsion of mucus by cilia," Am. Rev. Respir. Dis. **137**, 726–741.

Smith, D., 2015, "Play: The path to discovery or my Friday afternoon experiment," https://davethesmith.wordpress.com/2015/06/29/play-the-path-to-discovery-or-my-friday-afternoon-experiment/ (accessed November 21, 2021).

Smith, E., 2020, "Out damned spot: The Lady Macbeth hand-washing scene that became a coronavirus meme," https://www.penguin.co.uk/articles/2020/03/the-history-behind-the-lady-macbeth-coronavirus-meme.

Smith, G. D., 2011, *A to Z of Whisky* (Neil Wilson Publishing, Dumfries, Scotland).

Smith, N. M., H. Ebrahimi, R. Ghosh, and A. K. Dickerson, 2018, "High-speed microjets issue from bursting oil gland reservoirs of citrus fruit," Proc. Natl. Acad. Sci. U.S.A. **115**, E5887–E5895.

Smoluchowski, M., 1908, "Molekular-kinetische Theorie der Opaleszenz von Gasen im kritischen Zustande, sowie einiger verwandter Erscheinungen [Molecular-kinetic theory of the opalescence of gases in the critical state, and several related phenomena]," Ann. Phys. (Berlin) **330**, 205–226.

Sobac, B., A. Rednikov, S. Dorbolo, and P. Colinet, 2017, "Self-propelled Leidenfrost drops on a thermal gradient: A theoretical study," Phys. Fluids **29**, 082101.

Spagnolie, S. E., and P. T. Underhill, 2022, "Swimming in complex fluids," arXiv:2208.03537.

Speirs, N. B., Z. Pan, J. Belden, and T. T. Truscott, 2018, "The water entry of multi-droplet streams and jets," J. Fluid Mech. **844**, 1084–1111.

Squires, T. M., and T. G. Mason, 2010, "Fluid mechanics of microrheology," Annu. Rev. Fluid Mech. **42**, 413–438.

Squires, T. M., R. J. Messinger, and S. R. Manalis, 2008, "Making it stick: Convection, reaction and diffusion in surface-based biosensors," Nat. Biotechnol. **26**, 417–426.

Squires, T. M., and S. R. Quake, 2005, "Microfluidics: Fluid physics at the nanoliter scale," Rev. Mod. Phys. **77**, 977–1026.

Sreedhar, B. K., S. K. Albert, and A. B. Pandit, 2017, "Cavitation damage: Theory and measurements—A review," Wear **372–373**, 177–196.

Stauffer, D., 2018, *Introduction to Percolation Theory*, 2nd ed. (Taylor & Francis, London).

Stein, P. D., and H. N. Sabbah, 1976, "Turbulent blood flow in the ascending aorta of humans with normal and diseased aortic valves," Circ. Res. **39**, 58–65.

Stern, M. E., 1960, "The 'salt-fountain' and thermohaline convection," Tellus **12**, 172–175.

Stewartson, K., 1956, "On the steady flow past a sphere at high Reynolds number using Oseen's approximation," Philos. Mag. **1**, 345–354.

Stokes, G. G., 1851, "On the effect of the internal friction of fluids on the motion of pendulums," in *Mathematical and Physical Papers*, Cambridge Library Collection—Mathematics Vol. 3 (Cambridge University Press, Cambridge, England), pp. 1–10.

Stokes, G. G., 1880, "On the theories of the internal friction of fluids in motion, and of the equilibrium and motion of elastic solids," Trans. Cambridge Philos. Soc. **8**, 75–129.

Stokes, J. R., M. W. Boehm, and S. K. Baier, 2013, "Oral processing, texture and mouthfeel: From rheology to tribology and beyond," Curr. Opin. Colloid Interface Sci. **18**, 349–359.

Stone, H. A., and L. G. Leal, 1989, "The influence of initial deformation on drop breakup in subcritical time-dependent flows at low Reynolds numbers," J. Fluid Mech. **206**, 223–263.

Stroock, A. D., S. K. Dertinger, A. Ajdari, I. Mezić, H. A. Stone, and G. M. Whitesides, 2002, "Chaotic mixer for microchannels," Science **295**, 647–651.

Suja, V. C., A. Verma, E. Mossige, K. Cui, V. Xia, Y. Zhang, D. Sinha, S. Joslin, and G. G. Fuller, 2022, "Dewetting characteristics of contact lenses coated with wetting agents," J. Colloid Interface Sci. **614**, 24–32.

Sur, J., A. L. Bertozzi, and R. P. Behringer, 2003, "Reverse Undercompressive Shock Structures in Driven Thin Film Flow," Phys. Rev. Lett. **90**, 126105.

Sutera, S. P., and R. Skalak, 1993, "The history of Poiseuille's law," Annu. Rev. Fluid Mech. **25**, 1–20.

Sutterby, J. L., 1973, "Falling sphere viscometry. I. Wall and inertial corrections to Stokes' law in long tubes," Trans. Soc. Rheol. **17**, 559–573.

Suzuki, J., 2002, *A History of Mathematics* (Prentice-Hall, Englewood Cliffs, NJ).

Szeri, A. Z., 2010, *Fluid Film Lubrication* (Cambridge University Press, Cambridge, England).

Sznitman, J., and P. E. Arratia, 2015, "Locomotion through complex fluids: An experimental view," in *Complex Fluids in Biological Systems* (Springer, New York), pp. 245–281.

Szymczak, P., and B. Cichocki, 2004, "Memory effects in collective dynamics of Brownian suspensions," J. Chem. Phys. **121**, 3329–3346.

Tabeling, P., 2005, *Introduction to Microfluidics* (Oxford University Press, New York).

Tadmor, R., 2004, "Line energy and the relation between advancing, receding, and Young contact angles," Langmuir **20**, 7659–7664.

Tait, R. I., and M. R. Howe, 1971, "Thermohaline staircase," Nature (London) **231**, 178–179.

Tamang, J. P., P. D. Cotter, A. Endo, N. S. Han, R. Kort, S. Q. Liu, B. Mayo, N. Westerik, and R. Hutkins, 2020, "Fermented foods in a global age: East meets West," Compr. Rev. Food Sci. Food Saf. **19**, 184–217.

Tan, H., C. Diddens, P. Lv, J. G. M. Kuerten, X. Zhang, and D. Lohse, 2016, "Evaporation-triggered microdroplet nucleation and the four life phases of an evaporating ouzo drop," Proc. Natl. Acad. Sci. U.S.A. **113**, 8642–8647.

Tan, H., C. Diddens, M. Versluis, H.-J. Butt, D. Lohse, and X. Zhang, 2017, "Self-wrapping of an ouzo drop induced by evaporation on a superamphiphobic surface," Soft Matter **13**, 2749–2759.
Tanford, C., 2004, *Ben Franklin Stilled the Waves* (Oxford University Press, New York).
Tang, J., and R. P. Behringer, 2011, "How granular materials jam in a hopper," Chaos **21**, 041107.
Tao, R., M. Wilson, and E. R. Weeks, 2021, "Soft particle clogging in two-dimensional hoppers," Phys. Rev. E **104**, 044909.
Tao, Y., *et al.*, 2021, "Morphing pasta and beyond," Sci. Adv. **7**, eabf4098.
Tárrega, A., L. Durán, and E. Costell, 2005, "Rheological characterization of semisolid dairy desserts. Effect of temperature," Food Hydrocolloids **19**, 133–139.
Taylor, G. I., 1934, "The formation of emulsions in definable fields of flow," Proc. R. Soc. A **146**, 501–523.
Taylor, G. I., 1946, *Dynamics of a Mass of Hot Gas Rising in Air* (U.S. Atomic Energy Commission, Oak Ridge, TN).
Taylor, G. I., 1950, "The instability of liquid surfaces when accelerated in a direction perpendicular to their planes. I," Proc. R. Soc. A **201**, 192–196.
Taylor, G. I., 1967, "Low-Reynolds-number flows," http://web.mit.edu/hml/ncfmf.html (accessed December 16, 2020).
Tcholakova, S., N. D. Denkov, I. B. Ivanov, and B. Campbell, 2006, "Coalescence stability of emulsions containing globular milk proteins," Adv. Colloid Interface Sci. **123–126**, 259–293.
Tehrani-Bagha, A. R., 2019, "Waterproof breathable layers—A review," Adv. Colloid Interface Sci. **268**, 114–135.
Ten, A., P. Kaushik, P.-Y. Oudeyer, and J. Gottlieb, 2021, "Humans monitor learning progress in curiosity-driven exploration," Nat. Commun. **12**, 1–10.
Teoh, R., U. Schumann, A. Majumdar, and M. E. Stettler, 2020, "Mitigating the climate forcing of aircraft contrails by small-scale diversions and technology adoption," Environ. Sci. Technol. **54**, 2941–2950.
Teunou, E., J. J. Fitzpatrick, and E. C. Synnott, 1999, "Characterisation of food powder flowability," J. Food Eng. **39**, 31–37.
Thiffeault, J.-L., 2022, "The mathematics of burger flipping," Physica (Amsterdam) **439D**, 133410.
Thiffeault, J.-L., E. Gouillart, and O. Dauchot, 2011, "Moving walls accelerate mixing," Phys. Rev. E **84**, 036313.
Thimbleby, H., 1989, "The Leidenfrost phenomenon," Phys. Educ. **24**, 300.
This, H., 2006, *Molecular Gastronomy: Exploring the Science of Flavor* (Columbia University Press, New York).
Thomas, C. C., and D. J. Durian, 2015, "Fraction of Clogging Configurations Sampled by Granular Hopper Flow," Phys. Rev. Lett. **114**, 178001.
Thompson, C. V., 2012, "Solid-state dewetting of thin films," Annu. Rev. Mater. Res. **42**, 399–434.
Thomsen, V., 1993, "Estimating Reynolds number in the kitchen sink," Phys. Teach. **31**, 410–410.
Thomson, J., 1855, "On certain curious motions observable at the surfaces of wine and other alcoholic liquors," Philos. Mag. **10**, 330–333.
Thomson, J., 1892, "Bakerian lecture—On the grand currents of atmospheric circulation," Proc. R. Soc. London **51**, 42–46.
Thorpe, S. A., 1969, "Experiments on the instability of stratified shear flows: Immiscible fluids," J. Fluid Mech. **39**, 25–48.
Thurston, R., J. Morris, and S. Steiman, 2013, *Coffee: A Comprehensive Guide to the Bean, the Beverage, and the Industry* (Rowman & Littlefield, Washington, DC).
Timm, M. L., S. J. Kang, J. P. Rothstein, and H. Masoud, 2021, "A remotely controlled Marangoni surfer," Bioinspiration Biomimetics **16**, 066014.
To, K., P.-Y. Lai, and H. K. Pak, 2001, "Jamming of Granular Flow in a Two-Dimensional Hopper," Phys. Rev. Lett. **86**, 71–74.
Tobias, S., and F. A. Birrer, 1999, "Who will study physics, and why?," Eur. J. Phys. **20**, 365.
Todd, E. C., B. S. Michaels, D. Smith, J. D. Greig, and C. A. Bartleson, 2010, "Outbreaks where food workers have been implicated in the spread of foodborne disease. Part 9. Washing and drying of hands to reduce microbial contamination," J. Food Prot. **73**, 1937–1955.
Tokel, O., *et al.*, 2015, "Portable microfluidic integrated plasmonic platform for pathogen detection," Sci. Rep. **5**, 9152.
Touffet, M., M. H. Allouche, M. Ariane, and O. Vitrac, 2021, "Coupling between oxidation kinetics and anisothermal oil flow during deep-fat frying," Phys. Fluids **33**, 085105.
Toussaint-Samat, M., 2009, *A History of Food* (John Wiley & Sons, New York).
Townsend, A. K., and H. J. Wilson, 2016, "The fluid dynamics of the chocolate fountain," Eur. J. Phys. **37**, 015803.
Trávníček, Z., A. Fedorchenko, M. Pavelka, and J. Hrubý, 2012, "Visualization of the hot chocolate sound effect by spectrograms," J. Sound Vib. **331**, 5387–5392.
Trout, J. J., and T. Jacobsen, 2020, "The science of ice cream, an undergraduate, interdisciplinary, general education course taught in the physics program," Phys. Educ. **55**, 015009.
Trubek, A. B., 2000, *Haute Cuisine: How the French Invented the Culinary Profession* (University of Pennsylvania Press, Philadelphia).
Tuosto, K., *et al.*, 2020, "Making science accessible," Science **367**, 34–35.
Turchiuli, C., 2013, "Fluidization in food powder production," in *Handbook of Food Powders*, edited by B. Bhandari, N. Bansal, M. Zhang, and P. Schuck (Elsevier, New York), pp. 178–199.
Turner, J. S., 1966, "Jets and plumes with negative or reversing buoyancy," J. Fluid Mech. **26**, 779–792.
Tyvand, P. A., 2022, "Viscous Rankine vortices," Phys. Fluids **34**, 073603.
Ubbink, J., A. Burbidge, and R. Mezzenga, 2008, "Food structure and functionality: A soft matter perspective," Soft Matter **4**, 1569–1581.
Ungarish, M., 2009, *An Introduction to Gravity Currents and Intrusions* (CRC Press, Boca Raton).
Väisälä, V., 1925, "Uber die Wirkung der Windschwankungen auf die Pilotbeobachtungen [On the effect of wind variations on pilot observations]," Soc. Sci. Fenn. Commentat. Phys.-Math. **2**, 2–46, http://urn.fi/URN:NBN:fi:bib:me:I00331656400.
Vallis, G. K., 2017, *Atmospheric and Oceanic Fluid Dynamics* (Cambridge University Press, Cambridge, England).
van de Hulst, H., 1981, *Light Scattering by Small Particles*, Dover Books on Physics (Dover Publications, New York).
Van der Sman, R. G. M., 2007, "Moisture transport during cooking of meat: An analysis based on Flory-Rehner theory," Meat Sci. **76**, 730–738.
Van der Sman, R. G. M., 2012, "Soft matter approaches to food structuring," Adv. Colloid Interface Sci. **176–177**, 18–30.
Van Dorst, B., J. Mehta, K. Bekaert, E. Rouah-Martin, W. De Coen, P. Dubruel, R. Blust, and J. Robbens, 2010, "Recent advances in recognition elements of food and environmental biosensors: A review," Biosens. Bioelectron. **26**, 1178–1194.
Van Dyke, M., 1975, *Perturbation Methods in Fluid Mechanics*, 2nd ed. (Parabolic Press, Stanford).

Van Leeuwen, J., 2016, *The Aristotelian Mechanics: Text and Diagrams*, Boston Studies in the Philosophy and History of Science Vol. 316 (Springer, New York).
Varanakkottu, S. N., M. Anyfantakis, M. Morel, S. Rudiuk, and D. Baigl, 2016, "Light-directed particle patterning by evaporative optical Marangoni assembly," Nano Lett. **16**, 644–650.
Vassileva, N. D., D. van den Ende, F. Mugele, and J. Mellema, 2005, "Capillary forces between spherical particles floating at a liquid-liquid interface," Langmuir, **21**, 11190–11200.
Velasco, C., R. Jones, S. King, and C. Spence, 2013, "Assessing the influence of the multisensory environment on the whisky drinking experience," Flavour **2**, 23.
Vella, D., 2015, "Floating versus sinking," Annu. Rev. Fluid Mech. **47**, 115–135.
Vella, D., 2019, "Buffering by buckling as a route for elastic deformation," Nat. Rev. Phys. **1**, 425–436.
Vella, D., and L. Mahadevan, 2005, "The Cheerios effect," Am. J. Phys. **73**, 817–825.
Venerus, D. C., and D. N. Simavilla, 2015, "Tears of wine: New insights on an old phenomenon," Sci. Rep. **5**, 16162.
Versluis, M., C. Blom, D. van der Meer, K. van der Weele, and D. Lohse, **2006**, "Leaping shampoo and the stable Kaye effect," J. Stat. Mech. P07007.
Via, M. A., M. Baechle, A. Stephan, T. A. Vilgis, and M. P. Clausen, 2021, "Microscopic characterization of fatty liver-based emulsions: Bridging microstructure and texture in foie gras and pâté," Phys. Fluids **33**, 117119.
Vidakovic, L., P. K. Singh, R. Hartmann, C. D. Nadell, and K. Drescher, 2018, "Dynamic biofilm architecture confers individual and collective mechanisms of viral protection," Nat. Microbiol. **3**, 26–31.
Vieyra, R. E., C. Vieyra, and S. Macchia, 2017, "Kitchen physics: Lessons in fluid pressure and error analysis," Phys. Teach. **55**, 87–90.
Vilgis, T. A., 1988, "Flory theory of polymeric fractals-intersection, saturation and condensation," Physica (Amsterdam) **153A**, 341–354.
Vilgis, T. A., 2000, "Polymer theory: Path integrals and scaling," Phys. Rep. **336**, 167–254.
Vilgis, T. A., 2015, "Soft matter food physics: The physics of food and cooking," Rep. Prog. Phys. **78**, 124602.
Virot, E., and A. Ponomarenko, 2015, "Popcorn: Critical temperature, jump and sound," J. R. Soc. Interface **12**, 20141247.
Vitale, S. A., and J. L. Katz, 2003, "Liquid droplet dispersions formed by homogeneous liquid- liquid nucleation:'The ouzo effect,' " Langmuir **19**, 4105–4110.
Vithu, P., and J. A. Moses, 2016, "Machine vision system for food grain quality evaluation: A review," Trends Food Sci. Technol. **56**, 13–20.
Vollestad, P., L. Angheluta, and A. Jensen, 2020, "Experimental study of secondary flows above rough and flat interfaces in horizontal gas-liquid pipe flow," Int. J. Multiphase Flow **125**, 103235.
von Kármán, T., 1954, *Aerodynamics* (Cornell University Press, Ithaca).
Vorobev, A., T. Zagvozkin, and T. Lyubimova, 2020, "Shapes of a rising miscible droplet," Phys. Fluids **32**, 012112.
Vuilleumier, R., V. Ego, L. Neltner, and A. M. Cazabat, 1995, "Tears of wine: The stationary state," Langmuir **11**, 4117–4121.
Vulić, H., D. Doračić, R. Hobbs, and J. Lang, 2017, "The Vinkovci treasure of late Roman silver plate: Preliminary report," J. Rom. Archaeol. **30**, 127–150.
Wadsworth, F. B., *et al.*, 2021, "The force required to operate the plunger on a French press," Am. J. Phys. **89**, 769–775.
Walker, J., 1978, "The Amateur Scientist," Sci. Am. **239**, No. 5, 186–197.
Walker, J., 2010, "Boiling and the Leidenfrost effect," in *Fundamentals of Physics*, edited by D. Halliday, R. Resnick, and J. Walker (Wiley, New York), https://www.researchgate.net/publication/251331691_Boiling_and_the_leidenfrost_effect.
Walker, T. W., T. T. Hsu, S. Fitzgibbon, C. W. Frank, D. S. Mui, J. Zhu, A. Mendiratta, and G. G. Fuller, 2014, "Enhanced particle removal using viscoelastic fluids," J. Rheol. **58**, 63–88.
Walker, T. W., T. T. Hsu, C. W. Frank, and G. G. Fuller, 2012, "Role of shear-thinning on the dynamics of rinsing flow by an impinging jet," Phys. Fluids **24**, 093102.
Walls, D. J., E. Meiburg, and G. G. Fuller, 2018, "The shape evolution of liquid droplets in miscible environments," J. Fluid Mech. **852**, 422–452.
Walls, D. J., A. S. Ylitalo, D. S. L. Mui, J. M. Frostad, and G. G. Fuller, 2019, "Spreading of rinsing liquids across a horizontal rotating substrate," Phys. Rev. Fluids **4**, 084102.
Walters, R. M., G. Mao, E. T. Gunn, and S. Hornby, **2012**, "Cleansing formulations that respect skin barrier integrity," Dermatol. Res. Pract. 495917.
Wang, C., X. Yu, and F. Liang, 2017, "A review of bridge scour: Mechanism, estimation, monitoring and countermeasures," Nat. Hazards **87**, 1881–1906.
Wang, K., P. Sanaei, J. Zhang, and L. Ristroph, 2022, "Open capillary siphons," J. Fluid Mech. **932**, R1.
Wang, W., J. Giltinan, S. Zakharchenko, and M. Sitti, 2017, "Dynamic and programmable self-assembly of micro-rafts at the air-water interface," Sci. Adv. **3**, e1602522.
Wang, W., *et al.*, 2018, "Multifunctional ferrofluid-infused surfaces with reconfigurable multiscale topography," Nature (London) **559**, 77–82.
Wasin, M., 2017, "Marangoni effect," https://www.youtube.com/watch?v=y6RSGzxEjVM (accessed May 5, 2020).
Watamura, T., F. Iwatsubo, K. Sugiyama, K. Yamamoto, Y. Yotsumoto, and T. Shiono, 2019, "Bubble cascade in Guinness beer is caused by gravity current instability," Sci. Rep. **9**, 1–9.
Watamura, T., K. Sugiyama, Y. Yotsumoto, M. Suzuki, and H. Wakabayashi, 2021, "Bubble cascade may form not only in stout beers," Phys. Rev. E **103**, 063103.
Watson, E. J., 1964, "The radial spread of a liquid jet over a horizontal plane," J. Fluid Mech. **20**, 481–499.
Weaire, D., and S. Hutzler, 2001, *The Physics of Foams* (Clarendon Press, Oxford).
Weaire, D., S. Hutzler, S. Cox, N. Kern, M. D. Alonso, and W. Drenckhan, 2003, "The fluid dynamics of foams," J. Phys. Condens. Matter **15**, S65–S73.
We are KIX, 2014, "Can you walk on water?," https://www.youtube.com/watch?v=dts-LIdwK00 (accessed November 20, 2021).
Weber, C. A., D. Zwicker, F. Jülicher, and C. F. Lee, 2019, "Physics of active emulsions," Rep. Prog. Phys. **82**, 064601.
Weidman, P. D., and M. A. Sprague, 2015, "Steady and unsteady modelling of the float height of a rotating air hockey disk," J. Fluid Mech. **778**, 39–59.
Welti-Chanes, J., and J. F. Velez-Ruiz, 2016, Eds., *Transport Phenomena in Food Processing* (CRC Press, Boca Raton).
Wensink, H. H., J. Dunkel, S. Heidenreich, K. Drescher, R. E. Goldstein, H. Löwen, and J. M. Yeomans, 2012, "Meso-scale turbulence in living fluids," Proc. Natl. Acad. Sci. U.S.A. **109**, 14308–14313.
West, J. B., 2013, "Torricelli and the ocean of air: The first measurement of barometric pressure," Physiology **28**, 66–73.

Wettlaufer, J. S., 2011, "The Universe in a cup of coffee," Phys. Today **64**, No. 5, 66–67.
Whalley, P. B., 1987, "Flooding, slugging and bottle emptying," Int. J. Multiphase Flow **13**, 723–728.
Wheeler, A. P. S., 2012, "Physics on tap," Phys. Educ. **47**, 403–408.
Whitaker, S., 1986, "Flow in porous media I: A theoretical derivation of Darcy's law," Transp. Porous Media **1**, 3–25.
White, B. Y., and J. R. Frederiksen, 1998, "Inquiry, modeling, and metacognition: Making science accessible to all students," Cognit. Instr. **16**, 3–118.
White, F. M., and I. Corfield, 2006, *Viscous Fluid Flow*, 3rd ed. (McGraw-Hill, New York).
Whitesides, G. M., 2011, "The frugal way," Economist **17**, 154, https://www.economist.com/news/2011/11/17/the-frugal-way.
Wiegand, J. H., 1963, "Demonstrating the Weissenberg effect with gelatin," J. Chem. Educ. **40**, 475.
Williams, J. T., 2018, Ed., *Waterproof and Water Repellent Textiles and Clothing* (Woodhead Publishing, Sawston, England).
Williams, S. J., 2021, "Whiskey webs: Fingerprints of evaporated bourbon," Phys. Today **74**, No. 2, 62–63.
Williams, S. J., M. J. Brown, and A. D. Carrithers, 2019, "Whiskey webs: Microscale 'fingerprints' of bourbon whiskey," Phys. Rev. Fluids **4**, 100511.
Wilson, D. M., and W. Strasser, 2022a, "The rise and fall of banana puree: Non-Newtonian annular wave cycle in transonic self-pulsating flow," Phys. Fluids **34**, 073107.
Wilson, D. M., and W. Strasser, 2022b, "A spray of puree: Wave-augmented transonic airblast non-Newtonian atomization," Phys. Fluids **34**, 073108.
Wilson, R. N., 2007, *Reflecting Telescope Optics I: Basic Design Theory and Its Historical Development* (Springer, New York).
Wilson, T. A., G. S. Beavers, M. A. DeCoster, D. K. Holger, and M. D. Regenfuss, 1971, "Experiments on the fluid mechanics of whistling," J. Acoust. Soc. Am. **50**, 366–372.
Windows-Yule, C. R. K., J. P. K. Seville, A. Ingram, and D. J. Parker, 2020, "Positron emission particle tracking of granular flows," Annu. Rev. Chem. Biomol. Eng. **11**, 367–396.
Wong, T.-S., T.-H. Chen, X. Shen, and C.-M. Ho, 2011, "Nano-chromatography driven by the coffee ring effect," Anal. Chem. **83**, 1871–1873.
Woodcroft, B., 1851, Ed., *The Pneumatics of Hero of Alexandria: From the Original Greek* (Taylor, Walton, and Maberly, London).
World Health Organization, 2015, "WHO estimates of the global burden of foodborne diseases: Foodborne disease burden epidemiology reference group 2007–2015," https://apps.who.int/iris/handle/10665/199350.
Woxenius, J., 2015, "The consequences of the extended gap between curiosity-driven and impact-driven research," Transp. Rev. **35**, 401–403.
Wray, A. W., and R. Cimpeanu, 2020, "Reduced-order modelling of thick inertial flows around rotating cylinders," J. Fluid Mech. **898**, A1–A33.
Würger, A., 2011, "Leidenfrost Gas Ratchets Driven by Thermal Creep," Phys. Rev. Lett. **107**, 164502.
Wylock, C., A. Rednikov, B. Haut, and P. Colinet, 2014, "Non-monotonic Rayleigh-Taylor instabilities driven by gas-liquid CO_2 chemisorption," J. Phys. Chem. B **118**, 11323–11329.
Xiao, H., D. McDonald, Y. Fan, P. B. Umbanhowar, J. M. Ottino, and R. M. Lueptow, 2017, "Controlling granular segregation using modulated flow," Powder Technol. **312**, 360–368.
Xu, R.-G., and Y. Leng, 2018, "Squeezing and stick-slip friction behaviors of lubricants in boundary lubrication," Proc. Natl. Acad. Sci. U.S.A. **115**, 6560–6565.
Xue, N., S. Khodaparast, and H. A. Stone, 2019, "Fountain mixing in a filling box at low Reynolds numbers," Phys. Rev. Fluids **4**, 024501.
Xue, N., S. Khodaparast, L. Zhu, J. K. Nunes, H. Kim, and H. A. Stone, 2017, "Laboratory layered latte," Nat. Commun. **8**, 1960.
Yakhno, T., A. Sanin, V. Yakhno, V. Kazakov, A. Pakhomov, T. Guguchkina, and M. Markovsky, 2018, "Drying drop technology in wine and hard drinks quality control," in *Food Control and Biosecurity*, edited by A. M. Grumezescu and A. M. Holban (Elsevier, New York), pp. 451–480.
Yan, Z., L. Sun, J. Xiao, and Y. Lan, 2017, "The profile of an oil-water interface in a spin-up rotating cylindrical vessel," Am. J. Phys. **85**, 271–276.
Yang, H., X. Min, S. Xu, J. Bender, and Y. Wang, 2020, "Development of effective and fast-flow ceramic porous media for point-of-use water treatment: Effect of pore size distribution," ACS Sustainable Chem. Eng. **8**, 2531–2539.
Yang, N., R. Lv, J. Jia, K. Nishinari, and Y. Fang, 2017, "Application of microrheology in food science," Annu. Rev. Food Sci. Technol. **8**, 493–521.
Yang, Y., W. Chen, R. Verzicco, and D. Lohse, 2020, "Multiple states and transport properties of double-diffusive convection turbulence," Proc. Natl. Acad. Sci. U.S.A. **117**, 14676–14681.
Yang, Y., R. Verzicco, and D. Lohse, 2016, "From convection rolls to finger convection in double-diffusive turbulence," Proc. Natl. Acad. Sci. U.S.A. **113**, 69–73.
Yasuda, K., R. C. Armstrong, and R. E. Cohen, 1981, "Shear flow properties of concentrated solutions of linear and star branched polystyrenes," Rheol. Acta **20**, 163–178.
Yeoh, G. H., and K. K. Yuen, 2009, *Computational Fluid Dynamics in Fire Engineering: Theory, Modelling and Practice* (Butterworth-Heinemann, Oxford).
Yeomans, J. M., D. O. Pushkin, and H. Shum, 2014, "An introduction to the hydrodynamics of swimming microorganisms," Eur. Phys. J. Spec. Top. **223**, 1771–1785.
Yih, C.-S., 1963, "Stability of liquid flow down an inclined plane," Phys. Fluids **6**, 321–334.
Yoo, B., 2004, "Effect of temperature on dynamic rheology of Korean honeys," J. Food Eng. **65**, 459–463.
Yoshikawa, H. N., and J. E. Wesfreid, 2011, "Oscillatory Kelvin-Helmholtz instability. Part 2. An experiment in fluids with a large viscosity contrast," J. Fluid Mech. **675**, 249–267.
Yunker, P. J., M. A. Lohr, T. Still, A. Borodin, D. J. Durian, and A. G. Yodh, 2013, "Effects of Particle Shape on Growth Dynamics at Edges of Evaporating Drops of Colloidal Suspensions," Phys. Rev. Lett. **110**, 035501.
Yunker, P. J., T. Still, M. A. Lohr, and A. G. Yodh, 2011, "Suppression of the coffee-ring effect by shape-dependent capillary interactions," Nature (London) **476**, 308–311.
Zanini, M., C. Marschelke, S. E. Anachkov, E. Marini, A. Synytska, and L. Isa, 2017, "Universal emulsion stabilization from the arrested adsorption of rough particles at liquid-liquid interfaces," Nat. Commun. **8**, 1–9.
Zellner, D. A., E. Siemers, V. Teran, R. Conroy, M. Lankford, A. Agrafiotis, L. Ambrose, and P. Locher, 2011, "Neatness counts. How plating affects liking for the taste of food," Appetite **57**, 642–648.
Zenit, R., 2019, "Some fluid mechanical aspects of artistic painting," Phys. Rev. Fluids **4**, 110507.
Zenit, R., and J. J. Feng, 2018, "Hydrodynamic interactions among bubbles, drops, and particles in non-Newtonian liquids," Annu. Rev. Fluid Mech. **50**, 505–534.

Zenit, R., A. H. Kumar, A. Mansingka, T. Powers, M. Ravisankar, A. Sollenberger, and P. Tieze, 2020, "Make a pancake: Learn about viscosity," *Proceedings of the 73rd Annual Meeting of the APS Division of Fluid Dynamics, 2020*, https://meetings.aps.org/Meeting/DFD20/Session/L02.6.

Zenit, R., and J. Rodríguez-Rodríguez, 2018, "The fluid mechanics of bubbly drinks," Phys. Today **71**, No. 11, 44.

Zhang, Z., X. Zhang, Z. Xin, M. Deng, Y. Wen, and Y. Song, 2013, "Controlled inkjetting of a conductive pattern of silver nanoparticles based on the coffee-ring effect," Adv. Mater. **25**, 6714–6718.

Zhao, N., B.-w. Li, Y.-d. Zhu, D. Li, and L.-j. Wang, 2020, "Viscoelastic analysis of oat grain within linear viscoelastic region by using dynamic mechanical analyzer," Int. J. Food Eng. **16**, 20180350.

Zhmud, B., 2014, "Viscosity blending equations," Lube Mag. **121**, 24–9, https://www.lube-media.com/wp-content/uploads/2017/11/Lube-Tech093-ViscosityBlendingEquations.pdf.

Zhong, J.-Q., M. D. Patterson, and J. S. Wettlaufer, 2010, "Streaks to Rings to Vortex Grids: Generic Patterns in Transient Convective Spin Up of an Evaporating Fluid," Phys. Rev. Lett. **105**, 044504.

Zhu, S., M. A. Stieger, A. J. van der Goot, and M. A. I. Schutyser, 2019, "Extrusion-based 3D printing of food pastes: Correlating rheological properties with printing behaviour," Innovative Food Sci. Emerging Technol. **58**, 102214.

Zia, R. N., 2018, "Active and passive microrheology: Theory and simulation," Annu. Rev. Fluid Mech. **50**, 371–405.

Ziefuß, A. R., T. Hupfeld, S. W. Meckelmann, M. Meyer, O. J. Schmitz, W. Kaziur-Cegla, L. K. Tintrop, T. C. Schmidt, B. Gökce, and S. Barcikowski, 2022, "Ultrafast cold-brewing of coffee by picosecond-pulsed laser extraction," npj Sci. Food **6**, 1–9.

Zielbauer, B. I., J. Franz, B. Viezens, and T. A. Vilgis, 2016, "Physical aspects of meat cooking: Time dependent thermal protein denaturation and water loss," Food Biophys. **11**, 34–42.

Zoltowski, B., Y. Chekanov, J. Masere, J. A. Pojman, and V. Volpert, 2007, "Evidence for the existence of an effective interfacial tension between miscible fluids. Part 2. Dodecyl acrylate/poly (dodecyl acrylate) in a spinning drop tensiometer," Langmuir **23**, 5522–5531.

Zöttl, A., and H. Stark, 2016, "Emergent behavior in active colloids," J. Phys. Condens. Matter **28**, 253001.

Zuriguel, I., 2014, "Invited review: Clogging of granular materials in bottlenecks," Pap. Phys. **6**, 060014.

Zuriguel, I., A. Janda, A. Garcimartín, C. Lozano, R. Arévalo, and D. Maza, 2011, "Silo Clogging Reduction by the Presence of an Obstacle," Phys. Rev. Lett. **107**, 278001.

Zuriguel, I., *et al.*, 2014, "Clogging transition of many-particle systems flowing through bottlenecks," Sci. Rep. **4**, 7324.